TITLE

" STUDIES OF GALVANOSTATIC PULSE PLATING OF COPPER FROM SOLUTION CONTAINING COMPLEXING IONS "

Ph.D. Thesis by Choy Wan Yeow.

Department of Chemistry,
Bedford College,
University of London,
Egham,
Surrey.

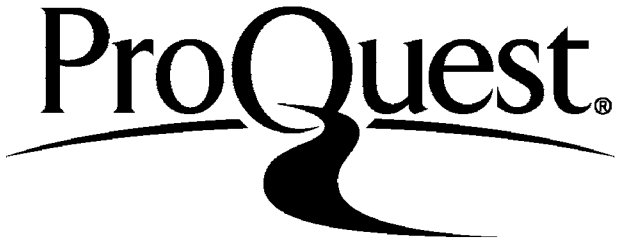

ACKNOWLEDGEMENTS

For making possible the voluminous research, time consuming experiments, endless discussions and above all the piecing together of all results in this thesis, I have incurred no small amount of indebtness to a number of persons to whom appreciation is hereby acknowledged.

Topping the list is my Supervisor, Dr. D.B. Hibbert who has most generously shared with me his knowledge, and experience through all the phases of this work. His guidance and encouragement have been the main confirmatory factors to the successful completion of this thesis.

In conjunction with the efforts of Dr. D.B. Hibbert are the support and assistance that have been made available to me by the staff of the Chemistry Department of Bedford College.

No less important are the patience and understanding shown by my wife. She has even further contributed by plodding through the ever changing manuscripts and eventually the fair copy on the typewritter.

I wish also to take this opportunity to pass my gratitude to my parents whose finiancial support I depend entirely for my education.

CONTENTS

.....continue

SUMMARY

The first part of this research work was the investigation of Galvanostatic pulse plating of copper and copper(I) halides from acid copper(II) halide solutions. The general stoichiometric equation for the reaction which occurs during the relaxation time was found to be

$$Cu^{2+} + Cu^{o} + 2X^{-} \longrightarrow 2\ CuX \qquad E(1\text{-}10,p24)$$

Further study showed that the rate determining step of reaction E(1-10) involves $CuCl^{+}$ in a first order reaction

$$\frac{d(CuCl)}{dt} = k_{CuCl^{+}} \left[CuCl^{+}\right] \qquad E(3\text{-}38,p174)$$

It is discovered here that the galvanostatic pulse plating technique has a great potential in the production of Cu^{o}/CuCl electrodes. These electrodes can be used in sea-water batteries. Control of the pulse plating conditions can produce electrodes of almost any desired composition of CuCl in the deposit of any required thickness and discharged capacity. The presence of a small amount of copper in the layer gives the electrodes conductivity which is an advantage for such electrodes.

The second part of the research involved studies of the electrodeposition of copper in electrolytes with and without 'addition agents'. It was found that the bright deposits obtained using solutions containing brighteners (dimethyl thiourea or thioglycolic acid) could consist of either small or large grains,instead of only small grains which had been frequently observed by others.

It was also found that those addition agents which gave bright deposits were easily oxidised in sulphuric acid.In the same sweep range (-72mV to -350mV vs SCE) the addition agents which did not give bright deposits did not oxidise significantly.

A postulation of the involvement of the brighteners is suggested. As the disulphide of dimethyl thiourea or thioglycolic acid could have been reduced during the deposition of copper, there are probably two electro-reduction processes taking place in solutions containing brighteners.

CHAPTER 1

INTRODUCTION

PART (1-1) Indsutrial Copper Electrodeposition Process.

Copper electrodeposition from acid copper sulphate solutions is extensively used in the industry e.g. for building up surfaces where the mechanical loading is not too high, production of electrotypes and printed circuits boards.

The copper electroplating process may be given as follows:-

(1) Racking or wiring.

(2) Pre-treatment ie. polishing, barreling and cleaning process.

(3) Electroplating.

(4) Post-treatment, including final rinsing and drying.

(5) Unloading from racks or wiring.

In an automatic plant, stages 2,3 and 4 are incorporated within one unit. The jigs or racks are conveyed to or from the plant with an automatic loader and unloader respectively.

The cleaning and electroplating process are the most important steps in the metal electroplating in general. Thus both of these processes will be discussed here.

The cleaning sequence can be summarised as preliminary cleaning, water rinsing, cathodic cleaning, water rinsing, acid dipping and water rinsing.

Preliminary cleaning or degreasing involves the removal of heavy oils, greases and soils from electrodes to be plated. In this process, the electrodes are immersed in a solvent vapour of trichloroethylene or perchloroethylene. The solvent vapour container is provided with heating elements in the base and a cooling coil round the top. This arrangement allows the solvent vapour to be recycled back to the base.

The cathodic cleaning process effects the removal of residual oxide or grease films. This process involve the use of an inert electrode as

anode and the electrode to be cleaned as cathode. The two electrodes are immersed in a cleaning solution which is commercially known as Activax. When the system is switched on, the hydrogen gas thus evolved, has a scouring effect upon the surface to be cleaned.

Hydrofluoric acid (2.5% vol/vol in water) and sulphuric acid (0.5% vol/vol in water) are used in the acid dipping step. This is carried out to ensure that any alkaline film present after the previous step is neutralised.

Electroplating is carried out in a glass, plastic or rubber lined tank. The process is usually carried out at room temperature but it may raised to 313 K if fast deposition is required. The maximum current density used at room temperature is 5 A dm^{-2} and 16 A dm^{-2} at 313 K. The composition of the solution is copper sulphate 200 g dm^{-3}, potash alum 12 g dm^{-3} and sulphuric acid 56 g dm^{-3}.

PART(1-2) REVIEW OF PREVIOUS WORK

Sect (1-2.1)

Electrochemical Reaction of Copper In Acidified Sulphate Solution.

Copper deposition from acid sulphate solution occurs in consecutive steps.[1] They are namely, the ion transfer across the electrified interface, i.e. the charge transfer reaction surface diffusion of adions to steps and diffusion along steps to kinks.

The mechanism of Copper deposition in acid copper sulphate system was studied by Mattsson and Bockris using a galvanostatic pulse technique[2]. They suggested that the mechanism involved the following steps.

$$Cu^{2+} + e \xrightarrow{slow} Cu^{+} \qquad E(1\text{-}1)$$

$$Cu^{+} + e \underset{\longleftarrow}{\xrightarrow{Fast}} Cu^{o} \qquad E(1\text{-}2)$$

The two step mechanism was confirmed by Peter and Cruser[3] using a chronopotentiometric technique. This involved the measurement of the potential-time variation at a working electrode during a short period of exhaustive electrolysis carried out

at constant current and under linear diffusion control. Hibbert,Sugiatro and Tseung[4] using the same galvanostatic transient method as Mattsson and Bockris, and Brown and Thirsk[5] using a rotating disk electrode also agreed with the above two step mechanism.

Bockris and co-workers,[2,6,7] have concluded from investigations carried out on the Cu/Cu^{2+} system in acid solutions that the rate determining step can be either due to a charge transfer step as E (1-1,p6) or surface diffusion of adatoms or adions. This was found to have depended on current density and types of surface preparation used. From all types of surface preparation used, it was concluded that the reaction is controlled by a surface diffusion process at low current density with the exception of surfaces obtained by electrodeposited copper where reaction control was shared with a charge transfer process. On the other hands when high current density was used,it was concluded that

reaction control is mainly due to a charge transfer process.

Slaiman and Lorenz[8] used a galvanostatic double pulse method to investigate the kinetics of the Cu/Cu^{2+} electrode system. They stated that the mechanism of the anodic dissolution and cathodic deposition would take place in three consecutive steps. The first step in the cathodic deposition process is the reaction shown in equation E(1-1,p6) The second and third consecutive steps are as followings:

$$Cu^{+} + (1 - V)e^{-} \rightleftharpoons Cu_{ads}^{v+} \qquad E\ (1\text{-}3\ )$$

$$Cu_{ads}^{v+} + Ve^{-} \rightleftharpoons Cu \qquad E\ (1\text{-}4\ )$$

The rates of reaction are that reaction E(1-3) and E(1-4) $>$ E(1-1) and $0 < V < 1$. They also suggested that the mechanism at a polycrystalline Cu/Cu^{2+} - electrode is not markedly influenced by surface diffusion processes. In other words, at $\eta > \pm$ 5mV, the direct charge transfer will take place at growth sites, e.g. kinks or screw dislocations.

Hurlen and co-workers[9] in 1978 reported that the fast Cu/Cu^{+} metal ion-transfer step reveals itself in the "Superpolarization" which appears in galvanostatic transients. Superpolarization is a peak occuring in the galvanostatic overpotential v s. time curve at the initial stage of the transient. The peak overvoltage numerically exceeds the final stationary overvoltage. They also claimed that the Cu/Cu^{+} step is kinetically accessible besides the slower Cu^{+}/Cu^{2+} step.

Karasyk and Linford[16] investigated the kinetic parameters for copper deposition on clean and "soiled" electrodes, using a galvanostatic method. The"soiled" electrodes are the electrodes containing film of stearic acid and paraffin oil. These electrodes were prepared by means of an evaporation technique. The electrodepositions were carried out from an acid copper sulphate solution and on flat plate copper electrodes. They found that the mean values of the cathodic transfer coeffieient (α_c) and exchange current density were 0.57 ± 0.02 and $(11.4 \pm 3.2)10^{-1} Adm^{-2}$ respectively for cleaned electrodes. These results are

in agreement with those reported by Mattsson and Bockris. For the soiled copper electrodes the values of a_c was found to be about 0.3. The exchange current density for the freshly prepared soiled (stearic acid) electrodes is higher than those for similar cleaned electrodes. Those non freshly prepared soiled electrodes (i.e. The film of stearic acid or paraffin oil remained on the electrode for 24 hour before the experiments) have exchange current densities which are close to those for clean electrodes.

They also reported that the typical values of the double layer capacitance were $(50\text{-}60)10^{-2}Fm^{-2}$ for clean electrodes and about $(7 - 26)\ 10^{-2}\ F\ m^{-2}$ for soiled electrodes. They suggested that this lowering of the capacity probably facilitates the transfer by making "leakge" of charged ions through the capacitance easier.

Bockris and Mattsson[2] found that the mean values of the double layer capacitance were $(78 \pm 6)10^{-2}\ Fm^{-2}$ for the copper electrodes used in the same acidified cupric sulphate solution as the above authors.

The values for He-prepared (i.e.copper electrodes prepared by melting in helium) and electrodeposited electrodes were not found to be significantly different. The reason given for the standard deviation from the mean of about 10% was there were some difficulties of taking tangents of,the overpotential at time t,η_t vs. t curve, at limitingly low over-potentials.

Slaiman and Lorenz[8] found the values of double layer capacitance and adsorption capacitance of copper electrodes in sulphate solution. The adsorption capacitance is related to adsorbed intermediates in the overall reaction, in this case to adatoms at the electrode surface. They found that the'adsorption capacity' was slightly affected by Cu^{2+} concentration but remained dependent on electrode surface treatment. The electrical double layer capacity of the electro-deposited copper electrodes was also found to be different from the group of different types of polished electrodes whose electrical double layer capacities were not significantly different from each other.

Examples of the cathodic values of the double layer capacitance found were $(50 \pm 5)10^{-2}Fm^{-2}$ and $(27 \pm 3.5)10^{-2}\ Fm^{-2}$ for the electrodeposited electrodes and the mechanical polishing electrodes respectively. The values of the adsorption capacitance of the above electrodes were found to be $(135 \pm 26)10^{-2}Fm^{-2}$ and $(55 \pm 8)10^{-2}\ Fm^{-2}$.

The values of the double layer capacitance of copper electrodes observed by the above authors show that their values are greatly affected by the surface treatments of the electrodes.

In crystallographical and morphological studies on copper deposition Pick and his co-workers[10,11,12] found that the surface geometry of the deposit was independant of plating time and that the scale of the surface features increased with time. The orientation and the purity of the cathode affect the initial mode of growth of deposits. Okada and Magari[17] agreed that the orientation of the cathode affect the copper deposit.

Damjanovic and co-workers[13] investigated copper deposition on single crystal planes. They found that the deposits on the (III) plane had the shapes of triangular and hexagonal pyramids, at low current density (i.e. less than 1 Adm^{-2}). At a higher current density (i.e. greater than 1 Adm^{-2}) it was found that the triangular and hexagonal pyramids transform into blocks and larger hexagonal layers. On the (110) plane, ridge types of deposits were found to have developed at all current densities (i.e. 0.2 A dm^{-2} to 3 Adm^{-2}). The observations were carried out up to an average thickness of the deposit corresponding to 10 coulomb cm^{-2}.

They also found that the morphology of the deposits obtained at 0.5 A dm^{-2} did not deviate markedly at different concentrations of solutions. The concentrations used were 0.25 mol dm^{-3} and 1 mol dm^{-3} copper sulphate in 0.1 mol dm^{-3} sulphuric acid.

Carneval and Cusminsky[14] observed that the morphology of the copper deposited on (001) copper surfaces was of similar overall shape and had epitaxial growth at an early stage of deposition.

The shape was mainly square pyramid or square block. The solutions used were simple acidic copper solutions (i.e. sulphate,chloride and citrate) and the current density used was less than 2 Adm^{-2}. The morphology of the deposits obtained, at higher current density (i.e. 5 Adm^{-2}) or from the complex solutions, deviate significantly. The shapes were of spheres, cauliflowers,dendrites,boulders of certain geometrical shape and nuclei without any characteristics.

Benn and Walker[15] studied the effect of the bath temperature,and current density on copper deposits from an acidified copper sulphate bath. They observed that the grain size decreased as the current density increased (in the range of 1 Adm^{-2} to 6.5 Adm^{-2}) at constant temperature. At constant current density, the grain size increased as the temperature increased (in the range of 273 K to 353 K). They also found that there is a strong correlation between a high hardness and a small grain size or factors which produce a small grain size. One of the earlier theories which has been proposed to explain this relationship is that the hardness was connected with the grain size

and,for a given grain size, differences in the hardness could be due to different packing within the crystal lattice. Another theory explained that a small grain size produced many grain boundries which blocked the slip planes along which deformation of the crystals would normally occur.

Sect:

1-2.2 Studies of Copper Reactions In Solutions Containing Halide Ions, And Copper Halide Electrodes.

It is a common practice to add chlorides (NaCl or HCl) to acidified copper sulphate electrolytes in copper refining processes. The chlorides are used to precipitate silver ions in the electrolytes and to minimize the codeposition of antimony and bismuth with copper.[18] Yao[19] suggested that the chloride concentration used should be from 0.01 to 0.05 g dm^{-3}. Chloride is also used as an so called "addition agent" in electroplating of bright copper deposits[20] Investigations of the effects of chloride ions on copper deposition has been carried out by several authors[18,19,21].

In 1944 Yao,[21] found that an increase of chloride concentration at low chloride concentration resulted in small increases in cathode polarization, hardness and a large decrease in grain size. However, at

chloride concentration greater than 0.015 g dm^{-3} cathode polarization and hardness decreased sharply with concentration. Also the grain size was observed to have increased. Acidified copper sulphate chloride ion solutions were used in his experiments.

In 1952, Beaver[22] patented the use of chloride for bright copper plating in an acid copper bath. He recommended that the range of chloride concentration to be used should be from 0.001 to 0.015 g dm^{-3}.

Mosher[23] suggested that in order to avoid obtaining coarse deposits in electrorefining processes 0.002 to 0.035 g dm^{-3} of chloride ions should be added to precipitate silver. There is little agreement among different authors regarding the range of concentrations of chloride to be used. This is probably because it depends on temperature and on concentrations of other bath constituents.

The effect of chloride may be markedly modified by the presence of other addition agents. It was

observed by Gauvin and Winkler [18] that the addition of gelatin to a solution containing chloride should be considerably increased powder formation of the deposit. They suggested a hypothesis to explain the addition agent effect of chloride in deposition. The hypothesis is that a small concentration of cuprous ions is always available to react with chloride ions due to the following reaction between the copper electrode and copper sulphate solution:

$$Cu^{2+} + Cu \rightleftharpoons 2\,Cu^{+} \qquad E\ (1\text{-}5)$$

As a result, at a concentration higher than some critical value, (i.e. 0.0089 g dm^{-3} Cl^{-} in 0.5 mole dm^{-3} copper sulphate solution) cuprous chloride precipitates in colloidal form since it has had no time to grow into a visible precipitate during electrolyiss. The colloidal cuprous chloride is then adsorbed by the deposit and therefore acts as a mild addition agent.

They also observed that a grey cuprous chloride film formed at the anode at chloride concentrations of $\geq$ 0.1 g dm^{-3}.

Bartlett, Cooper and Stephenson[24,25,26,27] studied the anodic behavious of copper in HCl solution without any Cu^{+} and Cu^{2+} ions being present initially by both electrochemical and optical methods. They reported that immediately after electrolysis began on anode layer grew until it was completely covered. The layer was of Cu (I) Cl by the reaction:[24]

$$Cu + Cl^{-} \longrightarrow CuCl + e^{-} \qquad E(1\text{-}6)$$

and grew to a thickness of 10^{-4}cm. In the steady state, the rate of the Cu (I) Cl layer formation reaction was equivalent to the rate of layer removal:

$$Cu\ Cl + Cl^{-} \longrightarrow Cu\ Cl_2^{-} \qquad E(1\text{-}7)$$

and the overall reaction was

$$Cu + 2Cl^{-} \longrightarrow Cu\ Cl_2^{-} + e^{-} \qquad E(1\text{-}8)$$

The formation of Cu^{2+} ions was also detected in the solution and the entrance into solution of

Cu^{2+} and the $Cu\,Cl_2^-$ complex were observed.[27] It was suggested that the Cu^{2+} ions went directly into the solution through the pores in the Cu(I) Cl layer.[26]

The corrosion of copper in solutions of copper (II) chloride was studied by Hurlen.[28,29] He found that layers of copper (I) chloride were formed which subsequently dissolved giving soluble species such as $Cu\,Cl_2^-$.

Hurlen[28] also suggested that the anodic dissolution and cathodic deposition reactions of copper in acidified Cu (I) Cl solution were diffusion controlled. The reactions were found to obey the relationship.

$$V = E_R + (RT/nF) \ln (1 \pm i/i_L) \qquad E\ (1\text{-}9)$$

where V = electrode potential vs. S.H.E.

E_R = The reversible potential of copper in electrolyte vs. S.H.E

i = current density A/dm^2

i_L = Limiting current density A/dm^2

The experiments were carried out with a current density of less than 1.0 A dm^{-2} .

Bonfiglio et al [38] agreed with Hurlen[28] that the anodic dissolution of copper in acid chloride media is diffusional in character. They concluded that the slow cuprous chloride complexes transer towards the bulk is the rate determining step. This is partially in agreement with Cooper and Bartlett[26] who suggested that diffusion of the $CuCl_2^-$ complex is the rate determining step.

Braun and Nobe[39] used a model, which assumes the formation of a CuCl film on the copper surface and diffusion of the chloride ions to the electrode as the rate determining step, to interpret their experimental data. They calculated that the values of K_2 and K_3 (complexation constants) were 6.67×10^4 and 1.81×10^5 respectively. They concluded that

in solutions with Cl^- concentration of less than 0.7 mol dm^{-3}, the complex, $CuCl_2^-$, is dominant, while at more concentrated chloride solutions, $CuCl_3^{2-}$ is the main complex formed. It can be seen that most investigators have agreed that the copper anodic dissolution process in chloride solution is mass transfer rather than activation controlled. Different anions species (Cl^-, $CuCl_2^-$ and $CuCl_3^-$) have been proposed by different investigators to be involved in the diffusion controlled rate determining step.[39] This shows, it is difficult to completely understood this reaction since different chloride complexes are involved.

Tseung and Mahmood[30] investigated the possibility of using an integrated chemical-electrochemical method for the recovery of copper from dilute solutions containing chloride and cupric ions. Their results showed that higher efficiency and rates in the recovery process were achieved.

The kinetics of copper (II) reduction in chloride media with and without the reducing agent $Na_2 SO_3$ were studied by Hibbert, Sugiarto and Tseung[4]. The results showed that, in the presence of chloride and sulphide ions, the $Cu Cl_2^-$ complex was formed. In the cathodic process, it was reported that the rate determining step was the reduction of the $Cu Cl_2^-$ complex. Anodically, the slow step was the oxidation of $Cu Cl_2^-$. It was observed that the copper deposited at the cathode, in the chloride solution, without reducing agent dissolved chemically at PH1. The reaction suggested was that the copper deposit reacts with chloride ions, to give copper chloride complex [i.e. reaction E(1-8,p19)]

Copper (I) chloride is used as a cathode for reserve sea water batteries,[31] which may be fabricated by mixing copper (I) chloride, an organic binder and graphite.

Margalit[32] investigated copper (I) halide/ sulphur mixes as cathodes for seawater activated cells: chloride, bromide and iodide were the

halides used. He concluded that CuI/sulphur pellets were the most promising materials among the halide-sulphur mixes. This was because the chloride/suplhur pellet disintegrated and the bromide-sulphur pellet changed colour indicating a chemical change during temperature and humidity tests.

A method of manufacture copper halide electrodes by direct reactions at a copper electrode using galvanostatic pulse technique was described by Yeow and Hibbert.[33] The reactions involved are the two step electrochemical reaction of copper plating as shown in equations E(1-1,1-2,p6) . and the chemical reaction involving copper,halides (X) and cupric ions in the plating electrolytes.

$$Cu^{2+} + Cu^{o} + 2\ X \longrightarrow 2\ CuX \qquad E\ (\ 1\text{-}10\ )$$

The electrodes made using the method may be more conducting, have a known discharge capacity,strongly binded and ultimately be more economical.

Copper deposits containing large amount of iodine, deposited from a cuprous iodide bath,were described by Schlotter.[34] He reported that the concentration of iodine in the deposit increased with current density,with a concentration as high as 0.63 per cent. At this concentration, the lattice constant increased from 3.604 to 3.609°A. The deposit has the interesting property of being photosensitive, turning from red to blue on exposure to light.

Winkler[35] and co-workers found that bormide and iodide added to sulphate baths have similar effect as chloride[18] on the deposits but less pronounced.

Mayanna[36] investigated the mechanism of the dissolution reaction of copper in acidic solution with and without the presence of iodine ions. The results obtained in both cases were consistent with the mechansim proposed by Bockris[2] except in the presence of iodide ions, the rate of the dissolution is decreased. The anodic Tafel slopes obtained for copper single crystal planes in the absence and

presence of iodide ions were the same. They suggested that this indicates the mechanism of the dissolution reaction on uninhibited and inhibited copper single crystal planes in sulphuric acid is the same.

Nageswar[37] studied the electrodeposition of copper on a copper single crystal (111) face in the presence of bromide ions. It was found that the pyramidal growth of copper deposited on Cu(111) from an acid copper sulphate bath without bromide ions. The pyramidal growth became truncated pyramids and transformed to a layer growth which gave rise to ridges and then to a polycrystalline deposit when bromide ions were present. These transitions of the surface features were in parallel with the increaments of concentrations of bromide ions from 10^{-3} to 10^{-10} mol dm^{-3}. The transition from one type of growth to another was more gradual at high current density (i.e. 1, 1.5 and $2 A dm^{-2}$).

Sect (I-2.3)

Studies of the Role of Addition Agents in the Electrodeposition of Copper.

The discovery of bright plating led to considerable savings of production costs in the field of electroplating. In particular, substantial savings in cost and effort have been made since a good deal of the hand finishing previously used can be eliminated.

The early history of bright plating has been reviewed by Rubinstein[55] and by Henricks.[56] The discovery of brighteners used in various plating baths was accidental in some cases, and in others it was the result of small scale trial and error experimentations.

Henricks[56] reviewed serveral theories proposed for the mechanism of bright plating. The most prominent of these theories are as follows:-

(1) Adsorption Theory:

Bancroft stated that "The crystal size is decreased when there are present at the cathode surface substances which are adsorbed by the deposited metal"

(2) Reducing Agent Theory:

Kern in 1909 stated that "The function of an addition agent in an electrolyte is to maintain a reducing menstruum around the cathode,which, in turn causes the deposit to form denser and smoother". He based his observations on the fact that reducing agents such as phenols,aromatic amines,refined the grain size of deposit,while oxidizing anions produced coarse or spongy deposits.

(3) Complex Ion Theory:

This theory was first proposed by Mathers in 1916 and then elaborated by him in 1939.Fuseya and his co-workers did some research to establish the validity of this theory and stated that effective addition agents form complex ions with the depositing metal.

(4) Cathode Interference Theory:

The conclusion that Hunt came to from his study of the structure of electrodeposited metals was that:"the crystalline structure of an electro-deposited metal will be governed by the relation of the metal ion concentration in the cathode film to the concentration of the other constituents of

that film. If the proportion of metal ions to inert particles is comparatively high,there will be little interference with crystal growth,and coarsely crystalline deposits will result. If,however, the proportion is low e.g. due to low degree of dissociation and complex ion formation, there will be considerable interference with crystal growth,with the consequent formation of many nuclei."

The theories described above explain some of the phenomena associated with brightener action but none of these completely explains all of the observed facts.

The surface structure is the principal factor which determines the brightness of electrodeposited metal.[141] Therefore, the effect of addition agents on grain size and crystal growth habit has been the subject of several investigations. In addition, most investigators studied the kinetics of copper electrodeposition using the same addition agents so that a successful theory of bright plating could be deduced.

Shreir and Smith[60] studied the effects of addition agents on the cathode polarization potential during the electrodeposition of copper and upon the superficial structure of the deposits. They found that addition agents (e.g.thiourea,citric acid and others) which cause an increase in polarization result in deposits of finer grain size. On the other hand those which decreased the overvoltage result in coarse-grained deposits.

They also reported that a concentration of thiourea of 10^{-5} mol dm^{-3} caused the formation of coarsely crystalline deposits. Conversely, a higher concentration of thiourea, 10^{-4} mol $^{-3}$ which has a higher polarization potential resulted in a fine grain and bright deposits. Sukava and Winkler[140] have reported that cystline + Chloride in copper sulphate gave coarse and irregular deposit when the polarization potential was lowest. Therefore, there is some agreement in their observation of the relationship between grain size and polarization potential with that of Shreir and Smith's.

Barnes and Storey[47] suggested that the crystal growth habit modifications (e.g. transformation of pyramid growth to cubic layer growth) produced by, additions of glucose, or urea, or glycine (i.e. concentration of less than 10^{-2} mol dm^{-3}), is basically due to the change of polarization. Also this effects was observed under the electrodeposition of single crystal copper surfaces can be simulated in uncontaminated solutions by changes in the current density. The electrochemical kinetics of the process has been altered by the addition agents but the crystal growth mechanism remained the same.

They found that a glycine concentration of 1×10^{-2} mol dm^{-3} causes crystalline material to be codeposited, with considerable distortion in the metal lattice. They interpreted this as an indication of surface adsorption and impurity incorporation.

Further work by Barnes[57] discovered that this compounds which contain divalent sulphur e.g. thioacetamide and thioxamide etc, in acid copper

baths reduced cathodic polarization and modified the crystal habit of copper diposited on the (100) surface of copper single crystal . He suggested that the divalent compounds form a barrier between the cathode surface and the electrode and prevent H^+ ion inhibition on the surface. Therefore, the ———HS^- anions become adsorbed on the metal surface in preference to other molecular or ionic species. As result the cathode surface is covered with an adsorbed film of different characteristics which affect the crystal growth habit.

Fischer[58] and his co-workers have also carried out an investigation into the effect of glycine additions to sulphate solutions on the surface topography of deposits formed on cubic-texture strip. They found that glycine additions failed to influnce the current density at which pyramid growth transformed to cubic layer growth, but that in the current density range of layer growth increased glycine concentration,up to a limiting value,enlarged the crystallite size. Above this limiting value,

the mean diameter of the grains was inversely proportional to the inhibitor concentration. Therefore both the glycine concentrations and thiourea concentrations have the same effect on the grain sizes of copper deposits.

Johnson and Turner[59] agreed with other investigators[57,60] that a small amounts of thiourea in the plating solution has a depolarization effect on the cathode. They suggested that this indicates the kinetics of copper electrodeposition is limited by surface diffusion of adatoms up to a higher current density with small amounts of thiourea than without it. Also higher thiourea concentration inhibits the surface diffusion of adatoms.

They also found that both thiourea and 1(-) cystine have similar behaviour as addition agents in acid copper plating. Both addition agents contain sulphur groups and they proposed that they are either hydrolysed or electrochemically reduced during plating to form sulphide ions which precipitate copper as CuS at the cathode surface.

Hoekstra et al,[46] carried out the radio tracer studies of the adsorption of thiourea on copper. It was found that thiourea was strongly adsorbed on the surface of a copper electrode. The adsorption took place even in the absence of applied potential, in acid copper plating bath with 0.01g dm^{-3} thiourea-S-35 . The adsorption of thiourea appeared to have no preference for any crystal face of copper. It was suggested that the adsorbed thiourea interferes with the crystal growth and resulted in obtaining bright deposit in their electrodeposition studies.

Evidence for adsorption also comes from the fact that, the additives get incoroperated into the electrodeposits. Llopis and co-workers, using radio tracers, found sulphur but not carbon, in the copper deposit when the plating bath contained thiourea.[59] Rogers and Ware[61] used radio tracer techniques and autoradiography have found that the nickel deposit contained sulphur. Also the amount sulphur increased with decreasing current density in a Watts plating solution containing thiourea as a brightener.

There is very little informatinn available regarding the values of double layer capacitance of copper during the electrodeposition or dissolution processes. Bockris and Enyo[6] measured the values of the double layer capacitance of copper electrodes in acidified cupric solutions with different anions (i.e. S_4^{2-}, Cl^-, ClO_4^-, Ac^- and $NH_2SO_3^-$).They found that the values of double layer capacitance varied between $(43 \pm 13)\ 10^{-2}\ Fm^{-2}$ and $(143 \pm 21)10^{-2}Fm^{-2}$ for acetate and aminosulphonate anions respectively.

No information was found regarding the study of the relationship between the surface crystal structure and the values of double layer capacitance of copper electrodeposition with or without addition agents.

Weil[62] has summarized the following facts about the sturcture of bright nickel deposits which he said most of the facts apply also to other plated metals. In order to be fully bright, nickel electrodeposits may either have fine grains or large grains.

If they have large grains there should not be any bounding crystal planes inclined to the surface. The boundaries of large grains are usually deep valleys. Therefore, bright, large grained deposits are rare in commercial plating. However, single-crystal deposits could be fully bright. Deposits with fine grains i.e. the grains having the difference in the height between the middle of the grain and the grain boundary, less than the wavelength of visible light (400 to 700,nm) and without crevices are bright. If there is a strong fibre axis, i.e. the same plane is essentially parallel to the surface in most grains, the boundaries between them would be expected to be shallow. When there is a strong fibre axis, the grains need not be very fine for a deposit to be bright. The banded structure is also generally observed in bright deposits but not all deposits showing the banded structure are fully bright.

CHAPTER 2

Part (2-1) Some Techniques for the study of Electrode Processes and Electrode deposit

Sect (2-1.1) Single Current Pulse Method

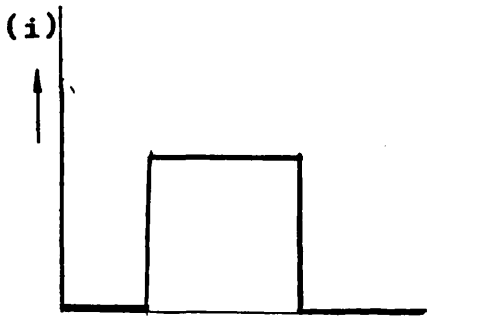

Fig (2-1)

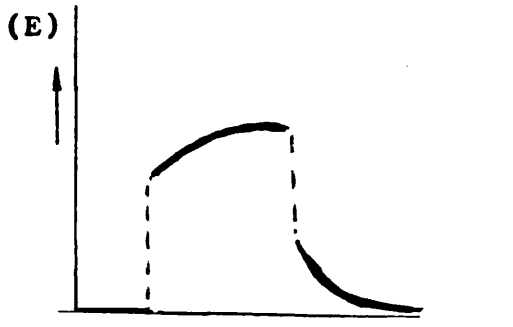

Fig (2-2)

This method is very useful for the study of kinetics of fast electrode reactions. (i.e. k_s up to 100 $cm\ s^{-1}$ [51]) A small rectangular current pulse (egg. ontime range of 0.5 ms to 50 ms used by Berzins and Delahay [51]) is used to stimulate a working electrode which is at equilibrium. The response of the working electrode during the passage of current is a change in potential as a function of time (t) fig (2-2)

The mathematical expression of η v.s. t, where η is the overpotential, is relatively complex even for a simple reversible charge-transfer process e.g.

$$O + ne \rightleftharpoons R \qquad E(2\text{-}1)$$

A linear relationship exists between η and $\sqrt{t}$ for a small displacement of potential from its equilibrium potential i.e. $\eta \ll RT/nF$ and $t > 5 \times 10^{-5}$s i.e. when the double layer charging current has become negligible. The relationship is shown as follows:-[52]

$$\eta = -\frac{RT}{nF}\left[\frac{1}{i_o} + \frac{2L}{nF}\sqrt{\frac{f}{\pi}} - RT\left(\frac{L}{nF}\right)^2 C_{dl}\right] i \qquad E(2-2)$$

with

$$L = \frac{1}{C_O^o\sqrt{D_O}} + \frac{1}{C_R^o\sqrt{D_R}} \qquad E(2-3)$$

C_{dl} = the double layer capacitance at the reversible potential.

i = Total Faradaic current.

C_O^o = Concentration in mol $/dm^3$ in bulk phase of O species.

i_o = Exchange current density.

D_O = Diffusion coefficient of species O

The exchange current density can be determined from the intercept at t = 0. The value of L can be obtained from the slope in the η vs. $\sqrt{t}$ plot.

The transfer coefficients cannot be evaluated using this method directly from a single transient but can be obtained from the dependance of the exchange current density on the concentration of O or R as shown in the equation below.

$$i_o = nFk_s C_O^{\alpha(1-\alpha)} C_R^{\circ\,\alpha} \qquad E(2\text{-}4)$$

Where k_s = rate constant, α = transfer coefficient. Thus α can be evaluated by varying the concentration of one of the reactants while the concentration of the other reactant is kept constant. The logarithm of exchange current density is plotted against the logarithm of the varying concentrations. Therefore α can be obtained from a straight line whose slope is either α or $1-\alpha$, depending which reactant concentrations are varried.

The main disadvantage in this method is that only a relatively small perturbation is permitted when E(2-2,p38) is to be used in the experimental calculation.

Thus this leads to lower signal-to-noise ratios and hence greater uncertainty in the measured kinetic parameters. The main advantage is that the experimental set-up is relatively simple and easy to correct for IR drop.[53]

Sect (2.1.2) **Potential Step Method:**

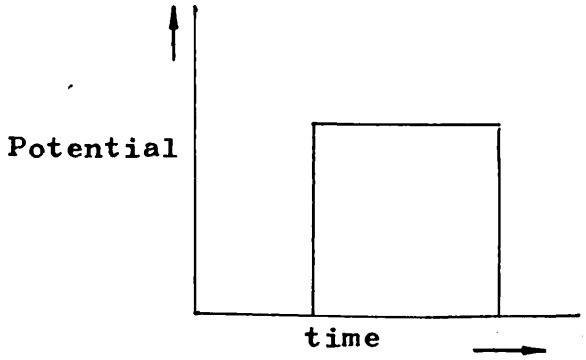

Fig (2-3)

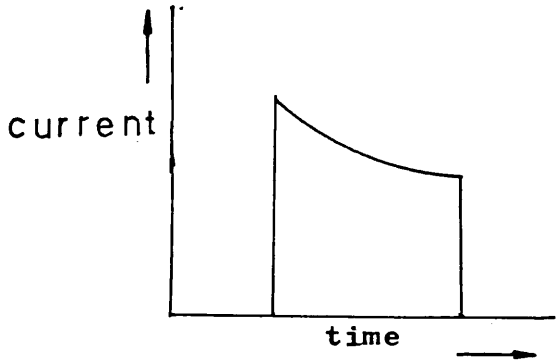

Fig (2-4)

In this method a potential step (Fig 2-3) is used to perturb an electrode which is in its equilibrium state and the resulting current is then measured as a function of time (Fig 2-4). The kinetic parameters can then be obtained using the current-time relationship.

The current-time and η equation is generally quite complicated, for example the current-time and η equation for the first order kinetics of the reaction (E2-1, p37) is as follows:[53]

$$i_f = i_o \left\langle \exp\left[-\frac{\alpha n F \eta}{RT}\right] - \exp\left[(1-\alpha)\frac{n F \eta}{RT}\right] \right\rangle A(t) \qquad E(2\text{-}5)$$

where $A(t) = \left[\exp(\lambda^2 t)\right] \operatorname{erfc}(\lambda t^{\frac{1}{2}})$ E(2-6)

and λ is a constant given by

$$\lambda = \frac{i_o}{nF}\left(\frac{1}{C_O^o\sqrt{D_O}}\exp\left[-\alpha\frac{nF}{RT}\eta\right] + \frac{1}{C_R^o\sqrt{D_R}}\exp\left[(1-\alpha)\frac{nF\eta}{RT}\right]\right) \qquad E(2\text{-}7)$$

where overpotential η is equal to the potential jump for small IR drop. The meanings of the symbols used are the same as those used in the single current pulse method.

Equation E(2-5,p41) indicates that the faradaic current density is equal to the value without diffusion control multiplied by a factor A(t). The factor A(t) considers the diffusion process and carries the value of time.

The io value of the reaction considered can be obtained easily with the aid of the monograms prepared by Oldham and Osteryoung[54] as shown on page (44). This is done by plotting the values of i_f v.s. $\sqrt{t}$ and from this a straight line is drawn through the points in the central portion of the curve. This straight line is then extrapolated to the Y-axis and the i_x value is obtained as shown in figure (2-5,p44).The ratio of i/i_x is then used to obtained the value of

$\frac{i_x}{io}$ from fig (2-6, p44). Thus io value can be evaluated using the value of i_x. The condition for the application of this method is $\frac{i}{io} \geqslant 0.9$ The value of α can be determined using the equation E(2-4, p39) This is carried out by plotting the values of log io with log C_O^o with a constant value of C_R^o . Therefore, the values of α can be evaluated.

The conditions for this process to be carried out efficiently are that the IR drop between working and reference electrodes must be small and for a short ontime step, correction of double layer charging is required.

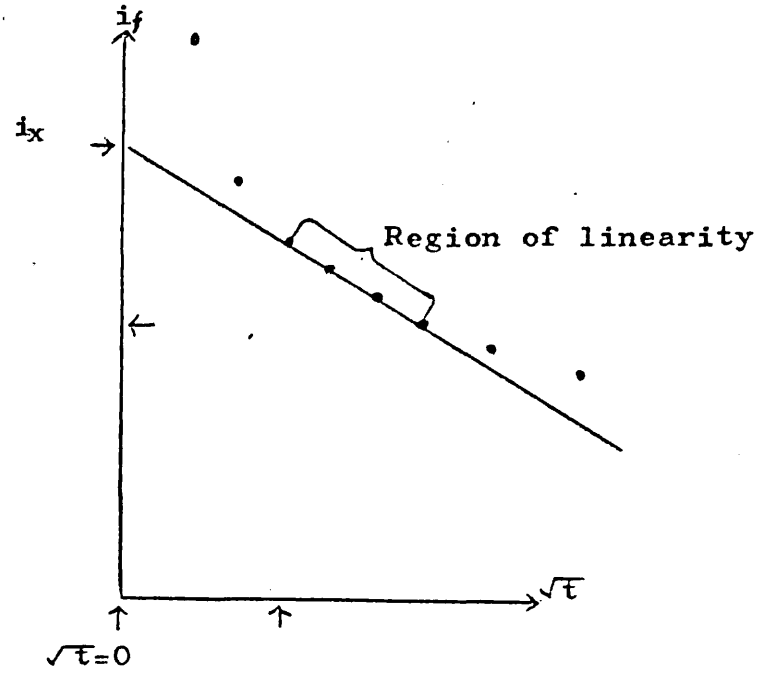

Fig (2-5). Typical chronoamperometric data points.

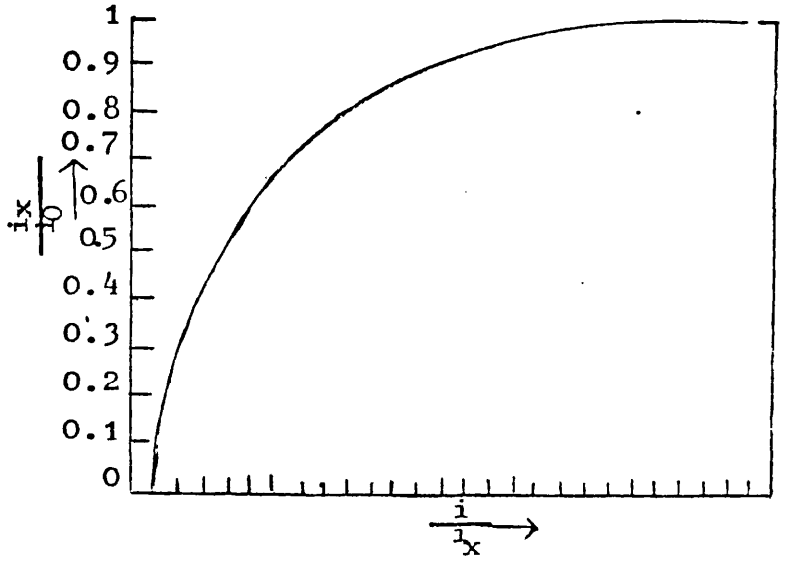

Fig (2-6) The curve shows i_x/i_0 as a function of i/i_x

Sect (2-1.3) Chronopotentiometry

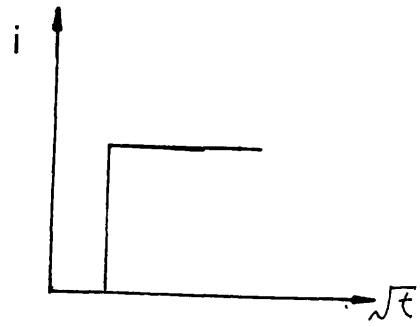

Fig (2-7)

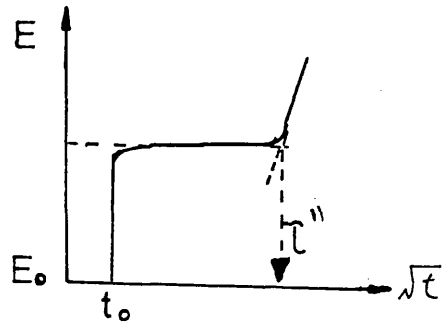

Fig (2-8)

This method uses a larger constant current pulse of longer duration (Fig $_{2-7}$) which will completely consume all the reactants at the electrode. A change of potential with time(t) is then studied and a typical chronopotentiogram obtained is shown in figure($_{2-8}$). The principal assumption of this method is that mass transport occurs only by linear diffusion under the influence of the concentration gradient.

The time required for the reactants to be completely reacted at the electrode is known as the transition time(τ'')[11]. The equation which relates

with concentration of the reaction of the reacting species O and the current density, for a plane electrode is as follows:[52]

$$\sqrt{\tau''} = \frac{nF\ C_O^o\ \sqrt{\pi Do}}{2i} \qquad E(2\text{-}8)$$

This method is relatively useful in evaluating the kinetic parameters for a one-step cathodic process with combined kinetic and diffusion control in which the back reaction is negligible for the following reaction:

$$O + ne \rightleftharpoons R \qquad E(2\text{-}9)$$

The relationship of the electrode potential with time after completion of double-layer charging is [52]

$$E = Eo + (RT/\alpha nF)(\ln[nF\ Co^o\ k_o\ /i\ ] + \ln\ [1-(\ t/\tau'')^{\frac{1}{2}}\ ]\ ) \qquad E(2\text{-}10)$$

Equation E(2-10) shows that the value of α can be obtained from the slope of the plot of E v.s. $\ln\ [1-(t/\tau'')^{\frac{1}{2}}\ ]$. Also with the known standard electrode potential, the standard rate constant of $[Ko \leq 10^{-4}\ cm\ s^{-1}]$ [53] can be determined.

This method can also be used to determine the extend to which reactants are adsorbed on the electrode surface. This is carried out by observing the number of transition times present on the potential v s. time plot. If both the adsorbed and diffusing species both undergo reaction at widely different potentials, two separate transitions times will be observed.

Sect (2-1.4) Methods for Measurement of Capacity at Electrode-Electrolyte Interfaces

There are a number of methods available for the measurement of double-layer capacitance (C_{dl}) on solid electrodes. The methods of measurement may be classified in two groups, namely, pulse methods and the alternating current method. Three pulse methods and one alternating current method will be described. A galvanostatic pulse method was used in this research.

Sect (2-1.4A) Square-wave pulse Method:

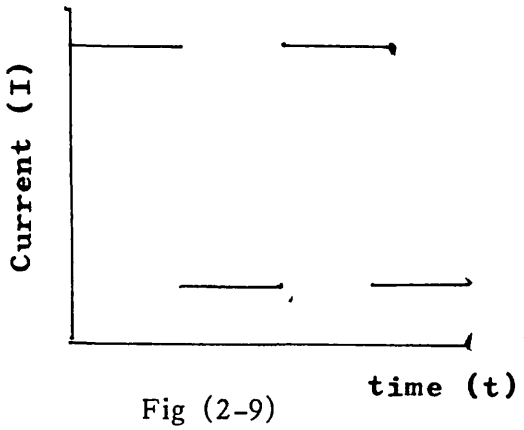

Fig (2-9)

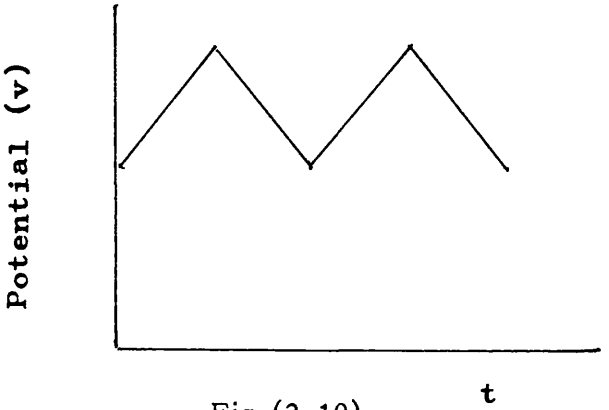

Fig (2-10)

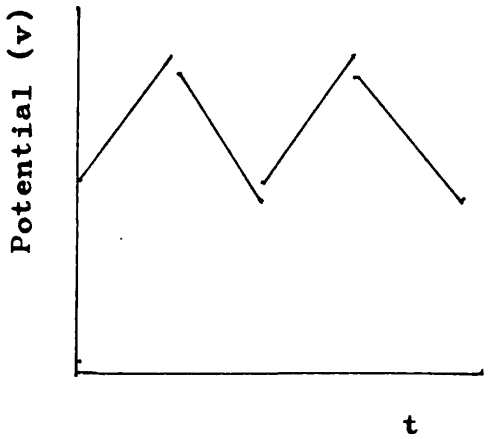

Fig (2-11)

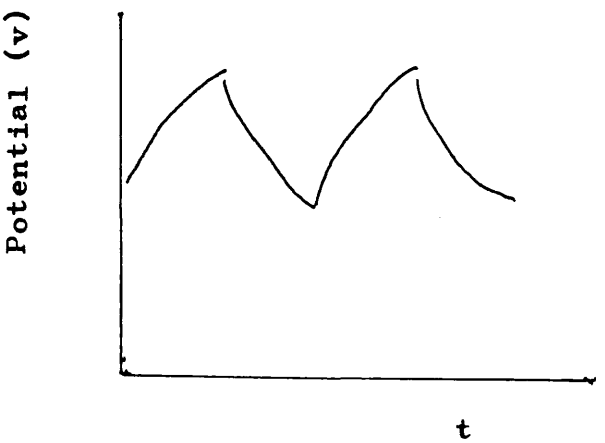

Fig (2-12)

The square wave pulse technique has been developed by Hackerman et al[63] and Cahan et al.[64] In this technique a repetitive constant current (I) square wave pulse is applied to the electrode (Fig. 2-9,p48). The direction of the current flow of the second half cycle is opposite to the first half cycle. The potential (V)-time response is varied under different conditions of the experimental set up. The potential-time response of figure (2-10,p48) if for the case when only pure double-layer capacitance of the electrode is measured. Figure(2-11,p48)shows the response of the case when ohmic potential (IR) drop is present in series which the double-layer capacitance. When faradaic current and ohmic drop are present, the response of this case is shown in figure (2-12, p48).

The value of the double-layer capacitance can be evaluated from the potential-time response of all three cases mentioned above. The linear portion of the slopes of the potential-time curves are used in conjunction with the applied known constant current, in the calculation of the values of the double layer

capacitance of the electrodes. The following equation is used in the calculation of the values of capacitance.

$$C = \frac{I}{dV/dt} \qquad E(2\text{-}11)$$

Sect (2-1.4B) **Triangular-Wave Pulse Method:**

Fig (2-13)

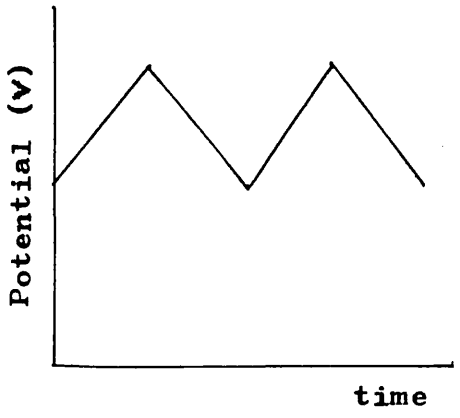

Fig (2-14)

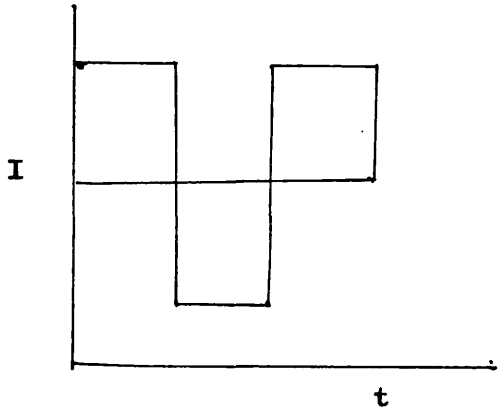

Fig (2-15)

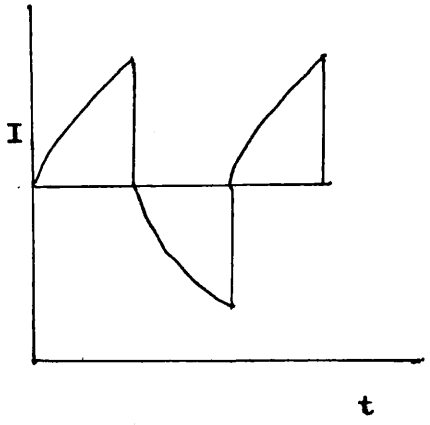

Fig (2-16)

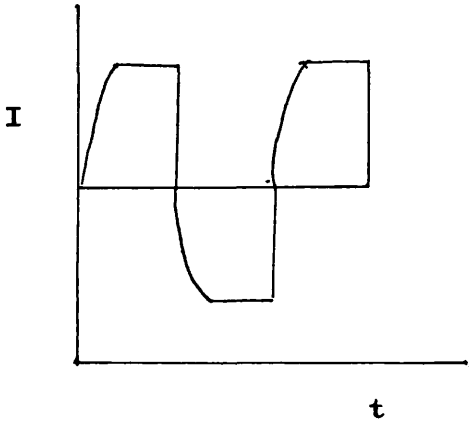

Fig (2-17)

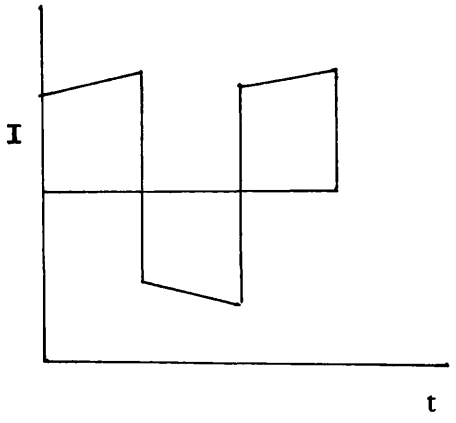

Gileadi et al [65,66] used this method to measure the double layer capacitance of a gold disk electrode in 10^{-3} mol dm^{-3} $HClO_4$ solution. A train of triangular wave pulse is applied on the working electrode. The frequency used is normally in the range of 10^2 - 10^4 cycles per second. The amplitude of voltage is from 1 to 20mV. The applied potential is increase from a lower potential to the peak potential in the first half of the cycle and decrease from the peak potential to the lower potential at the second half of the cycle (Fig. 2-13,p51)

Using the capacitance equation E(2-11,p50) the value of the double-layer capacitance can be evaluated when the current is measured. Alternatively, the response can be caliberated with known dummy capacitors since the square wave response is proportional to the current before the experiment. Thus during the experiment the values of the double-layer can be obtained directly from the caliberated screen or chart.

Four types of responses are shown in figures (2-14,p51) to (2-17,p51). Figure (2-14,p51) shows the response of only double-layer capacitance of the electrode. Figure(2-15,p51) shows the response of the double-layer capacitance in the preeence of ohmic drop of the electrode. In the system where the ohmic drop is compensated, the response of the double-layer capacitance of the electrode is shown in figure (2-16,p51). Figure (2-17,p51) shows the response of the double layer capacitance of the electrode when the ohmic drop is compensated and faradaic current is present.

The error due to the faradaic current in the measured capacity can be reduced by increasing the frequency and adjusting for optimum IR compensation. This error can be readily estimated using the following equation which relates the measured capacitance (Cm) to the true capacitance.

$$C = Cm \frac{im}{(1-p)\, i_{max} + P i_{min}} \qquad E(2\text{-}12)$$

Where P is the fraction of half-cycle during which sampling is made. i_{min} and i_{max} are the values of the current at the begining and at the end of the half-cycle, measured on a curve such as figure (2-17,p51)

Sect (2-1.4C) **Double Current Pulse Method:**

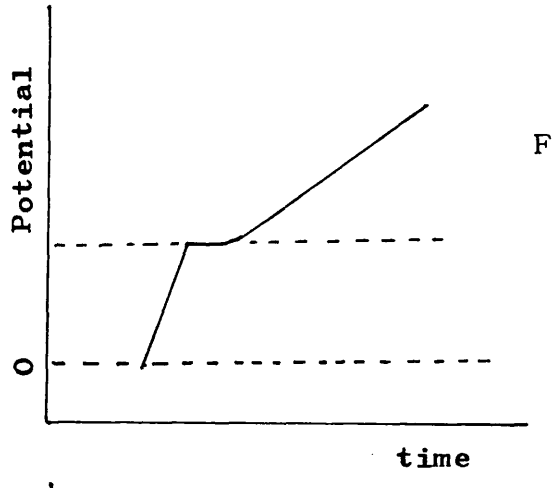

Fig (2-18)

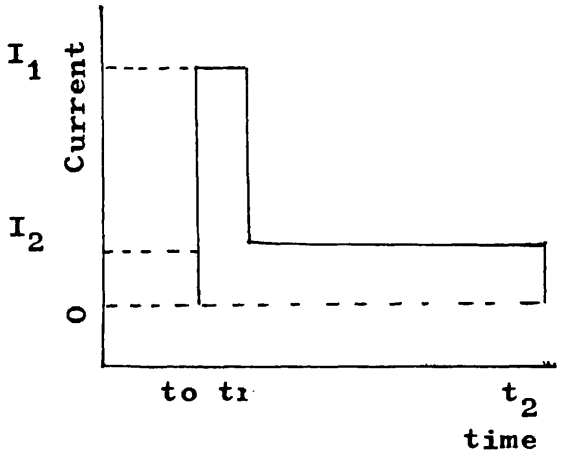

Fig (2-19)

Gerischer and Kruse[52] introduced the galvanostatic double pulse method in order to seperate diffusion overvoltage from charge-transfer overvoltage in the case of fast electrode processes.

Slaiman and Lorenz[8] in 1974, used this method to measure the double-layer capacitance and the adsorption capacitance (Cads) of copper-electrodes in acidified cupric sulphate solution.

In this method, two consecutive rectangular current pulses are used (Fig 2-19,p55). The first pulse is of a large current amplitude (I_1), and flows only for a short time t_1, e.g, 1-2 μs. This serves to charge rapidly the double layer. The amplitude and duration of the first pulse are adjusted so that the potential-time curve starts out flat at the begining of the second pulse ie $(dv/dt)_{t=t_1} = 0$. Once this is achieved, the slope of response of the first pulse (ie t = 0 to t = 1) is then due to the double layer charging with current I_1. Therefore, the double-layer capacitance is then calculated using the equation E(2-11, p50)

The slope of the potential-time curve of $t > t_1$, is then used to calculate the total values of the two capacitances (ie C_{dl} + Cads) as shown in the following equation.[8]

$$C_{dl} + Cads = \frac{I_2}{(dv/dt)_{t > t_1}} \qquad E(2\text{-}13)$$

As a result the value of the adsorption capacitance can then be evaluated.

Sect (2-1.5) **X-Ray Diffraction**

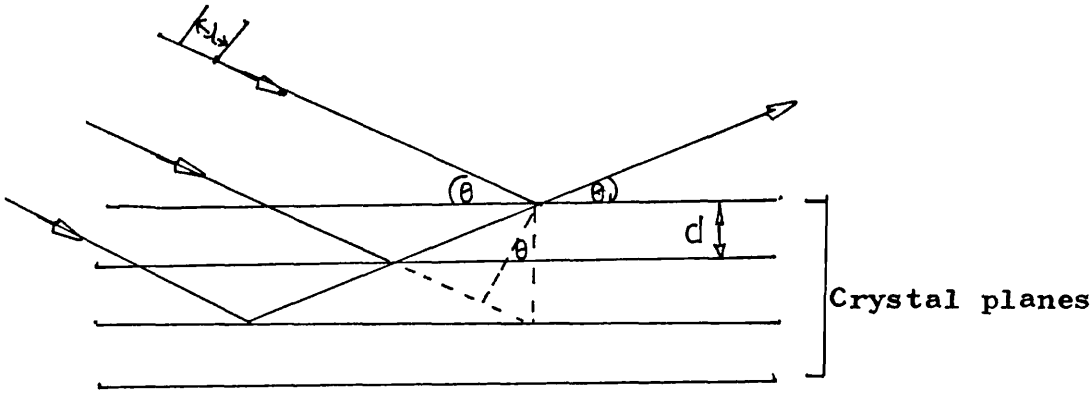

Fig (2-20)

X-ray diffraction (XRD) has been used in the structural studies of copper electrodeposit by various authors.[14,46,47] The mechanism of the "reflection" may be visualised by reference to fig (2- 20). The equation is used to determine the interplanar distance (d) of the crystal structure, through measurement of the angles (θ) at which x-rays are constructively

reflected from the cyrstal faces i known as the Bragg equation.[48]

$$n\lambda = 2\,d \sin\theta \quad E(2\text{-}14)$$

where (n= 1,2,3...) are called first, second...

...order reflections.

λ is the wavelength of the x-ray used.

The powder method is used to determine the interplanar spacings of crystalline powders. The Bragg equation is used in the calculation of the values of d.

The working principle of the powder method is that a beam of monochromatic x-rays is collimated by two pin holes in a lead sheet and this falls on the crystalline powder. The reflected rays normally have a shape of cones.

There are two different experimental arrangements that can be used in the powder method.[69] One of them involves the use of diffractormeter and the other involves the use of cylindrical camera when a diffractrometer is used. The specimen is shaped into a flat plate and is placed at the centre of rotation in the diffractrometer. A scanning chart recorder is used to record the reflected beam.

The powder is shaped into a cylinder when a cylindrical camera is used. A photographic film is used to record the reflected beams.

The x-ray pattern of the deposit obtained is then used to establish the orientation of the deposit and can also be used to identify the deposit.[68] Identification is carried out by comparing the calculated d spacings of the three most intense XRD pattern peaks with those d spacings values tabulated in the American J.C.P.D.S. Powder Diffraction File.

Sect(2-1.6) Atomic Absorption Spectrophotometry:

This technique is used for determining the concentration of an element in a sample by measuring the absorption of radiation in an atomic vapour produced from the sample at a wavelength that is specific and characteristic of the element under consideration. For example the wavelength of the most sensitive absorption line of copper is 324.75nm[70]

The atomic absorption spectrometer basically consists of a light source which generates a sharp

line spectrum, combustion chamber which converts the solution into atomic vapours, a monochromater which selects the resonance line to be measured a photo-multiplier and a chart recorder or digital display unit.[71]

The calibration curve of concentration against absorbance is obtained using the Beer-Lambert Law. According to this law, the absorbance (A) is proportional to the concentration of the analysed element. This law is followed within certain limits in atomic absorption spectrometry. The absorbance can be calculated as the inverse function of the transmission (T') of the flame.

$$A = \log 1/T' \qquad E(2\text{-}15)$$

For the evaluation of sample concentrations, the absorbance must be evaluated from the relation.

$$A = \log Io/I \qquad E(2\text{-}16)$$

Where Io and I are the indicator deflections corresponding to the pure solvent and sample respectively.

A standard working curve is normally plotted with the known concentration of standard solutions (x-axis) corresponding to the measured absorbance (Y-axis). This curve is then used in the determination of the unknown concentration of the solution of the same element.

Sect(2-1.7) Stereo Scanning Electron Microscopy:

The principle of the instrument is as follows. A primary beam of electrons from a heated element is focused into a fine beam and made to scan in a raster on the surface of interest. The electrons liberated from the surface by the beam are detected by scintillator -photomultiplier system. This is called the emissive mode. The resulting signals are used to modulate the brightness of a cathode-ray tube screen which is scanned in synchronism with the electron beam producing an image on the screen.

Scanning electron microscopes (S E M) have been used to study the morphology of copper deposits by some authors.[14,17,50] Micrographs (i.e.photography of the SEM image) of the deposit are usually taken during the

study of the morphology of copper deposits. The micrograph may be used in the calculation of grain size using the following equation:

$$\text{Actual grain size} = \frac{\text{Size of grain on micrograph}}{\text{magnification of micrograph}} \qquad E(2\text{-}17)$$

$$\text{where magnification of micrograph} = \frac{\text{Screen Magnification}}{\text{Constant}} \qquad E(2\text{-}18)$$

and constant is the ratio of screen size divided by micrograph size.

Sect (2-1.8) Cyclic Linear Sweep Voltammetry:

This technique has been used to measure the concentration of both the additive and the chloride content in different various types of copper bath by Tench and co-workers.[40-44]

In this method, the potential of the working electrode varies linearly with time at some known rate and the current is observed with respect to time.

The potential of the working electrode is scanned from an initial potential Ei to a second potential Er. At Er the direction of scan is,reversed and the potential swept back to Ei. This procedure can be repeated continuously if needed.

The cyclic voltammogram has a characteristic shape depending on the nature of the reaction.[45] Some examples are shown in figures (2-21 to 2-25,p65) It may be possible to predict the reaction mechanism from the cyclic voltammogram when used in conjunction with table (2-1,p66). The table contains the equations relating the peak potential (Ep) and peak current (Ip), with scan rate (ν).

Figure: 2-21

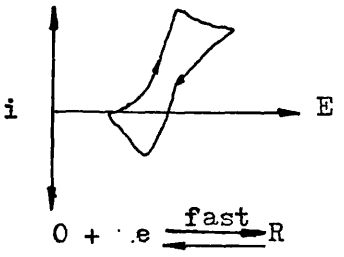

Fast reversible reaction

Figure: 2-22

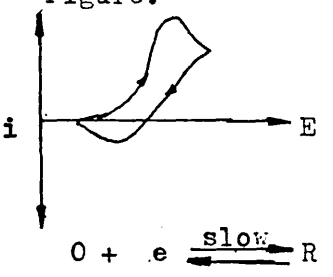

Slow reversible reaction

Figure: 2-23

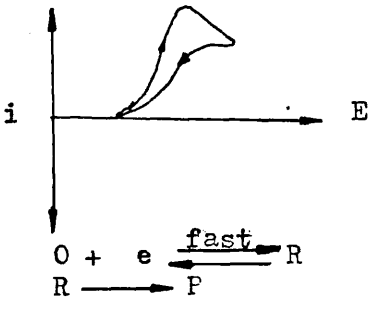

The Reversible reaction followed by a chemical reaction producing electroinactive P

Figure: 2-24

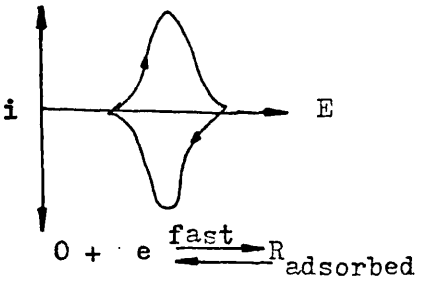

Fast adsorption reaction

Figure 2-25

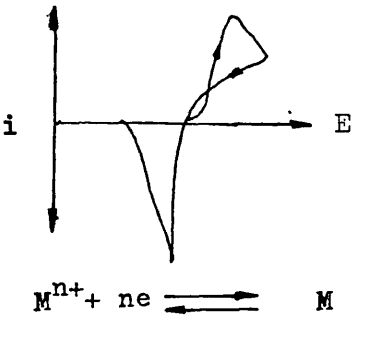

Reaction at inert electrode

Table: (2-1)

Cyclic voltammetry - diagnostic criteria for four illustrative mechanism. E_p=peak potietial, $E_{p/2}$=half peak potential, $\Delta E_p = E^f_p - E^b_p$, I_p = peak current density; superscripts f,b= forward and back reactions.

	$E^{\ominus}_p$(V)	ΔE_p(mV)	$E_p - E_{p/2}$(mV)	I_p^f	I_p^b/I_p^f
(a) $O + ne \underset{}{\overset{fast}{\rightleftharpoons}} R$	$E - \frac{0.029}{n}$	60/n	60/n	$I_p \propto \nu^{\frac{1}{2}}$	1.0
(b) $O + ne \overset{slow}{\rightleftharpoons} R$; $k^{\ominus}, \alpha$	Function k,α Shifts negative with ν $\frac{\partial E_p}{\partial \nu} = \frac{0.5RT}{\alpha nF}$ mV	Increases with ν. Function of $\nu, k^{\ominus}_a$	48/αn	$I_p \propto \nu^{\frac{1}{2}}$	1.0
(c) $O + ne \overset{fast}{\rightleftharpoons} R$; $R \xrightarrow{k} P$	Function of k. Shifts negative with ν $\frac{\partial E_p}{\partial \nu} = 30/n$ mV	Function of k	-	$I_p \propto \nu^{\frac{1}{2}}$	<1.0 Function of k,ν
(d) $O + ne \xrightarrow{fast} R_{ads}$	$E^{\ominus}$	0	-	$I_p \propto \nu$	1.0

Part (2-2) Fundamental Principles of Metal Deposition Processes.

Sect (2-2.1) Faradays's Law:

Electrodeposition is the process of depositing metals using an external source of current. On passing the current, the metal is deposited on the cathode. The process obeys Faraday's laws of electrolysis, which state that, the amount of chemical change produced by the electric current is proportional to the quantity of electricity passed. One mole of electrons (i.e. 1 Faraday or 96,490 coulombs) will produce $\frac{1}{2}$ mole of copper.

Sect (2-2.2) Overpotential

The deviation of the potential from the equilibrium value, when an external current flows through the electrode is called the overpotential and is expressed by: $\eta = \Delta\Phi - \Delta\Phi_e$ E(2-19)

where $\Delta\Phi$ is the potential difference across the interface through which a current density i is flowing. $\Delta\Phi_e$ is the equilibrium potential

difference (i.e. the potential difference where no current is flowing). Both $\Delta\Phi$ and $\Delta\Phi_e$ are absolute potentials which cannot be measured. To measure the overpotential a three electrode system has to be used i.e. a system consisting a working electrode, a counter electrode and a reference electrode. E_e is measurable and is the potential difference between the working and reference electrode when no current is flowing. E is measured as the potential difference between the working electrode and the reference electrode (assuming the ohmic potential drop is small) The overpotential is thus given by E-Ee.

The following are various types of overpotential which appear during the deposition process:

(1) Charge-transfer overpotential (η_{ct}), associated with the step involving charge transfer between the electrode and a molecule, ion, or atom.

(2) Crystallization overpotential (η_{cr}), which results from the energy barrier associated with incorporation of an atom into the crystal lattice of the electrode.

The sum of η_{ct} and η_{cr} is also known as the activation overpotential (η_a).

(3) Reaction overpotential (η_r) which is the result of a chemical reaction and is independent of the electrode potential. This overpotential when it is rate determining, hinders the current flow.

(4) Diffusion overpotential (η_d). This is associated with the rate-determingin mass transport of reactants from the bulk to the interphase. The sum of the reaction and diffusion overpotentials is sometimes known as the concentration overpotential η_c. The sum of the four overpotentials gives the total overpotential.

(5) Ohmic overpotential (η_Ω) this is introduced in the measurement of overpotential. This overpotential equals the IR drop across the surface film on the electrode or within the electrolyte.

Sect (2-2.3) Equilibrium exchange current density io:

In the study of electrode reactions, it is important to obtain the equilibrium exchange current density io values. A high value of io for a metal deposition process means that the metal can be deposited with little polarization. The io is decreased by the

presence of absorbed impurities or 'addition agents' since they interfere with the deposition process. In a multistep reaction, the step with the smallest io value generally determines the overall current. This is because the smaller the io is for the step, the lower is its conductivity.[79]

The io value is generally concentration dependent at constant η. Thus an equation can be obtained based on this property and this equation can be used to determine the electrochemical reaction order[79] of the charge transfer reaction.

$$\text{Picath} = \left(\frac{\partial \log io}{\partial \log Co}\right)_{C_{R\neq 0}} - \frac{a_{cF}}{RT}\left(\frac{\partial \Delta\Phi_e}{\partial \log Co}\right)_{C_{R\neq 0}} \qquad \text{E(2-20)}$$

where Picath is the order of the cathodic reaction of the reactant R. The drawback in this method is that it is necessary to know the overall reaction so that it is possible to determine the concentration dependence of the reversible potential on the concentration of a given species.

Sect (2-2.4) **Symmetry Factor**

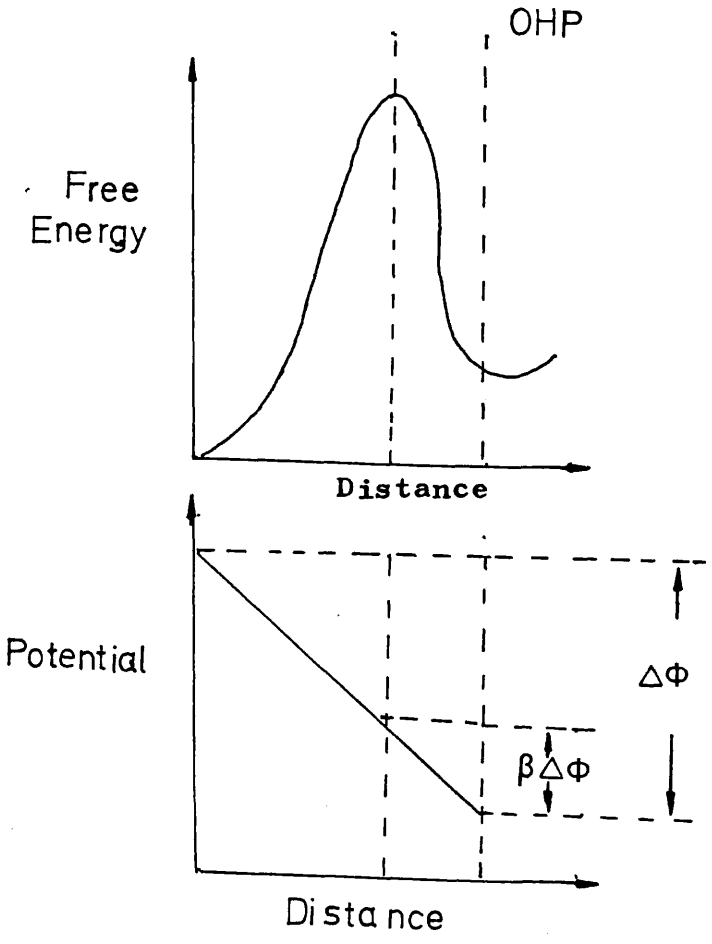

Fig: (2-26)

Fig:(2-27)

In the cathodic charge transfer reaction, the ion moves across the double layer from the solution side of the interface to the metal electrode. When the energy of the ion passes the summit of the energy barrier (Fig: 2-26). The summit has been lowered by the electrical work done, i.e. part of the total potential difference (i.e. from OHP to the summit) Fig 2-27 multiplied by the charge. Thus the symmetry factor β

$(0 < \beta < 1)$ is used in describing the amount of electrical work (i.e. $\beta \Delta\Phi F$) (Fig 2-27,p71)by which the energy barrier for the ion-to-electrode is lowered. Also β can be expressed as:

$$\beta = \frac{\text{Distance across double layer to summit}}{\text{Distance across whole double layer}} \qquad E(2\text{-}21)$$

Using a different approach where β is shown to be depended on the relative slopes of the potential-energy-distance curves, the definition of β obtained is[80]

$$\beta = \frac{\Delta E^{\neq}}{\eta F} \qquad E(2\text{-}22)$$

or

$$= \frac{\text{change of activation energy}}{\text{change of electrical energy}} \qquad E(2\text{-}23)$$

The symmetry factor was shown to represent the fraction of the input electrical energy by which the electrical part of the activation energy decreases. The decreases in activation energy mean an increases in the net rate of reaction. The practical significance of this can be seen when electrical energy is used in

direct synthesis of compounds. In this case the value of β determines how much change of rate of production of a substance will take place when the potential of a electrode is changed for given concentration of reactant.

Sect (2-2.5) Transfer Coefficient:

During electrodeposition, the excess negative potential increases the rate of transfer of metal ions across the double layer to the electrode where they get deposited. At the same time, it diminishes the rate of metal dissolution at the cathode. The extent to which the applied excess potential is effective in accelerating the deposition process at the cathode, as compared to that which slows the dissolution process is expressed by a fraction called transfer coefficient α .

For a single step and single electron process the value of α is the same as symmetry factors. For a multistep cathodic electrodeposition process, α is written as[79] $\alpha_c = \frac{\gamma_c}{\nu'} + r'\beta$ E(2-24)

where γ_c = number of electrons transferred preceding the rds for the cathodic process.

ν' = stoichiometric number of the reaction.

r' = a factor of the rds, when the rds is a charge-transfer step, r = 1 and when

the rds is a chemical step, r = 0.

Sect (2-2.6) Butler Volmer Equations:

The dependence of overpotential on current density for a one step, single-electron electrode reaction controlled by the charge transfer step is given by the Butler-Volmer equation.

$$i = i_o \left[\exp(1-\beta)\eta F/RT - \exp(-\beta)\eta F/RT \right] \qquad E(2\text{-}25)$$

The equation below is the general form of the Butler Volmer equation. This is also valid for a multistep overall electrode reaction. The reaction may be electron transfers in steps other than the rds and also the rds may have to occur η number of times per occurence of the overall reaction.

$$i = i_o \left[\exp -\alpha_c F\eta/RT - \exp \alpha_a F\eta/RT \right] \qquad E(2\text{-}26)$$

From equations (2-25)and equation (2-26) it can be seen that the transfer coefficients (α) play the same role in a multistep, η-electrons transfer

reaction as the β does in the single step, one electron charge-transfer reaction. That means the values determine how the input electrical energy ($F\eta$) affects the reaction rate.

Sect (2-2.7) Tafel Equation:

The theoretical rate equation (E2-26,p75) that is

$$i=i_o \left[\exp\left(\frac{-a_c F \eta}{RT}\right) - \exp\left(\frac{a_a F \eta}{RT}\right)\right] \qquad E(2-27)$$

where i_o, α , T and etc have their usual meaning and are defined in the appendix (p 303).For an activation overpotential which is more than -50mV, the deplating is negligible. Therefore, the second term of equation E(2-27) can be neglected and i can be written as

$$i = i_o \left[\exp\left(\frac{-a_c F \eta}{RT}\right)\right] \qquad E(2-28)$$

On rearranging,

$$\eta = \frac{RT}{a_c F} \ln i_o - \frac{RT}{a_c F} \ln i \qquad E(2-29)$$

Let $A = \frac{2.303RT}{a_c F} \log i_o$ E(2-30) $B = \frac{-2.303RT}{a_c F}$ E(2-31)

The Tafel equation is thus derived i.e.,

$$\eta = A + B \log_{10} i \qquad E(2-32)$$

Sect (2-2.8) **The Potential Time Transient At Constant Current Density:**

A constant current transient technique can be used to determine the rate determining step (rds) of a metal deposition process. A quantitative treatment involving the time variation of the overpotential and the rate determingin step in electrodeposition for a one electron process[67] is described as follows:

The total constant current density during the transient in this case is

$$i = i_{dl} + i_{ct} \qquad E(2\text{-}33)$$

and the current density for charging the double layer is determined by the capacity of the interface which is equal to

$$i_{dl} = C_{dl} \frac{d\eta_t}{dt} \qquad E(2\text{-}34)$$

In the charge-transfer step of the deposition reaction, ions from the OHP can only land on areas which are not already occupied. Hence,

$$i_c = FK_c (1 - \theta_t) C_M{}^{n+} \exp(-\beta F \Delta\Phi_e/RT) \exp(-\beta F \eta_t/RT) \qquad E(2\text{-}35)$$

multiplying E(2-35) by $\frac{(1-\theta_e)}{(1-\bar{\theta}_e)}$ and re-arranging the equation, the new expression of i_c can be written as

$$i_c = i_o \frac{1-\theta_t}{1-\theta e} \exp -\beta F\eta_t /RT \qquad E(2-36)$$

Assuming that both the fractions of surface covered by adions θ_c and θ_e are much less than unity.

$$i_c = i_o \exp -\beta F\eta_t/RT \qquad E(2-37)$$

The anodic current density depends on the average adion concentration and overpotential at the time t, in the following way,

$$i_A = F\ K_A\ \bar{C}_t \exp\left[(1-\beta)F\Delta\Phi_e/RT\right] \exp\left[(1-\beta)F\eta_t/RT\right] \qquad E(2-38)$$

$$= \left\{F\ K_A C_o \exp\left[(1-\beta)F\Delta\Phi_e/RT\right]\right\} \frac{\bar{C}_t}{C_o} \exp\left[(1-\beta)F\eta_t/RT\right] \qquad E(2-39)$$

The term in square bracket is the io. Hence,

$$i_A = io\ \frac{\bar{C}_t}{C_o} \exp(1-\beta)F\eta_t/RT \qquad E(2-40)$$

Since $i_{ct} = i_c - i_A$ E(2-41)

$$i_{ct} = io \exp -\beta F\,\eta_t/RT - i_o \frac{\bar{C}_t}{C_o} \exp(1-\beta)F\eta_t/RT \qquad E(2-42)$$

Considering small departures of overpotential from equilibrium, the exponentials can be linearized. Therefore,

$$i_{ct} = io\left[1+ (-\beta F\eta_t/RT)-\bar{C}_t/C_o\left\{1+ (1-\beta)F\eta_t/RT\right\}\right] \qquad E(2-43)$$

$$\text{or} \quad i_{ct} = io\left[(\bar{C}_t-C_o)/C_o+F\eta_t/RT\left\{\bar{C}_t/C_o(1-\beta)+\beta\right\}\right] \qquad E(2-44)$$

Also for small departures from equilibrium $\bar{C}_t/C_o \simeq 1$

Thus $\bar{C}_t/C_o\ (1-\beta)+\beta \simeq 1$ E(2-45)

As a result,

$$i_{ct} = io\left[\frac{\bar{C}_t-C_o}{C_o} - F\eta_t/RT\right] \qquad E(2-46)$$

Using the expressions E(2-34,p78) for i_{dl} and E(2-45) for i_{ct}, in equation E(2-33,p78) the constant current density switched on at t = 0 is given by

$$i= C_{dl}\frac{d\eta_t}{dt} + i_o\left[\frac{\bar{C}_t-C_o}{C_o} - F\eta_t/RT\right] \qquad E(2-47)$$

Sect (2-2.9) The Time Variation of The Overpotential When the Charge-transfer Step is Rate Determining.

In the case when the rate determining step is charge transfer, $C_t \simeq C_o$ [75]. Thus, from E(2-47,p80) the total current density in this case is

$$i = C_{dl} \frac{d\eta_t}{dt} - i_o F\eta_t/RT \qquad E(2\text{-}48)$$

Also using the low field law for rate determining charge transfer, at $t \longrightarrow \infty$ when the steady state overpotential η_∞ is obtained, the following relations holds:[74]

$$\eta_\infty = -RT/F \times i/i_o \qquad E(2\text{-}49)$$

On combining this relation with E(2-48)

$$-\left(\frac{d\eta_t}{dt}\right) = Fi_o/C_{dl}\, RT \times (\eta_\infty - \eta_t) \qquad E(2\text{-}50)$$

The negative sign indicates that the overpotential decreased with time (i.e. cathodic deposition process). This sign is not included in the integration of E(2-50)

Let $$\tau = \frac{C_{dl}\, RT}{Fi_o} \qquad E(2\text{-}51)$$

Substituting E(2-51) into E(2-50)

and rearranging gives

$$\frac{d\eta_t}{(\eta_\infty - \eta_t)} = \frac{1}{\tau}\, dt \qquad E(2\text{-}52)$$

Integrating equation E(2-52,p81) gives

$$-\ln (\eta_\infty - \eta_t) = \frac{t}{\tau} + K \qquad \text{E(2-53)}$$

where K is a constant, At $t=0$, $\eta_t = 0$

$$K = -\ln \eta_\infty \qquad \text{E(2-54)}$$

Substitute K into equation E(2-53) and rearranging, the result is

$$\ln \frac{\eta_\infty}{\eta_\infty - \eta_t} = \frac{t}{\tau} \qquad \text{E(2-55)}$$

Thus, the variation of the overpotential with time is given by

$$\eta_t = \eta_\infty (1 - \exp -t/\tau) \qquad \text{E(2-56)}$$

This equation is valid when $\beta \eta_t F/RT \ll 1$.

It is also of the same form as the equation describing the time variation of potential difference V_t across a parallel capacitor-resistor net-work when it is charged with a constant current

$$V_t = V_\infty (1 - \exp -t/\tau') \qquad \text{E(2-57)}$$

In the case of condenser charging, the rise time is defined as the time at which the magnitude of the exponent in the exponential term is equal to unity.[75]

Setting $t/\tau' = 1$ in equation E(2-57) implies that

$$\frac{V_t}{V_\infty} = 63\% \qquad \text{E(2-58)}$$

By adopting a similar criterion in the case of the buildup of the overpotential in the metal-deposition process, from equation E(2-56,p82) that

$$\frac{\eta_t}{\eta_\infty} = 63\% \qquad \text{E(2-59)}$$

When $t = \tau$

$$= RT\, C_{dl} / Fi_o \qquad \text{E(2-60)}$$

Sect (2-2.10) **The Time Variation of the Overpotential when the Surface Diffusion Step is Rate Determining:**

When the r d s is surface diffusion, then

$$\bar{C}_t = C_o \quad \text{and} \quad \left(\bar{C}_t - C_o\right) / C_o \neq 0 \qquad \text{E(2-61)}$$

Also when the time considered is longer than the time for charging the double layer, the double layer current can be considered virtually zero. Therefore, under these conditions, the total constant current density derived from E(2-47, p80) in this case is

$$i = io \left(\frac{\bar{C}_t - C_o}{C_o} - \frac{F \eta_t}{RT} \right) \qquad \text{E(2-62)}$$

The expression for the average adion concentration at any time t is given as[75]

$$\bar{C}_t - C_o = i/K_p F \left(1 - \exp -K_p t \right) \qquad \text{E(2-63)}$$

where kp is the proportionality constant.

Substituting equations E(2-63) into E(2-62) the result is

$$\eta_t = \frac{RTi}{F^2 K_p C_o} \left(1 - \exp -K_p t\right) - \frac{RT}{F} \frac{i}{i_o} \qquad \text{E(2-64)}$$

When t is approaching infinity, the overpotential is at steady state i.e. η_∞ . Using equation E(2-64) the expression for η_∞ is,

$$\eta_\infty = \frac{RT}{F^2}\frac{i}{K_p C_o} - \frac{RT}{F}\frac{i}{i_o} \qquad E(2\text{-}65)$$

Expanding equation E(2-64) and substitute E(2-65) into the expanded equation gives

$$\eta_t = \eta_\infty - \frac{RT}{F^2}\frac{i}{K_p C_o}\left[\exp -K_p t\right] \qquad E(2\text{-}66)$$

or

$$\ln(\eta_t - \eta_\infty) = -\ln\left[\frac{RT}{F^2}\frac{i}{K_p C_o}\right] - K_p t \qquad E(2\text{-}67)$$

This is the basic equation for the time variation of the overpotential, assuming that the deposition consists of a two-step charge-transfer plus a surface-diffusion reaction and the rate-determining surface diffusion is under near-equilibrium conditions.

Sect(2-2.11) The Mechanism of the Electrogrowth of Metals

The description of the electrogrowth of metals can be divided into two sections. The first concerns the path taken by an ion from a position in the bulk of the solution unitl it reaches a growth site and is incorporated into the crystal lattice (i.e.the process of deposition). The second concerns the process of electrolytic crystal growth.

(A) The Process of deposition

Fig (2-28)

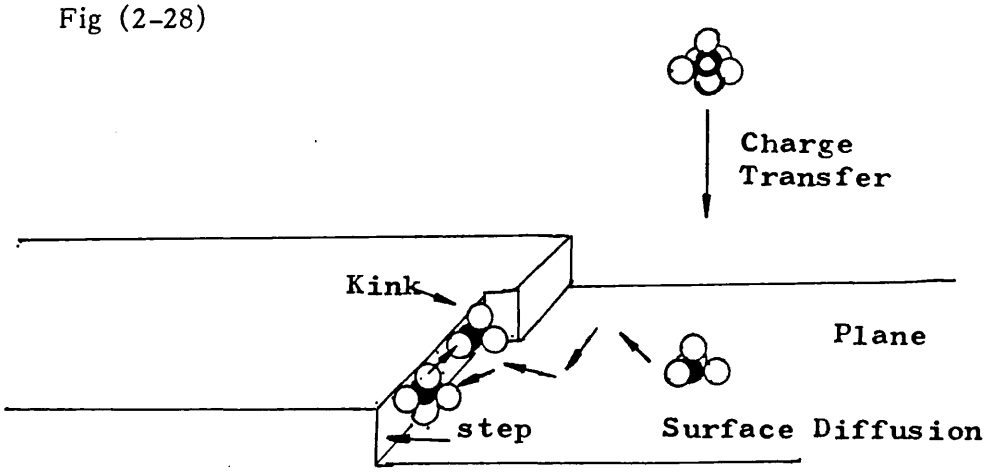

Consecutive stages involved in the Incorporation of an Ion at Kink Site.

The first step in the depostion process is that

the hydrated metal ion at the (OHP) acrosses the electrified interface, i.e. the charge transfer reaction.

The hydrated ion is then landed on a plane on the cathode which is the most favorable site. This is because there are more plane sites than the other sites such as holes, kinks, and steps. Also crossing over to a plane sites requires the minimum amount of distortion in the metal ion-water complex and hence the minimum energy change from this source.

After having landed on the plane, the partially hydrated adion must lose its water molecules in order to be incorporated into the metal lattice. This is carried out by surface diffusion from the smooth plane to a step, where it loses one more water molecule, and then move along the step to a kink site where another water molecule is lost, (Fig 2-28, p86) The process continues with further replacement of water molecules by coordinating metal atoms until,

finally, the series of actions ends when this 'ion', now without water molecules, gets embedded in the lattice.[67]

(B) The Process of Electrolytic Crystal Growth

As more and more adions get incorporated into a microstep, the step grows and advances. The step might be present originally at the emergence points of screw dislocation or due to other defects or might be formed by two-dimensional nucleation (i.e. adions condense together without random walking separately to steps).

If in the course of the step growth; it encounters adsorbed impurities, then further progress is stopped and a new microstep is formed over the older one. This may be repeated several times leading to the bunching of microsteps into a macrostep (Fig 2-29,p 91).The lateral growth of the deposit proceeds from various centres until the neighbouring lattices meet. The crystals which touch each other in a continuous fashion

to make up a metallic body are called grains.

In an early stage of electro-crystallization, the deposit tends to grow parallel to the substrate, this is known as epitaxial growth or 'paralled' growth. In prolonged electrodeposition, regardless of the type and nature of the starting substrate (e.g. various faces of a single crystal), a polycrystalline deposit will always form. In a polycrystalline deposit the orientation of each grain can be specified by giving the angles formed by the crystallographic directions of the crystal and the axes of a reference system fixed with respect to the macroscopic substrate. If one axis in all the crystallites is fixed relative to the substrate and the other two axes are randomly oriented then the polycrystal is said to have a preferred orientation. If all the three axes are randomly oriented then the polycrystal is said to exhibit random orientation.

There are several types of growth (i.e. also known as structural forms) of electrodeposits.Layer-type

structure is that most frequently observed and may have regular (Fig 2-30,p92)or irregular (Fig 2-31,p92) shapes. The block structure, or cubic layer formation, which may be regarded as a limiting case of the layer (Fig 2-32,p92), is also observed in electrodeposition. The ridge type of structure (Fig 2-33,p92) has been observed on copper electrodeposits. Pyramidal forms of growth are also often observed in copper electrodeposits[14,13] (Fig 2-34,p93). Apart from the above, other less frequently observed types of growth are spiral (Fig 2-35,p93),dendrites (Fig 2-36,p93)and cauliflowers.[10](Fig 2-37,p93). This classification is based on the visible surface topography of the electrodeposits. Several of these forms have been observed during copper deposition described in this thesis.

Fig: 2-29

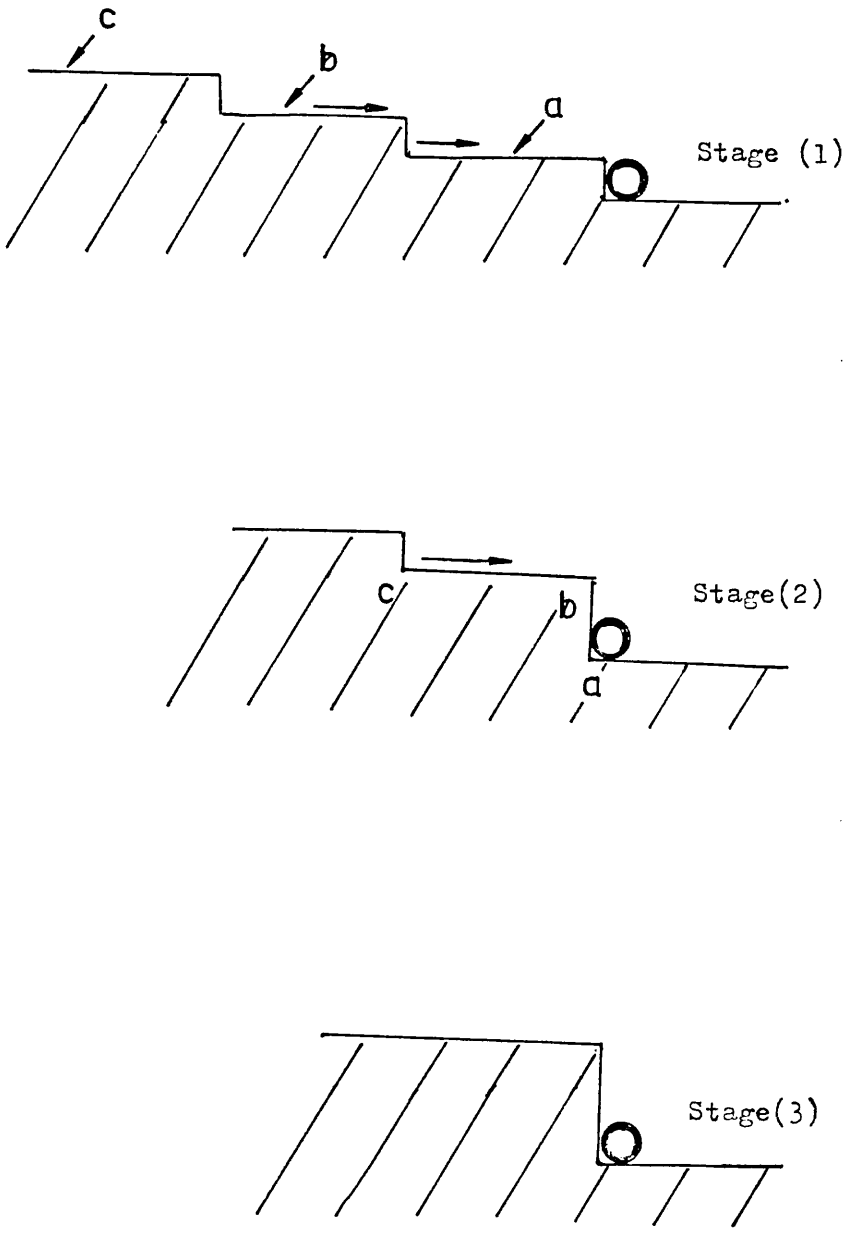

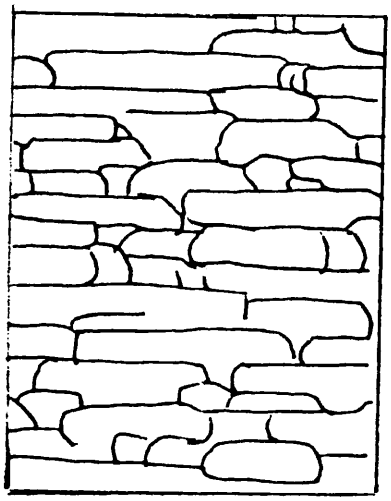

Fig (2-30)

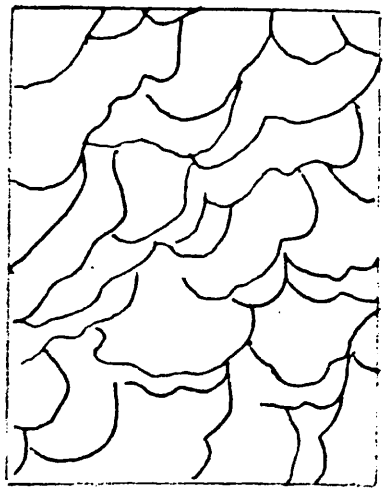

Fig (2-31)

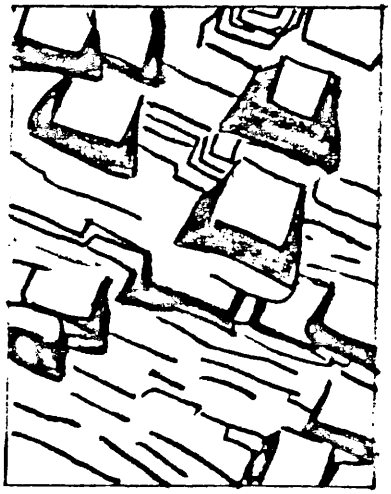

Fig (2-32)

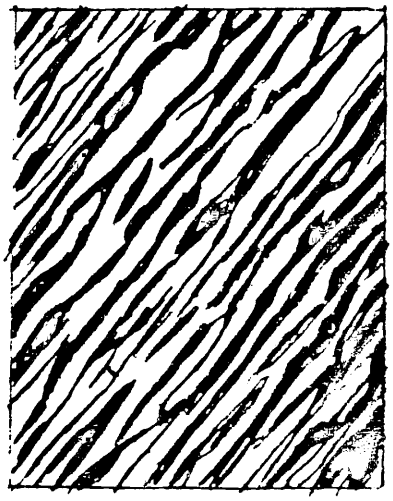

Fig (2-33)

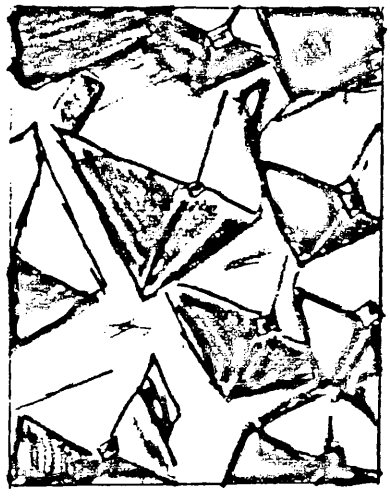

Fig (2-34)

Fig (2-35)

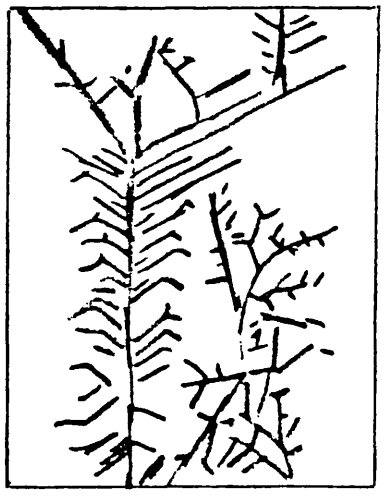

Fig (2-36)

Fig (2-37)

Sect(2-2.12) The Electrical Double Layer

Electrical double layers are found in nature wherever one has systems containing mobile charges, such as electrons, ions or orientable dipoles. These mobile charges distribute themselves under the combined influence of diffusion and potential gradients. The principal significance of double layers, wherever they occur is that they produce potential barriers which may strongly assit or inhibit the motion of charged species across their dimensions. Consequently, double layers often are the deciding factor determining the rate of an electrode reaction, influencing adsorption equilibria and establishing the electrical nature of a contact between dissimilar materials.

For a metal-solution interface, the first row of the electrical double layer of the charge metal electrode is largely occupied by water molecules which are dipoles. They orientate according to the charge on the electrode. When the electrode is highly positively charge, most of the water dipoles tend to 'flip up' so that the oxygen atoms are in contact with the electrode. The hydrogen end of the water points into the solution (fig 2-38,p96). When it is highly negatively charged the flipped up dipoles tend to turn around and are in a 'flopped down' state. Now the hydrogen ends are facing the electrode and the oxygen atom is toward the solution (fig 2-39,p96). Under these conditions there will be more flopped down dipoles than flipped up dipoles.

In addition to polar water molecules neutral organic molecules, e.g. organic additives also often get adsorbed on the electrode surface and form part of the double layer structure.

The charged electrode attracts ions carrying an opposite charge (or same charge as in the case of contact adsorption). These ions are held near the metal surface by an electrostatic force. In the absence of any contact adsorbed ions in the first row of the electrical double layer, excess charges exist both on the metal layer and in concentrated solutions on the outer layer of hydrated metal ions. This layer is referred as Outer Helmoholtz layer. The imaginary plane passing through the centre of the hydrated metals ions is called the outer Helmoholtz plane OHP (fig 2-40,p96). The first row is often occupied by some contact-adsorbing ions. As a result a new layer of excess charge between the metal electrode and the OHP is formed. The imaginary plane of these new layer of contact adsorbing ions is called the inner Helmoholtz plane IHP. Thus the double layer is no longer a double layer but a triple layer (fig 2-41,p96) and they behave like two capacitors connected in series. Therefore, the presence or absence of contact adsorption must influence the property of the interface for the storing charges i.e the capacity of the interface[77].

It is believed that when the water molecules on the surface of the electrode are not strongly attracted, the organic molecules present tend to replace them on the surface and vice versa[77].

Fig (2-38)

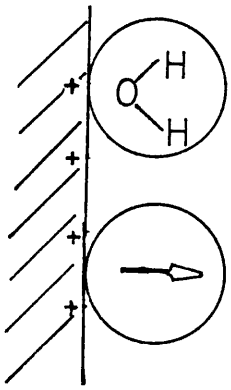

Fig (2-39)

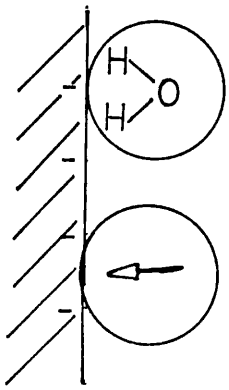

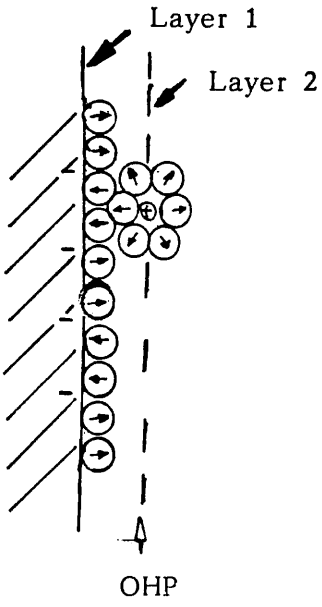

Fig (2-40)

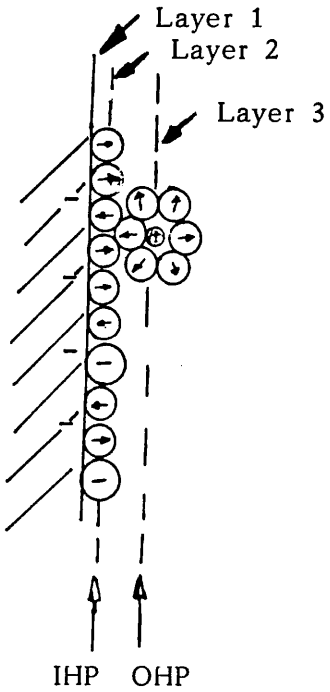

Fig (2-41)

The significance of this behaviour is that when the metal electrode is highly negatively or positively charged, the water molecules will be tightly held with their hydrogens or oxygen respectively on the surface (fig 2-42,44,p99). Therefore, few organic molecules can adsorb under such conditions. The condition at which the organic molecules will be tightly held (and thus more numorous) by the electrode is at the potential of zero charge (PZC). It has been reported that for copper electrode the PZC is 0.11 Volt vs SCE in an electrolyte consisting of 0.03 mol dm^{-3} copper sulphate and 0.05 mol dm^{-3} $Na_4P_2O_7$[78] .

There are three commonly known theories which describe the structure of the ionic double layer i.e. the arrangement of charges at an electrifiled interface. The first is the Helmoholtz-Perrin theory.They regarded the behaviour of the'double layer' of charges on the surface and those in solution as approximately to that of a parallel-plate condenser(fig 2-45,p100) having an electrical capacity C. Based on their model the equation which describes the relation between the excess charge density(q_M) on the electrode and the potential difference (V) across the double layer is

$$dV = \frac{4\pi d}{\varepsilon} \, dq_M \qquad E(2\text{-}68)$$

$$\frac{dq_M}{dV} = \frac{\varepsilon}{4\pi d} = C \qquad E(2\text{-}69)$$

Figure (2-46,p100) shows the Gouy-Chapman model of the double layer. The Gouy-Chapman point charge diffuse layer model theory describes the variation of capacity with potential. The Helmoholtz-Perrin theory does not predict such variation and the equation which predicts such variation is [99]

$$C = \frac{-dq_d}{d\Psi_M} \qquad E(2\text{-}70)$$

$$C = \left(\frac{\varepsilon z^2 e_o^2 n^0}{2\pi kT}\right)^{\frac{1}{2}} \cosh \frac{z e_o \Psi_M}{kT} \qquad E(2\text{-}71)$$

The above equation predicts that the differential capacity should show an inverted parabola dependence on the potential across the interface. In very dilute solution (0.001M) and at potentials near PZC, there are portions of the experimental curves which suggests that the interface behaving in a Gouy-Chapman way[99].

According to Stern there are two regions of charge separation (fig 2-47,p100). The first region is from the electrode to the Hemholtz plane. The second region is from this plane of fixed charges into the heart of the solution where the net charge density is zero. Therefore, this implies that there are two potential drops. The equation derived from Stern theory is[99].

$$\frac{1}{C} = \frac{1}{C_H} + \frac{1}{C_G} \qquad E(2\text{-}72)$$

where C_H is the Helmholtz-Perrin capacity

C_G is the Gouy-Chapman or diffuse charge capacity.

Fig (2-42)

(a) Negatively- charged electrode with excess of flopped-down dipoles.

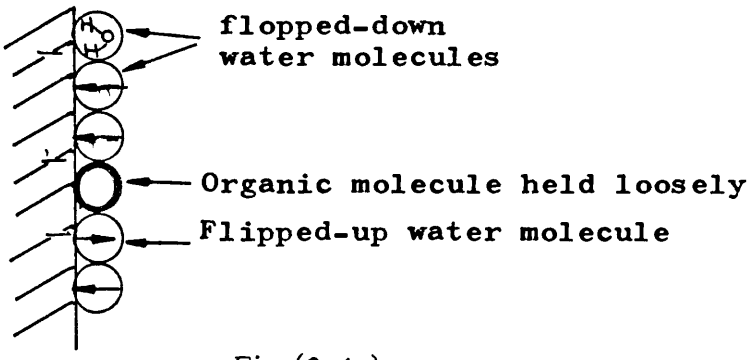

Fig (2-43)

(b) Uncharged electrode with equal numbers of flipped and flopped dipole.

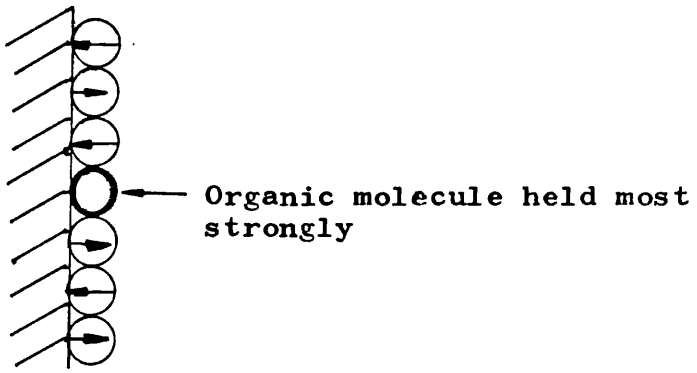

(c) Postively - charged electrode with excess of flipped-up dipoles.

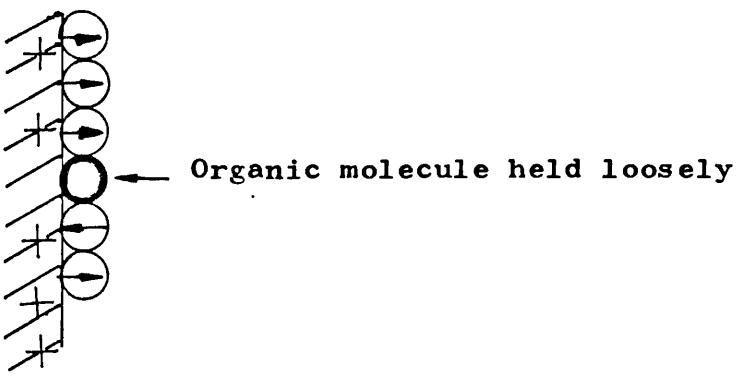

Fig (2-44)

Fig: 2-45

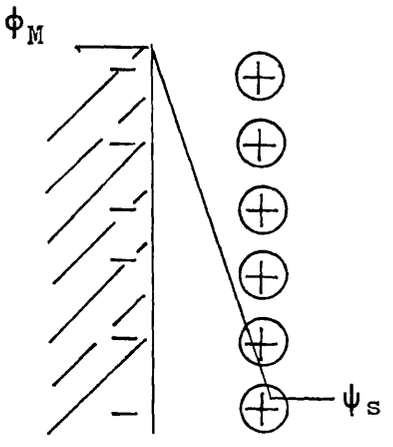

Fig: 2-46

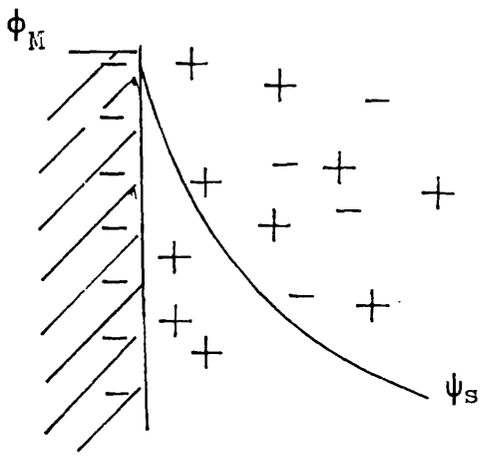

Fig: 2-47

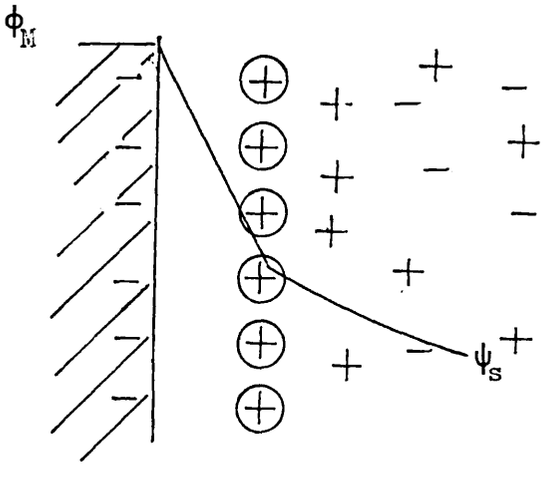

CHAPTER 3

Studies of Pulse Plating of Copper in Copper Halide Solutions

Introduction :

Studies of the efficiency of pulse methods on copper plating from acid baths have been carried out by various authors[83,103,104]. This investigation was instituted to observe the effect of additives on pulse plating and copper halides were chosen.

The corrosion of plated copper during the relaxation time to form Cu(I)halides [i.e. copper(I)chloride, copper(I)bromide, copper(I) iodide] shows that the halides might not be good additives to be used in order to improve the plate quality when pulse plating is used. Nevertheless copper(I)chloride is used as a cathode for reserved sea-water batteries[31] and CuBr and CuI can be used as electrode material for seawater activated cells. More studies were then carried out with this new method of producing copper(I)halide electrodes.

PART (3-1) EXPERIMENTAL

Sect (3-1.1) Materials:

Anodes:-

The anodes used were 4×10^{-2}m x 3×10^{-2}m copper foil (BDH. 99.999%)

Cathodes:-

The cathodes used were 2×10^{-2}m x 2×10^{-2}m copper foil (BDH) 99.999%) or 2×10^{-2}m x 2×10^{-2}m platinum foil (Johnson Matthey 99.999%) on which a thin layer of copper was plated from acid copper solution.

Reference Electrode:-

The reference electrode used in all experiments was a saturated calomel electrode. This saturated calomel electrode (S C E) has a potentail of + 270mV at 298 K vs standard hydrogen electrode.

Salt Bridge:-

An agar-agar type of salt bridge was used. The salt bridge was made of agar powder and pottasium chloride salt (Analar grade)[73].

Chemicals

All the chemicals in the experiments were of analar grade and used without further purifications.

Electrolytic Cells:-

The electrolytic cell used for pulse plating was made of perspex. It has a rectangular shape (fig 3-1,p103) and the dimensions of the cell are as follows:

Height = 1×10^{-1}m Length = 1.4×10^{-1}m

Width = 0.8×10^{-1}m

The glass electrolytic cell used for the controlled Potential coulometry experiment is shown on figure 4-1(p200). The cell consists of three compartments and the two main compartments have the same size. The third smaller compartment was used to hold the salt-bridge (agar). The dimensions of the large compartments are

Height = 1.50×10^{-1}m Diameter = 0.40×10^{-1}m

and the small compartment are

Height = 0.80×10^{-1}m Diameter = 0.15×10^{-1}m

The length of the bridge between the two main compartments is about 0.60×10^{-1}m and its diameter is 0.20×10^{-1}m.

Fig: (3-1)

ELECTROLYTIC CELL USED IN PULSE PLATING IN COPPER(I)CHLORIDE SOLUTION

1 Cathode(copper or Cu coated platinum)
2 Anode (copper)
3 Luggin capillary
4 Agar salt bridge
5 Saturated KCl solution
6 Saturated Calomel electrode
7 Magnetic stirrer
8 Electrical coil
9 N_2 gas inlet
10 Clamp+retort stand
11 Thermostated water bath
12 Support stand
13 Perspex box
14 Silicon washer
15 Teflon tape

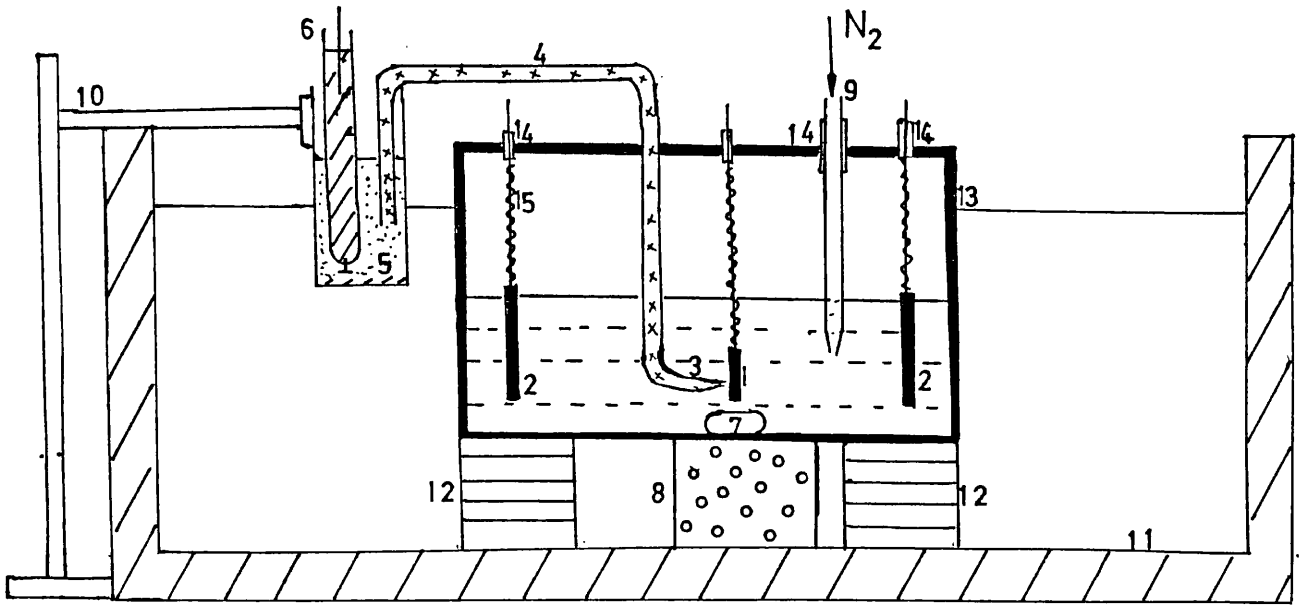

Sect(3-1.2) Electrode Pre-treatment:-

The following cleaning processes were used for all electrodes before they were placed into the electroplating bath.

(a) Degreasing:- Electrodes were immersed in chloroform for half an hour.

(b) Acid etching:- Electrodes were dipped into a 5 mol dm^{-3} nitric acid until clean and semi-bright electrodes were obtained . The average time required was about 15 seconds.

(c) Rinsing :- Electrodes were thoroughly rinsed in distilled water.

After the cleaning processes, electrodes (cathodes) were dried at a temperature of about $40^{o}C$. The electrodes were then stored under a N_2 atmosphere.

Platinum electrodes which were to be used as copper plated platinum cathodes, were plated in 0.34 mol dm^{-3} copper sulphate and 1.76 mol dm^{-3} H_2SO_4 solution.

The constant direct current used was 100 mA and the plating time was 5 minutes. The amount of copper coated was 0.0099 g $\pm$ 0.0002 g.

Sect (3-1.3) Corrosion of Copper in Solutions containing Halide ions :-

A clean copper foil was suspended from a balance (CI Electronics microforce 2) in a solution containing 1.76 mol dm^{-3} H_2SO_4, 0.34 mol dm^{-3} Cu^{2+} and KCl or KBr. The solution was thermostated to 25°C ($\pm$ 0.5°C). During this experiment the level of solution was adjusted in order to correct for the buoyancy of the electrode. The increase in weight of the foil was measured ($\pm$ 0.01 mg) with time. Similar experiments were attempted with solutions containing fluoride and iodide ions.

Sect (3-1.4) Galvanostatic Pulse Plating:-

The cell , ministat (Thompson Associates 125) and pulse generator (CERBI, Chemical Electronic Company) were set up as shown in Fig (3-2,p109). Copper was galvanostatically (300 mA) pulse plated from a series of electrolytes containing 1.76 mol dm^{-3} H_2SO_4 , 0.1 to 0.68 mol dm^{-3} $CuSO_4$, and 0.05 to 0.34 mol dm^{-3} KCl or KBr. The potential of the working electrode was monitored by an

oscilloscope against the SCE reference electrode connected to the Luggin capillary by a salt bridge. This cell was continuously purged with nitrogen during all experiments, and thermostatted to 25°C (± 0.5°C).

A train of rectangular wave pulses was produced by the pulse generator and the current controlled by a ministat working in a galvanostatic mode. The range of pulse periods (on time) was 2 to 30 ms, and off time of 10 to 1000 ms. Plated platinum electrodes were used when the deposited layer was to be analysed by atomic absorption spectrophotometry.

Sect(3-1.5) Controlled Potential Coulometry used in the Analysis of plated layer;-

This method is similar in the fundamental principle to the potential step method described in section (2-1.2, p41). In this research, this method was used to determine the amount of copper(I) halide present in copper/copper halide electrodes. The circuit diagram is shown on figure 3-3 (p110).

The experiment was carried out in nitrogen purged sulphuric acid (1 mol dm^{-3}) at 298 K . A potentiostatic

step, 0 V to 0.1V (vs.SHE) for copper(1) chloride,and to 0.05V for CuBr , was applied to the copper(1) halide electrode and the current measured with time. A charge passed as CuX was cathodically reduced to copper and X^- [E(3-1)] gave the amount of halide in the electrode. The anode used was a platinum electrode.

$$CuX + e \longrightarrow Cu + X^- \qquad E(3\text{-}1)$$

Sect(3-1.6) Atomic Absorption Spectrophotometry used in the analysis of plated layers.

The principle of this technique was briefly described in section (2-1.6,p60). In this experiment the standard solutions of 1,5,10 ppm of copper in 0.05 mol dm^{-3} HNO_3 were prepared. A ealiberation curve of absorbance vs. concentration of copper was then obtained using the above standard solutions (Fig 3-4,p111).

The copper/copper(1) halide deposits were dissolved in 5 mol dm^{-3} nitric acid. The sample solutions were then diluted to a range between 1 ppm to 10 ppm with 0.05 mol dm^{-3} HNO_3. These samples were analysed using the atomic absorption spectrophotometer.

Absorbance values of these samples obtained were then used to determined the concentrations of copper from the caliberation curve (p 111).

Wavelength of the spectrophotometer used was 327.4 nm and the band pass of 0.4 nm. Air flow and acetylene flow rates were 5.0 $dm^3 min^{-1}$ and 1.0 $dm^3\ min^{-1}$ respectively.

Sect (3-1.7) X-Ray Diffraction.

The principle of X-Ray diffraction was briefly described in section (2-1.5,p58) . In this experiment, the powder method was used to examine copper/copper (I) halide deposits. An X-Ray diffraction pattern of the deposit was obtained by placing fresh copper/copper (I) halide electrode at the focal plane of a Phillips diffractometer. For comparison the X-Ray pattern of a copper foil was also recorded.

THE CIRCUIT DIAGRAM FOR PULSE PLATING

Fig: (3-2)

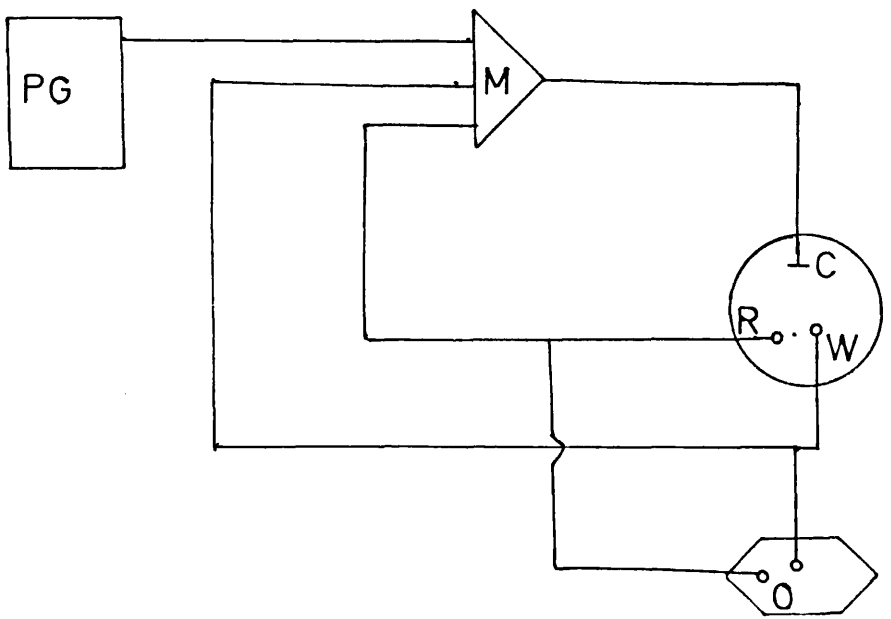

M: Ministat working as galvanostat
C: Counter electrode
W: Working electrode
R: Reference electrode
PG: Pulse generator
O: Oscilloscope

THE CIRCUIT DIAGRAM FOR THE CONTROLLED POTENTIAL COULOMETRY:

Fig:(3-3)

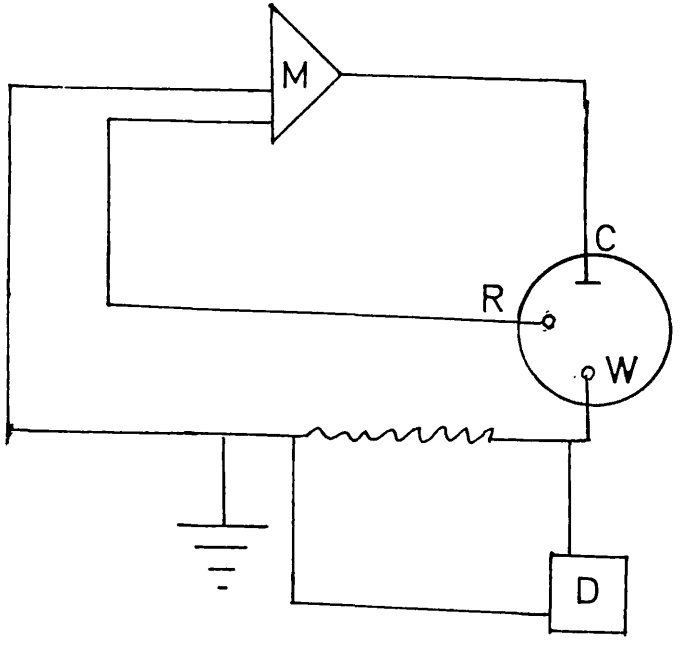

M: Ministat working as Potentiostat
C: Counter electrode (platinum)
W: Working electrode ($Cu^{o}/CuCl$)
R: Reference electrode (SCE)
D: Digital Voltmeter

THE ATOMIC ABSORPTION CALIBERATION CURVE:

Figure: (3-4)

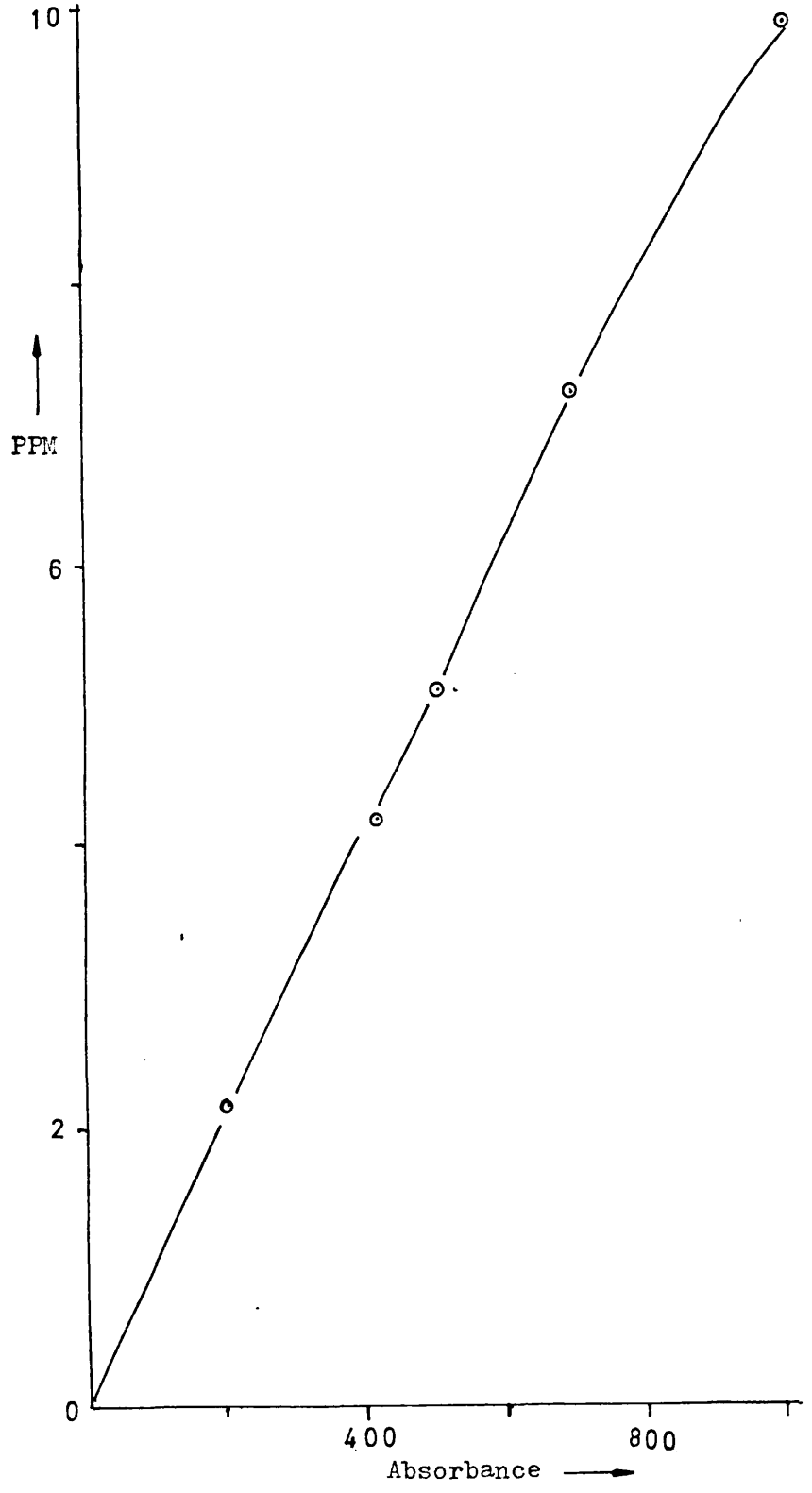

Part(3-2) CALCULATIONS AND RESULTS:

Sect(3-2.1) Corrosion of copper in Copper(II)Halide Solutions:

Figures (3-5,p125) and (3-6,p126) show the increase in weight (Δw) of a $8cm^2$ copper foil immersed in acid copper chloride and bromide solutions and 25^oC respectively. The compositions of the solutions of figure (3-5) and (3-6) are as follows:

Figure (3-5) $CuSO_4$ = 0.340 mol dm^{-3}

H_2SO_4 = 1.760 "

⬭ KCl = 0.100 "

⬬ KCl = 0.340 "

Figure (3-6) $CuSO_4$ = 0.340 "

H_2SO_4 = 1.760 "

• KBr = 0.100 "

ϴ KBr = 0.34 "

For solution containing bromide, the corrosion rate increases with increasing bromide concentration. In the case of chloride, the weight eventually decreases due to the dissolution of CuCl giving soluble copper chloride complexes. In iodide containing solution, the rate of reaction was very high between I^- and Cu^{2+}. A white precipitate of CuI was formed which easily scaled from the foil.

Figure (3-7,p127) shows a plot of the ratio of number of mol m^{-2}

of copper (I) chloride and number of mol m^{-2} of copper deposited vs. the ratio of the relaxation time (T_{off}) and pulse on time (T_{on}). The straight line drawn from the plot at low T_{off}/ T_{on} is taken to be the corrosion rate constant of a fresh copper surface. The composition of the solution of figure (3-7) is,

$CuSO_4$ = 0.34 mol dm^{-3}
H_2SO_4 = 1.76 "
KCl = 0.34 "

and the constant current used in the experiments was 0.34A. The pulse on times used were 2ms (•) and 10ms (o).

Figure (3-8,p128) shows the plot of number of mol m^{-2} of copper (I) chloride formed on the $8cm^2$ electrodes vs. the square root of the total copper (I) chloride formation reaction time. The pulse on time used was 10ms and the relaxation times used were 24ms, 90ms, 290ms. The composition of the solution was as follows:

$CuSO_4$ = 0.34 mol dm^{-3}
H_2SO_4 = 1.76 "
Cl^- = 0.1 "

The plots of the number of moles of Cu (1) Br formed on the surface area of the electrode vs. the total

reaction time]$^{1/2}$ are shown on figure (3-9,p129). The pulse on time used was 30ms and the relaxation times were 5ms, 70ms, 270ms and 1000ms. The constant current used was 334mA. The compositions of the solutions of the two plots in this figure are as follows:

(A) $CuSO_4$ = 0.34 mol dm^{-3}

KBr = 0.34 "

H_2SO_4 = 1.76 "

(B) $CuSO_4$ = 0.34 "

KBr = 0.1 "

H_2SO_4 = 1.76 "

These plots were carried out in order to establish a hypothesis of the movement of the corroding reactant through the layers of Cu^o deposited and the corroding product i.e. cuprous chloride or cuprous bromide.

Sect(3-2.2) Pulse Plating in Halide Solutions

Table (3-1,p155) shows the total amounts of copper present in the deposit which was determined by the atomic absorption spectrophotometry method (see p107). The deposit was obtained from solutions containing 0.34 mol dm^{-3} Br^- and 0.34 mol dm^{-3} Cu^{2+} in 1.76 mol dm^{-3} sulphuric acid.

The amount of copper chloride present in the deposit was obtained by coulometry of the reduction of CuCl as has been described in page (106). This method is only used in CuCl containing deposit and not CuBr containing deposit. This is because for a copper bromide containing deposit, the deposit flaked out easily from the electrode during the reduction process. Figures (3-11 to 3-16,p131-136) show the coulometric results of the reduction current flow through the electrode as a function of time. The deposits obtained in these cases were from solution containing 0.34 mol dm^{-3} Cl^-; 0.34 mol dm^{-3} $CuSO_4$ and 1.76 mol dm^{-3} H_2SO_4. The combination of the pulse on time and relaxation time in each case is not the same and is indicated on each figure.

The Copper electrodes which were coated with CuCl, CuBr and the copper foil were analysed by X-ray diffraction method (see p108). The deposits were prepared in acidic solution containing 0.34 mol dm^{-3} $CuSO_4$ and 0.34 mol dm^{-3}

of CuCl or CuBr. The pulse on time used was 10 ms and relaxation time was 90 ms. Figures (3-30 to 3-33.p150-153) show the response peaks with the angle of resolution θ . From these results the d-spacings of the deposits and their intensities were then calculated. The results are shown in table (3-2.p156) to (3-5.p159).

Figures (3-17,p137) and (3-18,p138) show the total weight percentage of copper/copper (1) chloride and copper/ copper (1) bromide deposits respectively as a function of relaxation time at constant pulse on time. The operating conditions for each curve shown in the figures are as follows:

Figure (3-17) $CuSO_4$ = 0.34 mol dm^{-3}

H_2SO_4 = 1.76 "

KCl = 0.1 "

Pulse on time = 2ms

KCl = 0.34 mol dm^{-3}

Pulse on time = 2ms

KCl = 1.0 mol dm^{-3}

Pulse on time = 2ms

Figure (3-18) $CuSO_4$ = 0.34 mol dm^{-3}

H_2SO_4 = 1.76 "

KBr = 0.1 "

Pulse on time = 30ms

KBr = 0.34 "

Pulse on time = 30ms

The effect of the bulk concentration of Cu^{2+} and Cl^- at constant pulse on time of 10ms and relaxation time of 90ms was studied. The amount of CuCl present in the deposit was analysed by the coulometry reduction method and is shown on figure (3-19.p139). This figure shows that the production of CuCl is influenced more by chloride concentration than copper concentration.

In addition the steady state plating of copper in the halide containing solution was also carried out. It was observed that the % wt efficiency of copper obtained in the chloride or bromide containing solutions were 100%. The compositions of the solutions were 0.1 or 0.34 mol dm^{-3} of halide. 0.34 mol dm^{-3} $CuSO_4$ and 1.76 mol dm^{-3} H_2SO_4. The direct current used was 334mA.

The following is the example of the calculation of the amount of copper electrochemically deposited by the pulse method. Example of the operation conditions used is·

(a) Pulse on-time = 10ms

(b) Relaxation time = 90ms

(c) Plating time = 106 minutes

(d) constant current = 334mA

Therefore, the amount of copper deposited (W_{pc}) is

$$= \frac{T_{on}}{T_{on}+T_{off}} \times \frac{\text{Plating time x current}}{\text{Faraday}} \times \frac{Mcu^{o}}{2} \qquad E(3-2)$$

$$= \frac{10}{90+10} \times \frac{106 \times 60 \times .334}{96490} \times \frac{63.540}{2}$$

$$= 0.070g$$

Also the % wt efficiency of the pulse plating is calculated using the subsequent formula,

$$\% \text{ wt efficiency} = \frac{\text{Measured weight } (W_E)}{W_{pc}} \times 100\% \qquad E(3-3)$$

Sect(3-2.3) The Equilibrium Concentrations of Cu^{2+} Complexes, Cu^{+} Complexes, Free Cu^{+} and Free Cu^{2+}

The 8 complexes formation equations (p184) show that in a solution containing Cu^{2+}, X^{-} and Cu^{o}. There is a possibility of 9 species of ions and copper X complexes present in the solution. The computer calculated the equilibrium concentration (EC) of the various species at different Cu^{2+} and X^{-} bulk concentrations were plotted as shown in figure (3-20 to 3-22,p140-142) and (3-23 to 3-28,p143-148).

Figures (3-20 to 3-22) show the EC of the Cu^{2+} complexes as a function of bulk Cl^{-} concentration. The bulk concentrations of Cu^{2+} for figures (3-20, 3-21) and (3-22) are 0.1 mol dm^{-3}, 0.34 mol dm^{-3} and 0.68 mol dm^{-3} respectively. In a solution of 0.1 mol dm^{-3} Cu^{2+} concentration, at a Cl^{-} concentrations of less than 0.15 mol dm^{-3}, the predominant complexes present in the solution are the $CuCl^{+}$ and $CuCl_2$. At total Cl^{-} concentration > 0.5 mol dm^{-3} the EC of the $CuCl_3^{-}$ and $CuCl_4^{2-}$ are much higher than $CuCl^{+}$. The $CuCl_2$ concentration of $CuCl^{+}$ is predominantly higher than the other 3 Cu^{2+} complexes at a Cl^{-} concentration of less than 0.5 mol dm^{-3}.

Figures (3-23, 3-24) and (3-25,p145) show the EC of free Cu^{2+}, Cl^{-}, $CuCl^{+}$ and $CuCl_2$ at 0.1, 0.34 and 0.68 mol dm^{-3} bulk concentrations of Cu^{2+} respectively. All these species have some influence in reaction of copper (I) chloride formation

at Cl^- of less than 0.7 mol dm^{-3}.

In the case where the solution containing bromide ions, the EC of these species which influence the copper bromide reaction are shown in figures (3-26,p146) to (3-28,p148). These curves have similar shape as the chloride curves (i.e. figures 3-23 to 3-25), when the Cu^{2+} bulk concentrations of the chloride and bromide containing solutions are the same. The EC of the similar species differ to certain extent between the two cases. For example, the free Cu^{2+} concentration in the bromide solutuon is much lower than in the chloride solution at the same bulk concentration of bromide and chloride.

Figure (3-29,p149) shows the rate of formation of the copper (I) chloride in chloride solution vs. $CuCl^+$ complex. The experimental data were obtained from the solution containing total concentrations of Cu^{2+} at 0.5, 0.34 and 0.68 mol dm^{-3}. There is a linear relationship between the rate of formation of Cu (I) Cl and the EC of $CuCl^+$.

Sect(3-2.4) The Rest Potential Differences of the Working Elcetrodes

The measured rest potential differences of the working electrodes in the chloride containing solution are shown on table (3-8,p162). The two theorectically calculated equilibrium potentials of a possible electrochemical corrosion reaction of E(3-4) and E(3-6) are also shown. For example, the possible equilibrium potentials of a copper electrode, in a solution containing bulk concentrations of Cu^{2+} = 0.68 mol dm^{-3} and Cl^- = 0.34 mol dm^{-3} are calculated as follows:

(A) Calculation of the equilibrium potential (E_1^c) of reaction:

$$Cu^o + Cl^- \rightleftharpoons CuCl + e \qquad E(3-4)$$

At standard conditions, the standard electrode potential of the above reaction is equal to 0.137 volt.

From the computer calculated results at a total concentrations of Cu^{2+} = 0.68 mol dm^{-3} and Cl^- = 0.34 mol dm^{-3}, the concentration of the free Cl^- ions = 1.422 x 10^{-3} mol dm^{-3}, and the $CuCl^+$ complex is 3.128 x 10^{-1} mol dm^{-3} (used in calculation of E_2^c).

The Nernst equation is used to calculate E_1^c and can be written as,

$$E = E^o + \frac{RT \times 2.303}{n\ F} \log \frac{\prod(\text{activities of reactants})}{\prod(\text{activities of products})} \qquad E(3-5)$$

Where E is the potential difference at a non standard condition and E^o is the potential difference at standard condition. The activity coefficients of the $CuSO_4$ solutions were used to calculate the activity of the Cl^-. It is assumed here that the other species do not affect the activity coefficient of the Cl^- ions.

(B) Calculation of the equilibrium potential (E_2^c) of reaction:

$$CuCl^+ + e \rightleftharpoons CuCl \qquad E(3-6)$$

The standard electrode potential in the Cu^{2+} deposition is 0.34 volt.[86]

$$Cu^{2+} + 2e \rightleftharpoons Cu^o \qquad E(3-7)$$

Since $\Delta G^o = -nFE^o$ E(3-8)

Therefore the standard free energy of the reaction E(3-7) is = -65.613 KJ $mole^{-1}$.

Also, the equilibrium constant value of the reaction E(3-9) is 631 mol dm^{-3}.

$$Cu^{2+} + Cl^- \rightleftharpoons CuCl^+ \qquad E(3-9)$$

Therefore the standard free energy of the reaction E(3-9) is = -RTln 631 J mol^{-1}

or = -15.973 KJ mol^{-1}

On subtracting E(3-9) from E(3-7), E(3-10) is obtained i.e.

$$CuCl^+ + 2e \rightleftharpoons Cu^o + Cl^- \qquad E(3-10)$$

and its free energy is -49.64 KJ mol^{-1}.

The standard electrode potential of the following CuCl reduction reaction is 0.137 volt.

$$CuCl + e \rightleftharpoons Cu^{o} + Cl^{-} \qquad E(3\text{-}11)$$

Therefore, its standard free energy is -13.219 KJ mol^{-1}.

The standard free energy of the $CuCl^{+}$ reduction reaction, E(3-6,p122) is obtained by subtracting the standard free energy of E(3-11) from E(3-10,p122). Thus the standard free energy is -36.421 KJ mol^{-1} and the standard electrode potential is 0.378 volt.

The Nernst equation E(3-5,p121) is then used to calculate the non-standard state equilibrium potential difference E_2^c .

Sect(3-2.5) The Potential Differences of The Working Electrode During Pulse Plating

Table 3-9 (p163) shows the measured mixed potentials of the copper electrodes during pulse plating. The calculated standard electrode potentials of the plating process involving the individual $CuCl^+$ ($E^c_{CuCl^+}$), $CuCl_2$ ($E^c_{CuCl_2}$) and free Cu^{2+} ions ($E^c_{Cu}2+$) are also shown on table 3-9. The standard free energy of reduction reaction involving $CuCl^+$ i.e. E(3-10) was found to be -49.64 KJ mol^{-1} (see p122). Therefore, its standard electrode potential is equal to 0.257 volt.

The plating reaction involving the $CuCl_2$ complex is shown as follow:

$$CuCl_2 + 2e \rightleftharpoons Cu^o + 2Cl^- \qquad E(3-12)$$

The standard electrode potential of E(3-12) is calculated in the following manner.

From the table (3-10,p164) it is shown that the equilibrium constant of the following reaction is 39.81 J mol^{-1}.

$$CuCl^+ + Cl^- \rightleftharpoons CuCl_2 \qquad E(3-13)$$

The standard free energy is calculated to be equal to -9.127 KJ mol^{-1}.

The standard free energy of E(3-12) is obtained by subtracting E(3-13) from E(3-10,p122) i.e. -40.513 KJ mol^{-1}.

The standard electrode potential of the Cu^{2+} reduction process E(3-7,p122) as mentioned in page 122 is 0.34 volt. The Nernst equation E(3-5,p121) was used to calculate the non-standard electrode potentials of the electrodeposition reactions involving the free Cu^{2+} ions, $CuCl^+$ and $CuCl_2$ complexes.

Fig: (3-5)

WEIGHT INCREMENT OF COPPER FOIL(8 cm^2) WITH TIME:

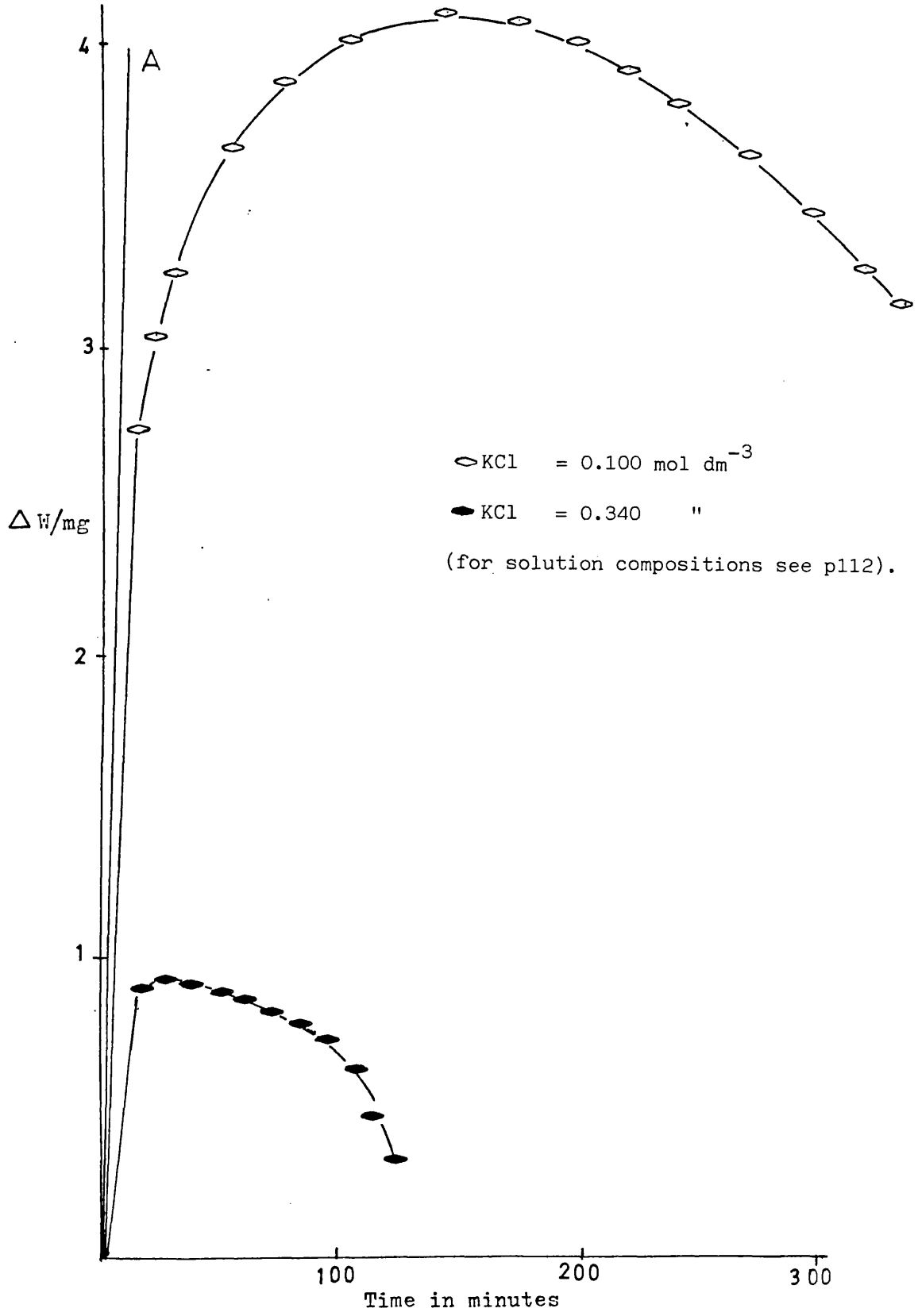

Fig: (3-6)

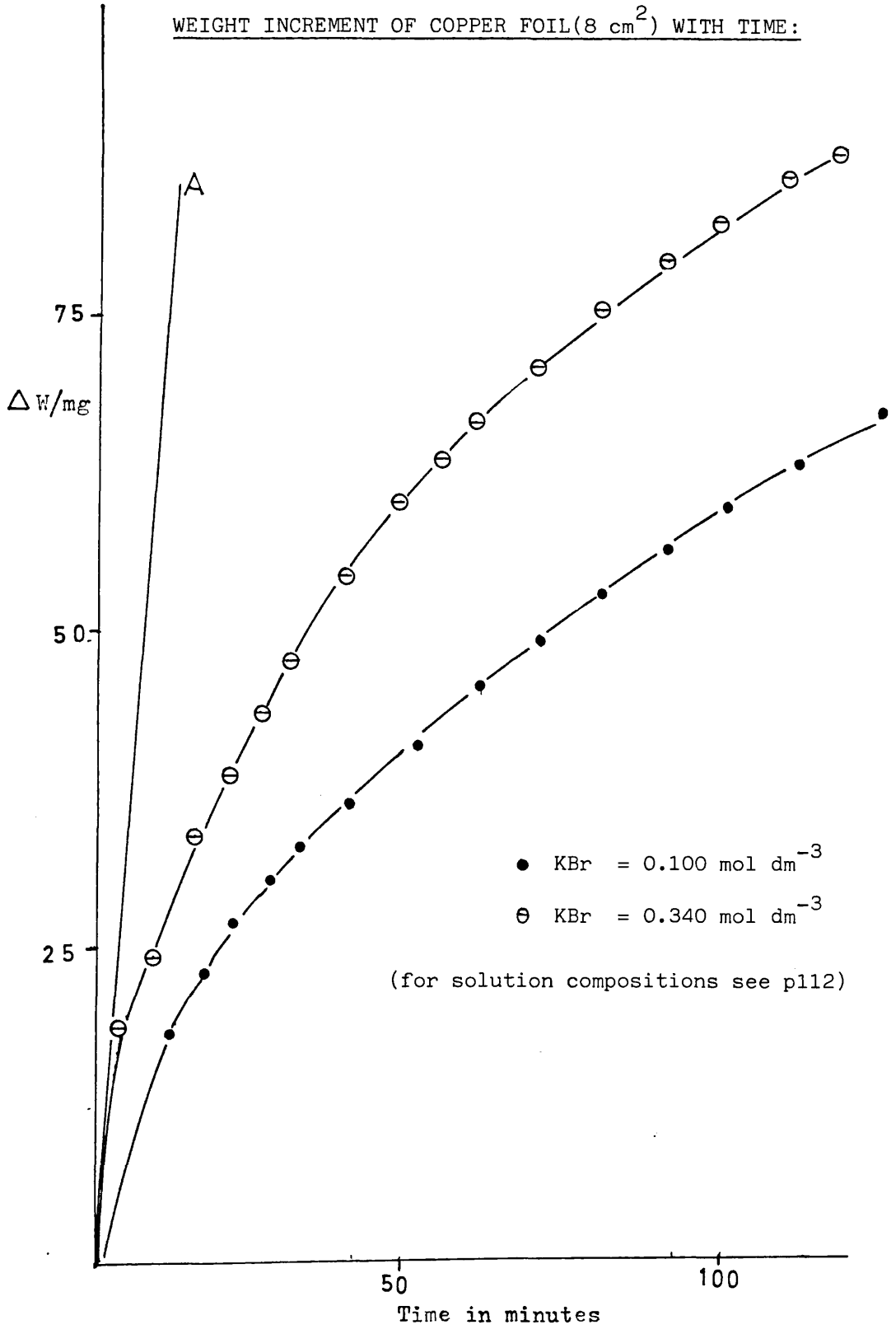
WEIGHT INCREMENT OF COPPER FOIL(8 cm^2) WITH TIME:
A
75
50
25
Δ W/mg
50
100
Time in minutes
● KBr = 0.100 mol dm^{-3}
Θ KBr = 0.340 mol dm^{-3}
(for solution compositions see p112)

Fig (3-7)

RARIO OF Cu(I)Cl AND Cu° VS RATIO OF T_{off} AND T_{on}:

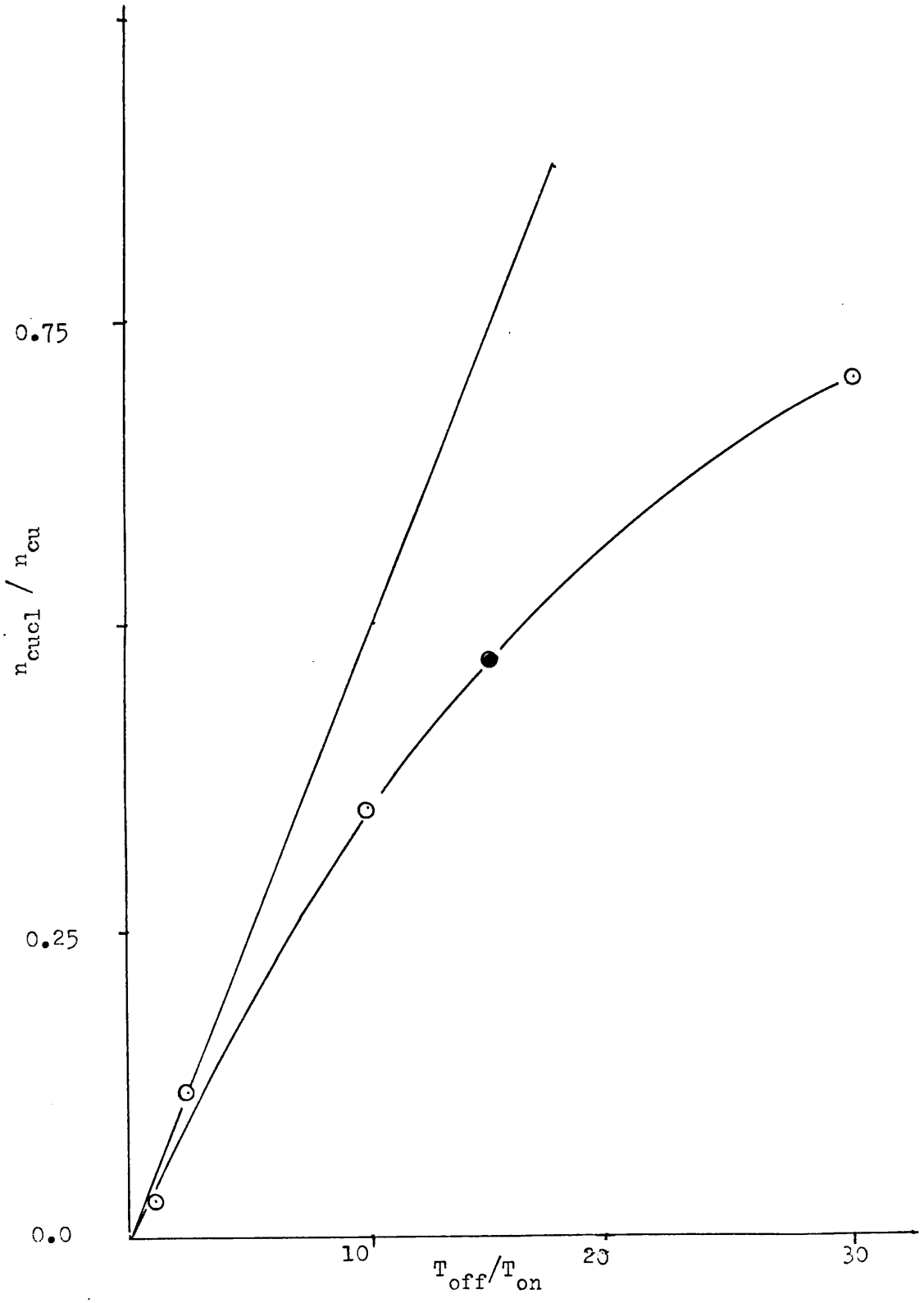

Fig (3-8)

AMOUNT OF COPPER (I)CHLORIDE FORMED VS (TOTAL REACTION TIME)$^{1/2}$:

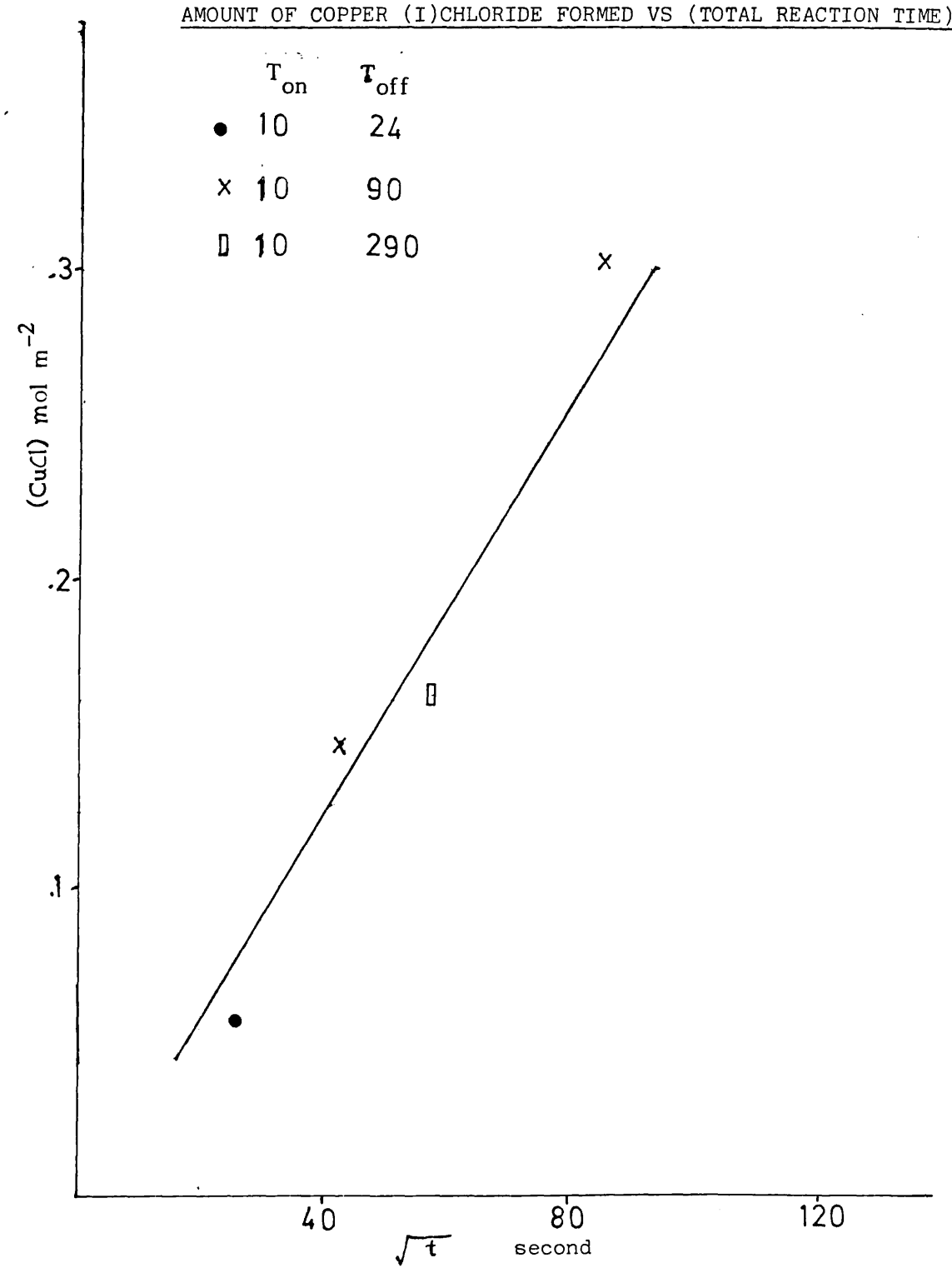

Fig (3-9)

AMOUNT OF COPPER(I) BROMIDE FORMED VS (TOTAL REACTION TIME)$^{1/2}$:

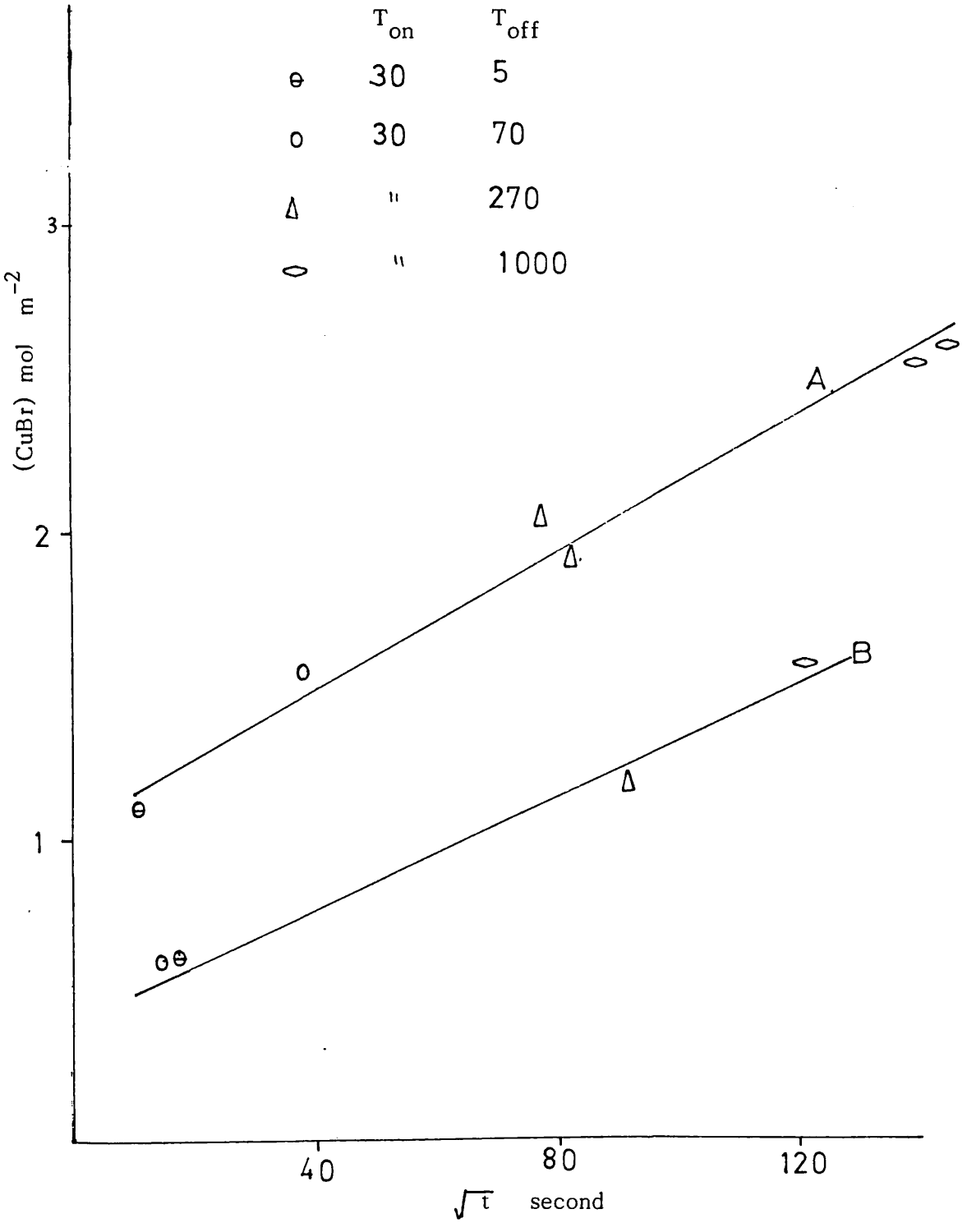

(3-10)

% WEIGHT EFFCIENCY OF COPPER DEPOSITION USING PULSE METHOD:

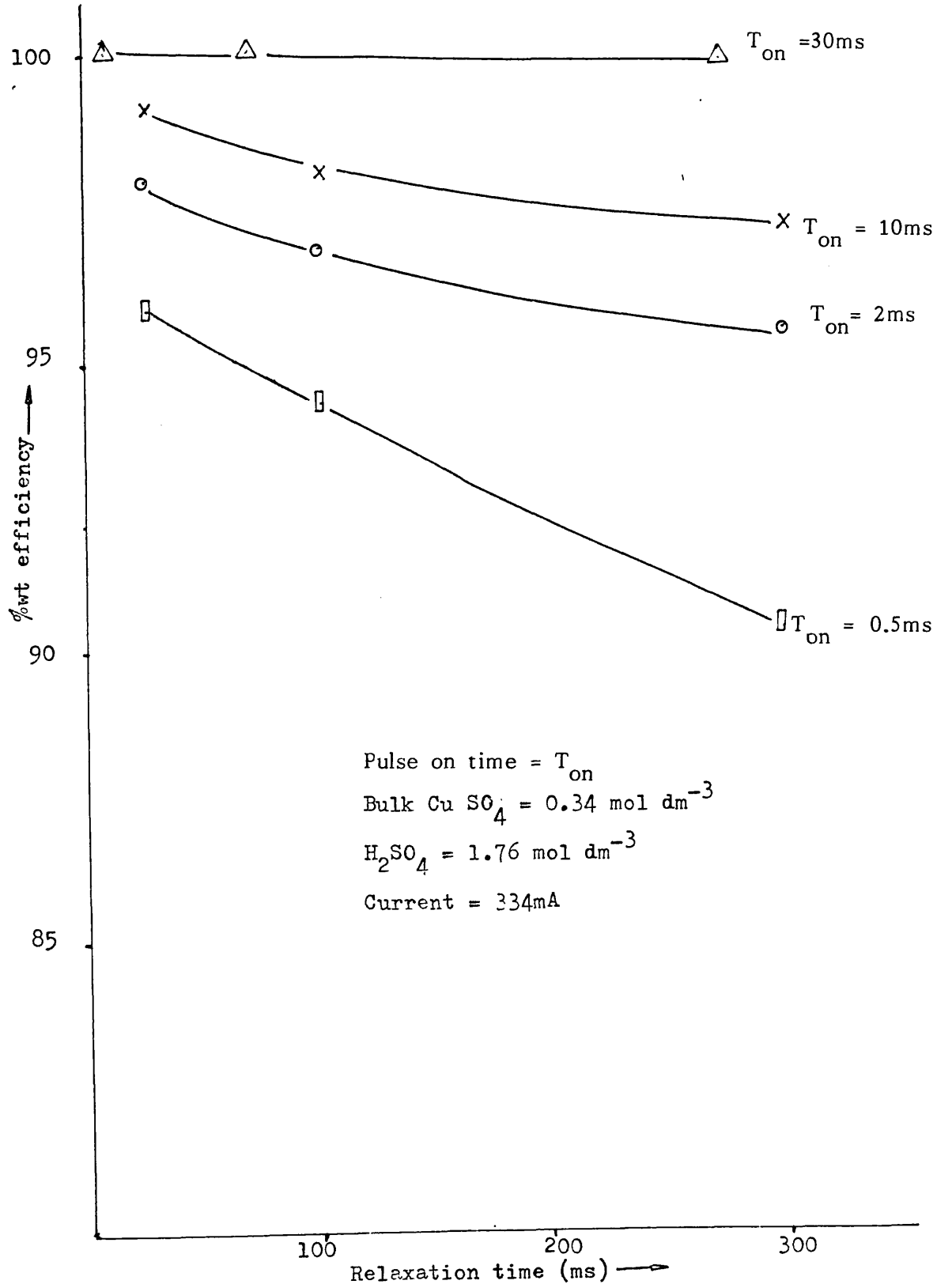

Figure (3-11)

COULOMETRIC PLOT OF $Cu^{o}/CuCl$ ELECTRODE:

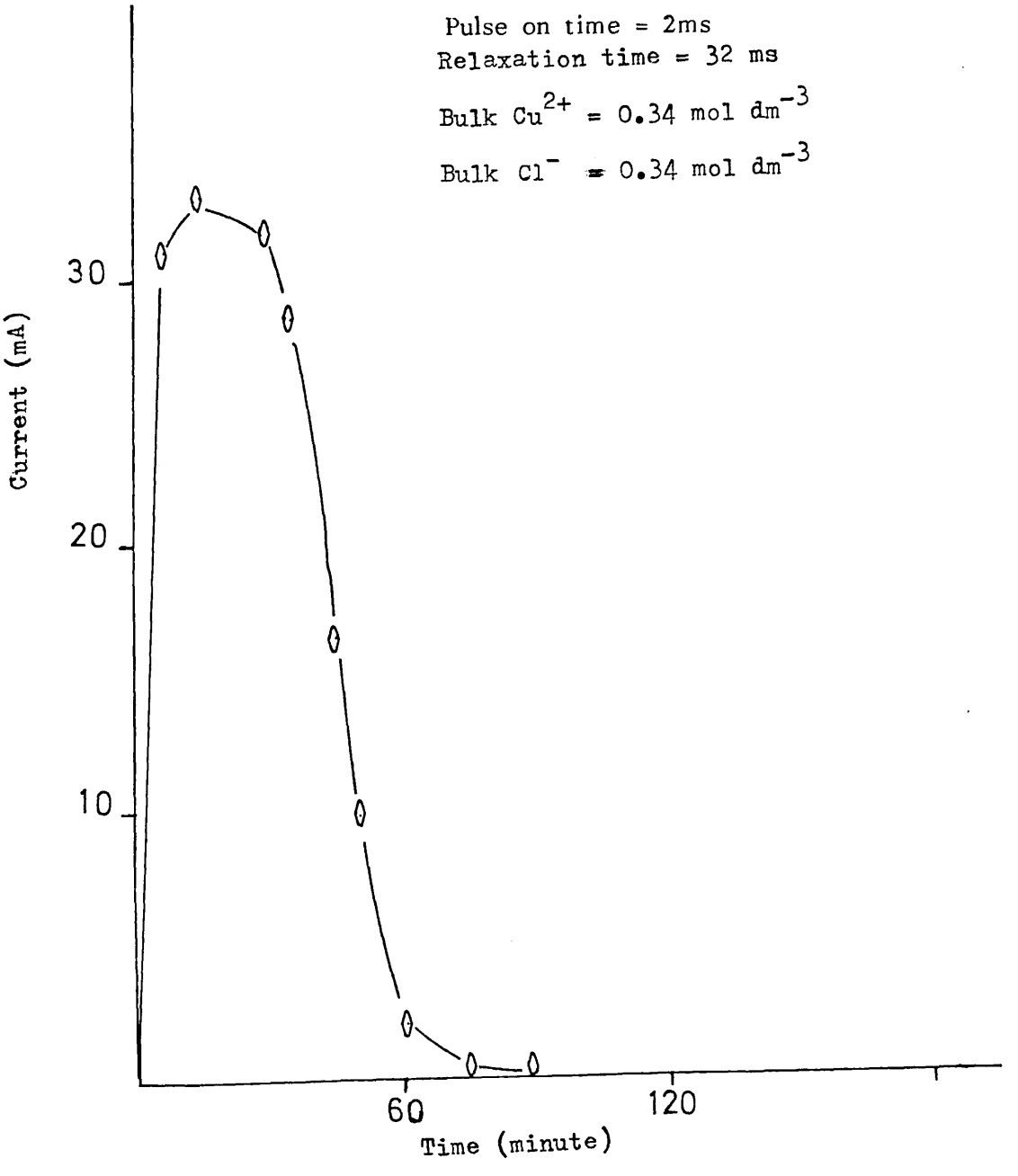

Figure (3-12)

COULOMETRIC PLOT OF $Cu^{o}/CuCl$ ELECTRODE:

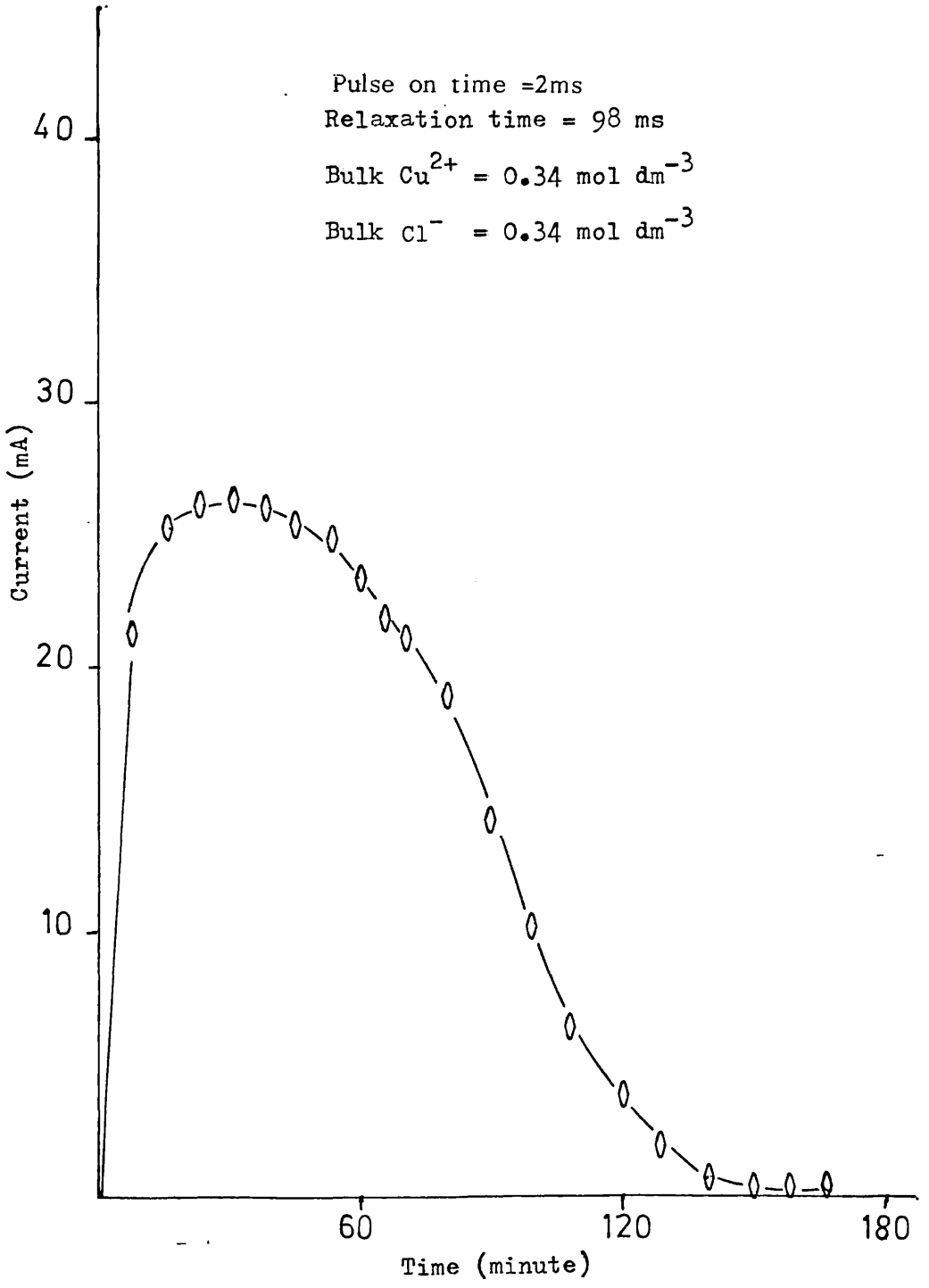

Figure (3-13)

COULOMETRIC PLOT OF $Cu^{o}/CuCl$ ELECTRODE:

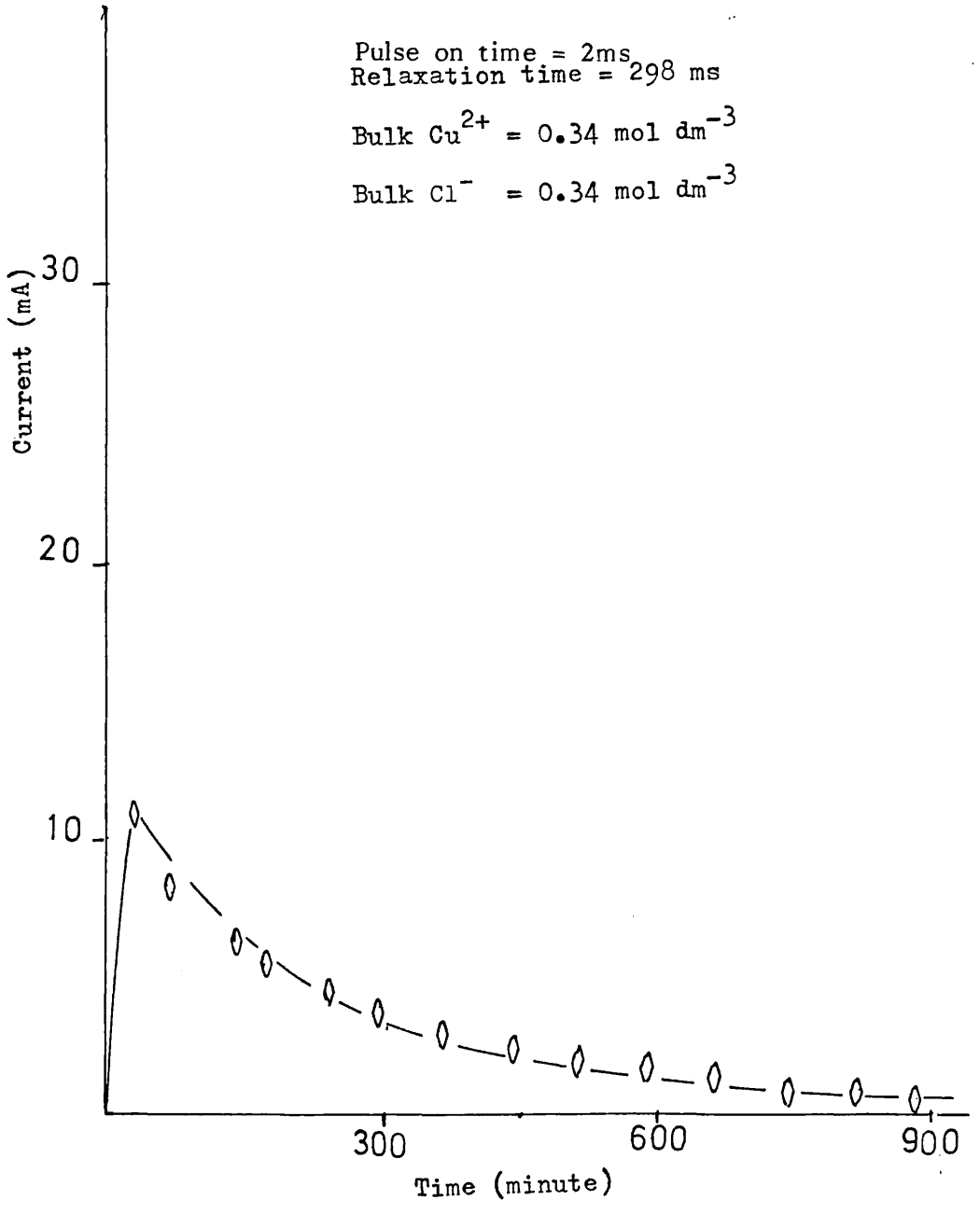

Figure (3-14)

COULOMETRIC PLOT OF $Cu^{o}/CuCl$ ELECTRODE:

Pulse on time = 10ms
Relaxation time = 24 ms
Bulk Cu^{2+} = 0.34 mol dm^{-3}
Bulk Cl^{-} = 0.34 mol dm^{-3}

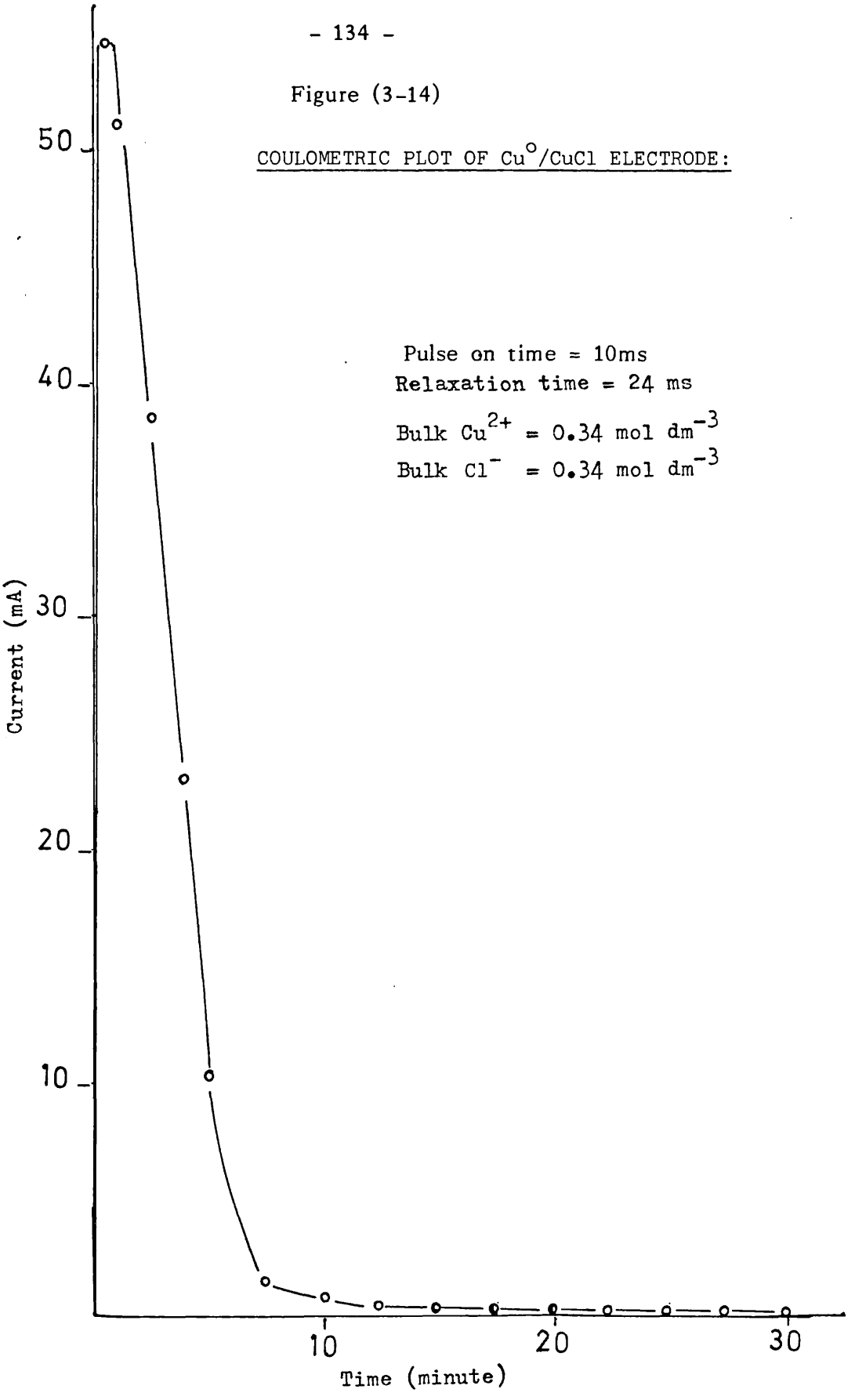

Figure (3-15)

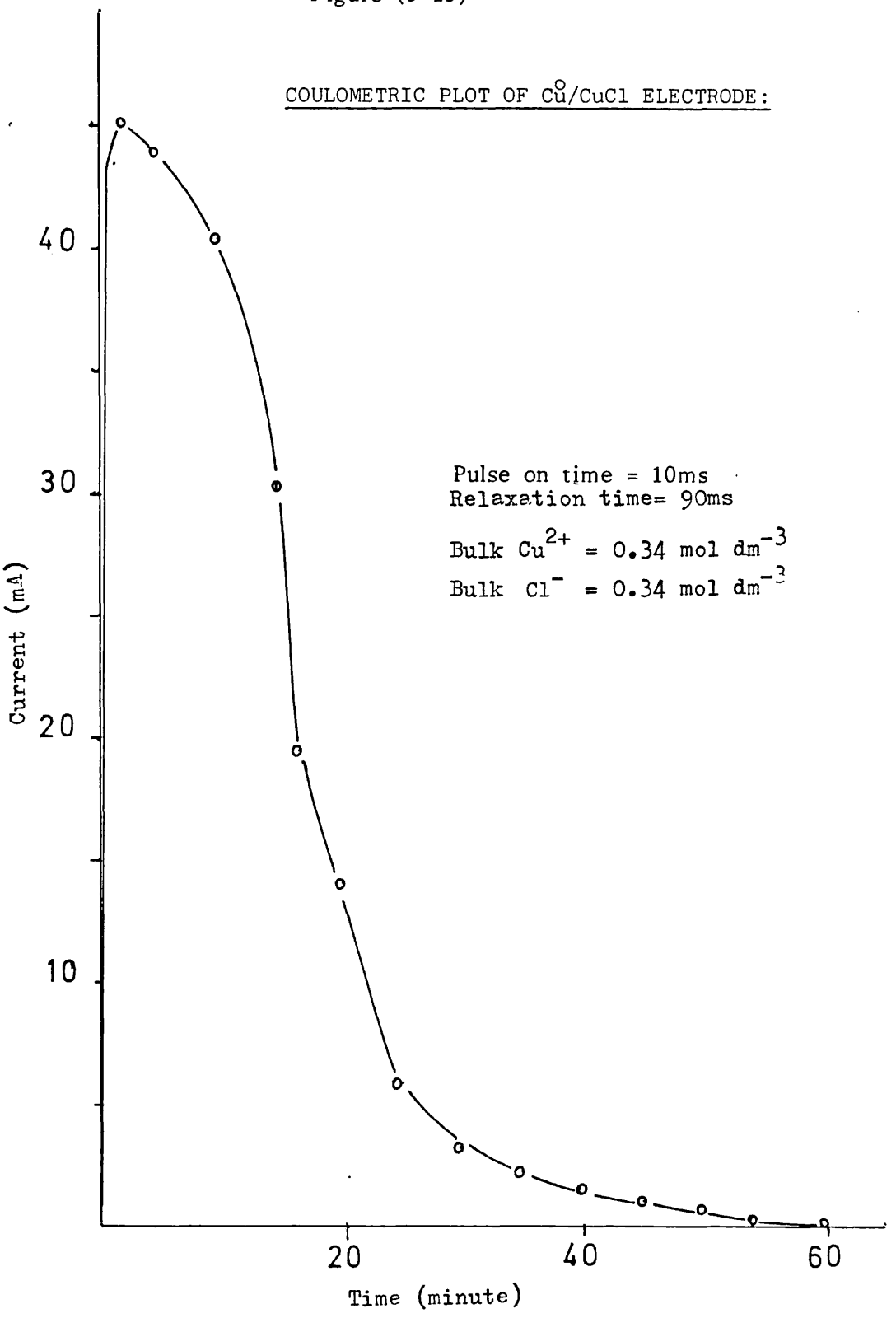
COULOMETRIC PLOT OF Cu°/CuCl ELECTRODE:
Pulse on time = 10ms
Relaxation time= 90ms
Bulk Cu2+ = 0.34 mol dm-3
Bulk Cl- = 0.34 mol dm-3
Current (mA)
40
30
20
10
20
40
60
Time (minute)

Figure (3-16)

COULOMETRIC PLOT OF Cu^{o}/CuCl ELECTRODE:

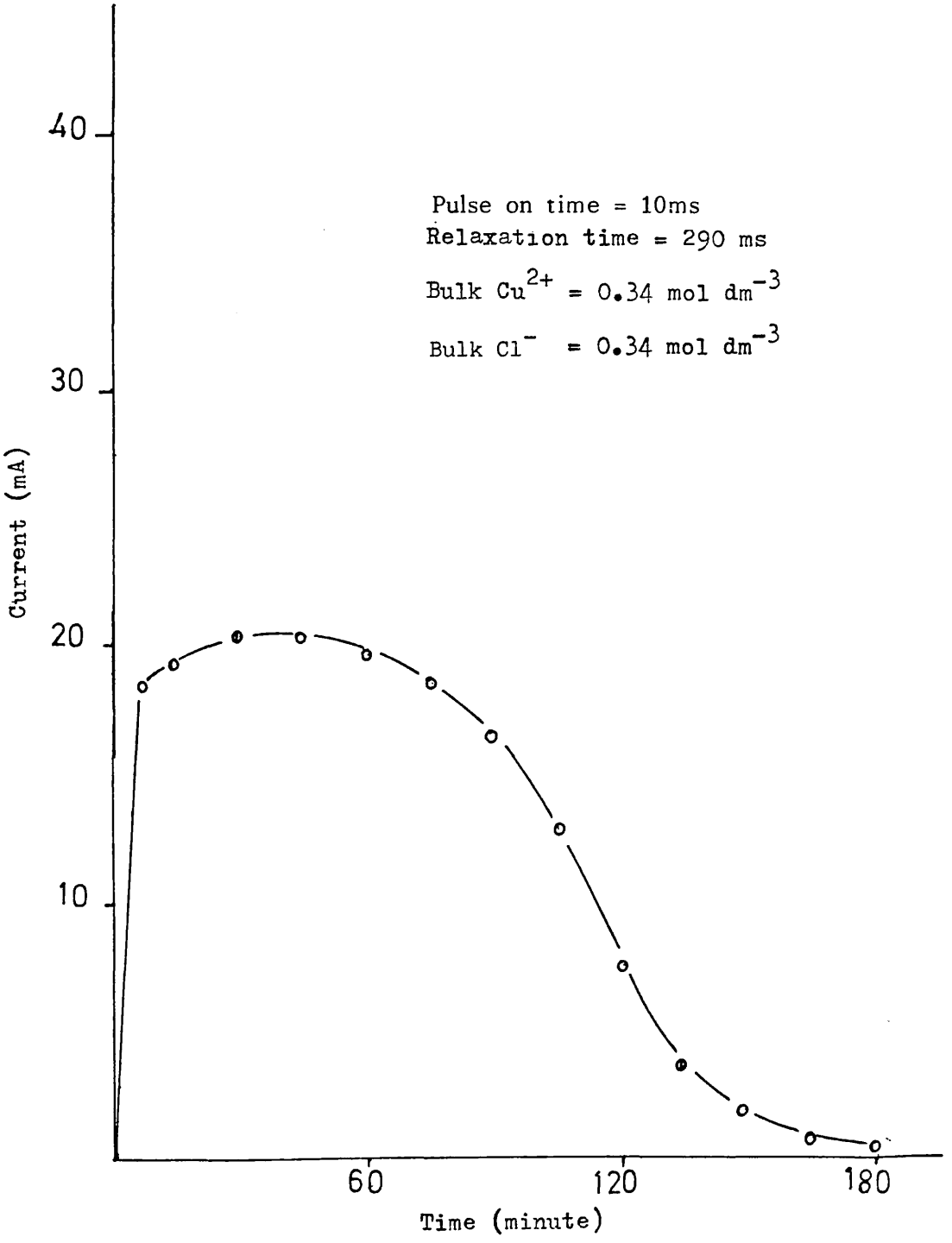

Figure (3-17)

% WEIGHT EFFICIENCY OF DEPOSITS VS RELAXATION TIME :

Current = 334 mA

Pulse on time = 2ms

	Bulk Cu^{2+} (mol dm^{-3})	Bulk Cl^{-} (mol dm^{-3})
□—□	0.34	0.34
⊕—⊕	0.34	0.10
△—△	0.34	1.0

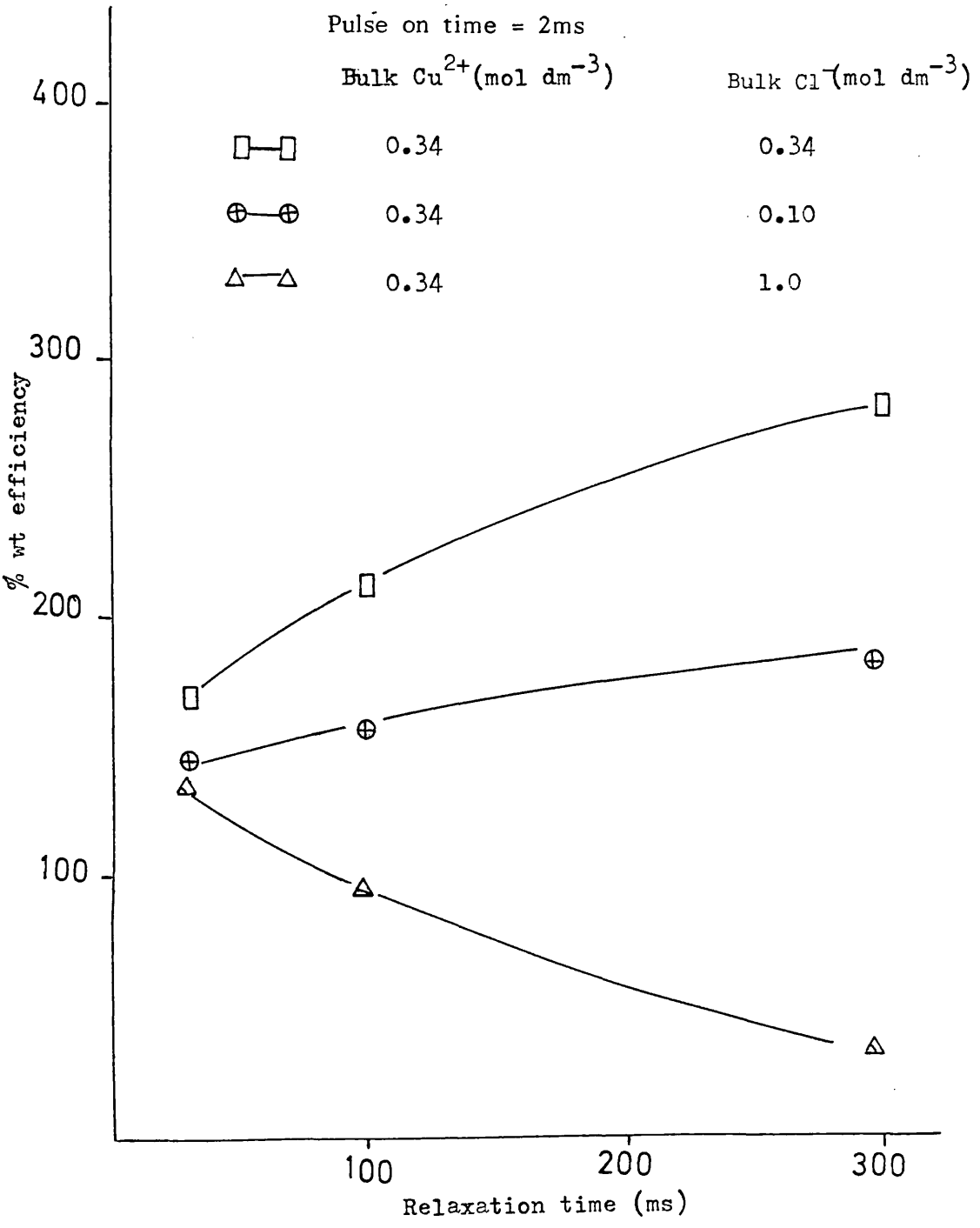

Figure (3-18)

% WEIGHT EFFICIENCY OF DEPOSITS VS RELAXATION TIME :

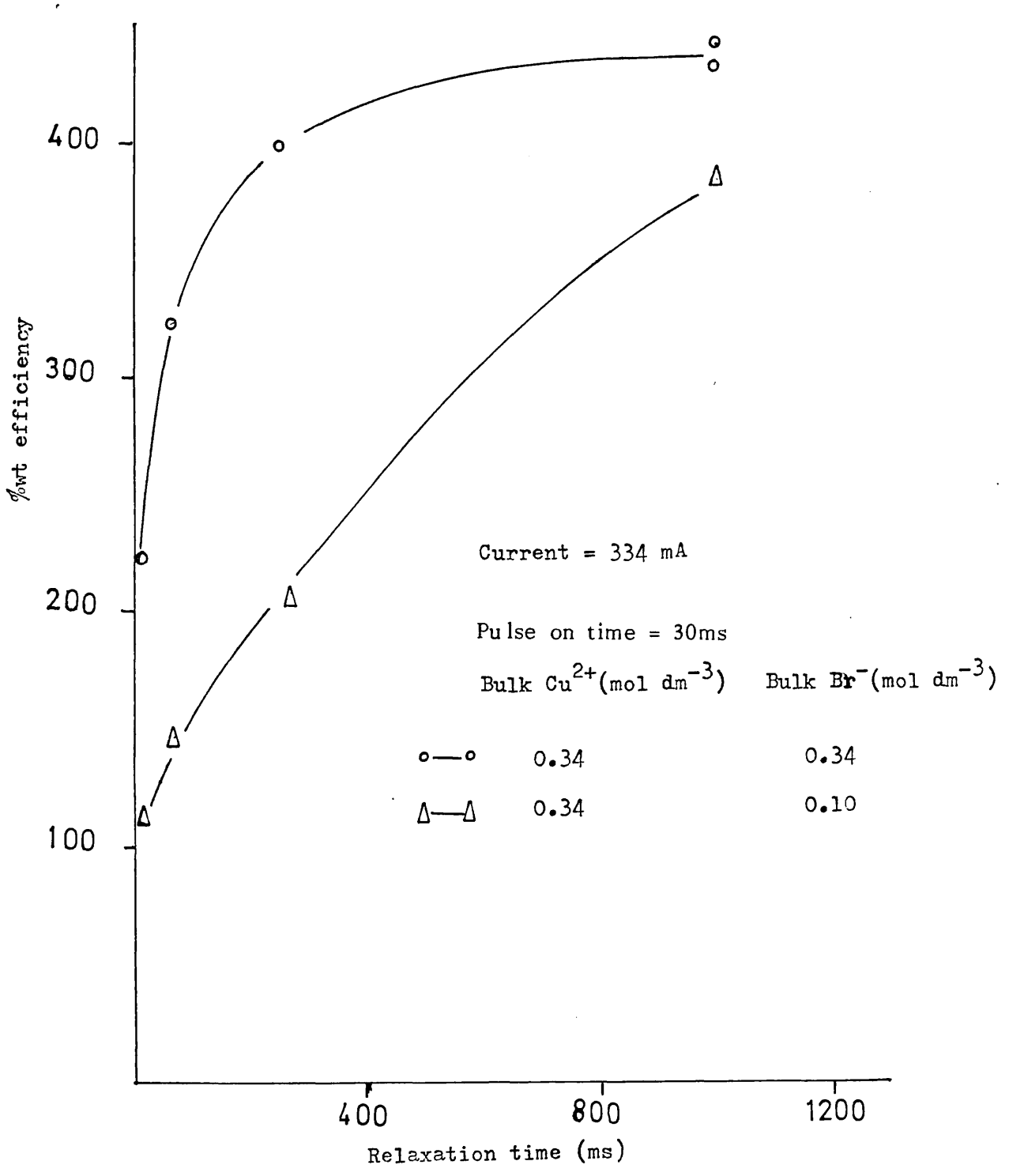

Figure (3-19)

WEIGHT OF Cu(I)Cl FORMED AT DIFFERENT Cu^{2+} AND Cl^- CONCENTRATIONS:

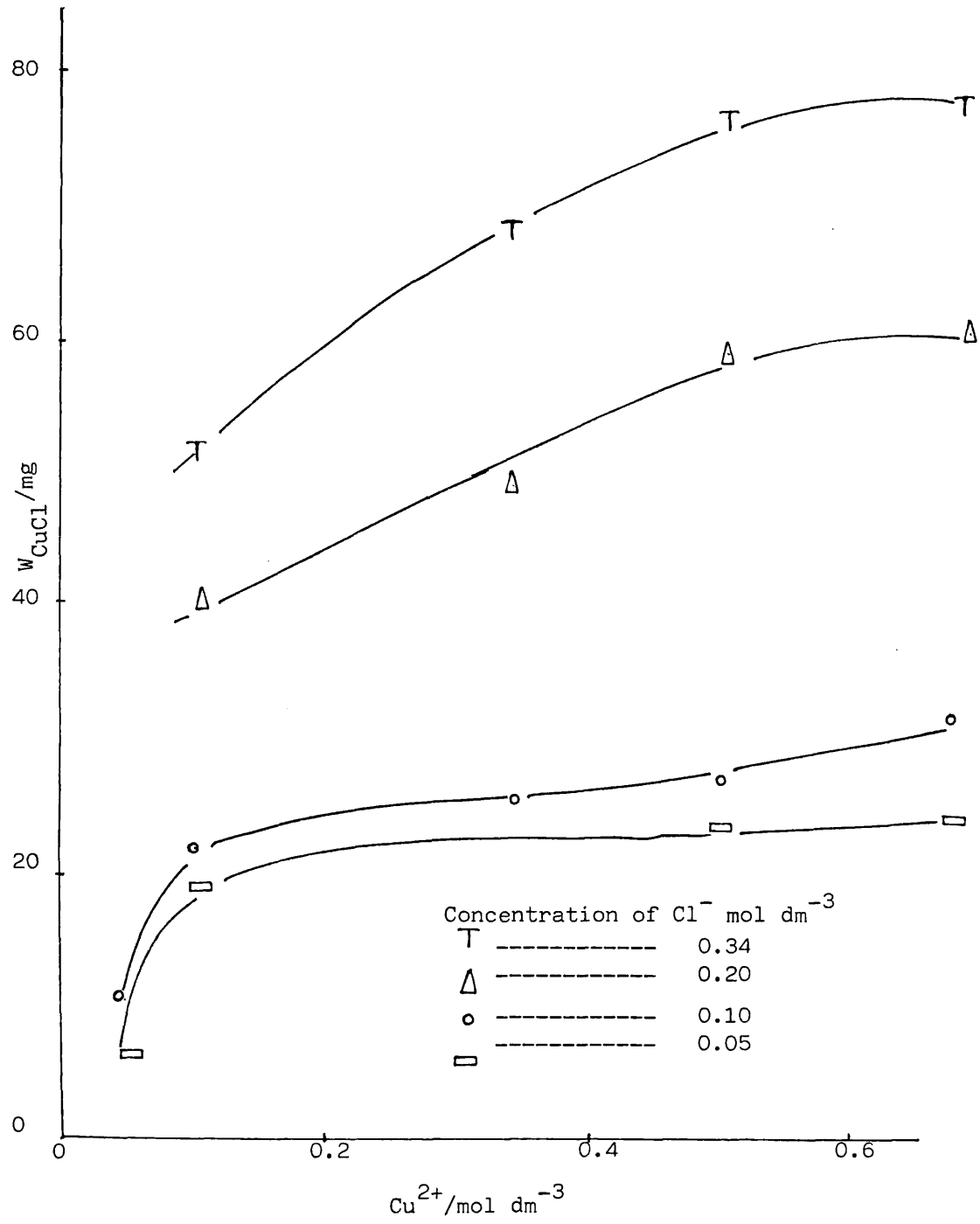

Figure (3-20)

EQUILIBRIUM CONCENTRATIONS OF COPPER CHLORIDE COMPLEXES:

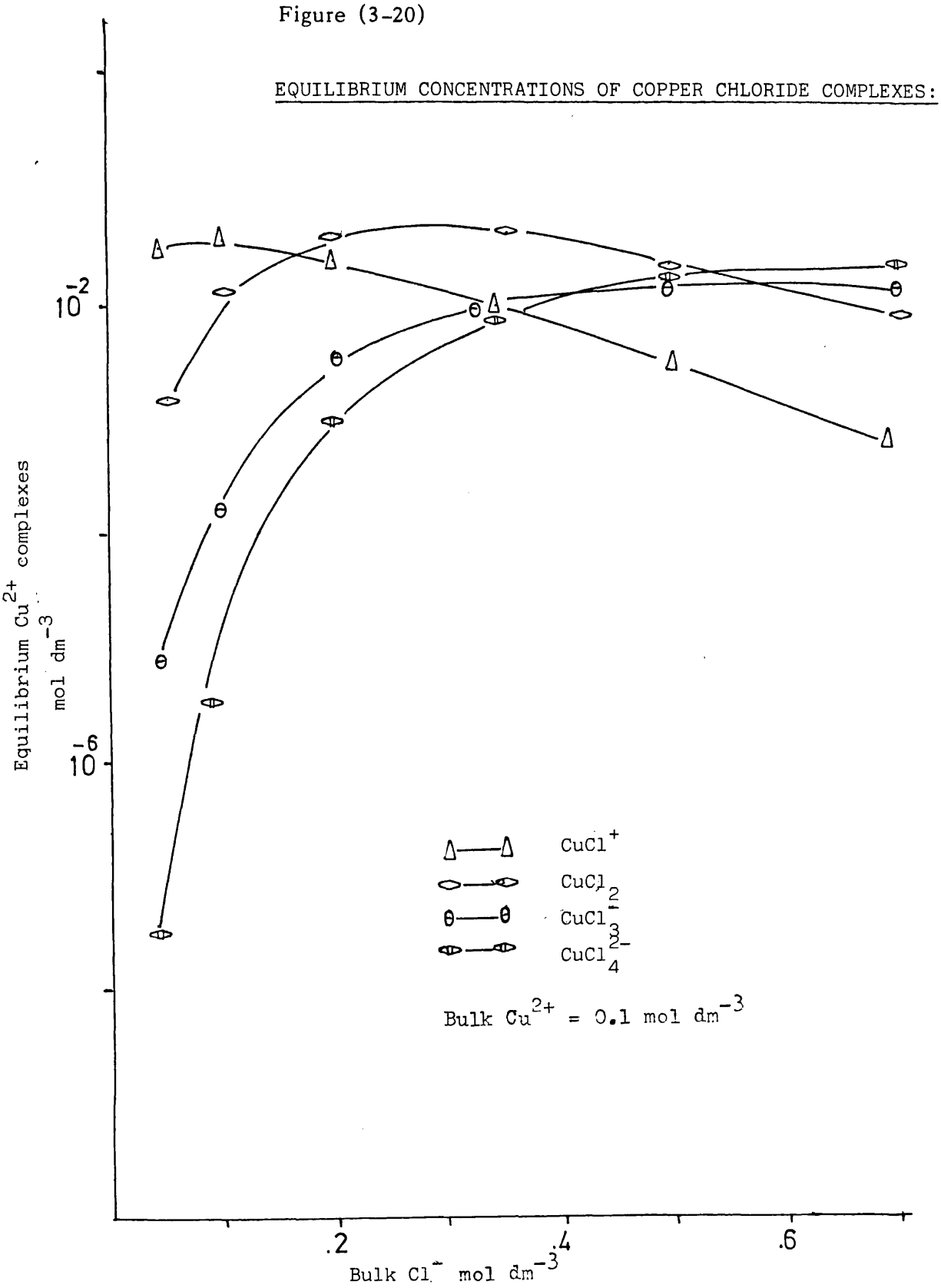

Figure (3-21)

EQUILIBRIUM CONCENTRATIONS OF COPPER CHLORIDE COMPLEXES:

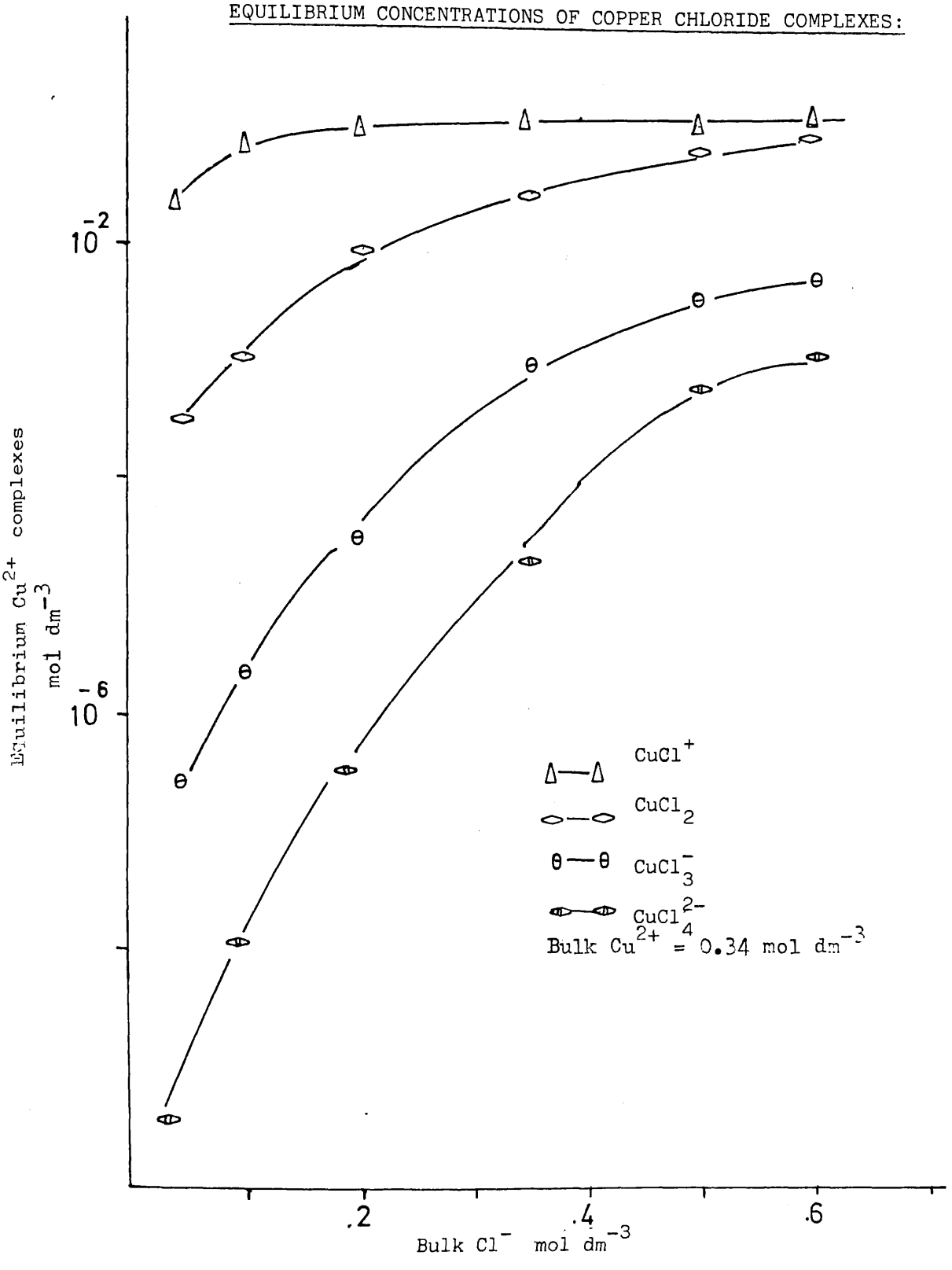

Figure (3-22)

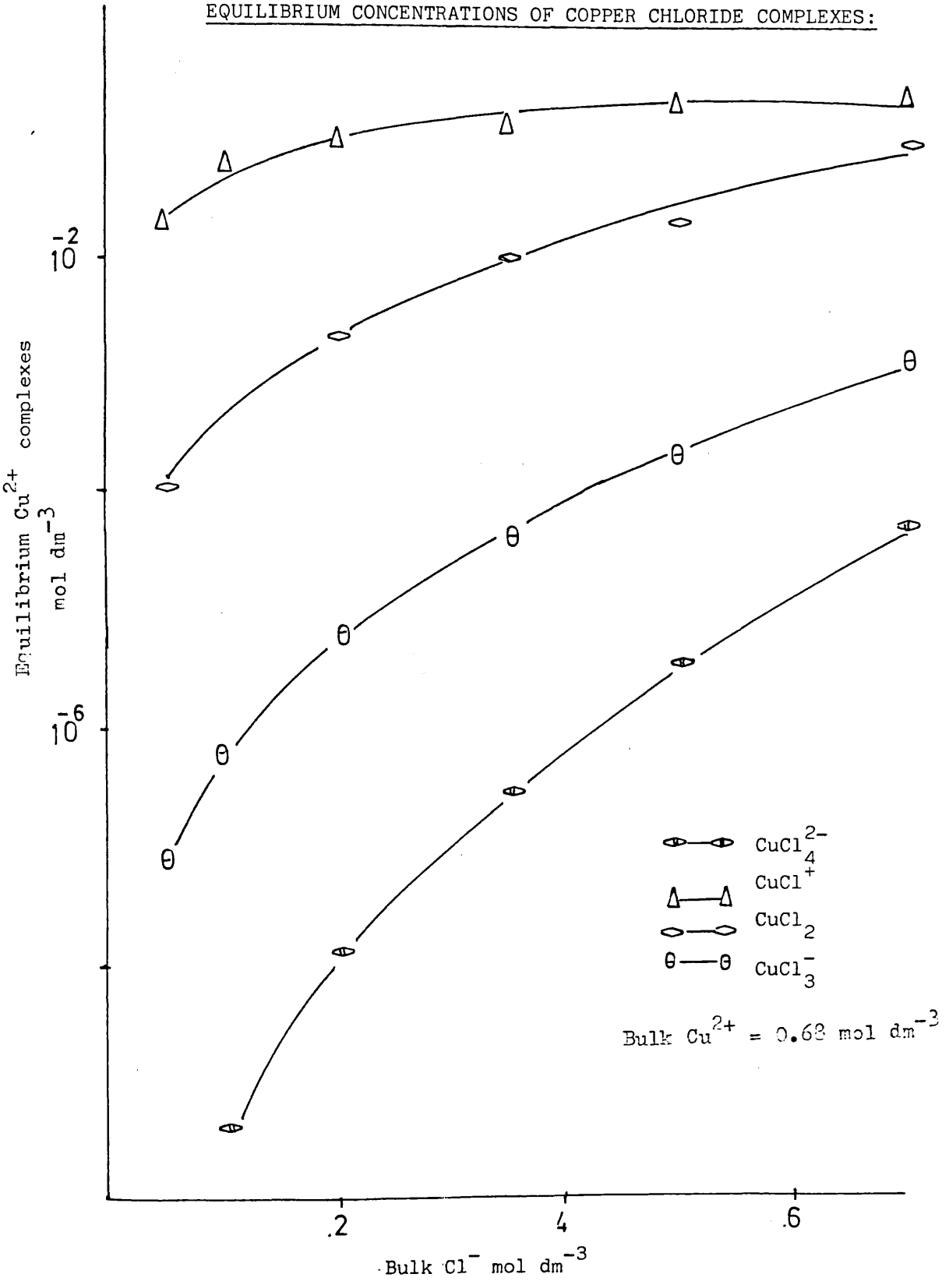
EQUILIBRIUM CONCENTRATIONS OF COPPER CHLORIDE COMPLEXES:
Equilibrium Cu^{2+} complexes mol dm^{-3}
10^{-2}
10^{-6}
.2
.4
.6
Bulk Cl^- mol dm^{-3}
$CuCl_4^{2-}$
$CuCl^+$
$CuCl_2$
$CuCl_3^-$
Bulk Cu^{2+} = 0.63 mol dm^{-3}

Figure (3-23)

EQUILIBRIUM CONCENTRATIONS OF COPPER CHLORIDE COMPLEXES AND IONS:

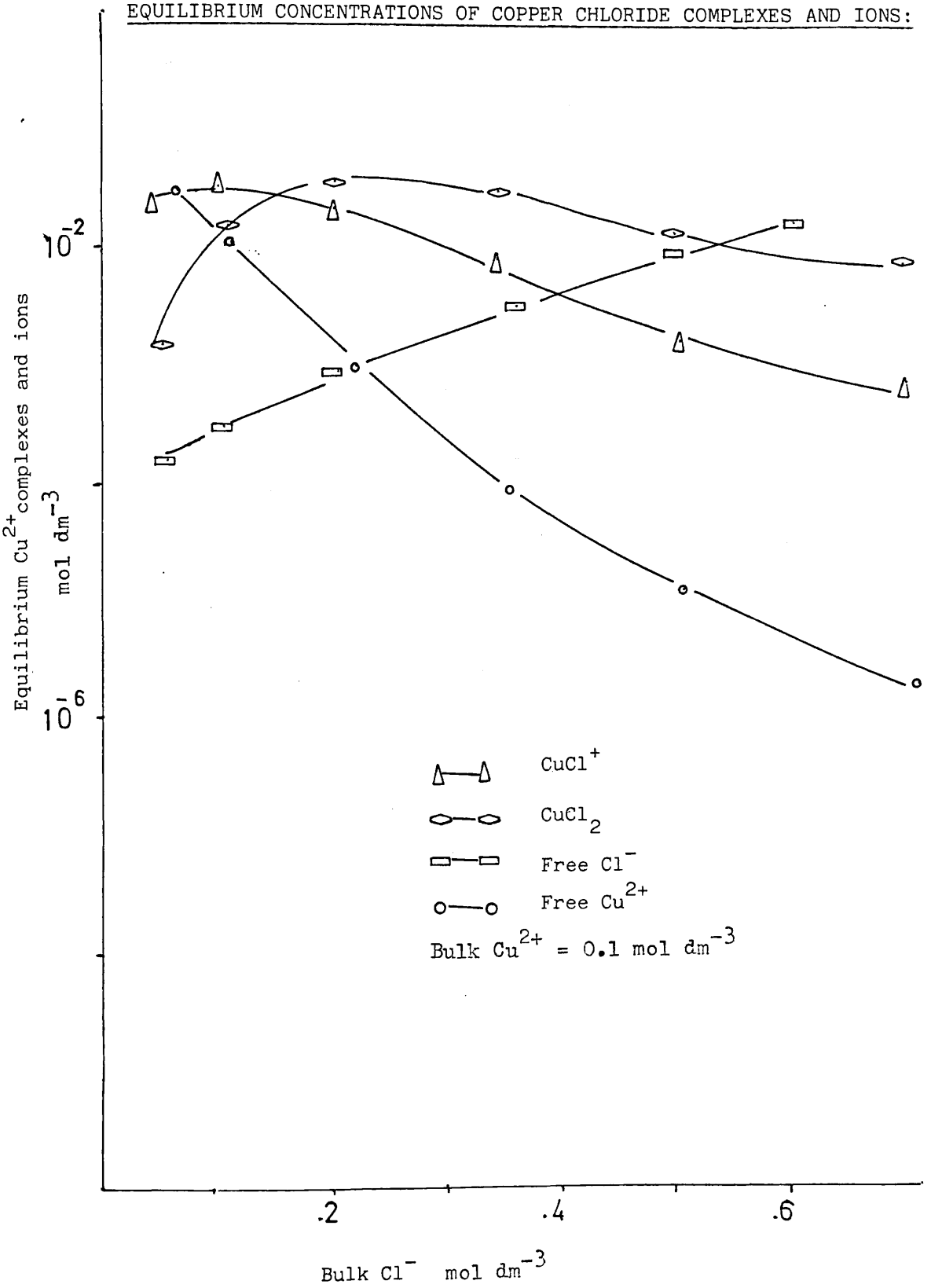

Figure (3-24)

EQUILIBRIUM CONCENTRATIONS OF COPPER CHLORIDE COMPLEXES AND IONS:

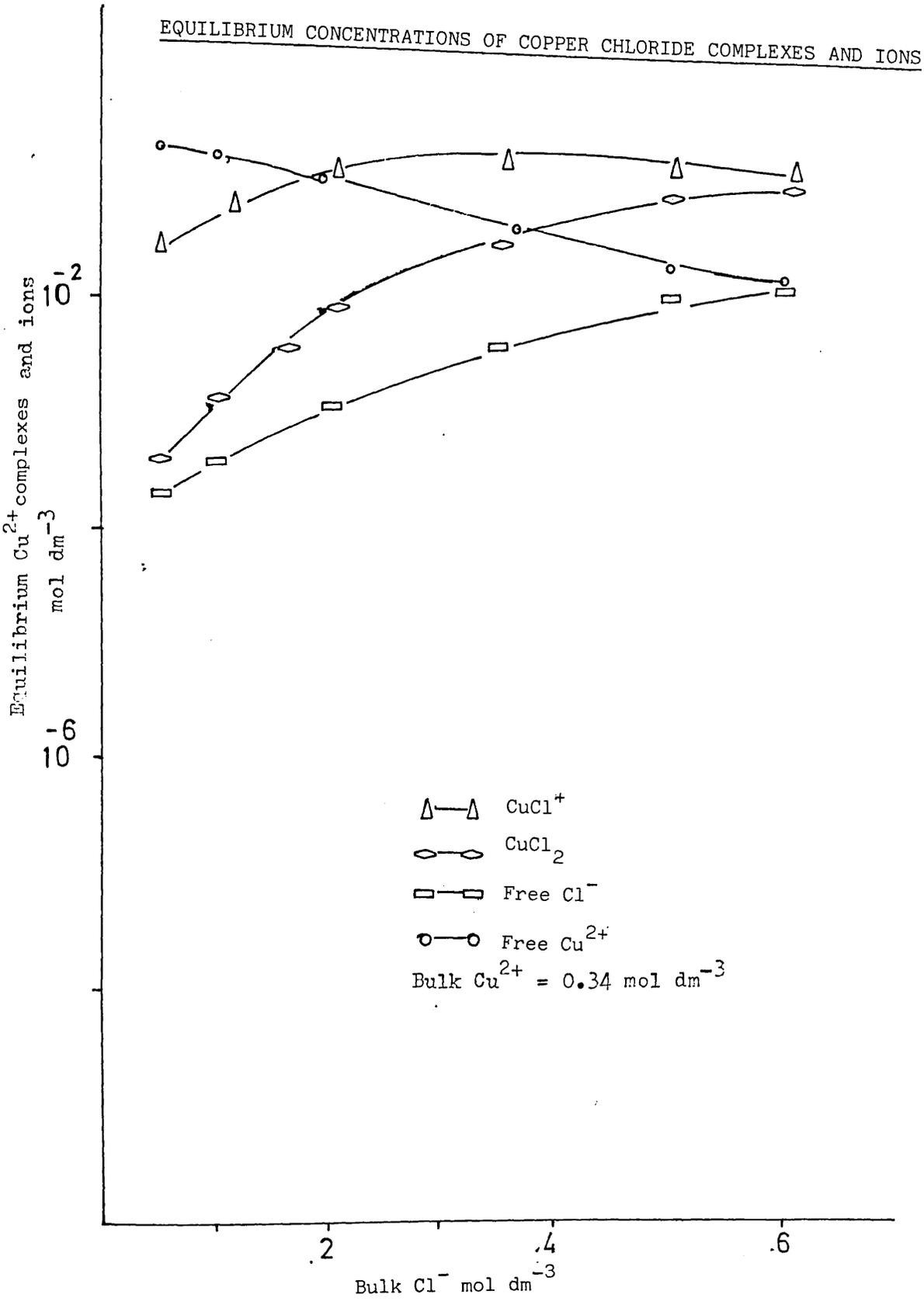

Figure (3-25) EQUILIBRIUM CONCENTRATIONS OF COPPER CHLORIDE COMPLEXES AND IONS:

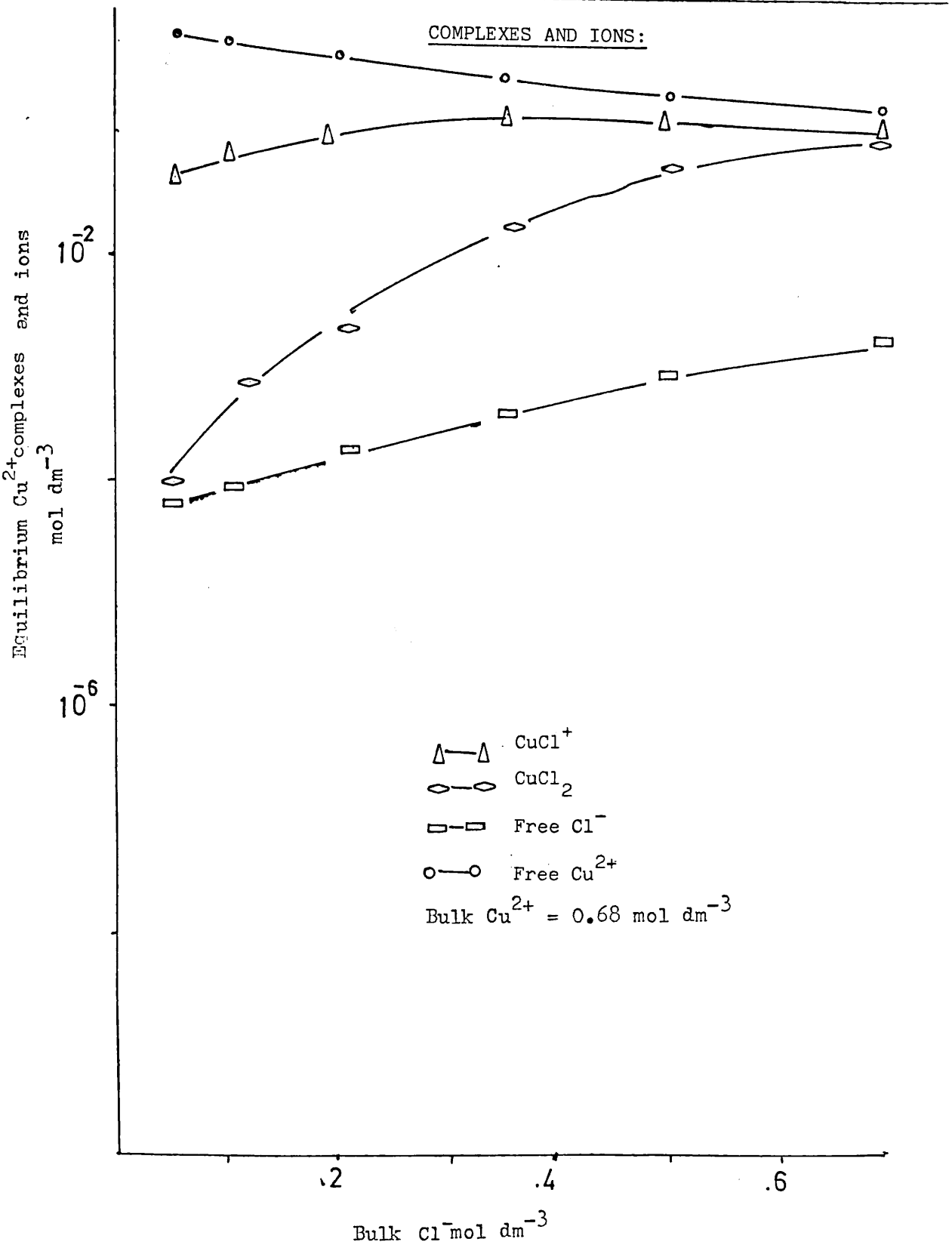

Figure (3-26)

EQUILIBRIUM CONCENTRATIONS OF COPPER BROMIDE COMPLEXES AND IONS:

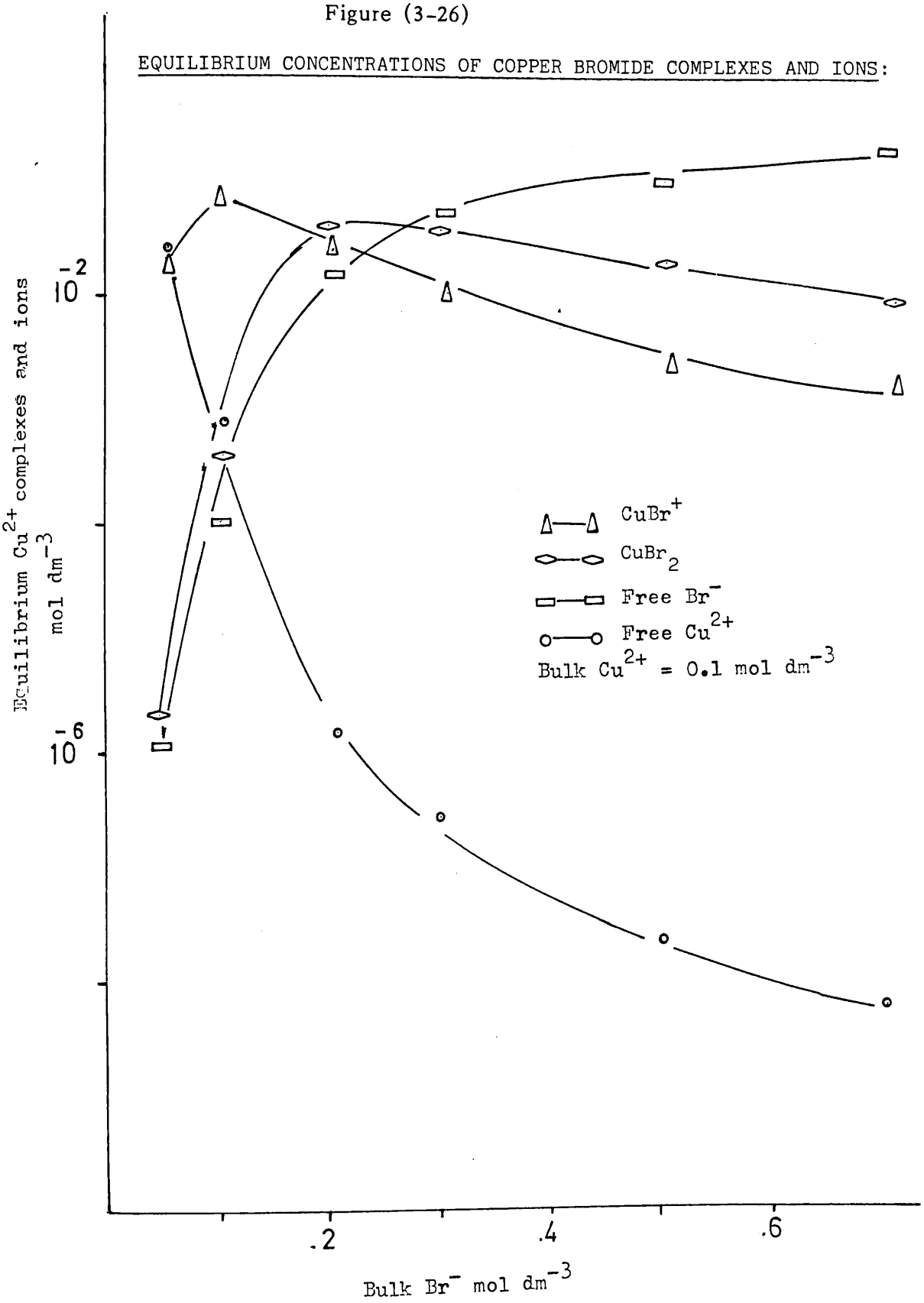

Figure (3-27)

EQUILIBRIUM CONCENTRATIONS OF COPPER BROMIDE COMPLEXES AND IONS:

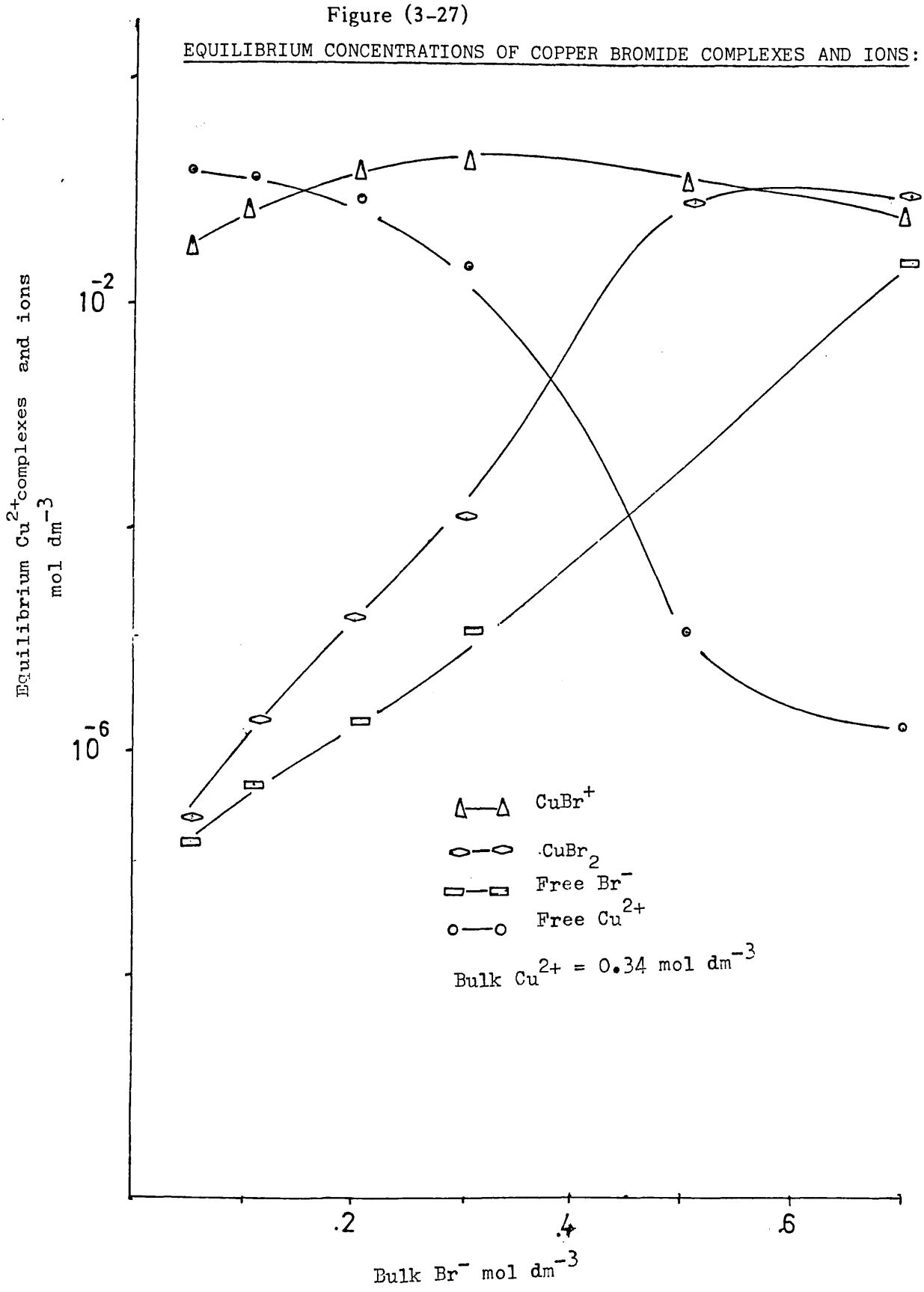

Figure (3-28)

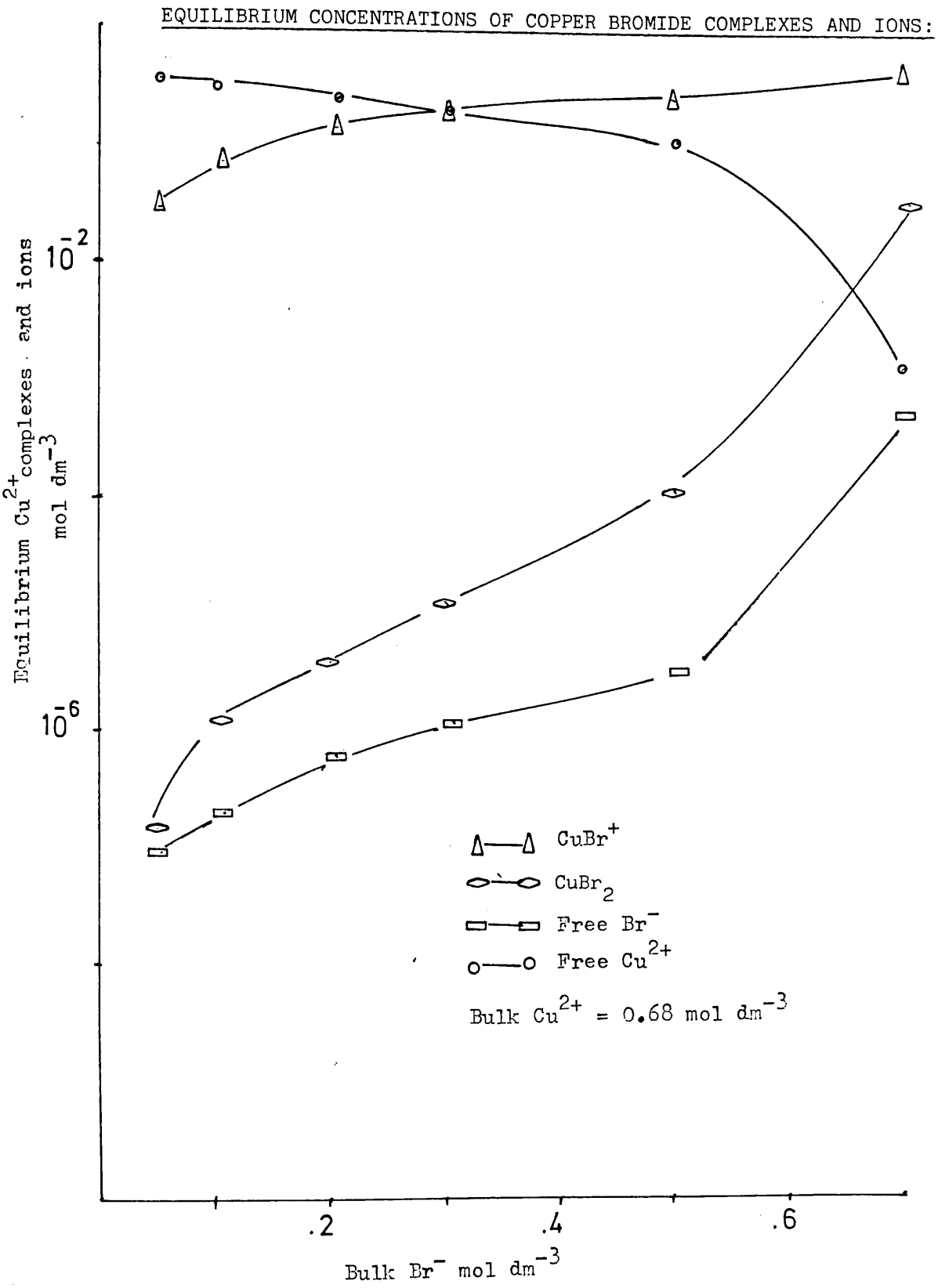
EQUILIBRIUM CONCENTRATIONS OF COPPER BROMIDE COMPLEXES AND IONS:
Equilibrium Cu2+ complexes and ions mol dm-3
10-2
10-6
.2
.4
.6
Bulk Br- mol dm-3
CuBr+
CuBr2
Free Br-
Free Cu2+
Bulk Cu2+ = 0.68 mol dm-3

Figure (3-29)

RATE OF COPPER(I)CHLORIDE FORMATION VS CONCENTRATION OF $CuCl^+$:

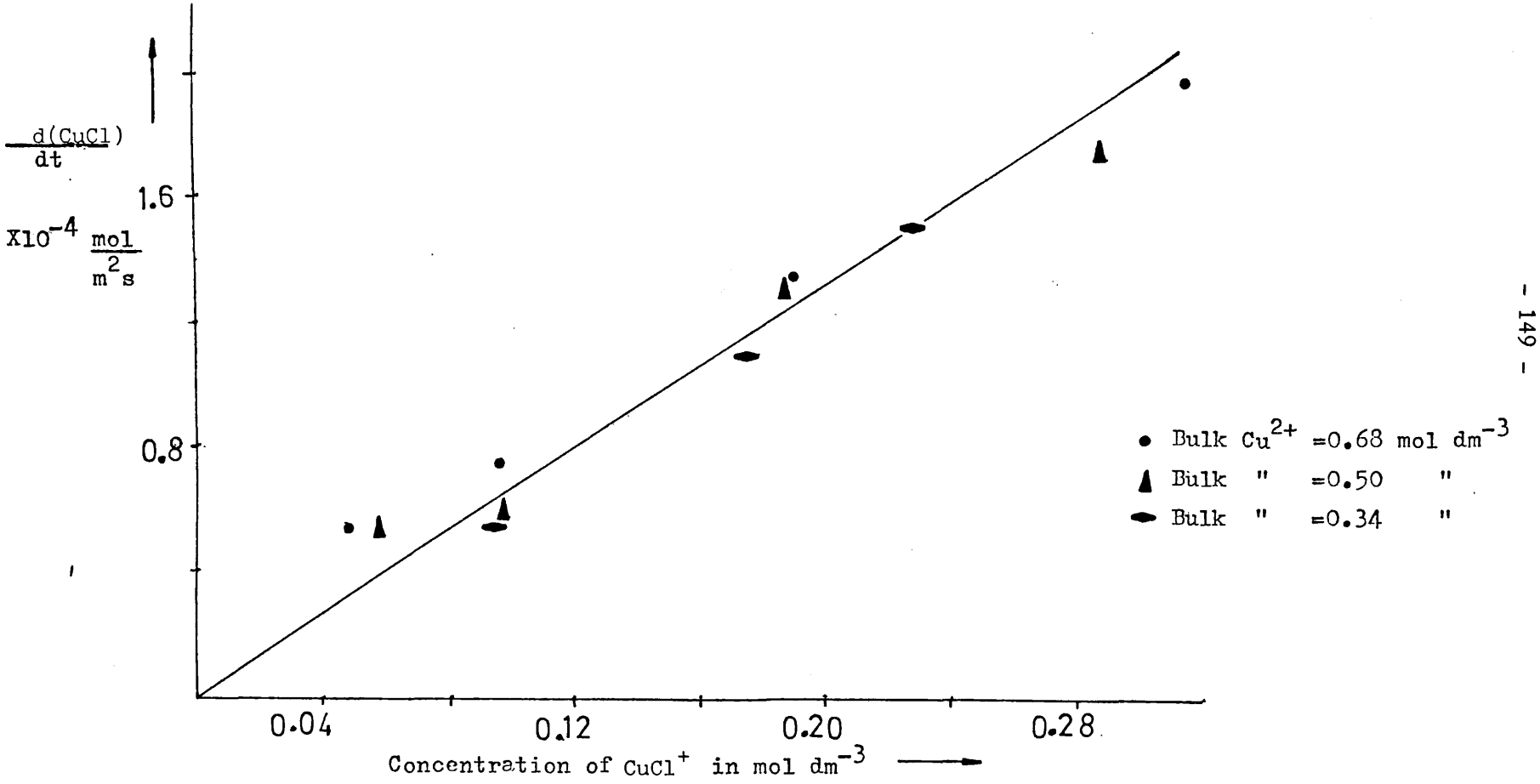

Figure (3-30)

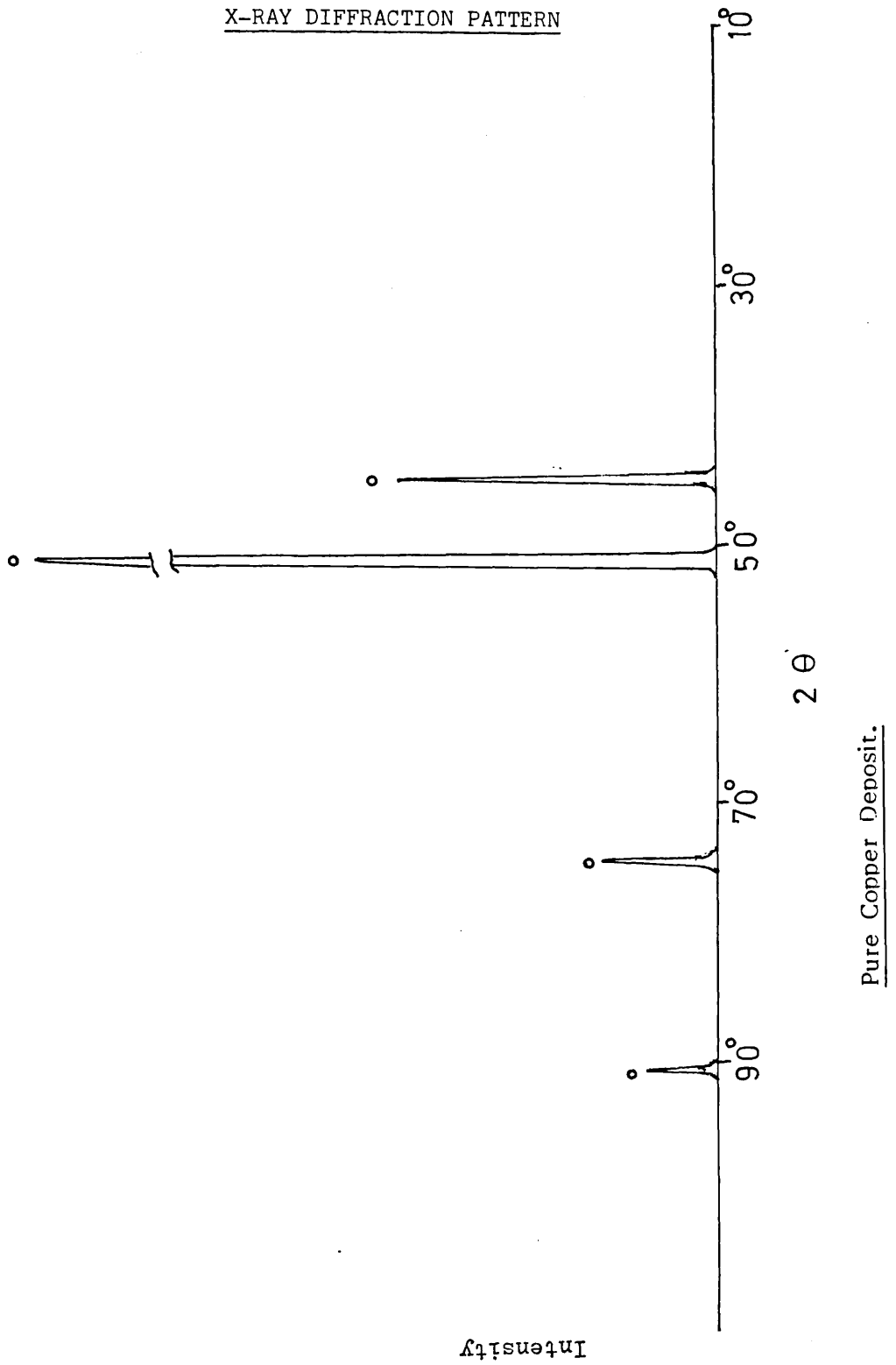
X-RAY DIFFRACTION PATTERN
10°
30°
50°
70°
90°
2θ
Intensity
Pure Copper Deposit.

Figure (3-31)

X-RAY DIFFRACTION PATTERN

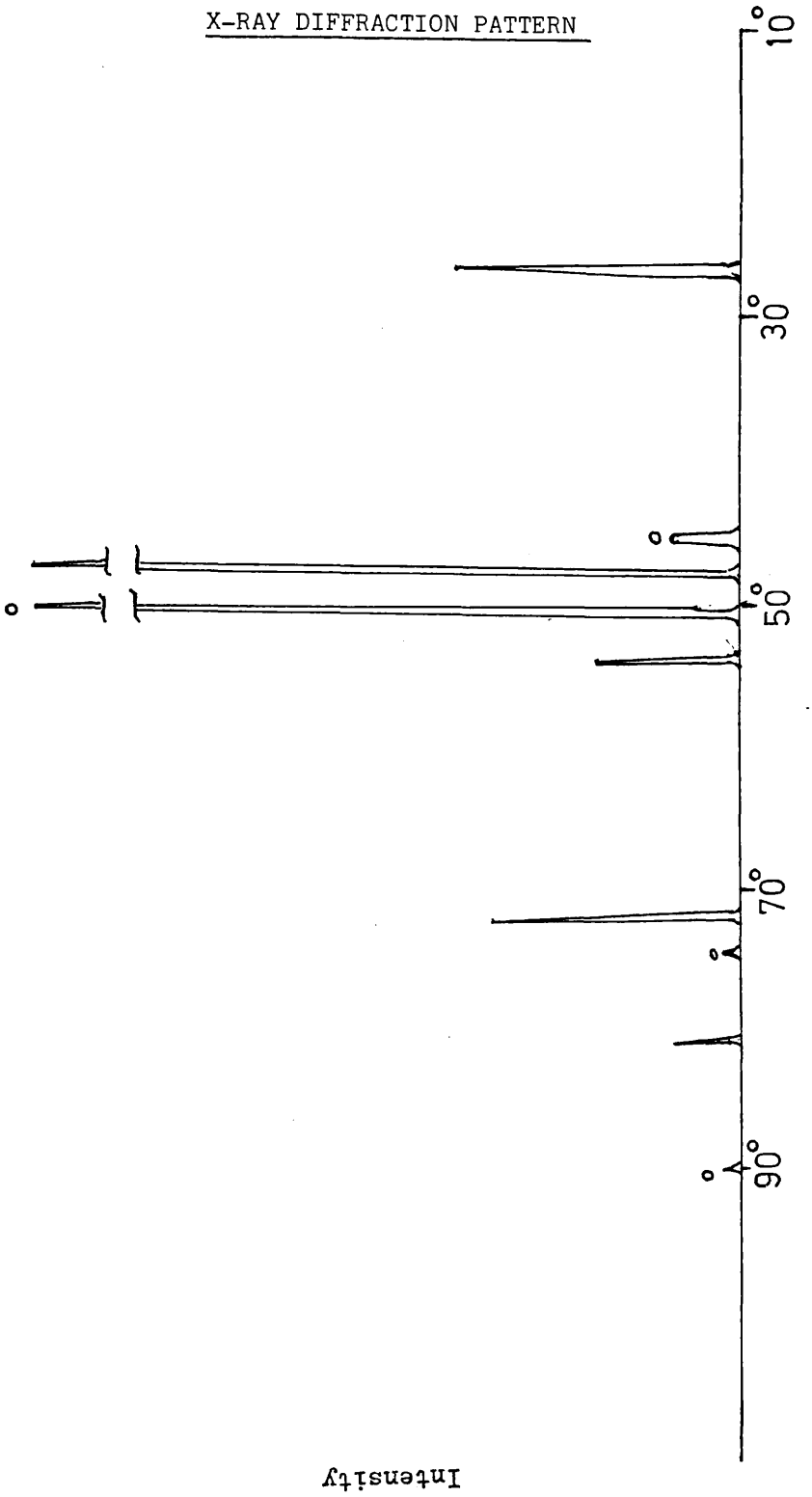

Copper Deposit with Copper Bromide.

Figure (3-32)

X-RAY DIFFRACTION PATTERN

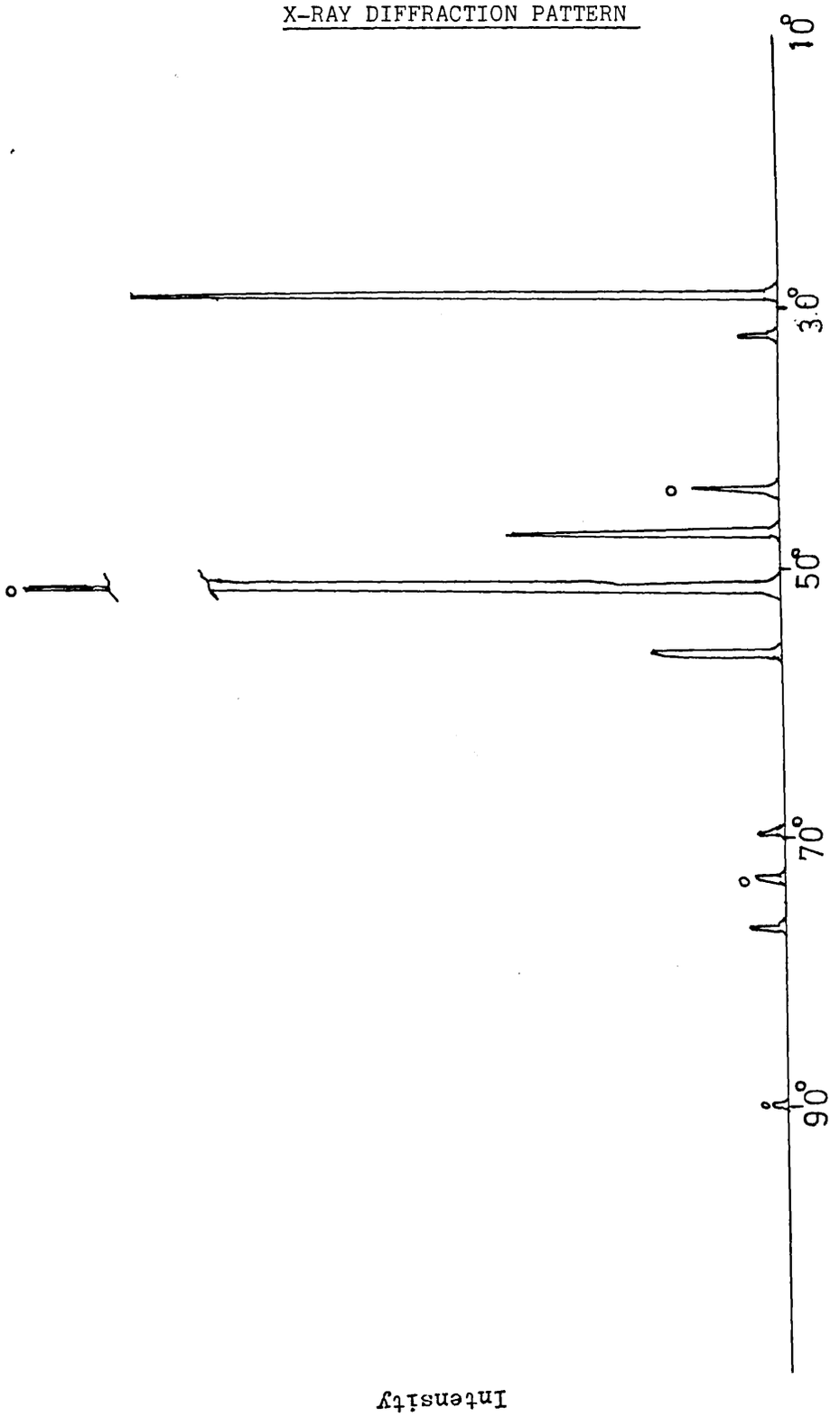

Copper Deposit with Copper (1) chloride.

Figure (3-33)

X-RAY DIFFRACTION PATTERN

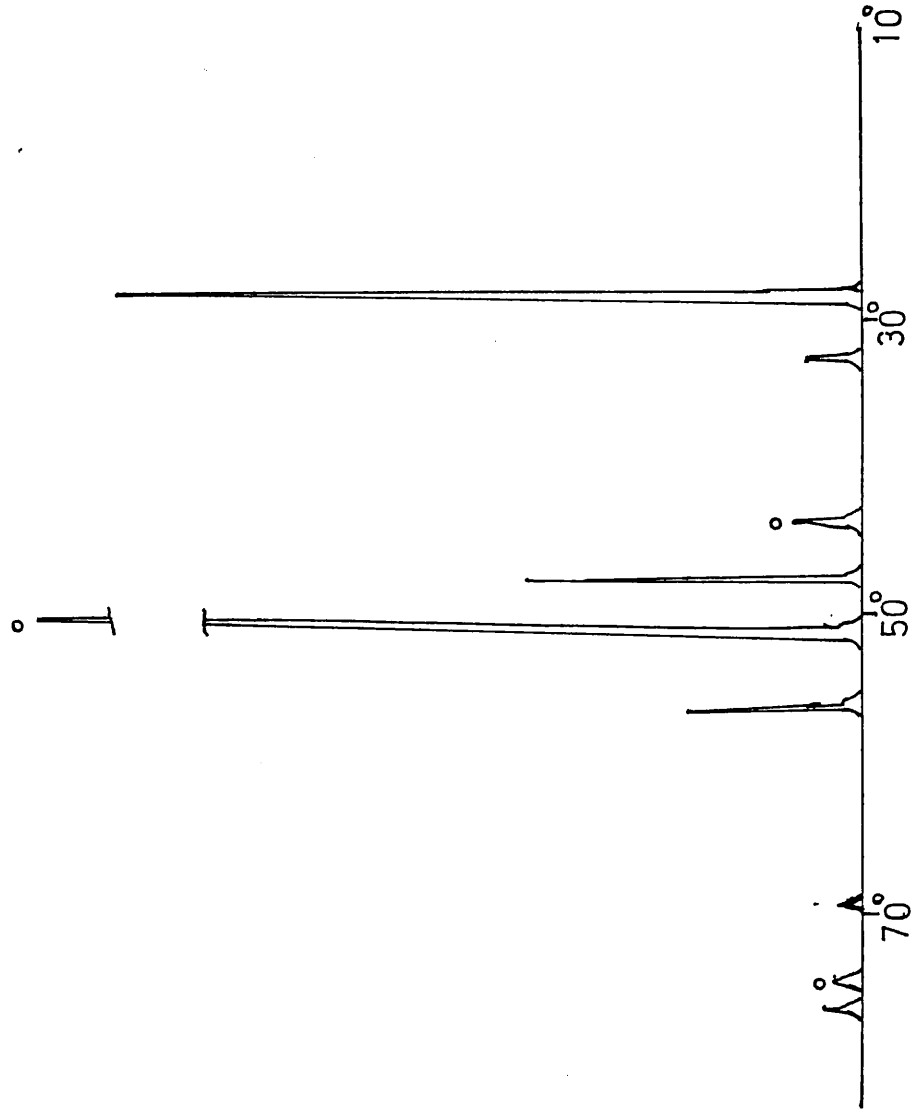

Copper Deposit with Copper (1) Chloride.

Figure (3-34)

{200 plane of copper}

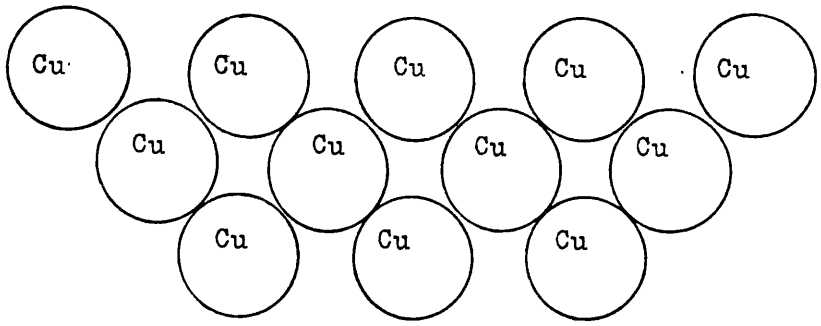

(A)

Figure (3-35)

{220 plane of copper(1) bromide.}

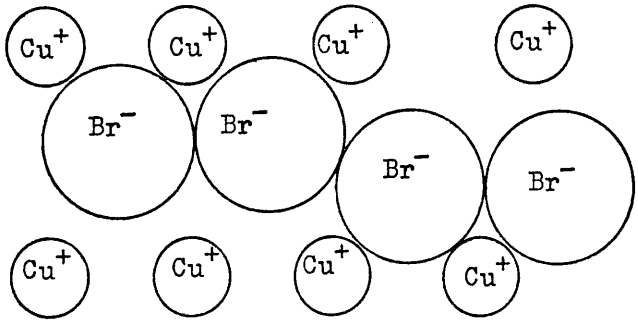

(B)

Table: (3-1)

WEIGHT OF COPPER DETERMINED BY ATOMIC ABSORPTION SPECTROPHOTOMETRY

T_{on} ms	T_{off} ms	Absorbance	ppm of Cu	Volume dm^3	Wt. of Cu g
30	5	454	3.9	25	0.0975
30	5	234	2.0	50	0.100
30	70	499	4.4	25	0.110
30	70	494	4.3	25	0.1075
30	1000	586	5.3	25	0.1325
30	1000	597	5.4	25	0.1350

T_{on} Pulse length T_{off} Relaxation time

Table (3-2)

Pulse-Plated Cu Deposit On Copper Foil

	$d/\mathring{A}_{theo}$	$d/\mathring{A}_{exp}$	I_{theo}	I_{exp}	h	k	l
Cu	2.088	2.090	100	100	1	1	1
	1.808	1.808	46	>800	2	0	0
	1.278	1.278	20	36	2	2	0
	1.090	1.091	17	21	3	1	1

Table (3-3)

Pulse-Plated Cu/CuBr Deposit On Copper Foil

	$d/\mathring{A}_{theo}$	$d/\mathring{A}_{exp}$	I_{theo}	I_{exp}	h	k	l
Cu	2.088	2.090	100	100	1	1	1
	1.808	1.807	46	>800	2	0	0
	1.278	1.275	20	36	2	2	0
	1.090	1.090	17	21	3	1	1
CuBr	3.290	3.302	100	100	1	1	1
	2.012	2.021	60	>800	2	2	0
	1.716	1.722	35	50	3	1	1
	1.308	1.308	10	90	3	3	1
	1.161	1.1634	10	23	4	2	2

Table (3-4)

Pulse-Plated Cu/CuCl Deposit On Copper Foil

	$d/\mathring{A}_{theo}$	$d/\mathring{A}_{exp}$	I_{theo}	I_{exp}	h	k	l
Cu	2.088	2.103	100	100	1	1	1
	1.808	1.804	46	>800	2	0	0
	1.278	1.284	20	31.8	2	2	0
	1.090	1.094	17	20.8	3	1	1
CuCl	3.120	3.164	100	100	1	1	1
	2.710	2.739	8	5.6	2	0	0
	1.915	1.929	55	45.1	2	2	0
	1.633	1.642	30	19.5	3	1	1
	1.354	1.358	6	3.6	4	0	0
	1.243	1.245	10	5.1	3	3	1

Table (3-5)

Pulse-Plated Cu/CuCl Deposit On Copper Foil

	$d/\mathring{A}_{theo}$	$d/\mathring{A}_{exp}$	I_{theo}	I_{exp}	h	k	l
Cu	2.088	2.094	100	100	1	1	1
	1.808	1.811	46	>800	2	0	0
	1.278	1.280	20	60	2	2	0
	1.090		17		3	1	1
CuCl	3.120	3.143	100	100	1	1	1
	2.710	2.722	8	4	2	0	0
	1.915	1.922	55	44.3	2	2	0
	1.633	1.637	30	22.2	3	1	1
	1.354	1.356	6	3.9	4	0	0
	1.243	1.245	10	4.4	3	1	1

Table: (3-6)

Pulse Length (PL) =10 ms Relaxation Time (RT) = 90 ms

Cu^{2+} mol/dm^3	Cl^- mol/dm^3	$W_{p.c.}$ g.	W_{Cucl} g.	W_E g.	Y
0.1	0.2	0.0703	0.1393	0.1528	0.636
0.34	0.1	0.0700	0.040	0.0952	0.576
0.34	0.2	0.0700	0.058	0.112	0.430
0.68	0.05	0.0689	0.0240	0.0854	0.48
0.68	0.20	0.070	0.0568	0.1113	0.425
0.68	0.34	0.0702	0.1870	0.1987	0.62

The mean value of Y =0.53$\pm$ 0.09.

Table: (3-7)

Bulk Concentration: Cu^{2+} =0.34 mol/dm^3 , Br^- =0.34 mol/dm^3

PL ms	RT ms	$W_{p.c.}$ g.	$W_{A.A}$ g.	W_E g.	Y
30	5	0.070	0.0975	0.1573	0.48
30	5	0.070	0.10	0.1562	0.46
30	70	0.070	0.110	0.2273	0.525
30	70	0.0693	0.1075	0.2170	0.52
30	1000	0.070	0.1325	0.2826	0.495
30	1000	0.070	0.135	0.295	0.495

The mean value of Y =0.50 $\pm$ 0.02

Table: 3-8

EQUILIBRIUM POTENTIALS OF REACTIONS E(3-4,p121 AND 3-6,p122) AND REST POTENTIALS

Total Cu^{2+} mol dm^{-3}	Total Cl^{-1} mol dm^{-3}	E_1^c vs. S.H.E. Volt	E_2^c vs. S.H.E. Volt	E_{rest}^{exp} Volt
0.1	0.05	0.356	0.249	0.238
0.1	0.1	0.320	0.259	0.201
0.1	0.34	0.240	0.213	0.155
0.34	0.05	0.414	0.235	0.270
0.34	0.10	0.392	0.252	0.261
0.34	0.34	0.332	0.274	0.162
0.68	0.05	0.443	0.225	0.283
0.68	0.10	0.424	0.242	0.273
0.68	0.34	0.381	0.273	0.179

Table: 3-9

THE STANDARD ELECTRODE POTENTIALS AND MEASURED MIXED POTENTIALS

Total Cu^{2+} mod dm^{-3}	Total Cl^{-1}	$E^{c}_{Cu\ 2+}$ vs. S.H.E. Volt	$E^{c}_{CuCl\ +}$ vs. S.H.E. Volt	$E^{c}_{CuCl_2}$ vs. S.H.E. Volt	E_m vs. S.H.E. Volt
0.1	0.05	0.285	0.302	0.306	0.19
0.1	0.1	0.272	0.289	0.293	0.15
0.1	0.34	0.218	0.226	0.230	0.13
0.2	0.05	0.289	0.316	0.345	0.16
0.2	0.34	0.285	0.270	0.300	0.13
0.34	0.20	0.285	0.316	0.349	0.14
0.68	0.05	0.297	0.334	0.372	0.18
0.68	0.10	0.297	0.333	0.371	0.19
0.68	0.34	0.293	0.326	0.364	-
0.2	0.1	0.287	0.311	0.341	-

Table: (3-10)

THE EQUILIBRIUM CONSTANT VALUES OF THE Cu^{+} AND COMPLEXES FORMATION REACTIONS

Copper Electrode in	Equilibrium Constants							
	K_1	K_2	K_3	K_4	K_5	K_6	K_7	K_8
Cu^{2+} + Cl^{-} solution	630.960	39.810	3.090	5.370	$1x\ 10^{-6}$	$3.98x10^{4}$	12.590	0
Cu^{2+} + Br^{-} solution	$4.780\ x\ 10^{5}$	36.310	4.786	2.344	$1x\ 10^{-6}$	$1.096\ x\ 10^{5}$	0	0

Part (3-3) DISCUSSION

Sect(3-3.1) The reaction between copper and copper (II) halide solutions :

In this study, the corrosive action of halide ions in copper (II) solutions has been confirmed. The overall reaction to give copper (I) halide is suggested to be

$$Cu + Cu^{2+} + 2X^{-} \longrightarrow 2CuX \qquad E(1\text{-}10,p24)$$

It was found that the order of reactivity of halides to equation E(1-10) is $F^{-} < Cl^{-} < Br^{-} < I^{-}$. This is supported by the thermodynamic data[81] which shows a similar increase in reduction potential for equation E(1-10), E^{o} = 0.401V, 0.607V, 1.08V for Cl^{-}, Br^{-} and I^{-} respectively.

The reaction with chloride is complicated by dissolution of CuCl giving $CuCl_2^{-}$ and possibly $CuCl_3^{2-}$. The dissolution process is seen from figure (3-5,p125). Where on increasing the concentration of chloride, the increase in weight of the foil is less by the reaction.

$$CuX + X^{-} \longrightarrow CuX_2^{-} \qquad E(3\text{-}14)$$

For X = Br^{-}, the experimental results (fig 3-6,p126) shows that the dissolution of CuBr is not so important. The equilibrium constant for equation E(3-14) is 2.8×10^{-2} for X = Cl and 4.5×10^{-3} for X = Br[81]. Conversion of $CuBr_2^{-}$ to further species is also less thermodynamically favorable[81].

For chloride and bromide solutions, the corrosion rate of fresh copper surface is great (fig 3-5,p125; 3-6,p126) and it is this fact which is used in the pulse plating experiments. During the pulse, certain amounts of copper is formed which during the relaxation time reacts to give the copper (I) halide. Optimum production of CuX occurs when the relaxation time is sufficient to allow reaction of the monolayer of plated copper, but not so great as to allow dissolution of the halide layer.

Sect (3-3.2) The Stoichiometry of the Reaction Forming CuCl and CuBr During Pulse Plating:

Noting that formation of CuX occurs only in the relaxation time of the pulse by corrosion of the newly plated. It is possible to obtain the stoichiometry of the reaction with respect to copper and halide ion and, thus, confirm that E(1-10, p165) is indeed the overall reaction which produces CuX. Analysis of the layers formed gives the total copper content and the total weight of the deposit. The total charge passed is also known, and by coulometry of the reduction of CuCl, the amount of CuCl may be determined (see page 106).

Experiments have established that in steady-state plating under the same conditions, 100% of wt efficiency for plating copper is obtained (see page 117). If the total charge passed during plating is Q coulombs, the copper deposited is Q/2F g atoms where F is the Faraday. If Q2 coulombs are passed during reduction of CuCl, the amount of CuCl formed is Q2/F mol. Let Y g atom of Cu^{o} react with 1 g atom of Cl^{-} during the formation of CuCl. Therefore , the amount of copper remaining after this reaction is

$$\left(Q/2F \times 63.54 - \frac{Y\ Q2}{F} \times \frac{63.54}{99.04}\right) \text{ g.}$$

The total weight of the deposit W_E is,

$$W_E = Q/2F \times 63.54 - Q2/F \times \frac{63.54}{99.04} \times Y + 99.04 \times \frac{Q2}{F} \qquad E(3\text{-}15)$$

Where $Q/2F \times 63.54 = W_{pc}$ E(3-16)

$Q_2/F \times 99.04 = W_{CuCl}$ E(3-17)

Therefore, the value of Y can be expressed as

$$Y = \frac{W_{pc} + W_{CuCl} - W_E \times 99.04}{63.54 \times W_{CuCl}} \qquad E(3\text{-}18)$$

Therefore, the value of Y can be obtained experimentally. Results during pulse plating in copper chloride gave $Y = 0.53 \pm 0.09$ (see table 3-6, p160). For copper bromide, the coulometric reduction process could not be used since the CuBr deposit flecked from the electrode surface during the experiment. Thus the atomic absorption method was used to analyse the copper deposit layer.

The mathematical calculation in obtaining the value Y, using this method is as follows:

Assuming 'A' mole of Cu^o reacted to give 2A mole of CuBr as shown in the equation below

$$\underset{A}{Cu^o} + Cu^{2+} + 2Br \longrightarrow \underset{2A}{2CuBr} \qquad E(3\text{-}19)$$

Also $W_E = W_{pc} - W_{pc}$ (reacted with bromide) $+ W_{CuBr}$ E(3-20)

or $$W_E = W_{pc} - (W_{AA} - W_{pc})\, A + (W_{AA} - W_{pc})2A^2 \quad \frac{M_{CuBr}}{M_{Cu^o}}$$ E(3-21)

Where W_{AA} = Weight of copper in deposit determined by atomic absorption spectroscopic method.

M_{CuBr} = Molecular weight of copper bromide

M_{Cu^o} = Molecular weight of copper

Since W_E, W_{pc}, W_{AA}, M_{CuBr} and $M_{Cu}o$ are all knowns, therefore the value of A can be determined from E(3-21) using a quadratic equation formula. Also the value of Y can be determined since Y = A/2 and the results obtained are shown in (table 3-7,p161). The mean value of Y obtained is = 0.50 ± 0.02.

The values of Y obtained for both CuCl and CuBr pulse plating confirmed that E(1-10,p165) is the general stoichiometric equation for the chemical reaction of copper in chloride, or bromide and Cu^{2+} containing solutions.

Sect (3-3.3) Calculation of Corrosion Rates

The rate of corrosion at a fresh copper surface may be determined from the formation of the copper (I) halide at different relaxation times. If conditions are chosen such that conversion to CuX is low, a constant corrosion rate may be assured.. Let N_{Cu} mol m^{-2} of copper be plated during the period of the pulse T_{on} sec, at a current density i Am^{-2} . Therefore

$$N_{Cu} = T_{on} \quad i/2F \qquad E(3-22)$$

At a corrosion rate of C mol sec^{-1} m^{-2} during the relaxation period, T_{off}, N_{CuX} mol m^{-2} are formed, i.e.,

$N_{CuX} = C\ T_{off}$

Thus

$$N_{CuX}/N_{Cu} = C/(i/2F) \times (T_{off}/T_{on}) \qquad E(3-23)$$

The ratio N_{CuX}/N_{Cu} calculated for a single pulse applies equally to any number of pulses. A plot of N_{CuX}/N_{Cu} against T_{off}/T_{on} should give, from its limiting slope at low relaxation times, a value for the corrosion rate C. Fig (3-7,p127) shows such a plot for the corrosion of copper in 0.34 mol dm^{-3} $CuSO_4$ and 0.34 mol dm^{-3} KCl. The limiting corrosion rate is 1.10×10^{-4} mol m^{-2} s^{-1}, which in terms of the increase in weight of a $8cm^2$ copper foil is 0.356 mg min^{-1} . This rate is drawn in Fig (3-5,p125) as line A. It is seen that the rate of corrosion by chloride stays close to the limiting value for several minutes until the effect of dissolution becomes important.

A similar plot for corrosion in bromide solution gave $C = 9.30 \times 10^{-4}$ mol m^{-2} s^{-1}, or 4.97 mg min^{-1} for an $8cm^2$ foil (line A in fig 3-6,p126). Thus for those metals which may be plated from solutions the pulse plating method may be used to give accurate values for corrosion rates at fresh metal surfaces.

The longest pulse on time used in the chloride containing solution in the experiments is 10ms with a constant current of 334mA. Theoretically, under this condition, approximately 0.682 monolayer of copper atoms will be plated on an $8cm^2$ electrode per pulse. The calculation is shown as follows:

Atomic radius[98] of Cu^o = 1.28 Å

Therefore area cover by one atom is

$= \pi r^2$ E(3-24)

$= 3.14 \times (1.28)^2 \times 10^{-20}$ m^2

$= 5.145 \times 10^{-20}$ m^2

Total area (apparent) of electrode

$= 8 \times 10^{-4}$ m^2

Mole of copper plated per 10ms pulse at 0.34 A

$$= \frac{T_{on} \times \text{Current}}{\text{Faraday} \times 2} \qquad \text{E(3-25)}$$

$$= \frac{10 \times 10^{-3}}{96490} \times \frac{0.34}{2}$$

$= 1.76 \times 10^{-8}$ g mole

Total number of atom is

= No of mole x Avogadro number E(3-26)

$= 1.76 \times 10^{-8} \times 6.024 \times 10^{23}$

$= 1.106 \times 10^{16}$

Therefore area cover by 10ms pulse is

= no. of atoms x area of one atom E(3-27)

$= 1.106 \times 10^{16} \times 5.145 \times 10^{-20}\ m^2$

$= 5.458 \times 10^{4}\ m^2$

Therefore the number of monolayer of copper deposited is

$$= \frac{\text{Area convered by all atoms}}{\text{Total (apparent) area}} \qquad E(3\text{-}28)$$

$$= \frac{5.458 \times 10^{4}\ m^{-2}}{8 \times 10^{-4}\ m^{-2}}$$

= 0.682

In practice, for each pulse the copper atoms might be deposited in more than 0.682 layer but cover a smaller area. Also the following pulse might be deposited at different surface of the electrode. Thus the electrode surface will be completely covered after a number of pulses. In the case of bromide containing electrolyte, the pulse length used was 30ms and with the same current. Thus for every pulse, there were more than 2 layers of copper atoms deposited.

The corrosion of the plated layers of copper atoms to form the solid copper halide probably takes place in the following manner. Initially the surface layer of the newly deposited copper atoms will be reacted with the corroding reactants. When the first layer of the deposit has been corroded to copper halide solid (CuX), the corroding reactant will have to move through the product to reach the inner layer of the deposit to react. As the product grows thicker, the

corroding reactant will find it harder to reach the inner Cu^{o}. Therefore, the corrosion reaction will slow down. Thus, the rate of the corrosion of copper atoms to CuX can be considered to be inversely proportional to the amount of solid product formed i.e.

$$\frac{d(CuX)}{dt} \propto \frac{1}{(CuX)} \qquad E(3\text{-}29)$$

or

$$\frac{d(CuX)}{dt} = \frac{k'_{CuX}}{(CuX)} \qquad E(3\text{-}30)$$

Re-arranging E(3-30) and integreating it the solution is

$$[CuX] = \sqrt{k_{CuX}\, t} \qquad E(3\text{-}31)$$

Where k'_{CuX} and K_{CuX} are constants, t is the total CuX formation reaction time and $[CuX]$ is the number of mol m^{-2}.

The above relationship of E(3-31) will hold when the dissolution of the product is not significant. E(3-31) shows that a plot of $[CuX]$ v s. $\sqrt{t}$ should be linear if the above hypothesis is right. Figures (3-8, p128) and (3-9,p129) show that the linear relationship hold. In addition, in an electrolyte with the bulk concentration of CuX^{2+} = 0.34 mol dm^{-3} and Cl^{-} = 0.1 mol dm^{-3}, the value of K_{CuX} was found to be 1.573×10^{-5} mol m^{-2} s^{-1}. (from fig 3-8,p128). In a bromide containing solution with the concentrations of Cu^{2+} = 0.34 mol dm^{-3} and Br^{-} = 0.1 mol dm^{-3} or 0.34 mol dm^{-3} the value of K_{CuX} were found to be 4.62×10^{-5} and 1.284×10^{-4} (fig 3-9,p129) mol m^{-2} s^{-1} respectively. This shows that the rate of reaction of Br^{-} is greater than Cl^{-} in the corrosion reaction.

Sect (3-3.4) Reaction occuring during relaxation time:

$$Cu^{+} + Cl^{-} \xrightarrow{k_{Cu^+}} CuCl \qquad E(3\text{-}32)$$

$$CuCl^{+} + Cu^{o} \xrightarrow{k_{CuCl^+}} CuCl + Cu^{+} \xrightarrow{Cl^-} 2CuCl \qquad E(3\text{-}33)$$

$$CuCl_2 + Cu^{o} \xrightarrow{k_{CuCl_2}} 2CuCl \qquad E(3\text{-}34)$$

$$CuCl_3^{-} + Cu^{o} \xrightarrow{k_{CuCl_3^-}} 2CuCl + Cl^{-} \qquad E(3\text{-}35)$$

$$CuCl_4^{2-} + Cu^{o} \xrightarrow{k_{CuCl_4^{2-}}} 2CuCl + 2Cl^{-} \qquad E(3\text{-}36)$$

$$CuCl + Cl^{-} \xrightarrow{k_{CuCl}} CuCl_2^{-} \qquad E(1\text{-}7,p19)$$

From the above equations, the rate of formation of copper (I) chloride can be written as follows:

$$\frac{d(CuCl)}{dt} = k_{Cu^+}[Cu^{+}][Cl^{-}] + k_{CuCl^+}[CuCl^{+}] + k_{CuCl_2}[CuCl_2] + k_{CuCl_3^-}[CuCl_3^{-}] + k_{CuCl_4^{2-}}[CuCl_4^{2-}] - k_{CuCl}[Cl^{-}] \qquad E(3\text{-}37)$$

Equation E(3-37) shows that the rate of formation of CuCl is directly proportional to the concentrations of Cu^{+}, $CuCl^{+}$, $CuCl_2$, $CuCl_3^{-}$, and $CuCl_4^{2-}$. Also inversely proportional to concentration of Cl^{-}. The computer calculated results (fig 3-20 to 3-22, p140 to 142) show that the equilibrium concentrations of $CuCl^{+}$ are significantly higher than the rest of the complexes at the bulk concentration of Cu^{2+} between 0.34 to 0.68 mol dm^{-3} and Cl^{-} of less than 0.5 mol dm^{-3}.

Thus the rate of formation of copper (I) chloride of E(3-37,p174) can be simplified to

$$\frac{d(CuCl)}{dt} = k_{CuCl^+}[CuCl^{+}] \qquad E(3\text{-}38)$$

Therefore, a plot of concentration of $[CuCl^+]$ v.s. $\frac{d[CuCl]}{dt}$ will yield a straight line. For the experiment carried out with Cu^{2+} concentrations of 0.34, 0.5 and 0.68 mol dm^{-3} and Cl^- concentrations of less than 0.5 mol dm^{-3}, a straight line plot was obtained as shown in figure (3-29,p149). The rate constant k_{CuCl^+} which is the gradient of the curve was found to be equal to 6.56×10^{-7} m s^{-1}. The corrosion rate of each particular bulk concentration of Cu^{2+} between 0.34 and 0.68 mol dm^{-3} and Cl^- of less than 0.5 mol dm^{-3} can be estimated from this plot. For the bulk concentration of Cu^{2+} = 0.34 mol dm^{-3}, the computer calculated value of the equilibrium concentration of $CuCl^+$ is 2.251×10^{-1} mol dm^{-3}. Therefore, from figure (3-29,p149) the rate of formation of CuCl or also known as corrosion rate is 1.44×10^{-4} mol m^{-2} s^{-1}. This value is reasonably closed to the value of the limiting corrosion rate evaluated by the previous method (see page 170) i.e. equal to 1.10×10^{-4} mol m^{-2} s^{-1}.

The above results indicated that during the relaxation time, the rate of formation of CuCl is directly proportional to $CuCl^+$ when $CuCl^+$ complex is the predominant species in the chloride containing solution.

Other possible reactions instead of E(3-33,p174) which also involved $CuCl^+$, Cu^o and Cl^- during the relaxation time are as follows:

$Cu^{o} + Cl^{-} \rightleftharpoons CuCl + e$ E(3-4,p121)

$CuCl^{+} + e \rightleftharpoons CuCl$ E(3-6,p122)

The above reactions are localised electrochemical corrosion reactions. The rate of formation of copper (I) chloride in this case is the same as E(3-38,p175). The pulse deposited copper acts as an electron sink area at which the dissolution of copper occurs. The interfacial $CuCl^{+}$ ions will consume the electrons liberated by the copper dissolution process. For these two processes to take place simultaneously, it is necessary and sufficient that the potential difference across the interface be more positive than the equilibrium potential of the Cu^{o} corrosion reaction i.e. E(3-4) and more negative than the equilibrium potential of the reduction of $CuCl^{+}$ of E(3-6).

The experimental results on table (3-8,p162) show that four out of nine of the measured rest "corrosion" potential difference across the interface fall within the two calculated "corrosion" equilibrium potential values. These values are the E_1^c , and E_2^c of reactions E(3-4) and E(3-6) respectively (see p121 for the calculations). Thus this suggests that it is not possible to confirm that the copper (I) chloride formation reaction is a chemical reaction according to E(3-33,p174) or a localised electrochemical corrosion reactions [i.e. E(3-4,p176) and E(3-6,p176)].

The above observations suggest that more investigations are needed to confirm the mechanism of the corrosion reaction during relaxation time. In addition more accurate values of the activity coefficients of the chloride containing copper sulphate solutions might be needed. It is assumed here the activity coefficients of the chloride containing cupric sulphate is equal to the activity coefficient of the pure $CuSO_4$ solution, at equal total Cu^{2+} concentration. This assumption might not be accurate enough for the calculations of E_1^c and E_2^c .

The computer calculated results of the equilibrium concentrations of free Br^-, free Cu^{2+} Br^+ and $CuBr_2$ complexes vs. the Br^- bulk concentration plots, have the same general trend as in the chloride plots (sse figure 3-23 to 3-28,p143, to p148). This is only true when both the Cl^- and Br^- containing solutions have the same Cu^{2+} bulk concentration and same Cl^- and Br^- ions bulk concentration. Since the equilibrium concentrations have

similar trend, this might suggest that the reaction mechanism of copper (I) bromide formation during the relaxation time is probably similar to chloride case. This is further supported by the overall copper (I) halide formation reaction equation E(1-10,p165) which is applicable to both chloride and bromide containing solutions.

Sect(3-3.5) Reactions of Copper Deposition Process During Pulse Plating.

During the pulse plating of pure copper in acid copper sulphate solution, the mechanism of the deposition is shown in equation E(1-1,1-2,p6) i.e.

$$Cu^{2+} + e \underset{\text{slow}}{\rightleftharpoons} Cu^{+} \qquad E(1-1)$$

$$Cu^{+} + e \underset{\text{fast}}{\rightleftharpoons} Cu^{o} \qquad E(1-2)$$

The % weight efficiency of the copper deposition based on Faraday's Law of electrolysis decreased as the pulse length is shorter and the relaxation time is longer in acidic copper sulphate solution (fig 3-10,p130). This is probably due to the double layer charging current effect and also corrosion of the deposited copper by the acidic enviroment. The trend of the decrease in efficiency of the results obtained (fig3-10,p130) agreed with those obtained by Cheh et al[83]. Their % efficiency by weight is lower than those obtained in this experiment. This is probably because they were using a rotating disk electrode. Thus this will accelerate the corrosion rate during relaxation time since the shear force acting on the rotating electorde is greater than a stationary electrode. It was observed by Cheh et al[83] that the amount of copper deposit corroded in their experiments depended on the rotation speed of the disk electrodes.

From the above experimental results (fig 3-10) it was decided that the minimum pulse length used in the experiments with different chloride or bormide containing electrolytes was 2ms. The % weight lost due to enviromental acidic corrosion was corrected for each experiment.

There are four possible species formed which Cu^{o} would be deposited from halides containing solutions. The most commonly known is the Cu^{2+} ions as shown in equation (3-7,p122). The other three complexes which could be involved in the deposition processes are shown in the following equations:

$$CuX^{+} + 2\ e \longrightarrow Cu^{o} + X^{-} \qquad E(3\text{-}39)$$

$$CuX_{2} + 2\ e \longrightarrow Cu^{o} + 2X^{-} \qquad E(3\text{-}40)$$

$$CuX_{3}^{-} + 2\ e \longrightarrow Cu^{o} + 3X^{-} \qquad E(3\text{-}41)$$

The theoretical electrode potentials of the copper electrode reactions of E(3-7,p122), E(3-39) and E 3-40) were calculated at different bulk concentrations of Cu^{2+} and Cl^{-} (see p124). This was carried out by assuming that the electorde potentials due to each species in the solution is not affected by the presence of the other species. The concentration of each species is obtained from the result of the computer program. The activities of each species were than used in the calculations.

The activity coefficients of the pure acidic Cu^{2+} solutions at different concentrations were obtained from CRC Hand book of chemistry and physics[87]. These values[87] were then assumed to be the same activity coefficients of the chloride containing solutions which had the same Cu^{2+} concentrations.

From table (3-9,p163) the electrode potentials of the $CuCl^+$ and $CuCl_2$ deposition reactions are slightly higher than the electorde potentials of the Cu^{2+} deposition reaction at each particular Cu^{2+} and Cl^- bulk concentration. This suggests that the free Cu^{2+} ions are more stable than the complexes. Therefore, thermodynamically the complexes are more likely to plate than free Cu^{2+}. The electrode potentials of the three reactions also decrease as the bulk concentrations of the Cl^- increase. Thus this indicates that the free Cu^{2+}, $CuCl^+$ and $CuCl_2$ become more stable at higher bulk Cl^- concentrations. The table also shows the measured mixed electrode in some of the experiments. These mixed potentials could not be used in comparing with the calculated equilibrium value. This is because the galvanostatic pulse technique used was affected by the copper halide formation reaction during the relaxation time.

From the computer calculated equilibrium concentration results, (fig3-20 to 3-22,p140 to 142) show that at different bulk concentrations of Cu^{2+} and Cl^-, the copper complexes, $CuCl^+$, $CuCl_2$ and $CuCl_3^-$ are present. Also figures (3-23 to 3-25,p143 to 145) show that free Cu^{2+} ions are present. Therefore, it is quite likely that the electordeposition of Cu^o during pulse on-time involves the Cu^{2+}, $CuCl^+$, $CuCl_2$ and $CuCl_3^-$.

Sect (3-3.6) The Production of Sea-Water Battery Anodes

Pulse method may be a useful method for the production of copper chloride anodes for reserve sea-water batteries. Various types of copper (I) chloride electrodes i.e. high conductivity (could be used in high power battery) or low conductivity can be easily manufactured without much alteration of the production procedures, by changing the pulse length and relaxation time combinations or the temperature of the plating bath or the chemical composition of the bath.

Figures (3-11 to 3-16,p131 to p136) show the copper (I) chloride electrodes which have different discharge rates i.e. different conductivities or power output. These electordes were obtained with different pulse combinations. At constant pulse length temperature and concentration of solution, the discharge rate or conductivity of the electrode is inversely proportional to relaxation time. This is because more pulse deposited Cu^{o} been reacted to form Cu (I) Cl (fig 3-17,p137) or Cu (I)Br (fig 3-18,p138) as in the case of bromide containing solution.

This method also does not seem to consume much energy in the production of copper (I) chloride. The energy is mainly used in pulse plating and maintaining the temperature of the plating solution (i.e. within the range of $298k^{o}$ to $313^{o}k$). The other methods such as the extrusion of the copper chloride mixture melt and the dipping of copper plate into molten copper (I) chloride, the amount of heat energy used in the melting of copper (I) chloride seem to be considerable higher than the total energy used in the pulsed method.

Sect(3-3.7) Structure of The Copper Halide Deposits

The copper foil electordes used in this work were oriented along the (200) plane (fig3-30,p150) table (3-2,p156). From the X-ray results (fig3-31,p151) table (3-3,p157),copper bromide appears to have been deposited with the (200) plane upper most. The X-ray results of the copper (I) chloride (fig3-32,3-33,p152,153) table (3-4 and 3-5,p158,159) do not indicate that copper chloride have been deposited with the (220) plane uppermost.

Copper crystallizes in a face-centered cubic arrangement with a unit cell length of $3.615^{o}A$[84]. The (200) plane of copper is shown in figure (3-34,p154). Copper bromide exhibits a zinc blende structure in which copper is found in tetrahedral holes formed by bromide ions with a = $5.691^{o}A$[85].(Fig 3-35,p154)gives the (220) plane of CuBr in which the radius of Cu^{+} and Br^{-} are $0.96^{o}A$, respectively[85]. It is seen that the Cu - Cu distance in the X direction of the two planes is quite similar (3.6 A^{o} in copper and 4.0 A^{o} in copper (I) bromide), and thus, a CuBr lattice may be built up the insertion of bromide ions with a limited relaxation of copper ions from the underlying lattice. Such an obvious orientation is not seen with CuCl. Dissolution of CuCl as $CuCl_2^{-}$ may result in the re-organization of the CuCl layers.

Sect(3-3.8)

The Computer Program Used In Determining The Equilibrium Concentrations of the Complexes and Ions:

The following equations show the various complex formation equilibrium reactions when a copper foil is immersed in a solution containing halide and Cu^{2+} ions.

$$Cu^{2+} + X^- \xrightleftharpoons{K1} CuX^+ \qquad E(3\text{-}42)$$

$$CuX^+ + X^- \xrightleftharpoons{K2} CuX_2 \qquad E(3\text{-}43)$$

$$CuX_2 + X^- \xrightleftharpoons{K3} CuX_3^- \qquad E(3\text{-}44)$$

$$CuX_3^- + X^- \xrightleftharpoons{K4} CuX_4^{2-} \qquad E(3\text{-}45)$$

$$Cu^o + Cu^{2+} \xrightleftharpoons{K5} 2Cu^+ \qquad E(3\text{-}46)$$

$$Cu^+ + 2X^- \xrightleftharpoons{K6} CuX_2^- \qquad E(3\text{-}47)$$

$$CuX_2^- + X^- \xrightleftharpoons{K7} CuX_3^{2-} \qquad E(3\text{-}48)$$

$$Cu^+ + X^- \xrightleftharpoons{K8} CuX \qquad E(3\text{-}49)$$

The stability constants of the above reactions (i.e.when X = Cl^- or Br^-) were obtained from the stability constant book[81].

The equilibrium constants of the reactions were calculated from the known stability constant values. Examples of the calculations are as follows:

(A) The stability constant for the reaction

$$Cu^{2+} + Cl^- \rightleftharpoons CuCl^+ \qquad E(3\text{-}9,p122)$$

is = 2.8.

Therefore the equilibrium constant is the $antilog_{10}$ of 2.8 that is equalled to 630.960

(B) The gross constants $\beta'3$ for the following reaction.

$$CuCl_2^- + Cl^- \rightleftharpoons CuCl_3^{2-} \qquad E(3\text{-}50)$$

is = 5.70. The $\beta'3$ values for the preceding two reactions is 4.60. The following gross constant formula is used in the calculation.

$$\beta'_n = \prod_{i=1}^{n} Ki \qquad E(3\text{-}51)$$

or

$$\beta'_n = K_1 \times K_2 \times K_3 \ldots\ldots\ldots K_n \qquad E(3\text{-}52)$$

therefore, in this example,

$$\log \beta'_3 = \log \beta'_2 \times \log K'_3$$

or $\log K'_3 = \log \beta'_3 - \log \beta_2$

therefore, $K'_3 = 12.59$

The calculated equilibrium cosntants for the most likely reactions (i.e. E3-42 to 3-49) to occur in a solution containing halide ions, Cu^{2+} and Cu^o are shown on table (3-10,p164). The total amount of the halide and the Cu^{2+} ions are known. (i.e. assuming no significant amount of solid Cu^o dissolves into solution), Also there must be charge balance in the solution. There are 8 unknown species in the solution and there are as follows:

$$Cu^{2+},\ X^-,\ CuX^+,\ CuX_2,\ CuX_3^-,\ CuX_4^{2-},\ CuX_2^-,\ CuX_3^{2-}$$

Therefore, with the eight interconnected equilibrium reaction equations and their known equilibrium constant, it is possible to calculate the equilibrium concentrations of each particular complex and ions.

A computer program was written by Dr. Hibbert and was adopted to use in solving the above problem. This program is only valid if the amount of Cu(X) formed is small, as the loss of X^- or the increase in Cu^{2+} is not taken into account.

A binary search routine converging technique which uses the fact that $0 < [Cu^{2+}]$ free $\leq [Cu^{2+}]$ total was used in the program. A list of the program is shown in the appendix Page (291). The following page is the simplified flow chart of the program.

Figure 3-36

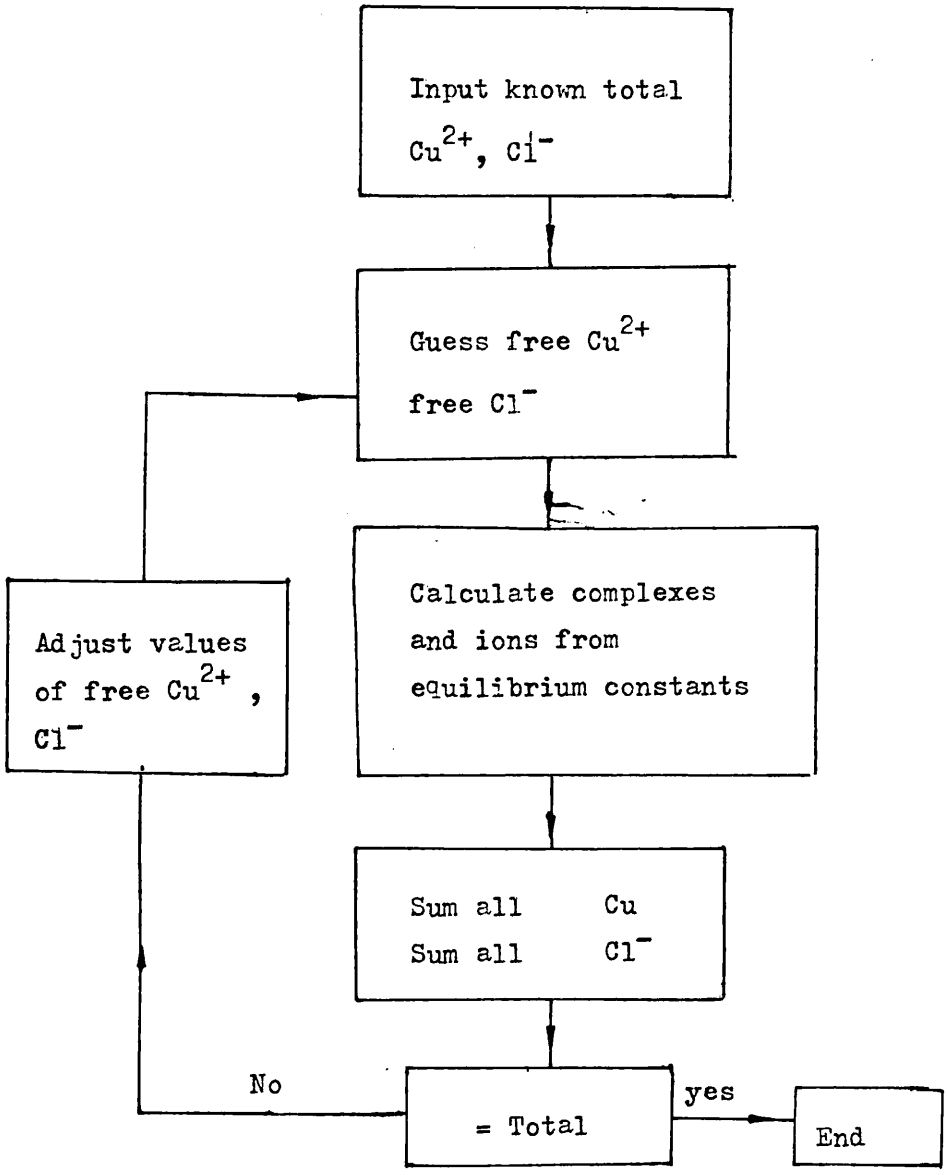
Input known total
Cu^{2+}, Cl^-
Guess free Cu^{2+}
free Cl^-
Calculate complexes
and ions from
equilibrium constants
Adjust values
of free Cu^{2+} ,
Cl^-
Sum all Cu
Sum all Cl^-
No
= Total
yes
End

CHAPTER 4

Studies of the Addition Agents in Copper Deposition:

Introductions:

Studies of bright copper plating with addition agents have been carried out by various authours[59,61,140]. Very often investigation covered only a specific area such as the study of the effect of some addition agents on the kinetics of copper electrodeposition from a sulphate bath by Turner and Johnson[59] or the effect of thiocompounds on the structure of copper electrodeposits by Barnes[57].

The studies carried out here involve not only the kinetics of electrodeposition of copper but the various other related subjects including the morphological studies of the deposits. The steady state overpotential build up time was examined . The double layer capacitance during the pulsed plating of samples which were used for morphological studies were also examined. The characteristics of each of the addition agents were examined by cyclic voltammetric method.

The inclusion of the sulphur atoms or compounds in the deposits was also investigated.

Composition of the acidified copper electrolytes with addition agents used, were either obtained from the United States Patent papers[20,106] or the heterocyclic compounds such as imidazole and histamine.

Part (4-1) EXPERIMENTAL

Sect(4-1.1) Materials:

Anodes:

The anodes used were 4×10^{-2} m x 4×10^{-2}m copper foil (BDH 99.999%) for all the experiments except the cyclic voltammetric experiments. In this experiment, the anodes used were the pure platinum foil (Johnson Matthey 99.999%). The dimension of these anodes was 2×10^{-2}m x 2×10^{-2} m.

Cathodes:

The cathodes used in all the experiments were 2×10^{-2}m x 2×10^{-2}m pure copper foil.

Salt Bridge:

The same type of salt bridge was used as those described on page 102.

Chemicals:

The analar grade (BDH) and reagent grade (BDH) chemicals were used in the experiments. The reagent grade chemicals used are imidazole, histamine, janus green B, thioglycolic acid, dimethyl thiourea, propionamide and polyvinyl alcohol. No further purifications were carried out on any of the chemicals used.

Electrolytic Cell:

The electrolytic cell used was made of glass and is shown on figure(4-1,p200).

Reference Electrode:

The reference electrode used in the experiments was the same saturated calomel electrode described on page (101).

Sect(4-1.2) Electrode Pre-treatment:

The cleaning processes of the electrodes used were the same as those described on the chloride experiments (p104).

Sect(4-1.3) Measurement of Overpotentials at Different Current Densities:

The experimental set up consists of the electrolytic cell (fig 4-1,p200), the ministat (Thompson Associate 125) the oscilloscope and the pulse generator (CERB1, chemical electronic Co). The circuit diagram of this system is shown on page 201 (fig 4-2).

In the study of the relationship between cathode over-potentials and current densities, a pulse on time of 30ms and relaxation time of 0.7 ms was used. A train of galvanostatic rectangular wave pulses was produced by the pulse generator.

A time of less than one minute was used for recording a single set of current density, potential difference and IR drop of the working electrode. This was carried out in order to minimise the change of working electrode surface.

Experiments were carried out at $25^{o}C \pm 0.5^{o}C$ and with different electrolytes. Compositions of electrolytes are shown on page 247 (table 4-3). Solutions were purged with N_2 and vigorously stirred.

Sect(4-1.4) Electromicroscopic (EM) study of the Deposits :

The deposits were obtained using the same experimental set ups shown in figure (4-1,p200). The pulse on time and relaxation time used were 30ms and 0.7ms respectively. The electrodepositions were carried out with different electrolytes and at different current densities. The electrolytes were purged with N_2 and maintained at $25^oC \pm 0.5^oC$.

Equal amount of deposits were plated on all the working electrode i.e. (0.0386g). As a result, all the deposits obtained probably had the same thickness. The electroplating time used for obtaining 0.0386g of the deposit at 6.25 mA cm^{-2} was 40 minutes. Therefore, for the subsequent higher current densities used in the electrodepositions, shorter plating times were required.

Deposits were subsequently rinsed in distilled water and dried in an oven (i.e. at $35^oC \pm 0.5^oC$). The drying process took about 45 minutes. Dried deposits were stored in a bottle which had been purged with N_2.

Small pieces of deposits (0.5cm x 0.5 cm) were cut from the centre portion of cathodes. These pieces of deposited cathodes were then used in electromicroscopic study. These observations were carried out at different magnifications such as x 1000, x 5000, x 10,000. Frequently, micrographs of deposits were taken.

Sect(4-1.5) Capacitance Measurements:

The initial linear increment of potential difference with time (i.e 20 μs <) of the working electrode was measured . Measurements were taken during the pulse plating process in obtaining deposits for electromicroscopic study.

Results obtained were then used to calculate the double layer capacitance of working electrodes which were used in electromicroscopic study. Calculated results are shown on table (4-4,p248) .

Sect(4-1.6) Steady State Overpotential Time (Tss):

The operating conditions (i.e. on time, relaxation time, temperature, N_2 purging and stirring)used were similar to those in the E.M. study experiment. The experimental set up was also the same.

In this experiment, the time for the overpotential (i.e. potential difference - IR drop) to virtually attain its steady state value was recorded. The T_{ss} values were measured at C.Ds range from 6.25 mA cm^{-2} to 62.5 mA cm^{-2}. This experiment was carried out in four different solutions and using different copper cathodes on each occasion. The compositions of the electrolytes and the results obtained are shown on table (4-12,p256).

Sect(4-1.7) Cyclic Voltammetric Plots:

Platinum anodes and pure copper cathodes were used here. The circuit diagram of this experiment set up is shown on fig (4-2, p201) . Electrolytes were stirred and purged with N_2. The SCE reference electrode was used. A working electrode was placed closed to the tip of agar-agar salt bridge in order to minimise ohmic drop. Copper sulphate was not added into the electrolytes and compositions of these solutions are shown on page (245,246) .

The copper working electrode was initially potentiostatically swept from -72 mV to -351 mV vs. SCE . Subsequently direction of the voltage scan was reversed. The sweep rate applied was 40 mV S^{-1} and the cyclic triangular wave was used. Results obtained are shown on figures (4-1, 4-2, p245,246) .

Sect(4-1.8) Sodium Azide Test:

Deposits used for this test were obtained using the same method as those deposits obtained for EM study.

N_2 will be liberated immediately when a trace of a sulphide, thiousulphate or thiocyanate is added into a solution of sodium azide and iodine. The above trace compounds each acts as a catalyst.[100] The chemical equation for this reaction is as follows:

$$2Na\ N_3 + I_2 \longrightarrow 2NaI + 3N_2 \qquad E(4\text{-}1).$$

Sodium azide-iodine reagent was prepared by dissolving 3 g of sodium azide in 100ml of 0.1 N iodine. A 3mm square sample was cut from the deposited working electrode. This sample was then dropped into 10 ml of sodium azide-iodine solution. Qbservation of N_2 evolution was then carried out. The above procedure was repeated with deposits obtained from different electrolytes or at different C.Ds.

C.Ds. used in the galvanostatic pulse plating process were 3.75, 6.25, 12.5 and 62.5 mA cm^{-2}. Different electrolytes were used in the depositions, and the compositions are as follows:-

(i)	Cu^{2+}	=	80.00	g dm^{-3}
	H_2SO_4	=	196.00	"
(ii)	Cu^{2+}	=	200.00	"
	H_2SO_4	=	15.00	"
	Dimethyl thiourea	=	0.030	"
	Janus green B	=	0.05	"
(iii)	Cu^{2+}	=	80	"
	H_2SO_4	=	196.	"
	Thioglycolic Acid	=	0.01	"
	NaCl	=	0.05	"
	Propionamide	=	0.10	"
	Ployvinyl alcohol	=	0.06	"

Sect (4-1.9) Detection of CuS by Spot Tests :

Small pieces of deposits (4mm x 4mm) were cut from the same plated electrodes which were used for sodium azide test. The samples were placed on a spot plate which was placed in a fume cupboard. Then a drop of pottasium cyanide was applied on the sample. The concentration of KCN solution used was 0.1 mol dm^{-3} .

The colour changes of samples were then observed and recorded . Electrolytes and current densities which were used to prepare the deposits are shown on page 198. Results obtained are shown on table (4-14,p258).

Fig: (4-1)

THE GLASS ELECTROLYTIC CELL USED IN COPPER DEPOSITIONS

1 Working electrode (copper)
2 Counter electrode (copper or platinum)
3 Lugin capillary
4 Agar salt bridge
5 Saturated Kcl solution
6 Saturated Calomel electrode
7 Magnetic stirer
8 Electrical coil
9 N_2 gas inlet
10 Clamp retort stand
11 Thermostatted water bath
12 Glass tube

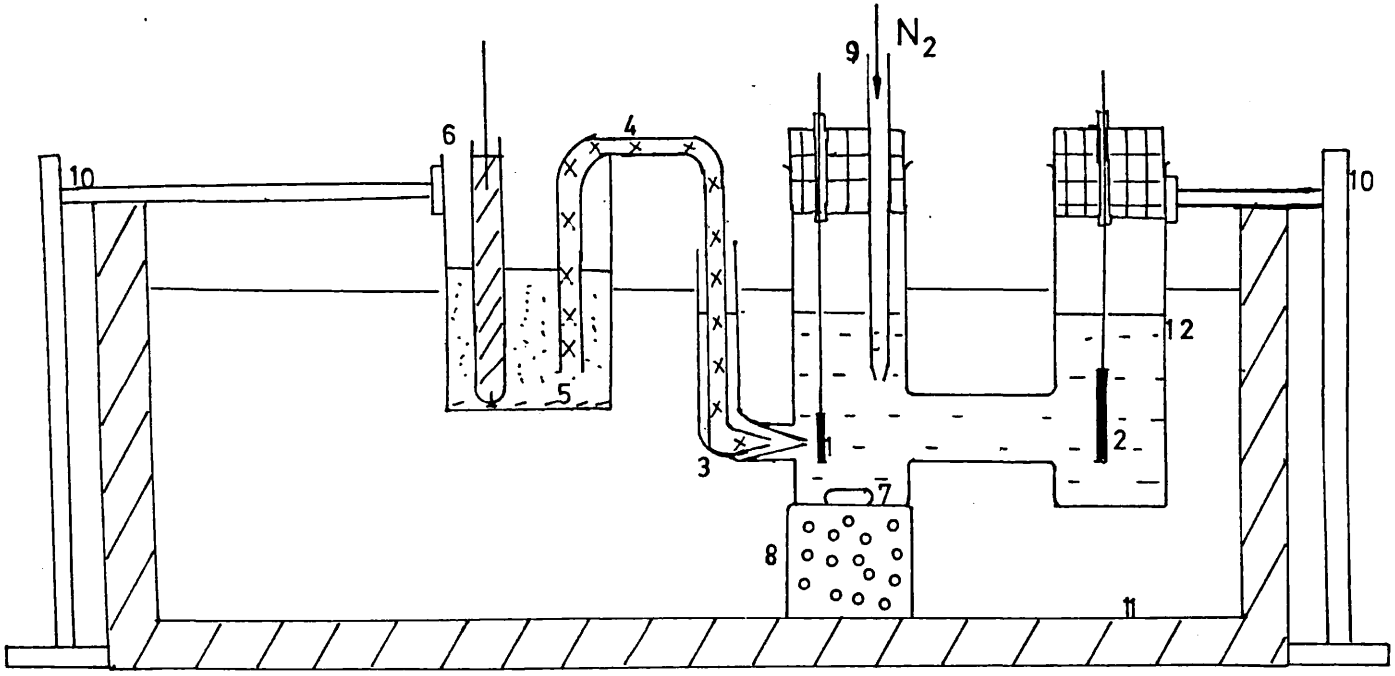

Fig: (4-2)

CIRCUIT DIAGRAM FOR THE CYCLIC VOLTAMMETRIC STUDIES

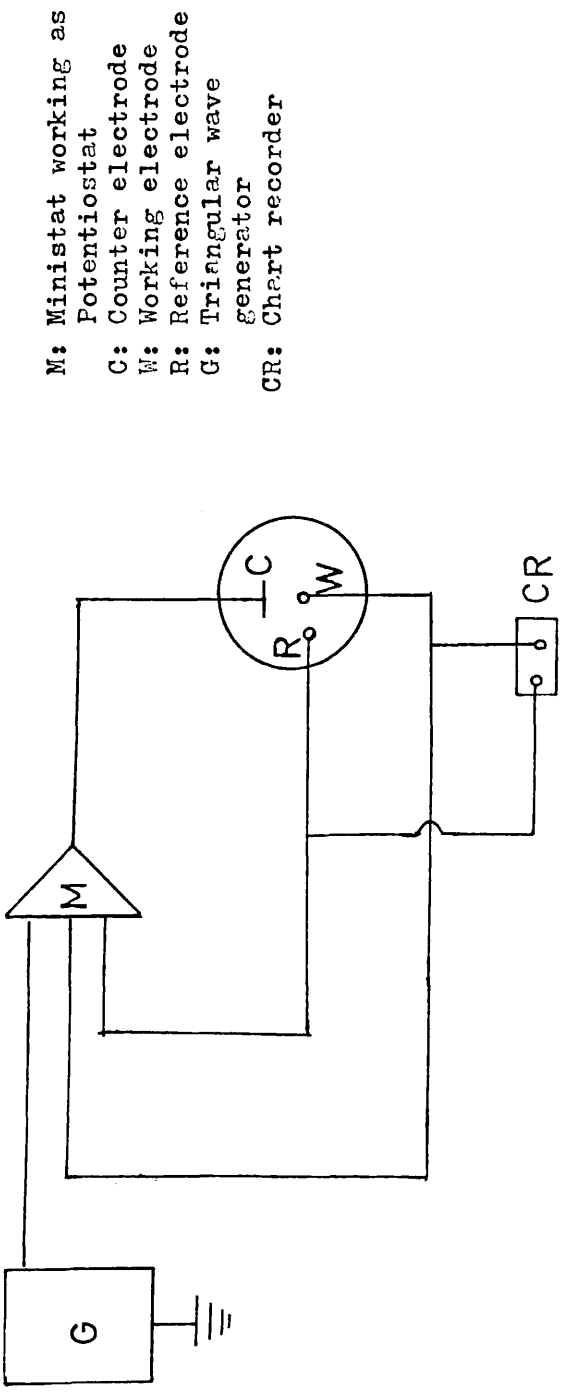

Part(4-2) RESULTS AND CALCULATIONS

Sect(4-2.1) Relation between Cathode Overpotential η_c and Current Density (i)

The cathode overpotential data (iR corrected) vs $\log_{10} i$ data were plotted as shown in figures (4-6 to 4-11,p219-224). Each figure represents the η vs $\log_{10} i$ plots for each type of solution. All these figures show good linear Tafel relations except with those experimental results obtained from solutions containing dimethyl thiourea and thioglycolic acid (fig 4-10,4-11,p223-224).

Five sets of experimental overpotential and current density results were obtained from acidic cupric sulphate solution without any addition agents. For those solutions which contained addition agents, two or three sets of experimental results were obtained for each solution (table 4-4,p248). For each set of the results, a different copper electrode was used. In general these results are fairly reproducible for each particular composition of solution.

The solution compositions for these figures mentioned above are shown in Table (4-3,p247). Exchange current densities and transfer coefficients were evaluated using the Tafel equation (E2-32,p77) and the above cathode overpotential vs. $\log_{10} i$ plots. The Tafel equation is as follows:

$$\eta = A + B \log i \qquad \text{E(2-32,p77)}$$

The α_c is determined from the slope B which is equal to $\frac{0.059V}{\alpha_c n}$ in this case. The i_o is obtained from extrapolation to the current density axis at $\eta = 0$ (A= Blog i_o). The α_c and i_o values obtained from figures are shown on table (4-4,p248).

Sect(4-2.2) Measurements of Double layer capacitance and Steady-State Overpotential Time.

The double layer capacitance (C_{dl}) of the copper electrodes were calculated from equation (E2-11,p50) i.e.

$$C = \frac{I}{dv/dt} \qquad E(2\text{-}11)$$

where dv/dt is equivalent to the change of overpotential with time (i.e. $d\eta/dt$) and I is equivalent to the constant current density (i.e. i). $d\eta/dt$ in this case is a measured initial rise of overpotential with a time of a very short duration i.e. between 10 μs to 20 μs (fig 4-5,p218).

Results (table 4-5 to 4-11,p249-255) obtained from the double layer capacitance experiments show that the C_{dl} values of the electrolytes containing $CuSO_4$ were generally higher than those electrolytes containing addition agents. The values were in the range of 31.25 $\mu F.\ cm^{-2}$ to 40.0 $\mu F\ cm^{-2}$ at different current densities. Also, results show that in each particular type of electrolyte, the double layer capacitance could vary at different current densities.

The steady-state overpotential time i.e

time that is taken for the overpotential to virtually attain its steady state value (T_{ss}) (see fig 4-4,p218), was recorded at different galvanostatic pulsed current densities and in different electrolytes. Results(table 4-12, p256) show that for those solutions containing brighteners, the T_{ss} are very much longer than for pure copper sulphate solutions. Also as the current densities increase, the T_{ss} values decrease in most cases.

Sect(4-2.3) Cyclic Voltammetric Analysis of Copper Electrodes in Solutions Containing Addition Agents:-

Experiments were carried out in stirred solutions containing different types of addition agents. Some of which are known as efficient brighteners, such as dimethyl thiourea and thioglycolic acid, which have a $\diagdown c - s$ group attached to the compound. The cyclic voltammograms obtained at a sweep rate of 40 mV/s for a copper working electrode in each type of solution are reproducible. Typical voltammograms are shown in figures (4-39 to 4-51, p232-244). The composition of the solution for each figure is shown in tables (4-1, 4-2, p245, 246).

The shape of the voltammograms of figures (4-39 to 4-42, 4-47, 4-49, p232-242) look similar and oxidations occur between approximately -72 mV to -82 mV in both sweep directions. The oxidative currents measured were less than 0.025 mA cm^{-2}. The reductions occur between a variable potential to -350 mV. All reducing currents measured were less than 0.025 mA cm^{-2}. The solutions contained addition agents which are not brighteners or levelling agents. Also figures (4-39 and 4-40) were obtained from pure sulphuric acid.

Figures (4-44,p237) and (4-45,p238) show that in acid solutions containing dimethyl thiourea and thiourea, the oxidation currents are significant (> 0.7 mA cm^{-2}). Also oxidation occurs predominantly between -72 mV to -215 mV (fig 4-44) and -72 mV to -255 mV (fig 4-45) in both sweep directions. Reductions occur in both sweep directions from -300 mV to -351 mV (fig 4-44) and -330 to -351 mV (fig 4-45).

In the acid solution containing janus green (B), reduction occurs very predominantly in both sweep directions (fig 4-43,p236). The maximum reduction current density measured was about 0.0688 mA cm^{-2}.

The voltammogram of an acid solution containing both janus green (B) and thiourea (fig 4-46,p236) shows that at potentials between -150 mV and -73 mV, oxidation occurred predominantly. Also at potentials between -195 mV to -350 mV reduction occurred significantly.

Figure (4-50,p243) shows that in a solution of propanoamide and sulphuric acid, the oxidation current measured was quite large between -72 mV to -82 mV in both sweep directions. The reduction current densities were less than 0.019 mA cm^{-2} throughout the reduction portion of the voltammogram.

In solution containing only thioglycolic acid and H_2SO_4, in both directions of the sweep between -255 to -72 mV, the oxidation reaction occurred very significantly (fig 4-14,p241). The maximum oxidation current measured was about 0.275 mA cm^{-2}. At a potential of > 290 mV and in a cathodic sweep, low magnitude reduction current density was measured (i.e. 0.003 mA cm^{-2}).

In the acid solution containing thioglycolic acid, propanoamide, polyvinyl alcohol and sodium chloride, oxidation again prevails in both sweep directions between -255 mV to -72 mV (fig 4-51,p244). The maximum oxidation current measured from the voltammogram was about 0.486 mA cm^{-2}. Again very low reducing currents occurred at potentials between -290 mV to -350 mV.

Sect(4-2.4) Electron Microscope Studies on Copper Electrodes in Sulphate Plating Baths with and without Addition Agents:

Measured grain sizes and the macroscopic appearance of the deposits are tabulated, tables (4-5,p249 to 4-11,p255) . The deposits were obtained from various plating baths and at different current densities.

Micrographs of the deposits (4-12,4-14,4-15,p225) obtained with the stereo scan electron microscope were use in the estimations of the grain sizes. The longest length of six grains in a micrograph were measured with an accurate ruler. Equation (E2-18,p63) was then used to calculate the actual lengths of these grains and the results were taken to be thegrain sizes. The standard deviation and mean of six grain sizes were calculated. The following are various micrographs of the deposits obtained from different plating baths.:

Figures (4-12 to 4-15,p225) are micrographs of deposits obtained from 0.321 mol dm^{-3} $CuSO_4$ and 2.0 mol dm^{-3} H_2SO_4 solutions. Figure (4-12,p225) shows that at 6.25 mA cm^{-2} the grains have square-based pyramids growth. The central portion of these grains consist of square base pyramids. At some distance from the peaks, layers become visible. Also thickness of the layers increases as they spread across the surface towards

.....continue

the edges of the face. The average grain size measured is large (i.e. 12.12$\pm$ 1.75 um, table 4-5,p249).

At 25 $mAcm^{-2}$, the pyramidal features of the grains is no longer visible. The grains have irregular shape (fig4-13,p225). At $50mAcm^{-2}$, the grains are more distinctive and like boulders of irregular shape. Also macroscopically rough edges begin to appear on the electrodes. The average grain size is slightly bigger (i.e.4.17 $\pm$ 0.68) than those obtained at $25mA/cm^2$ (i.e. 2.99 $\pm$ 0.333 μm).

At the highest C.D. carried out on these experiments (i.e. $100mAcm^{-2}$), the boulder-like grains had truncated into clusters of grains which appear like cauliflower (fig4-15,p225). The grain size has increased to about 6.1 μm.

Macroscopic appearance of the above deposits obtained at current densities of 6.25 $mAcm^{-2}$ and 25 $mAcm^{-2}$ were smooth and dull. At 50mA cm^{-2} and 100 mA cm^{-2}, edges of the electrodes were rough and deposits were a dull metallic copper in colour.

The micrographs of those deposits obtained in, 0.321 mol dm^{-3} $CuSO_4$, 2.0 mol dm^{-3} H_2SO_4 and 3.21×10^{-4} mol dm^{-3} imidazole, are shown in figure(4-16 to 4-18,p226).

Reasonably large grains [i.e. 6.3 $\pm$ 0.970 μm table (4-6,p250)] of boulder type were observed on the deposit obtained at 6.25 mA cm^{-2}. At higher current densities, grains of smaller sizes and irregular shape were formed. Some of them grouped together and formed a lump (fig 4-17,4-18,p226). At 50mA cm^{-2} and 100 mA cm^{-2} the deposits around the edges of the electrodes were rough.

Table 4-6 (p250) shows that macroscopic appearance of the deposits obtained were similar to those plated from 0.321 mol dm^{-3} pure $CuSO_4$ solution.

Figures (4-19 to 4-22,p227) show surface features of the deposits obtained from 0.321 mol dm^{-3} $CuSO_4$, 2.0 mol dm^{-3} and 0.000321 mol dm^{-3} histamine. At the lowest current density, the deposit has a boulder type of grain . The grain size is 14.51 $\pm$ 1.274 μm (table 4-7,p251). At current densities of 25, 50 and 100 mA cm^{-2}, the deposits again have irregular shape grains (4-20 to 4-22,p227) and their average grain size is less than 1.91 $\pm$ 0.448 μm (table 4-7, p251). The physical appearance of the deposits obtained at 100 mA cm^{-2} had rough edges aound its electrode. At a lower current density the deposits were dull and smooth.

In a solution containing 0.802 mol dm^{-3} $CuSO_4$, 0.153 mol dm^{-3} H_2SO_4 and 0.050 g dm^{-3} Janus green B the forms of grains obtained are shown on figures (4-23 to 4-26,p228). At the lowest current density surface feature of the grains is quite similar to those grains obtained from histamine - $CuSO_4$ solution at current densities of 50 mA cm^{-2} and 100 mA cm^{-2}. Grains obtained at higher current density are smaller than those obtained at 6.25 mA cm^{-2} (table 4-8 ,p252). The grains seemed to be more rounded in shape since their protrusions from the base are no longer pyrimidal in shape (fig 4-24 to 4-26,p228). Macroscopically at all current densities, no rough edges had been observed on the deposited electrodes.

The micrographs of the deposits obtained from solutions containing 0.000289 mol dm^{-3} dimethyl thiourea, 0.802 $CuSO_4$ and 0.153 mol dm^{-3} H_2SO_4, are shown on page 229. Figure (4-27,p229) shows the grains present on a brown-precipitate type of deposit. The shape of the grains is spherical and they cluster in lumps. The grain average size is quite small [0.52 ± 0.06 μm, table(4-9, p253)]. Macroscopically, the deposits consists of 2 different types. One of which is the dark brown precipitate type and the other a bright deposit. The deposits obtained at 25 mA cm^{-2} and 50 mA cm^{-2}

also have the same macroscopic appearance. The micrographs of bright deposit type (4-28 to 4-30,p229) show that grains of deposit obtained at current densities greater than 25 $mA \cdot cm^{-2}$ are spherical. Also they do not cluster into big lumps. In addition, the grains form a reasonably smooth microscopic surface. At 100 $mA\ cm^{-2}$, macroscopically only smooth bright deposits were observed and no rough edges occured on the electrodes.

Deposits obtained from solutions containing 0.000289 $mol\ dm^{-3}$ dimethyl thiourea , 0.802 $mol\ dm^{-3}$ $CuSO_4$ 0.153 $mol\ dm^{-3}$ H_2SO_4 and 0.05 g Janus green B, are shown on figures (4-31 to 4-34,p230). Grain sizes are shown on table (4-10,p254). The deposit obtained at 6.25 $mA\ cm^{-2}$ has small spherical grains (1.67 ± 0.24 μm). Grains cluster together and also appear like cauliflower. At higher current densities, the average grain sizes are smaller (i.e. 0.71μm <) and do not form a cauliflower type of deposit (fig 4-32- to 4-34,p230). Macroscopically only one type of deposit is present on each electrode at all current densities. Only bright deposits obtained at 100 $mA\ cm^{-2}$ and the microscopic surface of this electrode appears to be reasonably smooth (fig 4-34,p230) .....

continue next page

Figures (4-35 to 4-38, p231) show the surface features of deposits obtained from thioglycolic acid containing solution. The composition of the solution is as follows:

Thioglycolic acid = 0.010g dm^{-3}

Polyvinyl alcohol = 0.06 g dm^{-3}

Propanoamide = 0.1 g dm^{-3}

Na Cl = 0.05 g dm^{-3}

$CuSO_4$ = 80 g dm^{-3} (i.e. 0.321mol dm^{-3})

At current density of 6.25 mA cm^{-2}, the deposit consists of small spherical grains and spongy precipitate types (fig4-35,p231). The average size of small spherical grains is taken to be the grain size [i.e. about 0.86 μm, table (4-11,p255)]. Deposits obtained at 25 mA cm^{-2} appear to consist of small grain type (fig 4-36,p231). The microscopic surface of the deposit is relatively smooth and is bright.

At 50 mA cm^{-2}, the deposits obtained are microscopically very smooth and it is impossible to measure the grain sizes. Also, there are cracks present on the deposits (fig 4-37, p231). Macroscopically, the deposits are very bright and no rough edges were formed on the electrodes.

Figure (4-38,p231) shows the deposit obtained at 100 mA cm^{-2} has large grains and appears to be oval or egg shaped. They also appeared to be very smooth and grouped together to form a dough-like structure. No cracks were observed on the deposits obtained at this current density. Macroscopically, deposits were bright and edges of it were smooth.

Sect(4-2.5) Sodium Azide Test:

A solution of sodium azide (NaN_3) and of iodine (KI_3) does not react by itself. On the addition of a trace of a sulphide, thiosulphate or thiocyanate, which act as a catalysts , there is an immediate evolution of N_2 (see E(4-1),p197).

A small piece of copper deposit (see p197 for experimental detail) was dropped into 10 ml of NaN_3 + KI_3 solution. It was to observe if N_2 would evolve.Results (table 4-13,p257) show that all deposits obtained at different current densities and from electrolytes containing $\rangle$C - S brighteners were embedded with either sulphide, thiosulphate or thiocyanate. No N_2 was evolved when deposits obtained from pure acidic copper sulphate solution and pure copper foil were tested.

Sect (4-2.6) Detection of CuS by Spot Tests:

The experimental results obtained from this test are tabulated (table 4-14,p258) .Most of the samples obtained from deposits plated in solution containing brighteners reacted with KCN solution. They changed from their original colour (i.e. bright, dark brown and brown/yellow) to black when in contact with KCN solution. In addition, tiny bubbles also appeared on the surface of samples.

The tests carried out on those samples which were obtained from acidified cupric sulphate solution had no apparent reaction with KCN solution. This also applies to pure copper foil samples.

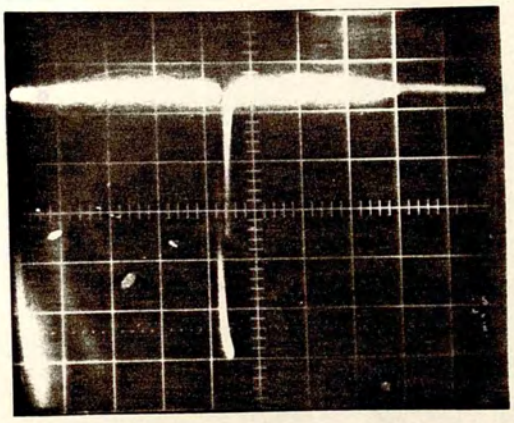

Fig (4-3)

Response for over -potentia! measurement showing IR drop

X-axis = 5 ms

Y-axis = 20 mV

Fig (4-4)

Response for steady state overpotential time measurement

X-axis = 0.1 ms

Y-axis = 20 mV

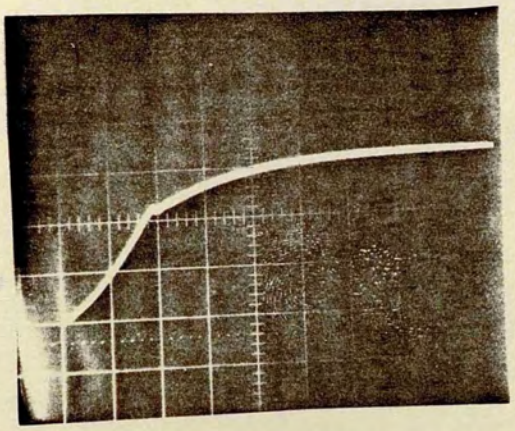

Fig (4-5)

Response for double layer capacitance measurement

X-axis = 20 μs

Y-axis =100 mV

Figure : (4-6) TAFEL PLOT:

$CuSO_4$ solution (see p247 for composition details)

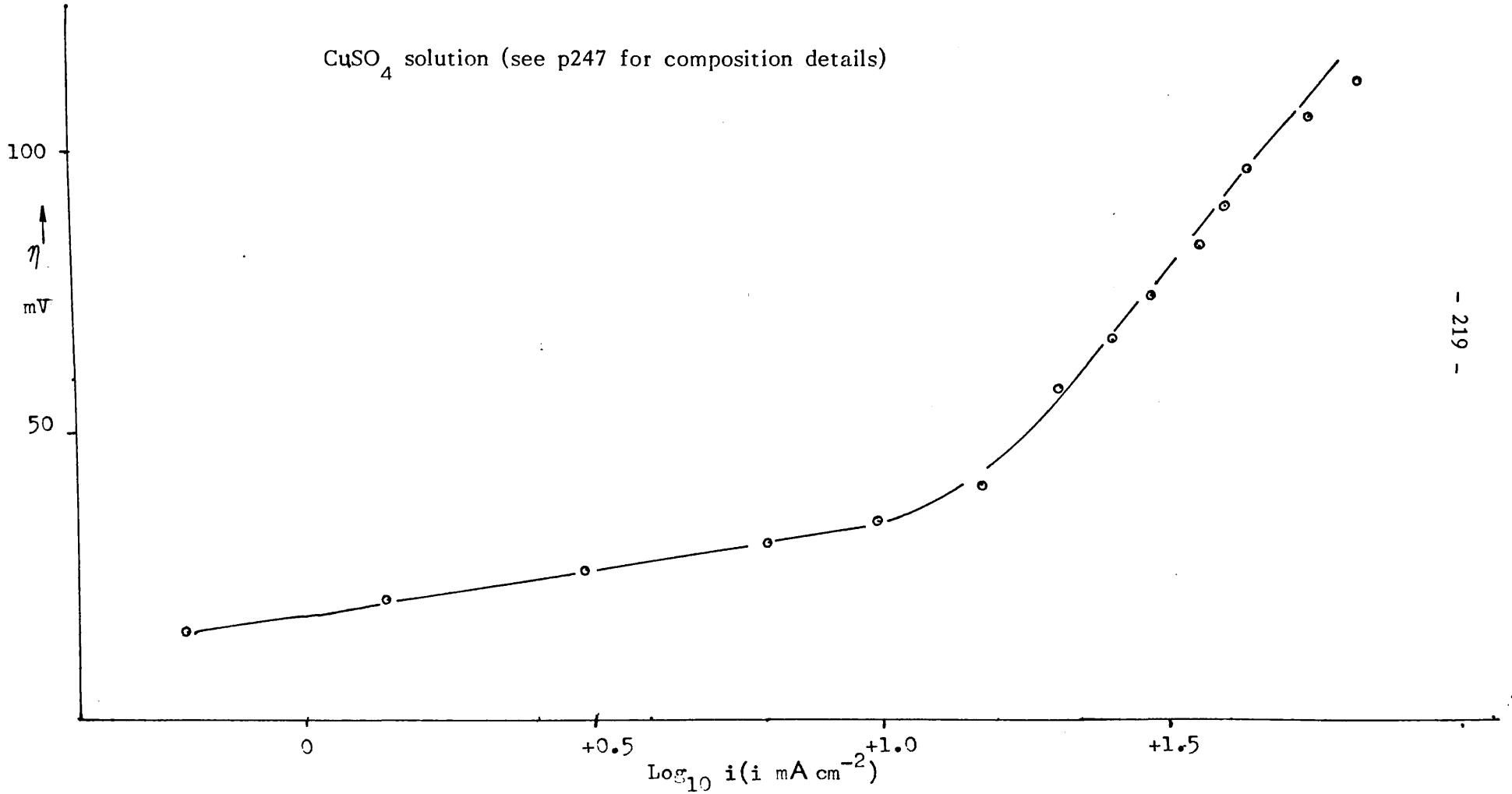

Figure:(4-7) TAFEL PLOT:

$CuSO_4$ solution (see p247 for composition details)

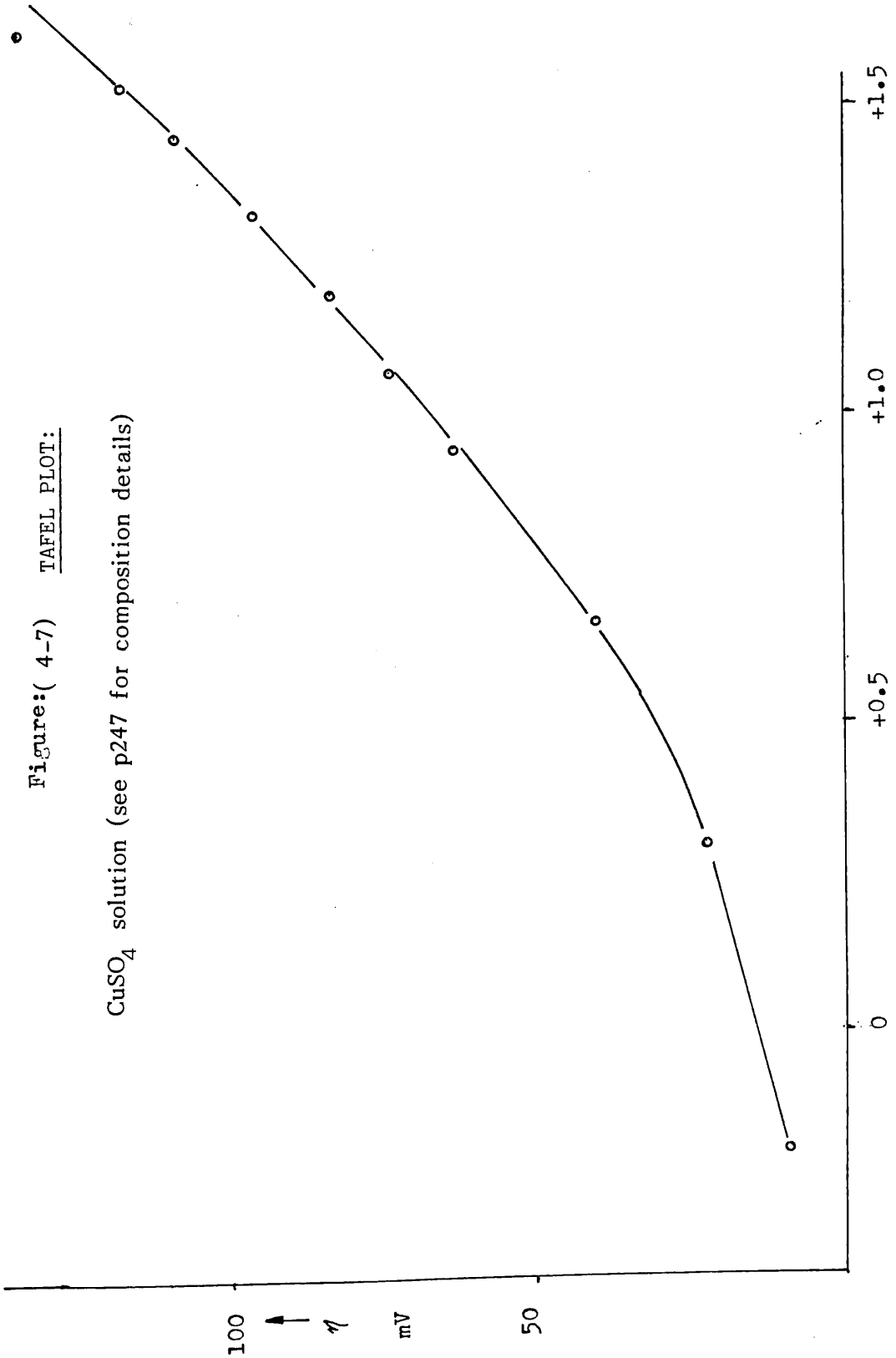

Figure: (4-8) TAFEL PLOT

$CuSO_4$ solution with imidazole (see p247 for compositon details)

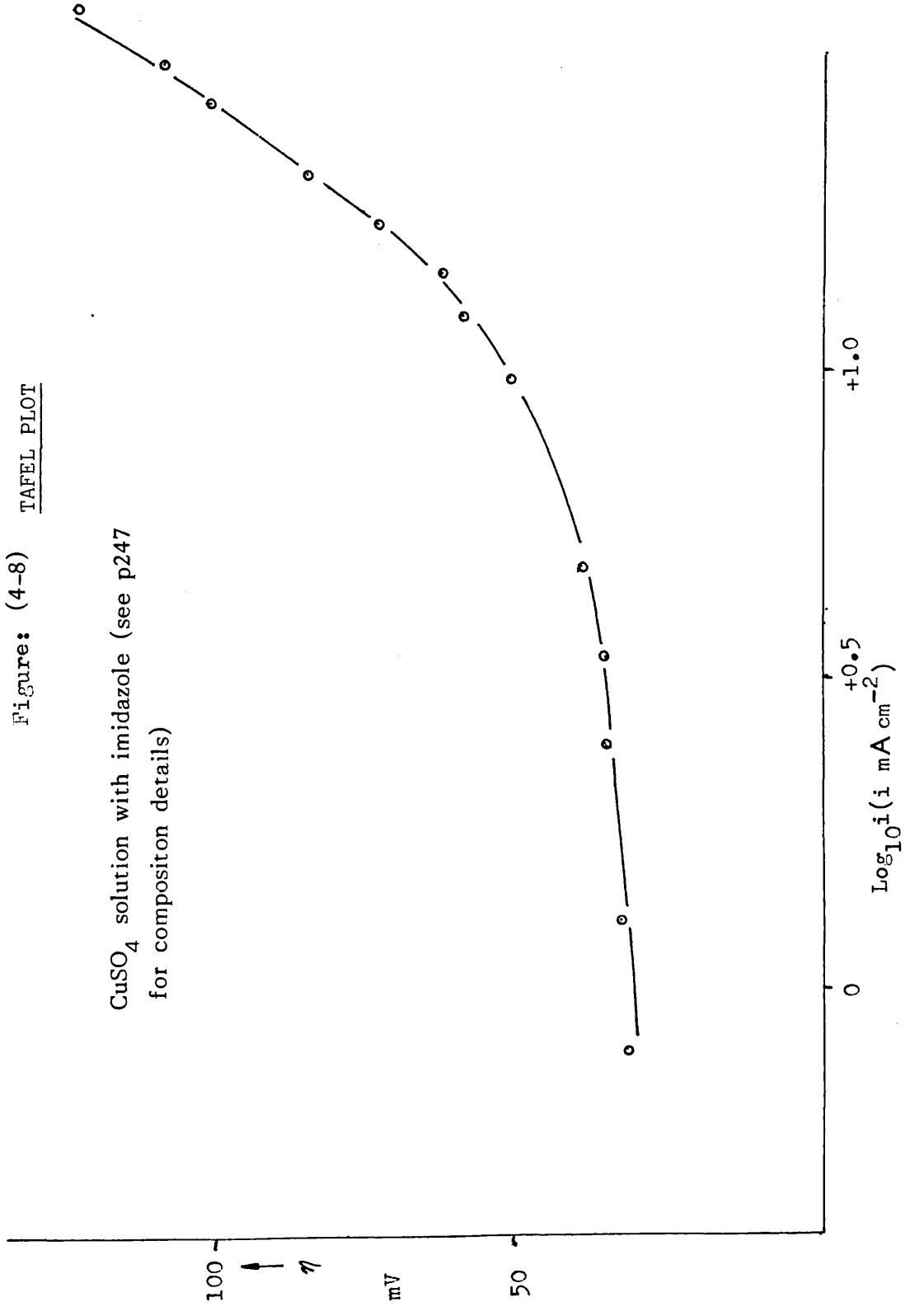

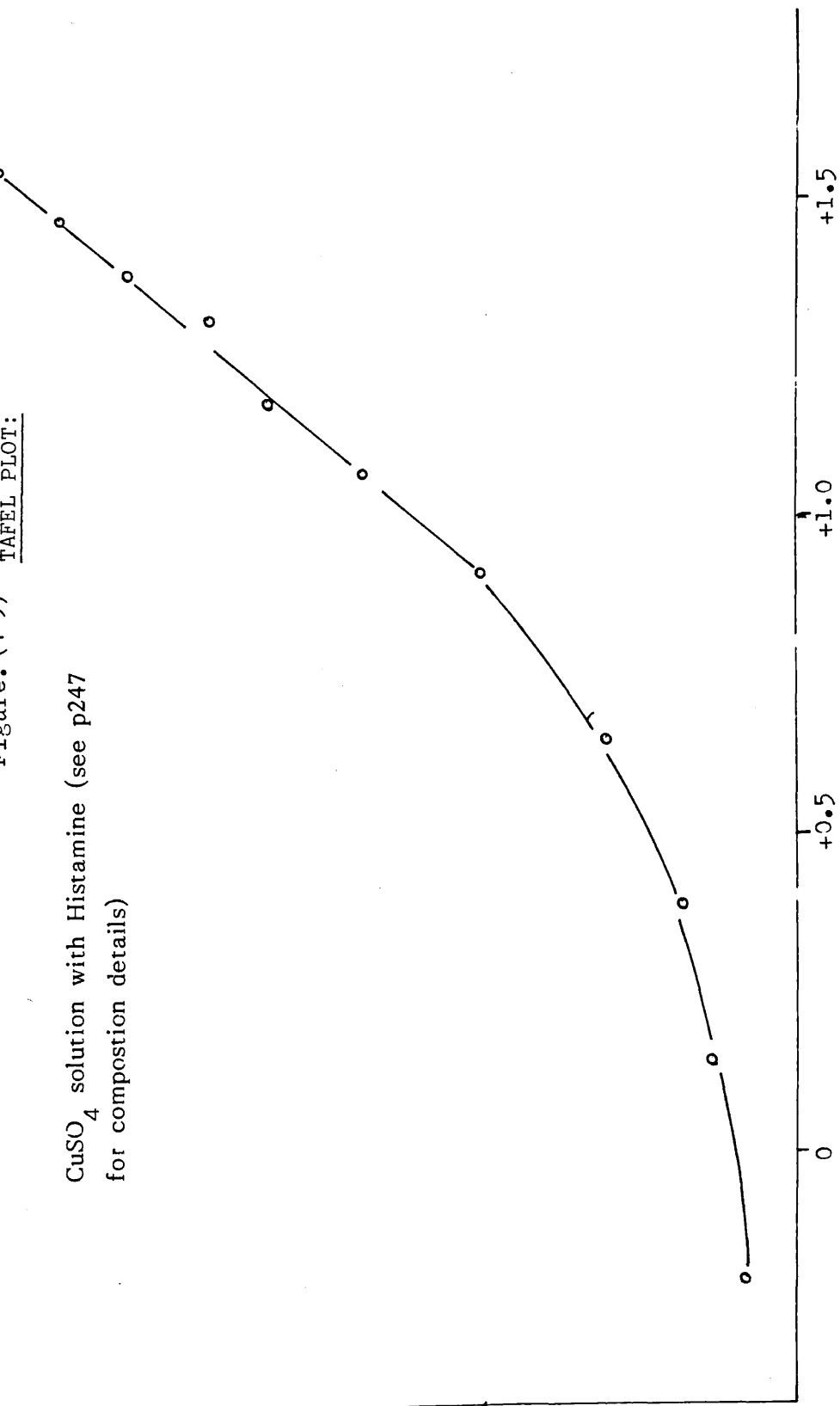

Figure: (4-9) TAFEL PLOT:

$CuSO_4$ solution with Histamine (see p247 for compostion details)

Figure: (4-10) TAFEL PLOT:

$CuSO_4$ solution with dimethyl thiourea
(see p247 for compositon details)

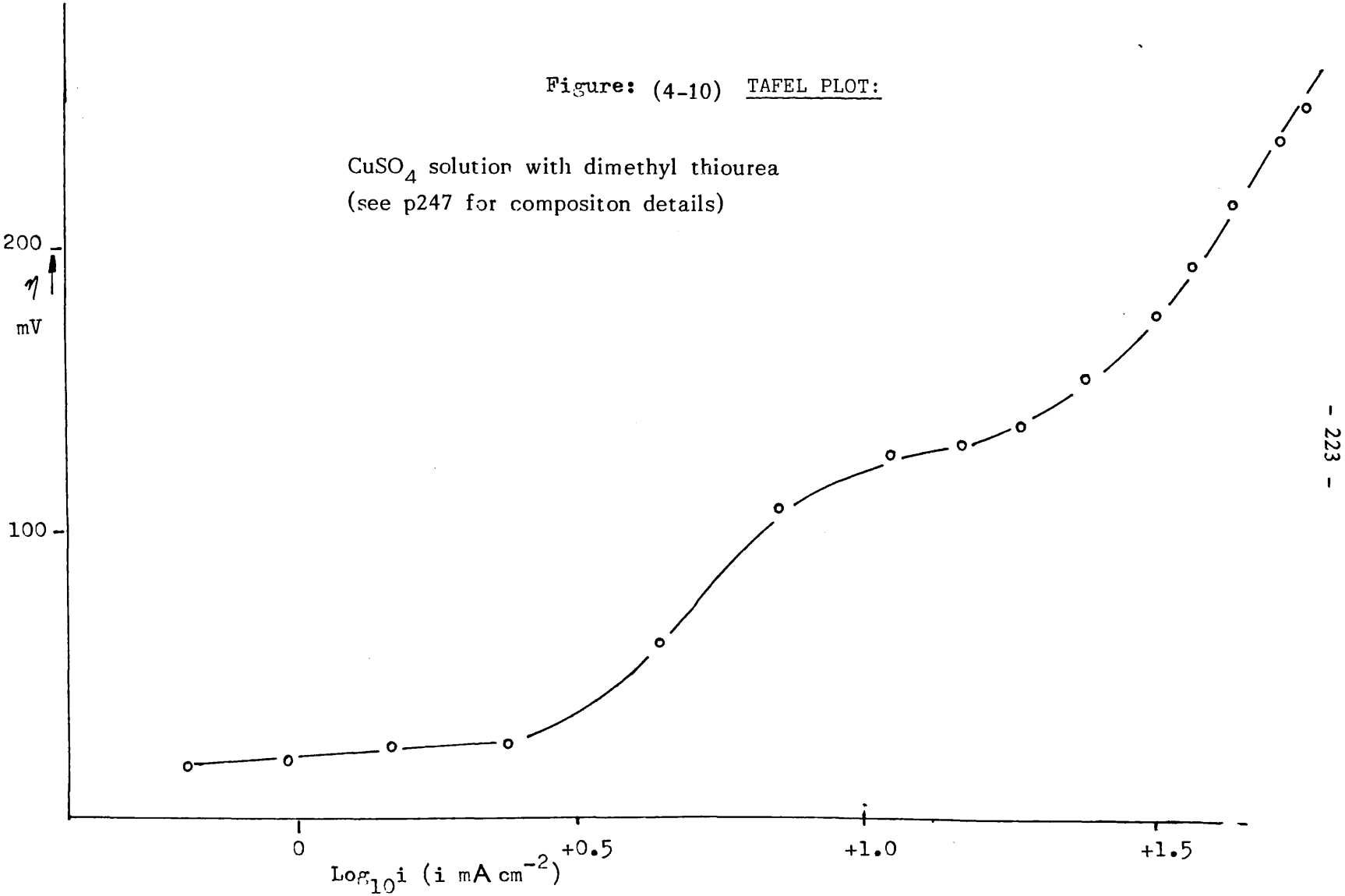

Figure: (4-11) TAFEL PLOT:

$CuSO_4$ solution with Thioglycolic acid
(see p247 for compositon details)

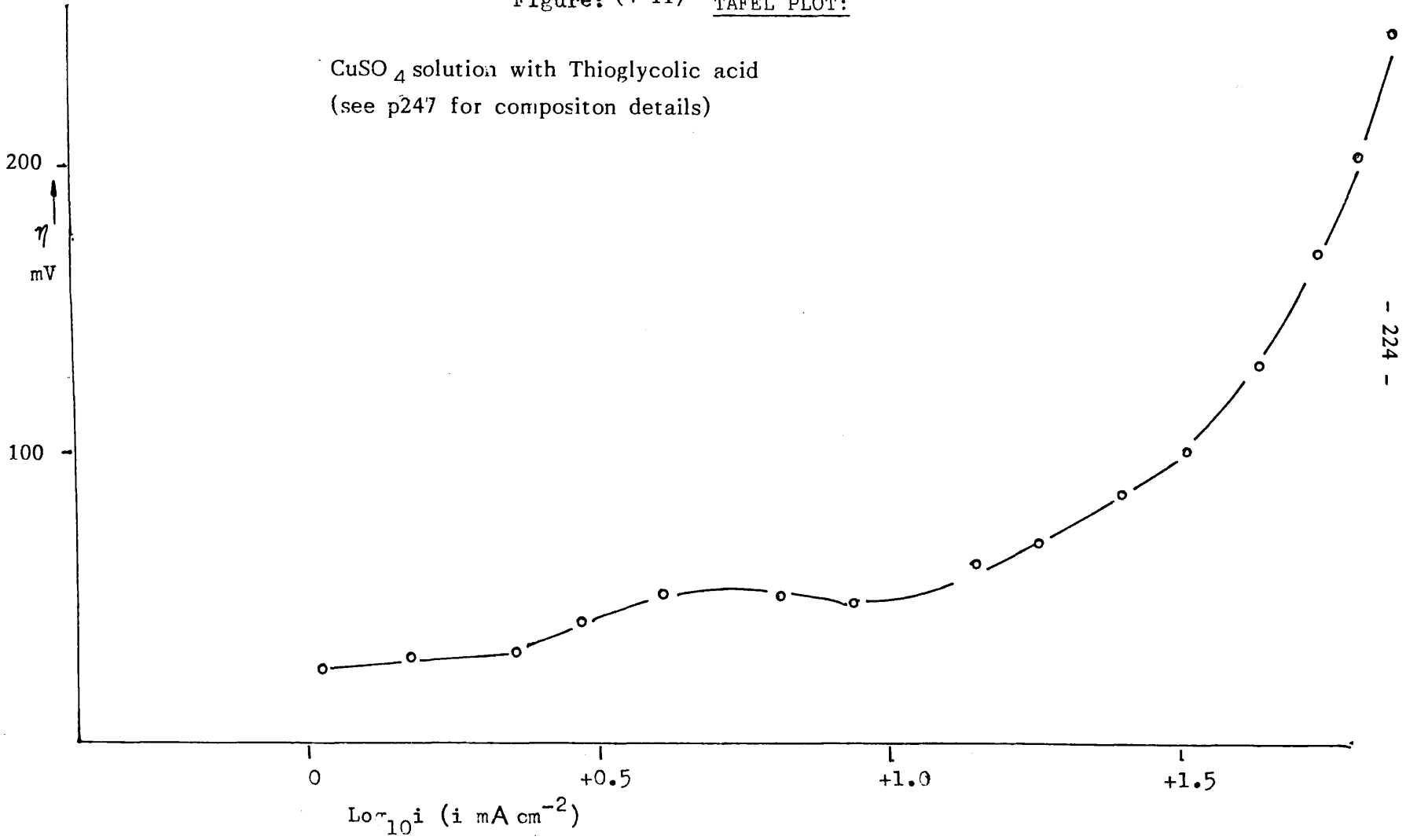

⟵⟶ 5.5 μm

Figure: (4-12)
Magnification: x 2.1K
Current Density: 6.25mA cm^{-2}

⟵⟶ 1.1 μm

Figure: (4-13)
Magnification: x 11K
Current Density: 25mA cm^{-2}

⟵⟶ 1.1 μm

Figure: (4-14)
Magnification: x 11K
Current Density: 50mA cm^{-2}

⟵⟶ 1.1 μm

Figure: (4-15)
Magification: x 11K
Current Density: 100mA cm^{-2}

$CuSC_4$ solution (see p249 for composition details).

1.2 μm

Figure: (4-16)
Magnification: x 10K
Current Density: 6.25mA cm^{-2}

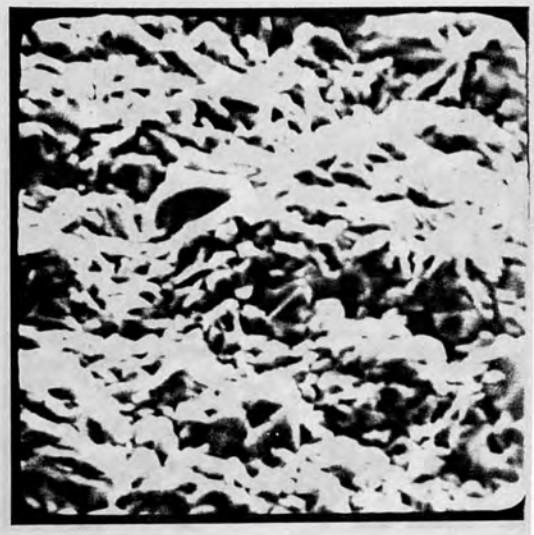

1.12 μm

Figure: (4-17)
Magnification: x 10.5K
Current Density: 25mA cm^{-2}

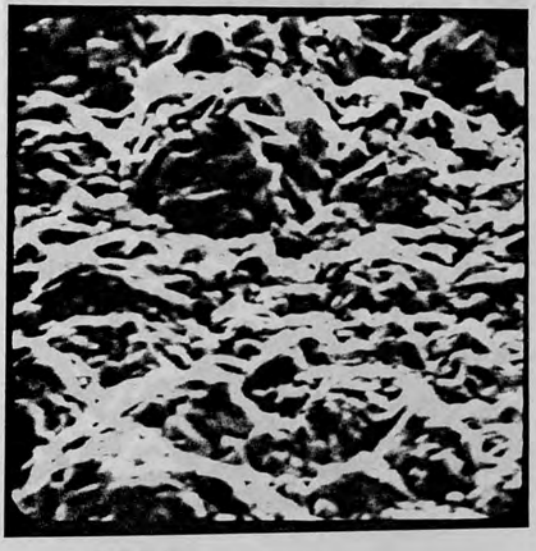

1.12 μm

Figure: (4-18)
Magnification: x 10.5K
Current Density: 50mA cm^{-2}

$CuSO_4^-$ solution with Imidazole (see p250 for composition details).

2.4 μm

Figure: (4-19)
Magnification: x 5K
Current Density: 6.25 mA cm^{-2}

0.96 μm

Figure: (4-20)
Magnification: x 12K
Current Density: 25 mA cm^{-2}

0.98 μm

Figure: (4-21)
Magnification: x 11.8K
Current Density: 50 mA cm^{-2}

0.98 μm

Figure: (4-22)
Magnification: x 11.8K
Current Density: 100 mA cm^{-2}

$CuSO_4$ solution with Histamine (see p251 for composition details).

1.13 μm

Figure: (4-23)
Magnification: x 10.2K
Current Density: 6.25mA cm^{-2}

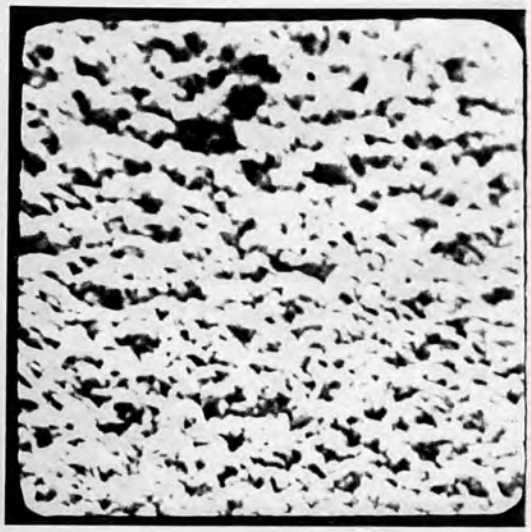

1.13 μm

Figure: (4-24)
Magnification: x 10.2K
Current Density: 25mA cm^{-2}

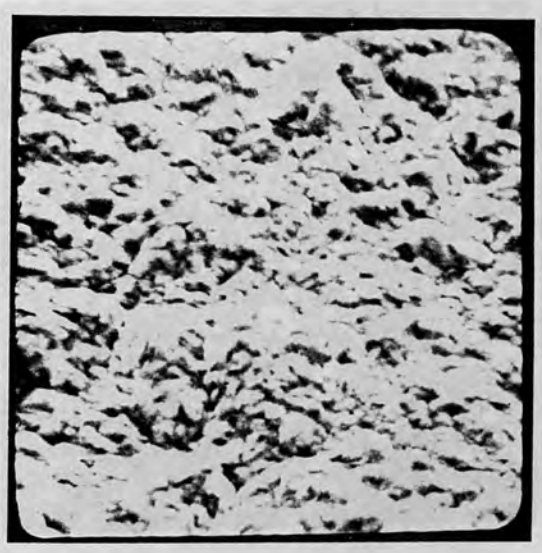

1.21 μm

Figure: (4-25)
Magnification: x 9.5K
Current Density: 50mA cm^{-2}

1.1 μm

Figure: (4-26)
Magnification: x 11K
Current Density: 100mA cm^{-2}

$CuSO_4$ solution with Janus green B (see p252 for composition details).

1.28 µm

Figure: (4-27)
Magnification: x 9K
Current Density: 6.25mA cm^{-2}

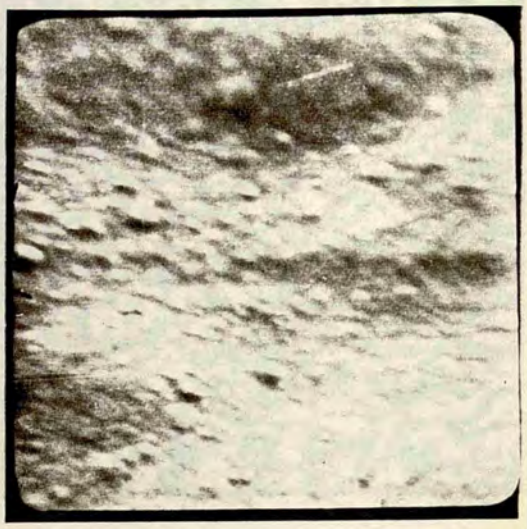

1.2 µm

Figure: (4-28)
Magnification: x 10K
Current Density: 25mA cm^{-2}

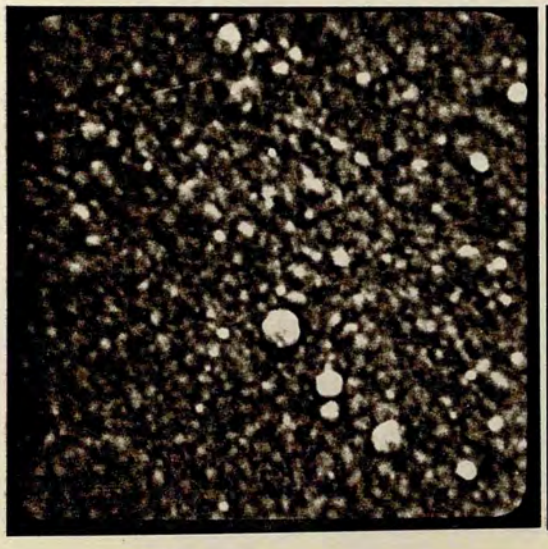

1.13 µm

Figure. (4-29)
Magnification: x 10.2K
Current Density: 50mA cm^{-2}

1.2 µm

Figure: (4-30)
Magnification: x 10K
Current Density: 100mA cm^{-2}

$CuSO_4$ solution with Dimethyl thiourea (see p253 for composition details).

1.2 μm

Figure: (4-31)
Magnification: x 10K
Current Density: 6.25mA cm^{-2}

1.14 μm

Figure: (4-32)
Magnification: x 10.1K
Current Density: 25mA cm^{-2}

1.13 μm

Figure: (4-33)
Magnification: x 10.2K
Current Density: 50mA cm^{-2}

1.13 μm

Figure: (4-34)
Magnification: x 10.2K
Current Density: 100mA cm^{-2}

$CuSO_4$ solution with Janus Green B and Dimethyl thiourea (see p254 for composition details).

5.7 8 µm

Figure: (4-35)
Magnification: x 2K
Current Density: 6.25mA cm^{-2}

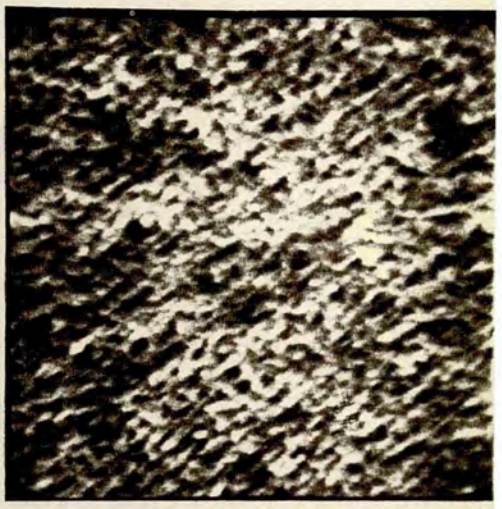

1.2 µm

Figure: (4-36)
Magnification: x 10K
Current Density: 25mA cm^{-2}

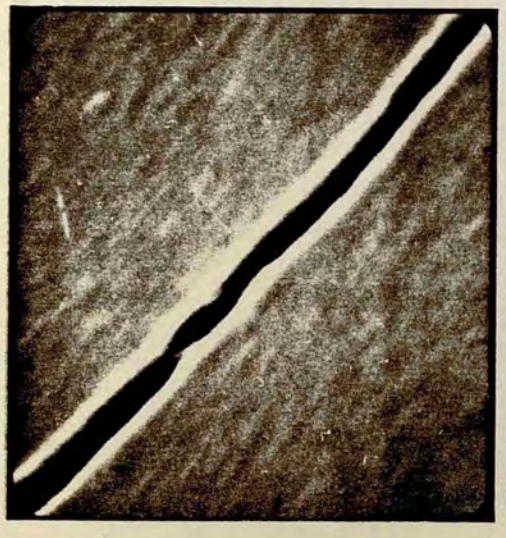

1.2 µm

Figure: (4-37)
Magnification: x 10K
Current Density: 50mA cm^{-2}

5.7 8 µm

Figure: (4-38)
Magnification: x2K
Current Density: 100mA cm^{-2}

$CuSO_4$ solution with Thioglycolic acid (see p255 for composition details)

Figure: (4-39) CYCLIC VOLTAMMOGRAM:

H_2SO_4 solution (2.0 mol dm^{-3})

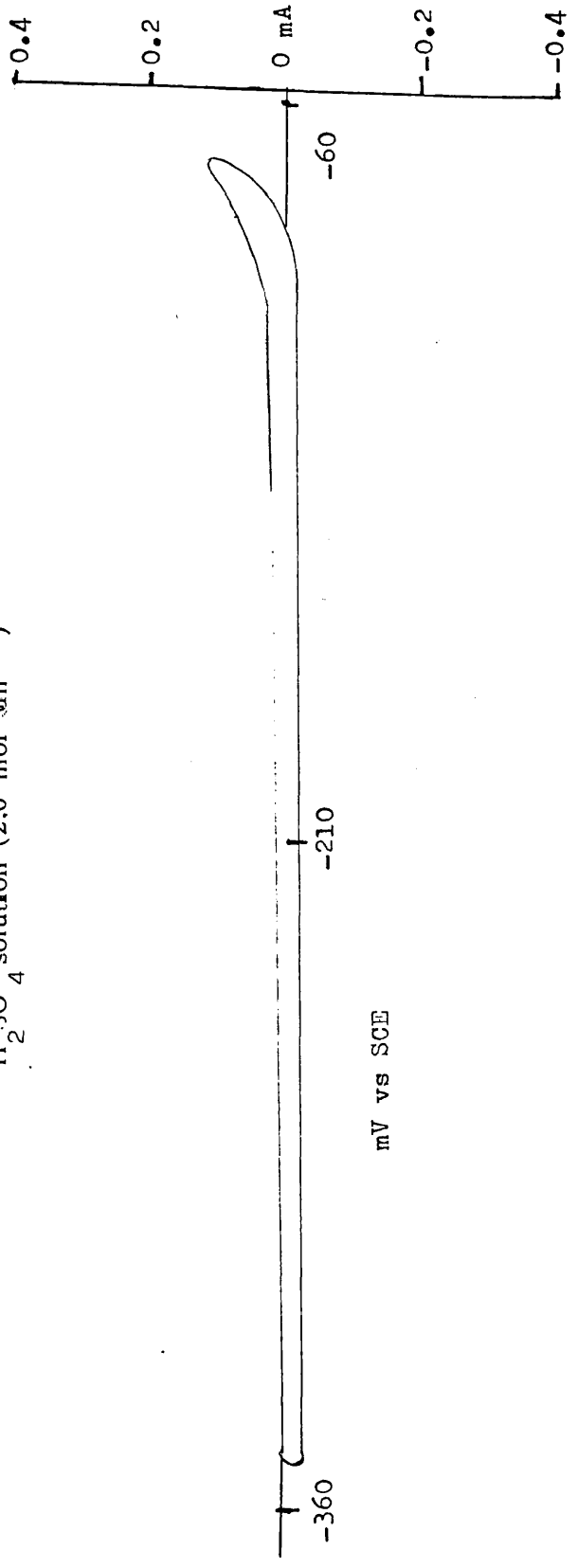

Figure: (4-40) CYCLIC VOLTAMMOGRAM:

H_2SO_4 solution (0.153 mol dm^{-3})

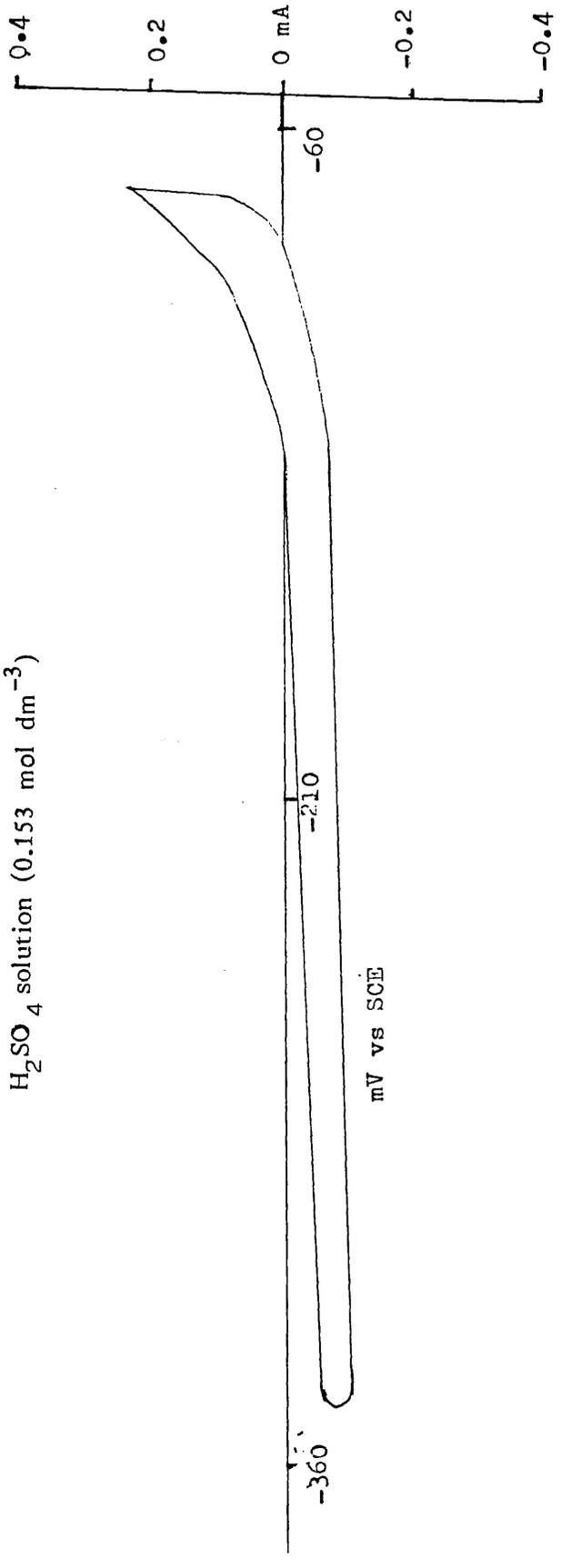

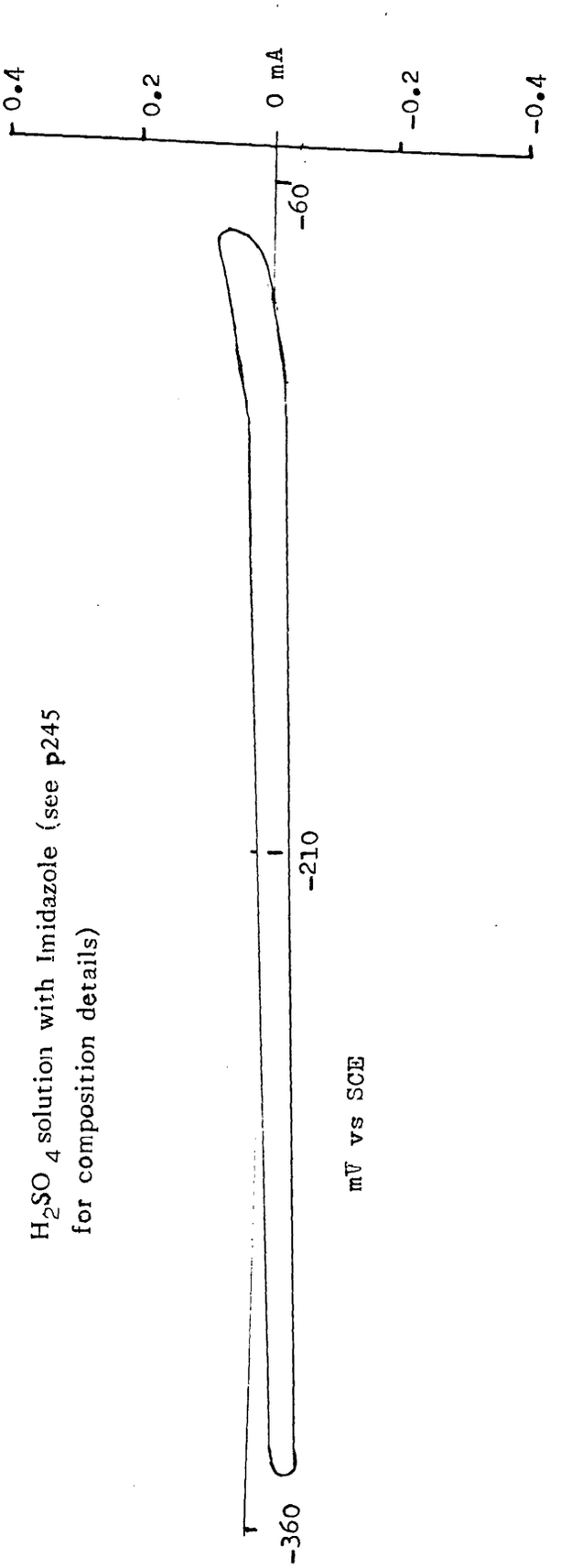

Figure: (4-41) CYCLIC VOLTAMMOGRAM:

H_2SO_4 solution with Imidazole (see p245 for composition details)

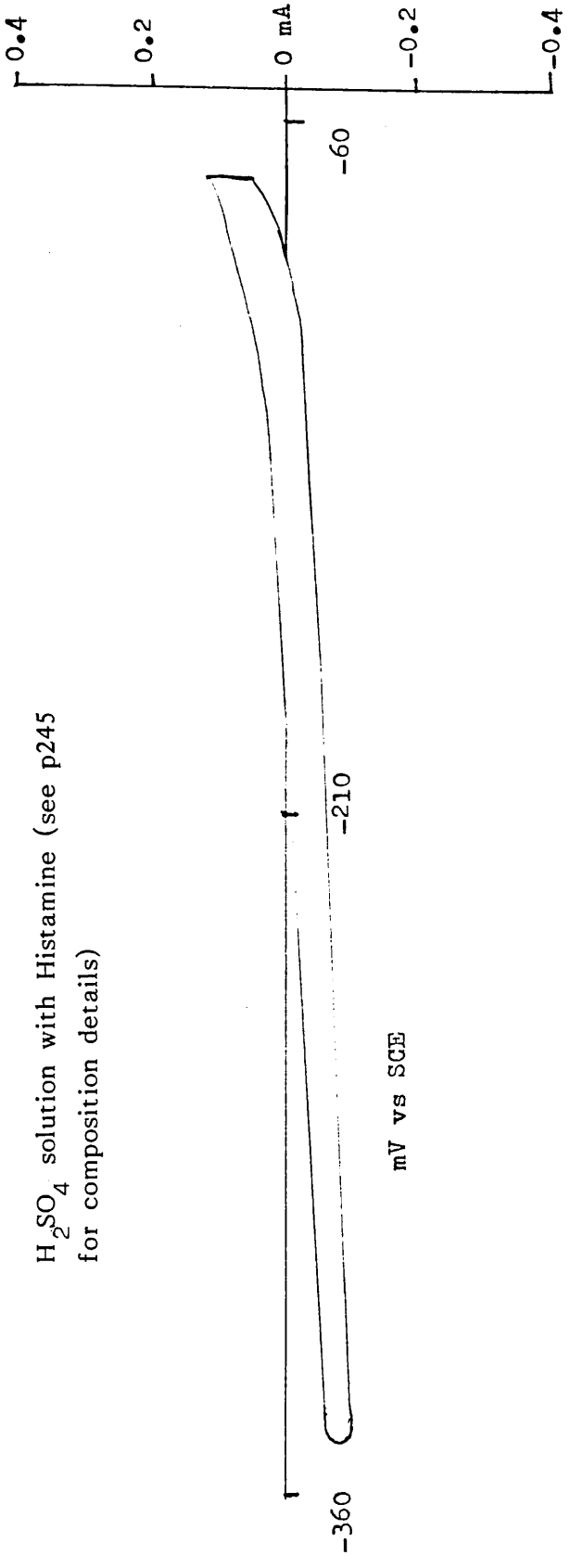

Figure: (4-42) CYCLIC VOLTAMMOGRAM:

H_2SO_4 solution with Histamine (see p245 for composition details)

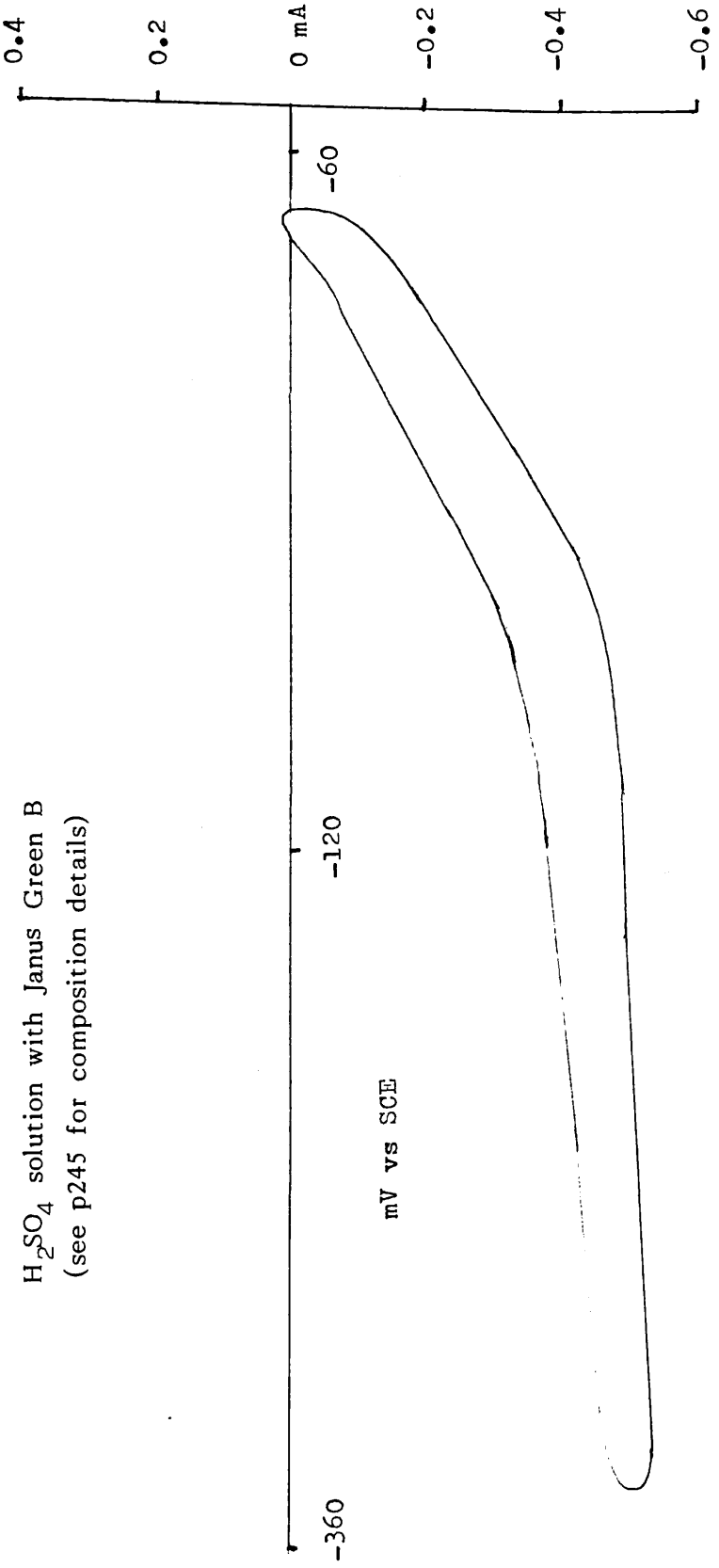

Figure (4-43) CYCLIC VOLTAMMOGRAM:

H_2SO_4 solution with Janus Green B
(see p245 for composition details)

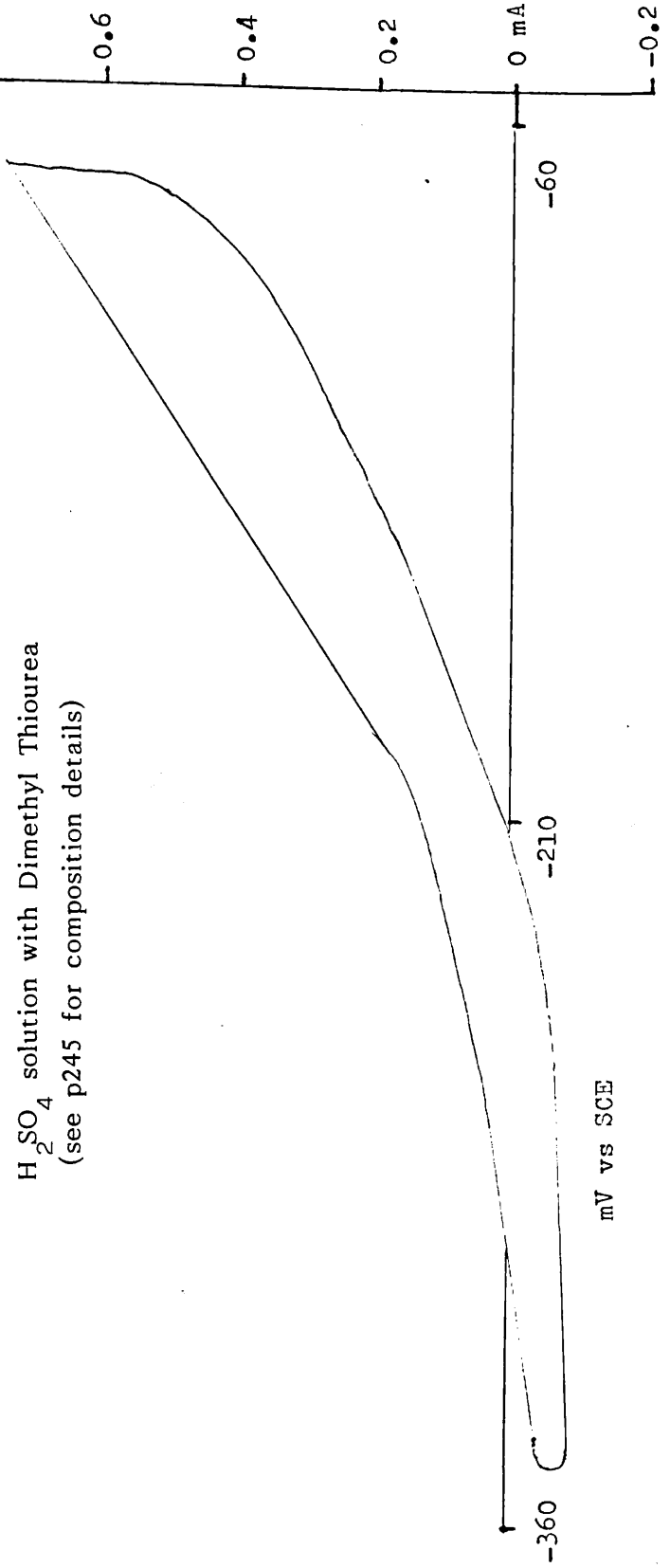

Figure: (4-44) CYCLIC VOLTAMMOGRAM:

H_2SO_4 solution with Dimethyl Thiourea
(see p245 for composition details)

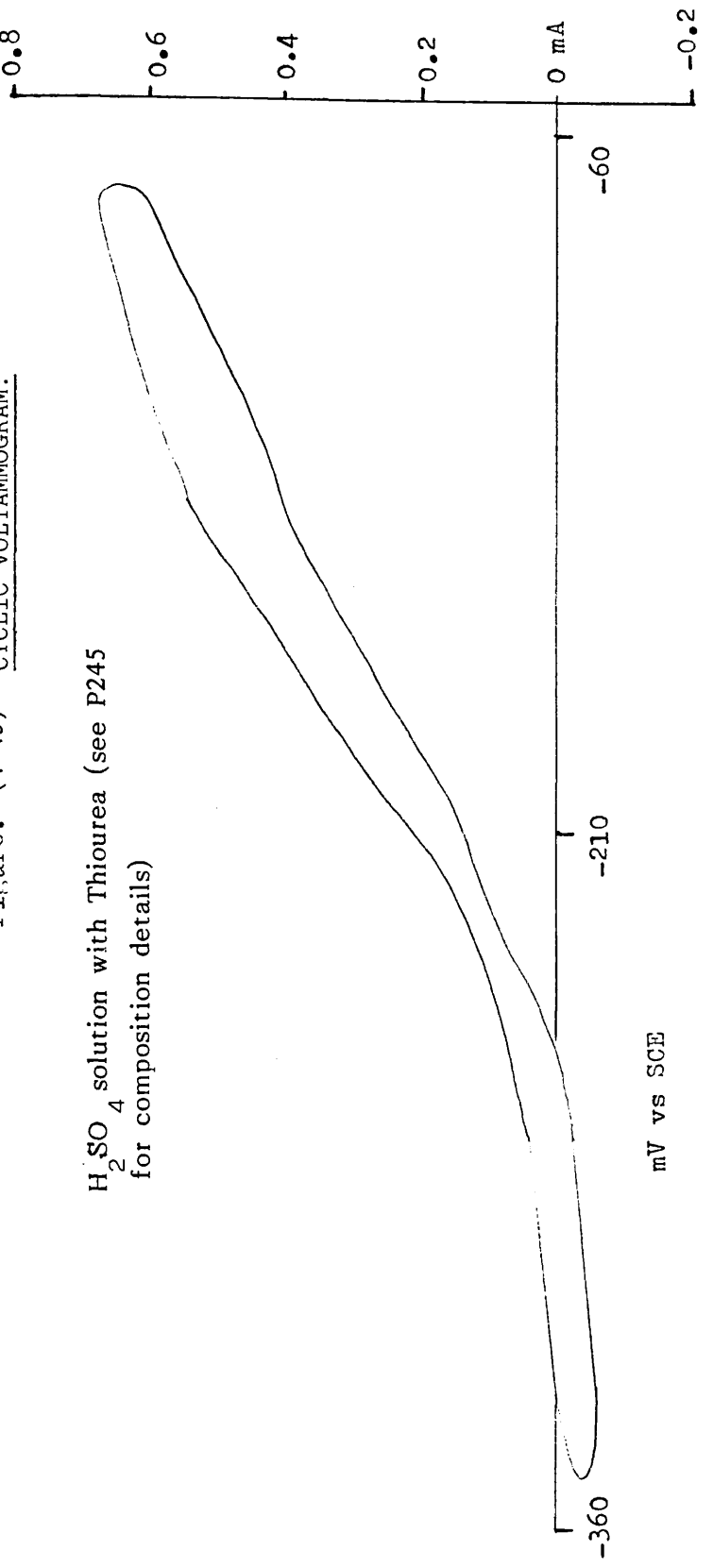

Figure: (4-45) CYCLIC VOLTAMMOGRAM:

H_2SO_4 solution with Thiourea (see P245 for composition details)

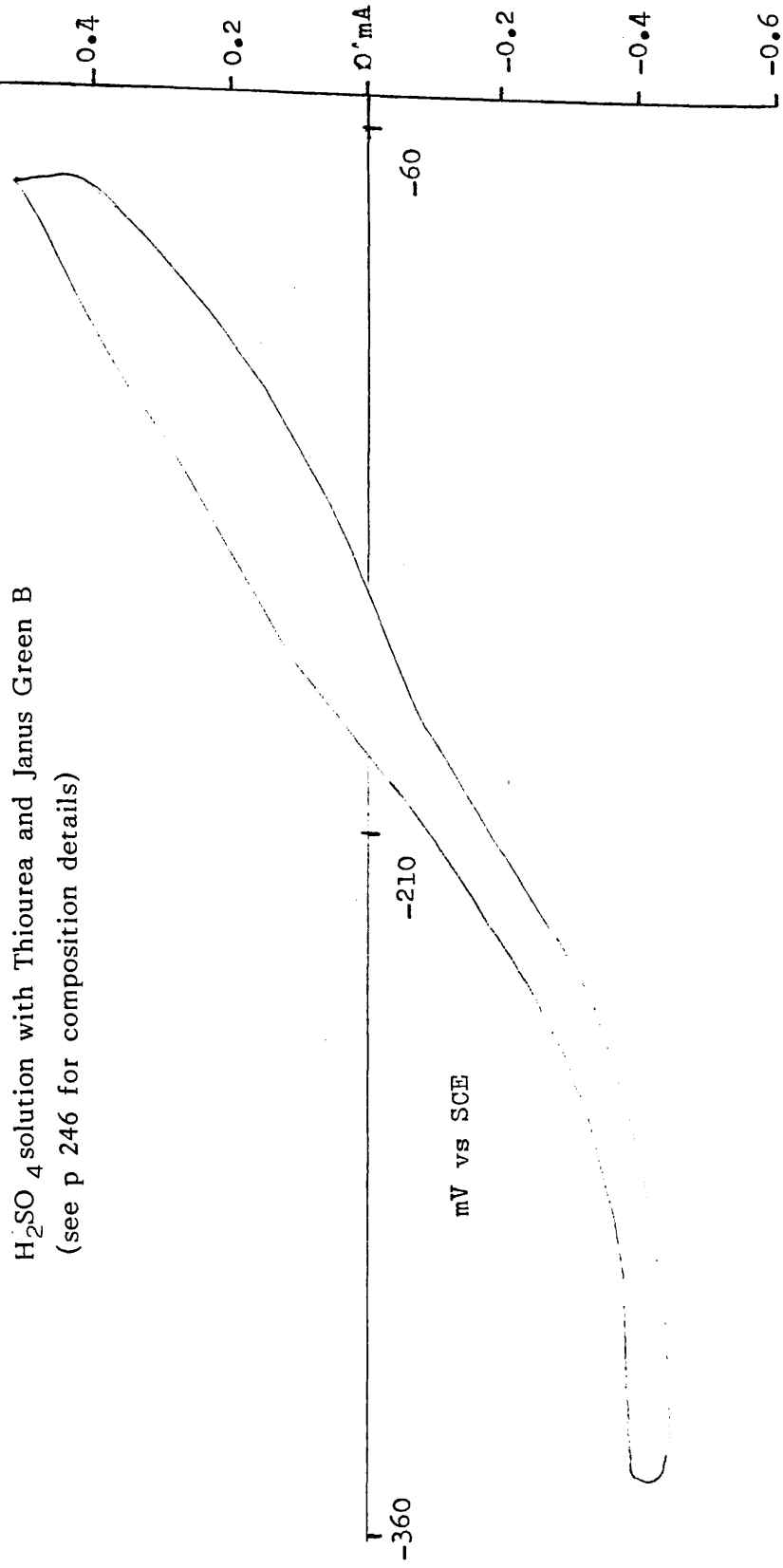

Figure: (4-46) CYCLIC VOLTAMMOGRAM:

H_2SO_4 solution with Thiourea and Janus Green B
(see p 246 for composition details)

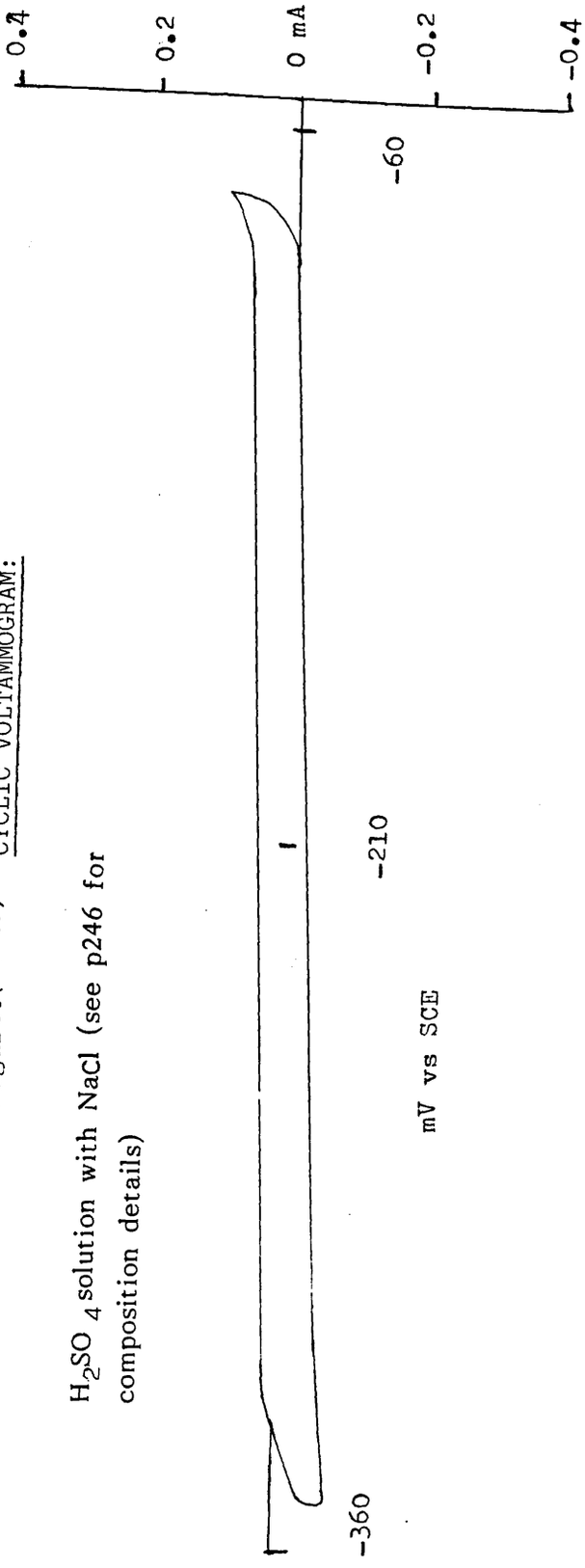

Figure:(4-47) CYCLIC VOLTAMMOGRAM:

H_2SO_4 solution with NaCl (see p246 for composition details)

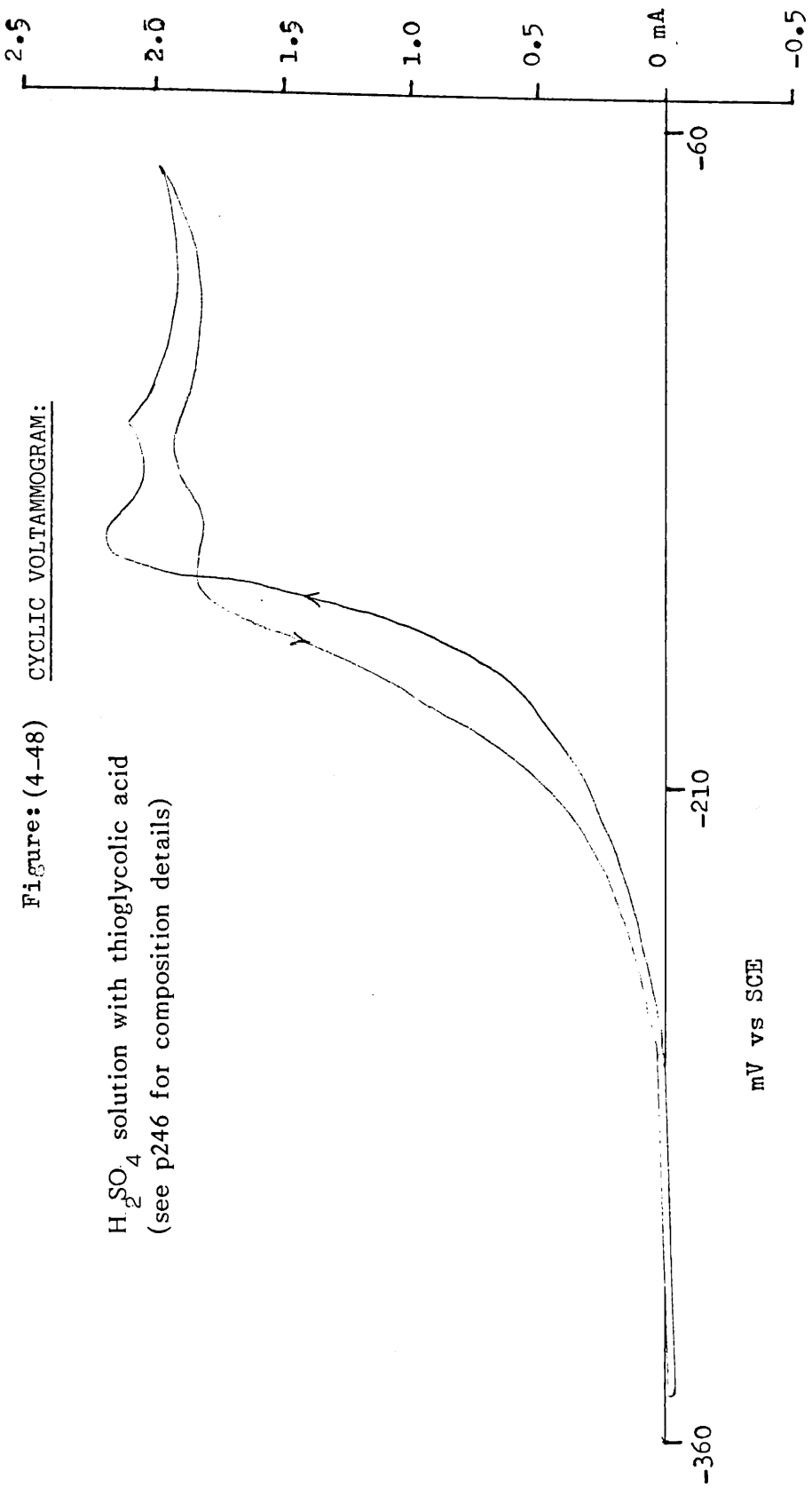

Figure: (4-48) CYCLIC VOLTAMMOGRAM:

H_2SO_4 solution with thioglycolic acid
(see p246 for composition details)

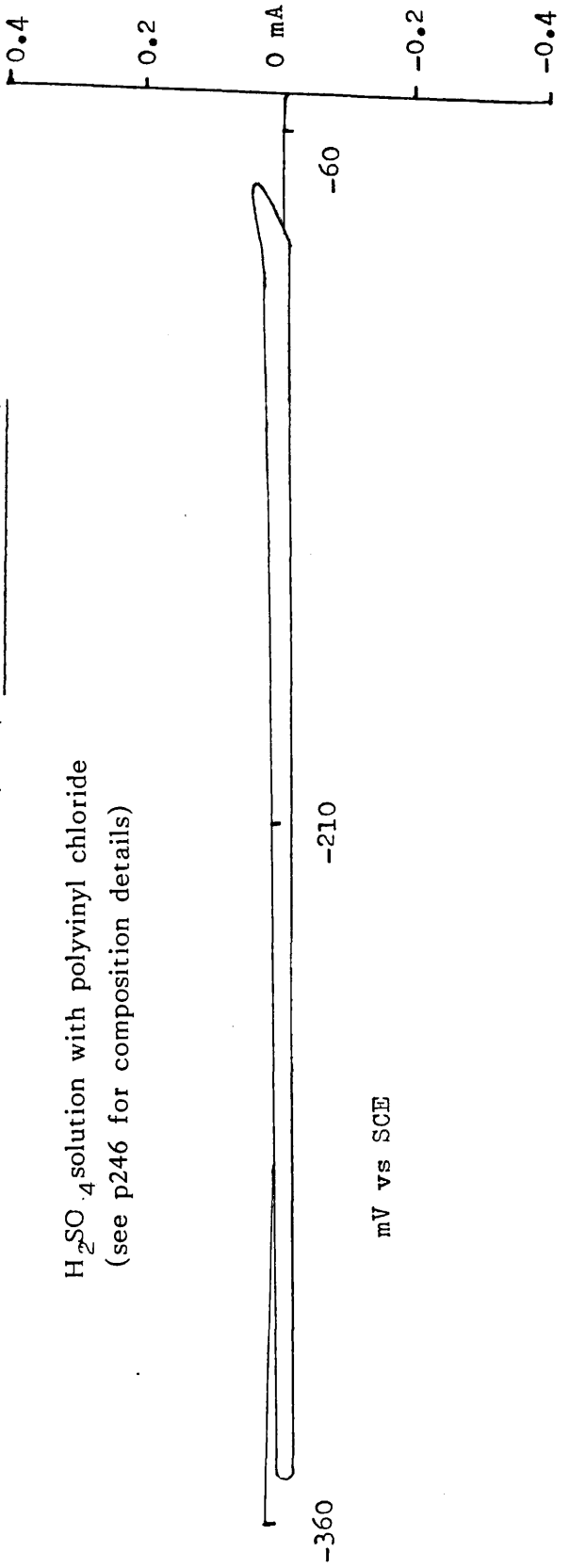

Figure: (4-49) CYCLIC VOLTAMMOGRAM:

H_2SO_4 solution with polyvinyl chloride
(see p246 for composition details)

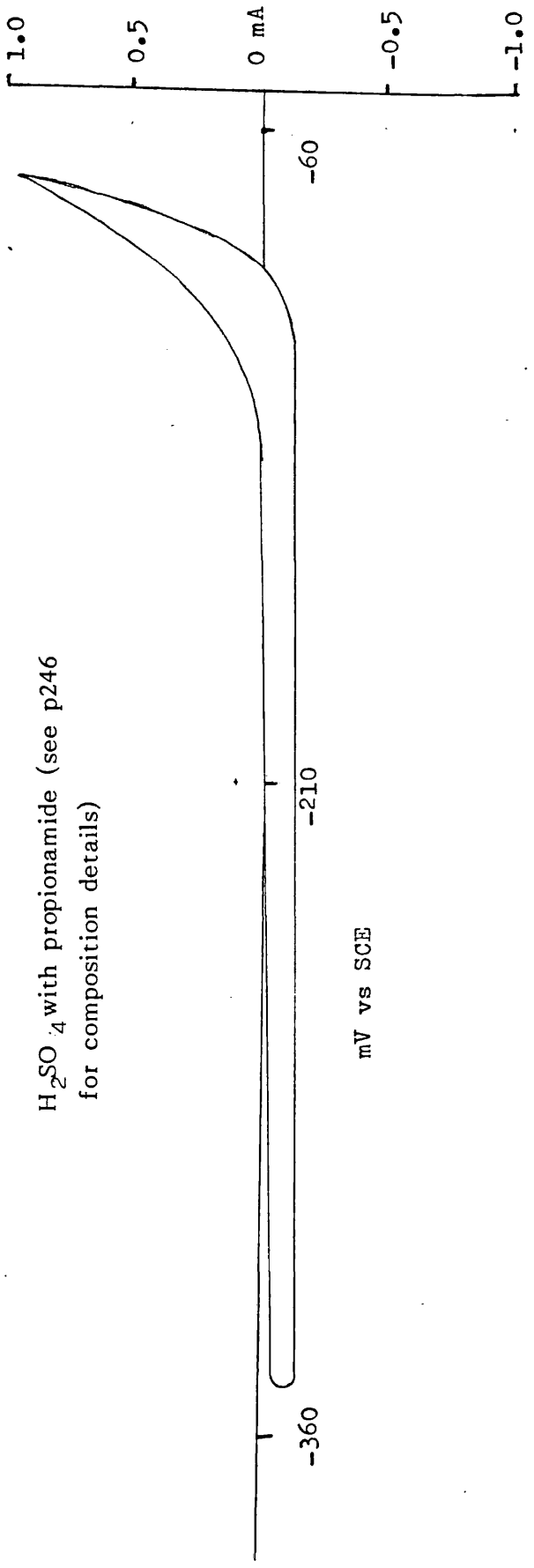

Figure:(4-50) CYCLIC VOLTAMMOGRAM:

H_2SO_4 with propionamide (see p246 for composition details)

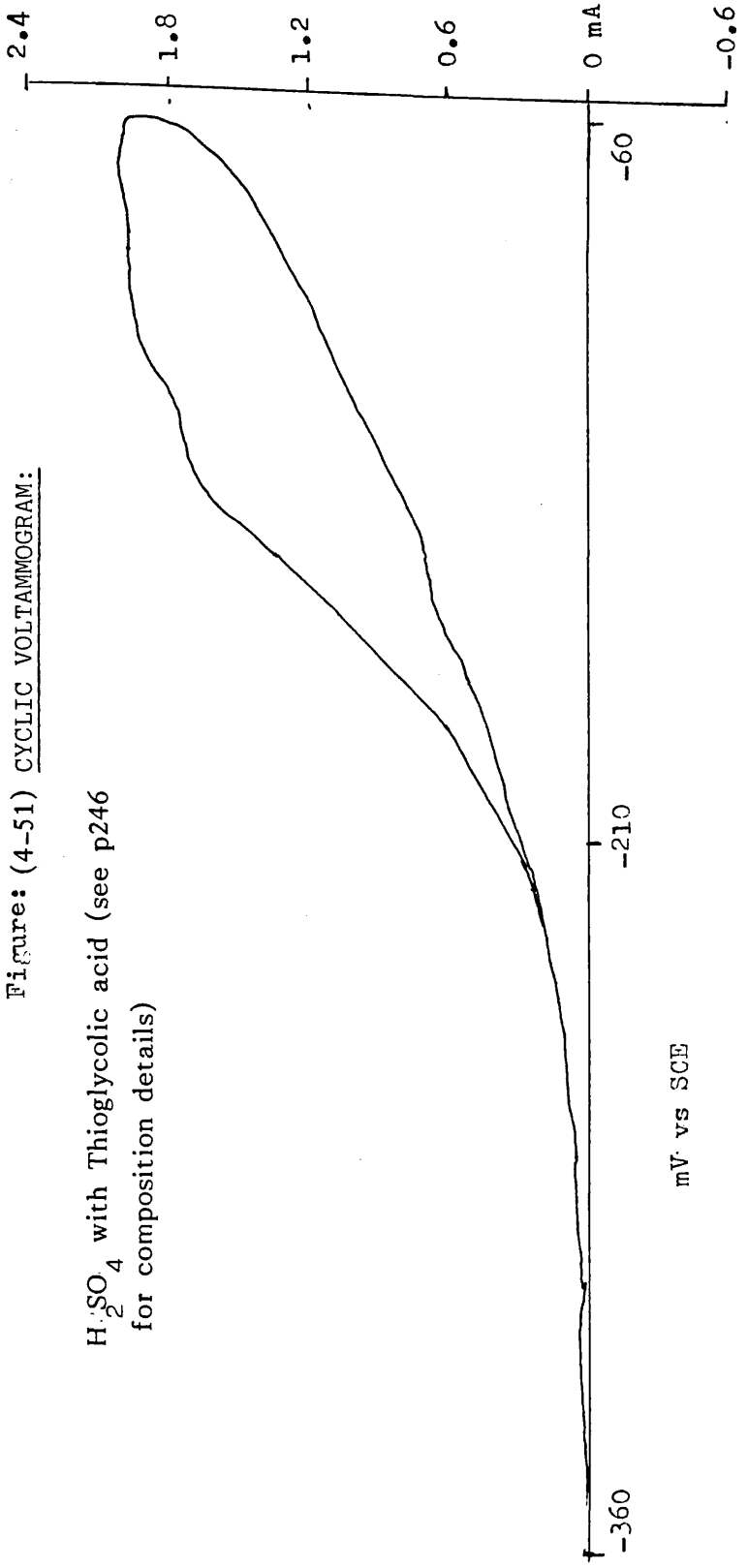

Figure: (4-51) CYCLIC VOLTAMMOGRAM:

H_2SO_4 with Thioglycolic acid (see p246 for composition details)

Table: (4-1) COMPOSITIONS OF ELECTROLYTES:

Figure	Conc. of H_2SO_4 mol dm^{-3}	Additives	Conc. of Additives g dm^{-3}	Potential (vs SCE) mV at i=0 Anodic direction	Cathodic direction
4-39	2.0	-	-	-270	-83
4-40	0.153	-	-	-142	-84
4-41	2.0	imidazole	0.022	-210	-88
4-42	2.0	Histamine	0.036	-195	-86
4-43	0.153	Janus Green B	0.050	-80	-72
4-44	0.153	Dimehtyl Thiourea	0.030	-300	-215
4-45	0.153	Thiourea	0.027	-325	-255

Table: (4-2) COMPOSITIONS OF ELECTROLYTES:

Figure	Conc. of H_2SO_4 mol dm^{-3}	Additives	Conc. of Additives g dm^{-3}	Potential (vs SCE) mV at i=0	
				Anodic direction	Cathodic direction
4-46	0.153	Thiourea Janus Green B	0.027 0.050	-190	-157
4-47	2.000	Sodium Chloride	0.050	-307	-94
4-48	2.000	Thioglycolic acid	0.010	-290	-285
4-49	2.000	polyvinyl alcohol	0.060	-240	-82
4-50	2.000	Propionamide	0.100	-180	-94
4-51	2.000	Thioglycolic acid Polyvinyl alcohol Propionamide Sodium Chloride	0.010 0.060 0.100 0.050	-276	-276

Table: (4-3) COMPOSITIONS OF ELECTROLYTES:

Figure	Conc. of $CuSO_4$ mol dm^{-3}	Conc. of H_2SO_4 mol dm^{-3}	Additives	Conc. of Additives g dm^{-3}
4-6	0.802	0.153	-	-
4-7	0.321	2.0	-	-
4-8	0.321	2.0	Imidazole	0.022
4-9	0.321	2.0	Histamine	0.036
4-10	0.802	0.153	Janus Green Dimethyl thiourea	0.05 0.03
4-11	0.321	2.0	Thioglycolic acid Propionamide Polyvinyl alcohol NaCl	0.01 0.10 0.06 0.05

TAble: (4-4) Electrode Kinetic Parameters for Copper Deposition

Electrolytes mol dm^{-3}	Additives g dm^{-3}	Cathodic Transfer coefficient (α_c)	Exchange current densities (mA cm^{-2})	Double layer Capacitance μF cm^{-2}
Cu_{2+} = 0.321 H2SO4 = 2.00		(1) 0.53 (2) 0.49	(1) 3.02 (2) 4.42	34.42 $\pm$ 3.31
Cu^{2+} = 0.802 H2SO4 = 0.153		(1) 0.5 (2) 0.41 (3) 0.472	(1) 6.82 (2) 7.76 (3) 6.92	
Cu^{2+} = 0.321 H_2SO_4 = 2.00	H = 0.036	(1) 0.49 (2) 0.51 (3) 0.44	(1) 3.32 (2) 3.26 (3) 5.12	15.47 $\pm$ 5.64
Cu_{2+} = 0.321 H_2SO_4 = 2.00	I = 0.022	(1) 0.431 (2) 0.42 (3) 0.41	(1) 5.25 (2) 5.37 (3) 7.41	19.70 $\pm$ 4.11
Cu^{2+} = 0.802 H_2SO_4 = 0.153	DT = 0.030 JGB = 0.05	(1) 0.203 (2) 0.23	(1) 7.24 (2) 5.0	11.69 $\pm$ 1.01
Cu^{2+} = 0.321 H_2SO_4 = 2.00	TA = 0.010 PA = 0.10 PV = 0.06 NaCl = 0.050	(1) 0.29 (2) 0.28	(1) 18.2 (2) 19.49	8.68 $\pm$ 2.67

Abbreviation: H = Histamine, I =Imidazole, DT = Dimethyl thiourea, JGB = Janus Green B,
TA = Thioglycolic acid, PA = Propionamide, PV = Polyvinyl alcohol

Table: (4-5)

GRAIN SIZE, APPEARANCE OF DEPOSITS AND DOUBLE LAYER CAPACITANCE:

Current density ($mA\ cm^{-2}$)	Average grain size (μm)	Double layer capacitance ($\mu F\ cm^{-2}$)	Macroscopic appearance of deposit
6.25	12.12 ± 1.75	31.25	smooth dull
6.25	13.83 ± 1.472	31.25	smooth, dull
25.00	2.99 ± 0.333	35.71	smooth, dull
25.00	2.63 ± 0.263	33.33	smooth, dull
50.00	4.17 ± 0.679	33.33	rough edge,dull
100.00	6.10 ± 0.443	40.00	rough edge,dull

Electrolyte composition: copper sulphate 0.32 mol dm^{-3}

sulphuric acid 2.00 "

Measured rest potential: 7.88 ± 0.99 mV vs SCE

Table: (4-6)

GRAIN SIZE, APPEARANCE OF DEPOSITS AND DOUBLE LAYER CAPACITANCE:

Current density (mA/cm^2)	Average grain size (μ m)	Double layer capacitance ($\mu F/cm^2$)	Macroscopic appearance of deposit
6.25	6.30 ± 0.969	15.63	smooth, dull
25.0	0.97 ± 0.112	15.63	smooth, dull
50.0	1.35 ± 0.323	20.0	rough edge, dull
50.0	1.19 ± 0.226	22.22	rough edge, dull
100.0	---	25.0	rough edge, dull

Electrolyte composition : imidazole : 3.21×10^{-4} mol dm^{-3}
copper sulphate : 0.321 "
sulphuric acid : 2.00 "

Measured rest potential : 13.1 ± 0.89 mV vs SCE

Table: (4-7)

GRAIN SIZE, APPEARANCE OF DEPOSITS AND DOUBLE LAYER CAPACITANCE:

Current density mA cm^{-2}	Average grain size (μ m)	Double layer capacitance ($\mu F\ cm^{-2}$)	Macroscopic appearance of deposit
6.25	14.51 $\pm$ 1.274	12.50	smooth, dull
25.00	1.19 $\pm$ 0.125	8.33	smooth, dull
50.00	1.91 $\pm$ 14.28	14.28	smooth, dull
100.00	1.42 $\pm$ 0.275	22.22	rough edge, dull
100.00	1.73 $\pm$ 0.172	20.0	rough edge, dull

Electrolyte composition : histamine 3.21×10^{-4} mol dm^{-3}
copper sulphate 0.321 "
sulphuric acid 2.00 "

Measured rest potential : 10.68 $\pm$ 1.92 mV v s SCE

Table: (4-8)

GRAIN SIZE, APPEARANCE OF DEPOSITS AND DOUBLE LAYER CAPACITANCE:

Current density $mA\ cm^{-2}$	Average grain size (μm)	Double layer capacitance ($\mu F\ cm^{-2}$)	Macroscopic appearance of deposit
6.25	1.70 ± 0.463	6.25	smooth, dull
25.00	0.44 ± 0.082	20.00	smooth, dull
50.00	0.63 ± 25.00	25.00	smooth, dull
100.00	0.79 ± 0.074	23.50	smooth, dull

Electrolyte composition : janus green $0.05\ g\ dm^{-3}$
copper sulphate 0.802 mol dm^{-3}
sulphuric acid 0.153 "

Measured rest potential : 62.35 ± 2.38 mV vs SCE

Table: (4-9)

GRAIN SIZE, APPEARANCE OF DEPOSITS AND DOUBLE LAYER CAPACITANCE:

Current density mA cm^{-2}	Average grain size (μ m)	Double layer capacitance (μ F cm^{-2})	Macroscopic appearance of deposit
6.25	0.52 $\pm$ 0.058	12.5	Layer, d brown/bright
25.00	0.30 $\pm$ 0.089	12.5	Layer, d brown/bright
50.00	0.44 $\pm$ 0.135	14.7	Layer, d brown/bright
100.00	0.48 $\pm$ 0.122	20.00	smooth, bright
100.00	0.52 $\pm$ 0.19	18.2	smooth, bright

Electrolyte composition : Di methyl thiourea 2.89×10^{-4} mol dm^{-3}
copper sulphate 0.802 "
sulphuric acid 0.153 "

Measured rest potential : 45.8 $\pm$ 1.83 mV vs SCE d;dark

Table:(4-10)

GRAIN SIZE, APPEARANCE OF DEPOSITS AND DOUBLE LAYER CAPACITANCE:

Current density $mA\ cm^{-2}$	Average grain size (μ m)	Double layer capacitance ($\mu F\ cm^{-2}$)	Macroscopic appearance of deposit
6.25	1.67 ± 0.2422	10.4	smooth, dark brown
25.00	0.70 ± 0.126	12.5	smooth, dull
50.00	0.82 ± 0.222	11.37	smooth, dull
100.00	0.49 ± 0.098	12.5	smooth, bright

Electrolyte composition : Di methyl thiourea 2.89×10^{-4} mol dm^{-3}
Janus green B 0.05 g dm^{-3}
copper sulphate 0.802 mol dm^{-3}
sulphuric acid 0.153 mol dm^{-3}

Measured rest potential : 57 ± 0.82 mV vs SCE

Table: (4-11)

GRAIN SIZE, APPEARANCE OF DEPOSITS AND DOUBLE LAYER CAPACITANCE:

Current density (mA cm^{-2})	Average grain size (µm)	Double layer capacitance (µF cm^{-2})	Macroscopic appearance of deposit
6.25	A. 0.84 ± 0.205 B. 0.88 ± 0.210	A. 5.00 B. 4.17	A. smooth brown/yellow B. smooth brown/yellow
25.00	A. 0.70 ± 0.109 B. 0.84 ± 0.093	A. 8.33 B. 10.00	A. smooth, bright B. smooth, bright
50.00	A. very small B. very small	A. 10.00 B. 10.00	A. smooth, bright B. smooth, bright
100.00	A. 6.83 ± 0.516 B. 5.39 ± 0.803	A. 11.10 B. 10.87	A. smooth, bright B. smooth, bright

Electrolyte composition:

Thioglycolic acid	1.435×10^{-5}	mol dm^{-3}
sulphuric acid	2.00	"
copper sulphate	0.321	"
propionamide	0.10	g dm^{-3}
polyvinyl alcohol	0.06	"

Measured rest potential: 6.475 ± 0.34 mV vs. SCE

Table: (4-12) STEADY STATE OVERPOTENTIAL TIME:

Electrolytes mol dm^{-3}	Additives g dm^{-3}	T_{ss} (ms) at different current densities (mA cm^{-2})					
		6.25	12.5	25.0	37.5	50.0	62.5
Cu^{2+} = 0.321 H2SO4 = 2.00		3.0	0.65	0.48	0.35	0.25	0.15
Cu^{2+} = 0.802 H2SO4 = 0.153		3.0	0.65	0.52	0.56	0.4	0.36
Cu^{2+} = 0.802 H_2SO_4 = 0.153	DT = 0.030 JGB = 0.05	3.3	1.56	1.45	1.4	1.36	1.36
Cu^{2+} = 0.321 H_2SO_4 = 2.00	TA = 0.010 PA = 0.10 PV = 0.06 Nacl = 0.050	3.1	1.4	0.96	0.90	0.90	0.80

Abbreviation: DT = Dimethyl thiourea, JGB = Janus Green B, TA = Thioglycolic acid,
PA = Propionamide, PV = Polyvinyl alcohol

Table: (4-13) Sodium Azide Test on samples from different current densities and electrolytes.

Electrolyte mol dm^{-3}	Additives g dm^{-3}	Current Densities mA cm^{-2} 3.75	6.25	12.5	62.5
Cu^{2+} = 0.802 H_2SO_4 = 0.153	DT = 0.030 JGB = 0.050	N_2 evolved	N_2 evolved	N_2 evolved	N_2 evolved
Cu^{2+} = 0.321 H_2SO_4 = 2.00	TA = 0.010 PA = 0.1 PV = 0.06 NaCl = 0.050	N_2 evolved	N_2 evolved	N_2 evolved	N_2 evolved
Cu^{2+} = 0.321 H2SO4 = 2.00		No N_2 evolved	No N_2 evolved	No N_2 evolved	No N_2evolved
Pure copper foil		No N_2 evolved			

Abbreviations: DT = Dimethyl thiourea, JGB = Janus Green B, TA = Thioglycolic acid,
PA = Propionamide, PV = Polyvinyl alcohol

Table: (4-14) CuS spot Tests on samples from different current densities and electrolytes.

Electrolytes mol dm^{-3}	Additives g dm^{-3}	mA cm^{-2}	Colour changes of sample	Presence of gas bubbles
$CuSO_4$ = 0.321 H_2SO_4 = 2.0	No	(1) 3.75 (2) 12.50 (3) 50.0 (4) 62.5	(1) reddish brown; No (2) reddish brown; No (3) reddish brown; No (4) reddish brown; No	No No No No
$CuSO_4$ = 0.321 H_2SO_4 = 2.0	TA = 0.010 PA = 0.100 PV = 0.060 NaCl = 0.050	(1) 3.75 (2) 12.50 (3) 50.0 (4) 62.5	(1) brown/yellow to black (2) bright to black (3) bright to black (4) bright to black	Yes Yes Yes Yes
$CuSO_4$ = 0.802 H_2SO_4 = 0.153	DT = 0.030 JGB = 0.050	(1) 3.75 (2) 12.50 (3) 50.0 (4) 62.5	(1) dark brown to black (2) dark brown to black (3) bright; No (4) bright; No	Yes Yes No No
Copper foil			reddish brown; No	No

Abbreviation ; see Table: (4-13)

Part (4-3)DISCUSSION

Sect (4-3.1) The Effect of Addition Agents on the Kinetics of Copper Electrodeposition:

The electrodeposition of copper studied in this work falls into 3 groups according to the compositions of the solution, and the effect which they produce.

(1) Solutions with pure acidic copper sulphate solution. This solution does not give bright deposit.

(2) Solutions with an heterocyclic compound such as

imidazole

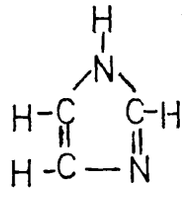

and histamine

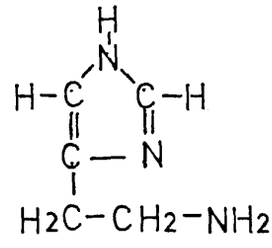

Both the addition agents had no effect in brightening the deposit.

(3) Solutions with a group of addition agents containing a brightener such as dimethyl thiourea or thioglycolic acid. Both of the brighteners are sulphur containing compounds. Bright deposits are obtainable from these solutions.

The cathodic transfer coefficients (α_c) for the acidic cupric sulphate solution without any addition agent was found to be 0.48 $\pm$ 0.05. This value agreed with results obtained by Bockris et al[2,6], using electrodeposited copper electrodes.

According to the following equation[97] the i_o value is proportional to activities of the reducible and oxidisable reactants in solution.

$$i_o = nF\, k^o\, a_{red}^{(1-\alpha_c)}\; a_{ox}^{(\alpha_c)} \qquad E(4-2)$$

For electrodeposition of copper from pure copper sulphate solution, reducible ions are predominantly Cu^{2+} and the oxidisable species is the copper electrode. Since the activity of solid is equalled to one, the relationship between i_o and the ions in pure copper electrolyte can be expressed as

$$i_o = nF\, k^o\, a_{Cu^{2+}}^{(1-\alpha_c)} \qquad E(4-3)$$

The above derived equation predicts that the value of i_o is proportional to square root of the activity of the Cu^{2+} ions. This agrees reasonably with experimental observations here. The i_o value for a 0.32 mol dm^{-3} Cu^{2+} solution was found to be 3.7 mA cm^{-2} at 25°C (table 4-4, p248). At the same temperature, the i_o values for the 0.802 mol dm^{-3} solution was found to be 7.2 ± 0.5 mA cm^{-2}.

The α_c values for solutions containing imidazole or histamine are not appreciably different from those of pure acidic cupric sulphate solution (i.e. table 4-4, p248). This suggests that the mechanism of the metal-solution exchange reaction of group (2) addition agents is probably the same as those of pure copper sulphate solution.

The cathode potential-$\log_{10}$ i curves obtained from solutions containing dimethylthiourea and janus green B (fig 4-10,p223) show that at a current density of 3 mA cm^{-2}, the overpotentials are higher than the overpotential obtained from pure cupric sulphate solution (fig 4-6,p219). Also there is an inflexion on each curve and a depolarizing effect on the electrode is indicated at 10 mA cm^{-2}. The presence of this inflexion probably implies that surface diffusion of adsorbed ions to the steps (fig 2-28,p86) is still playing a significant role in determining the rate of reaction. This is because for a predominantly charge transfer rate determining reaction in Cu^{2+} deposition, the curve of the cathode potential-$\log_{10}$i at this high field region (i.e. $>$50 mV) is linear. Also the steady state overpotential time (T_{ss}) (table 4-12,p256) values from dimethyl thiourea solutions is much longer than those obtained from pure $CuSO_4$ solution. In addition, the inflexion probably indicates that there is also a possibility of the occurence of a second reaction instead of only the Cu^{+} deposition process. The consequence of this additional reaction might affect the shape of the curve and the surface diffusion rate of adsorbed ions.

The α_c derived from the Tafel slope of the linear portion of the curve was much lower [i.e. about 0.202 (table 4-4,p248)] than the values obtained from pure $CuSO_4$ solution. The Tafel exchange current density in this case is slightly less than those values obtained from pure cupric sulphate solution.

Turner and Johnson[59] also carried out the kinetics studies of copper sulphate solution containing thiourea. Their α_c values and shape of the curves are closely similar to the results obtained here.

The α_c and i_o obtained from solutions with thioglycolic acids and other addition agents are about 0.29 and 29 mA cm^{-2} respectively. The anomaly of higher i_o values suggest that it is easier for copper to plate out from solution. A similar type of inflexion is also present on each curve (fig 4-11,p224) but to a lesser degree.

Sect(4-3.2) Double Layer Capacitance and Adsorption

The double layer capacitance average results (table 4-4,p248) show that the presence of addition agents had lowered the C_{dl} values. This lowering of C_{dl} values is much more significant in solutions containing brighteners. From the measured double layer capacitance values, the number of molecules which adsorbed on the electrodes can be calculated. The following assumptions are made.

(1) A blocked site on the electrode by the organic molecules does not contribute to the double layer capacitance.

(2) The area of the electrode deposit does not change between the measurements of $C_{dl(Cu^{2+})}$ and $C_{dl(organic)}$

The calculations are carried out as follows:

(A) Calculation of the area covered per molecule:-

The following sitting positions on the electrode have been decided. It is assumed here that, the higher the electronegativity of an atom or group of atoms the more likely that atom or group of atoms will be attracted to a negatively charged surface.

(i) Imidazole Molecule:

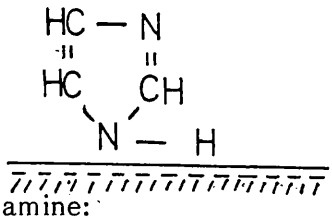

fig(4-52)

(ii) Histamine:

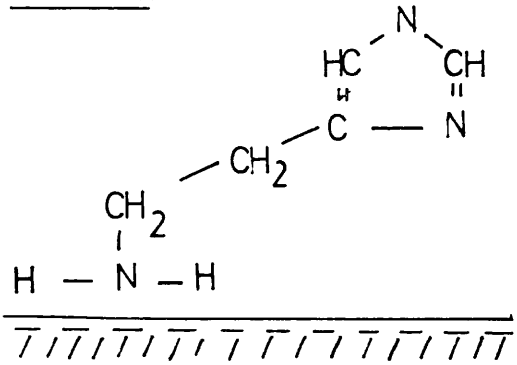

fig (4-53)

(iii) Disulphide of Dimethyl Thiourea:

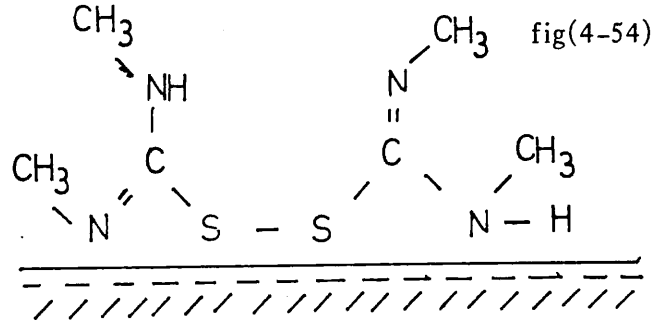

fig(4-54)

(iv) Disulphide of Thioglycolic Acid:

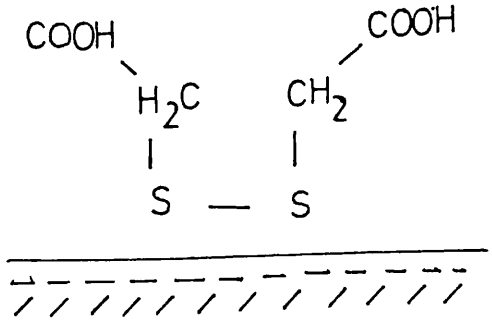

The covalent radii of the atoms are:[101]

-H- = 0.31 Å , -N- = 0.70 Å

=N = 0.63 Å -S- = 1.04 Å

The radius of a molecule that covers the surface is taken to be the sum of the radii of the adsorbed atoms. Area covered by these molecules is π x (the total radius of adsorbed atoms)^2. Therefore, the areas covered by different molecules are as follows:

Imidizole Area = 3.202 $(\text{Å})^2$

Histamine Area = 5.471 $(\text{Å})^2$

Disulphide of Dimethyl thiourea Area = 50.99 $(\text{Å})^2$

Disulphide of thioglycolic Acid Area = 13.85 $(\text{Å})^2$

(B) Caculation of area covered by organic molecules from C_{dl} measurement

Let $C_{dl(Cu^{2+})}$ be the capacitance of the electrode in $CuSO_4/H_2SO_4$

Let $C_{dl(organic)}$ be the capacitance of the electrode in $CuSO_4/H_2SO_4$/addition agents.

True area $(Area)_{cu^{2+}}$ of electrode in $CuSO_4/H_2SO_4$ is

$$(Area)_{Cu^{2+}} = \frac{C_{dl(Cu^{2+})} \times \text{Apparent Area } (8cm^2)}{17} \qquad E(4-4)$$

True area $(Area)_{organic}$ of electrode in $CuSO_4/H_2SO_4$/addition agents

$$(Area)_{organic} = \frac{C_{dl(organic)} \times 8\ cm^2}{17} \qquad E(4-5)$$

Therefore area covered by organic is

$$= (Area)_{cu^{2+}} - (Area)_{organic} \qquad E(4-6)$$

The total number of molecules adsorbed is

$$= \frac{(Area)_{Cu^{2+}} - (Area)_{organic}}{\text{Area of one molecule}} \qquad E(4-7)$$

Calculated values of the number of adsorbed molecules for imidazole, histamine, disulphide of dimethyl and thioglycolic acid are 2.163×10^6, 1.630×10^6, 0.210×10^6 and 0.836×10^6 respectively. There are less brightener molecules being adsorbed, than the histamine and imidazole molecules, on the electrode. This is probably because their sizes are very much larger than imidazole and histamine.

Sect (4-3.3) The Reactions involving the Brighteners:

Postulating the rate determining mechanism of the depcsition of shiny copper deposits in an industrially used plating bath is difficult. This is because more than one addition agent is used in the bath so that a bright and smooth deposit can be obtained. Some of the addition agents have their specific functions. For example some addition agents increase the brightness of the deposit and they are known as brighteners (e.g.dimethyl thiourea). Levelling agents such as janus green B (i.e. Diethyl safranine azo phenol) decreases surface roughness. Frequently it is required to combine various addition agents to obtain a shiny deposit.

From the sodium azide tests on the copper deposits obtained from different baths, it was deduced that sulphur was embedded from sulphur containing addition agents (table 4-13,p257). Rogers and Ware[61] also found that incorporated sulphur in nickel deposits was from thiourea instead of sulphate.

Inclusion of sulphur in copper deposits from experiments here suggest that dimethyl thiourea and thioglycolic acid used in plating baths are involved significantly in electrodeposition of bright copper deposit.

The following are the chemical properties of dimethyl thiourea and thioglycolic acid.

Di-methyl thiourea is a thione and thioglycolic acid is a thiol. Their structural fomulae are as follows:

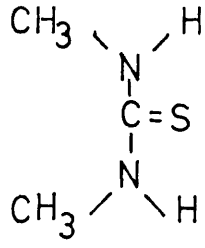

(Dimethyl thiourea)

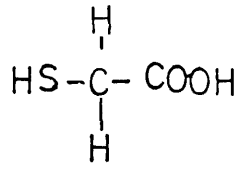

(thioglycolic acid)

The main structural difference between a thiol and a thione is that the thiol has a hydrogen atom attached to the sulphur and the thione does not.

One of the properties of thiols and thiones is that tautomerism exists between them[90]. It was suggested that thiourea exists as a thiol since it is easily oxidised in acidic solution to salts of unstable formamidine disulphide.[88] The two structural forms of thiourea are as follows:

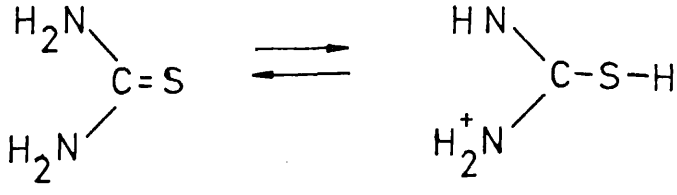

(Thione)

(Thiol)

Since the structure of thiones and thiols are closely related, therefore their reactions in electrodeposition of bright deposit are probably similar.

One of the products of the chemical reaction between Cu^{2+} and thiourea is formamidine disulphide.[46] Thus, it is very likely that dimethyl thiourea will react with Cu^{2+} present in the plating bath to form disulphide. The reaction is probably as follows:

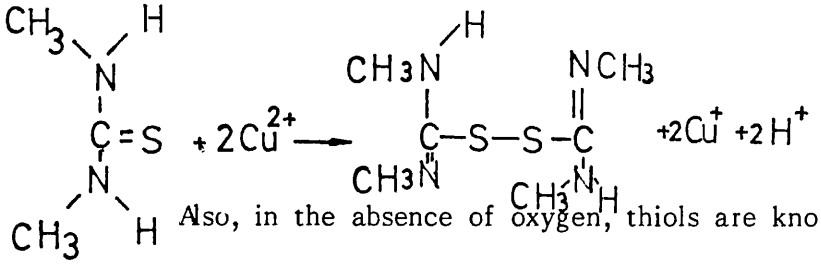

E(4-8)

Also, in the absence of oxygen, thiols are known to be oxidised by ions of transition metals which may exist in different states[89]. The oxidation reaction of thioglycolic acid shown below probably occurs in the N_2- purged plating bath.

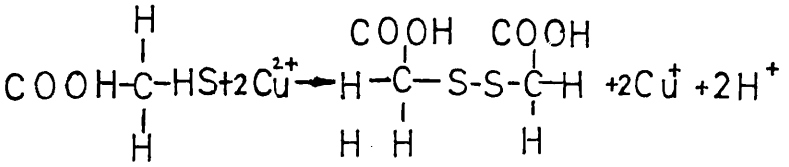

E(4-9)

The above two reactions show that it is possible for some of dimethyl thiourea and thioglycolic acid to be chemically oxidised into their respective disulphides. When these happen, the disulphides are probably adsorbed on copper electrode as well. Thus copper electrodes are probably covered by adsorbed layers of thioglycolic acid and its disulphide or by dimethyl thiourea and its disulphide.

Results showed that sulphur was present in the copper deposit, obtained from a plating bath containing dimethyl thiourea and thioglycolic acid (table 109). This suggests that there are probably more than one electro-chemical reactions taking place on the cathode.

It is postulated that there are probably at least 2 electrochemical reductions occuring on the cathode. The most likely electrochemical reaction is the reduction of Cu^{2+} to Cu^{o}. This is because there is a large amount of Cu^{2+} ions present in the solution.

The second possible electrochemical reduction process is the reduction of chemically formed disulphides back to dimethyl thiourea or thioglycolic acid. It is known that disulphides can be reduced to free thiols electrochemially[91] and a high yield of thioglycolic acid from dithioglycolic acid was obtained in 2N sulphuric acid at a lead electrode at - 0.55V *vs.* S.C.E..[95]. The electroreductions of both disulphides into thioglycolic acid and dimethyl thiourea are probably as follows:

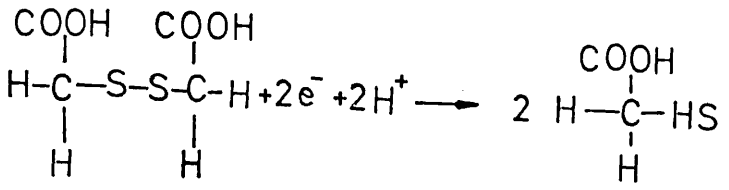

E(4-10)

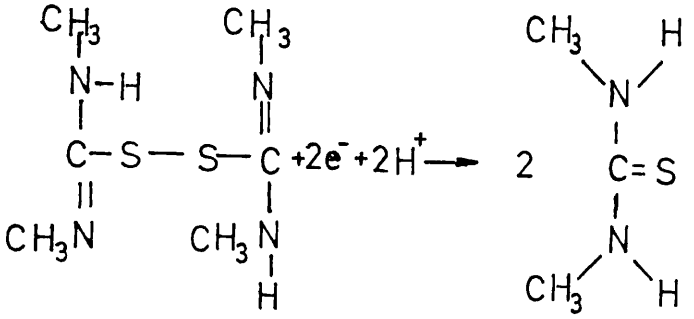

E(4-11)

The chemical oxidation reactions of dimethyl thiourea and thioglycolic acid E(4-8,4-9,p266) and the electroreduction of their disulphides show that they are interconvertable in cupric sulphate solution. These possibilities of interconversion of addition agents explains why that only small amount of brighteners are normally required for plating baths.

Turner and Johnson[59] suggested that sulphur was embedded in deposit of thiourea containing acidic cupric sulphate solution. Their explanation was that thiourea molecules come apart during the electroreduction process since, only sulphur and no carbon was detected in the deposit. The products of this reduction are NH_4CN and H_2S. The H_2S will then react with copper electrode and form CuS precipitate at the cathode surface. Following their suggestion, the electrochemical reduction of dimethyl thiourea and thioglycolic acid is probably as follows:

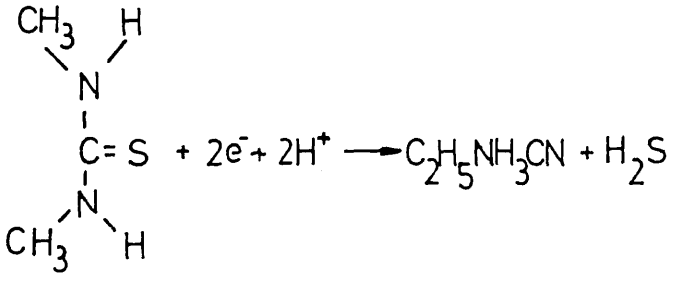

E(4-12)

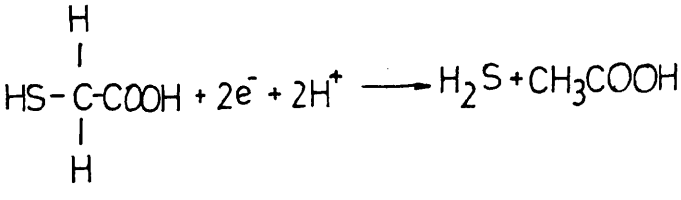

E(4-13)

In this experiment, sodium azide tests (p197) were carried out to detect the presence of sulphur compound such as sulphide, thiousulphate and thiocyanate in the deposit. The results (table 4-13,p257) show that at least one of the above compounds were present.

In order to confirm the inclusion mechanism of sulphur in deposits suggested by Turner, a detection of CuS spot tests (p199) were carried out. In principle when a drop of KCN is in contact with a copper sulphide (CuS) suspension which is placed on a spot plate, the brown colour due to copper sulphide disappear at once. This is due to the following chemical reaction[100],

$$CuS + 4KCN = K_2[Cu(CN)_4] + K_2S \qquad E(4\text{-}14)$$

Results from the tests (table 4-14,p258) carried out indicated that the above reaction probably does not occur This is because in most samples which contained sulphur (sodium azide test) changed from their original colour (dark brown, brown/yellow, bright brown) to black. In addition gas bubbles were also formed on the samples. The solid product of this test could probably be any of these black copper solids i.e. CuS , Cu_2S, CuO, CU_2O. The derivation from these tests is that the inclusion mechanism of sulphur in deposit suggested by Turner might not be applicable in the experiment carried out here.

More investigations are required in order to determine how sulphur are incorporated into deposits. It is also essential to know the form of sulphur present in the deposit . Dye and Klingenmaier [92] found that the brightener, fuchsin ($C_2OH_2ON_3Cl$) in its original form was embedded in nickel deposits. Therefore there is a possibility that dimethyl thiourea or thioglycolic acid or their respective disulphides be embedded in copper deposits.

Sect (4-3.3) Qualitative studies of the Electrochemical reactions in various solutions using Cyclic Voltammetric Techniques:-

Cyclic voltammetric studies were performed in pure sulphuric acid and in suphuric acid containing addition agents which were used in morphological studies. The solution contains each individual addition agent or a group of addition agents which were used in the bright plating process. The solution was stirred since deposits used for morphological studies were obtained in stirred electrolytes, and the aim of this experiment was to qualitatively differentiate the electrochemical behaviour of various addition agents. A short sweep range was used (i.e. -72mV to -350mV v s. S.C.E.) in order to avoide the anodic dissolution of the Cu^{o} working electrode and the hydrogen evolution at more negative potential. Tables (4-1,p245) and (4-2,p246) show the composition of electrolytes and potentials of the curve at i=o in both sweep directions.

For those solutions containing addition agents such as imidazole, histamine, Nacl and polyvinyl alcohol (fig 4-41,4-42, 4-47,4-49, between p234,p242) the voltammograms obtained were quite similar to those voltammograms obtained from pure sulphuric acid (fig 4-39,4-40,p232 and p 233). This suggests that these addition agents probably does not oxidise or reduce within the potentials of -72mV to - 351 mV v s. S.C.E.

In solution containing propanoamide, an anodic reaction seem to occur at the initial sweep range of -72mV to -90mV v s. S.C.E. (fig 4-50,p243). The voltammogram obtained from a solution containing janus green (B) (fig 4-43,p236) shows that throughout the whole sweep range cathodic reduction occurred significantly. This suggests that janus green B is reasonably reducible in sulphuric acid solution.

Results (fig 4-44,p237; 4-45,p238; 4-48,p241) show that the brighteners, thiourea, dimethyl thiourea and thioglycolic acid, oxidised anodically in a large part of the sweep range. It is known that the major products of the anodic oxidation of thio acids are the corresponding disulphides and anodic oxidation of thiourea is a convenient method for the preparation of corresponding formamidine disulphide salts[96]. The anodic oxidation of dimethyl thiourea and thioglycolic acid used in these experiments are probably as follows:

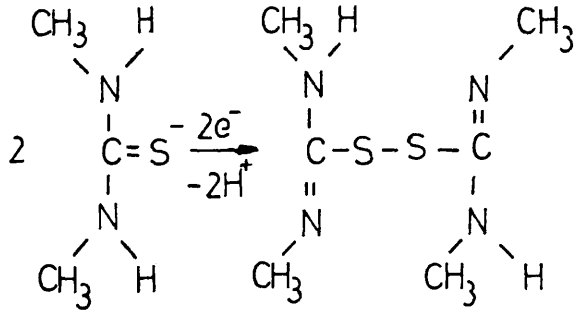

E(4-10)

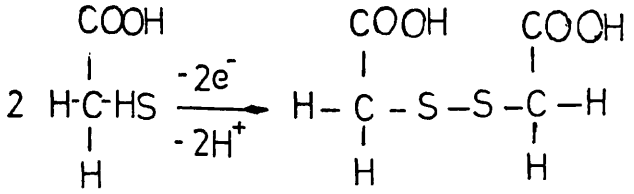

E(4-11)

In solution containing janus green B and thiourea, the voltammogram (fig 4-46,p239) indicated that anodic oxidation of thiourea takes place in the initial part of the sweep range (i.e. -72mV to -150mV) and the remainder part of the sweep range was predominantly due to cathodic reduction of janus green (B).

The voltammogram fig (4-51, p244) obtained from a solution containing thioglycolic acid, polyvinyl alcohol, NaCl and propionamide show that in 3/4 of the entire range of the sweep potential, anodic oxidation is predominant. These reactions are probably the oxidation of thioglycolic acid and propionamide.

The results obtained show that the sulphur containing brighteners are easily oxidised in sulphuric acid. Also organic compound such as janus green B are easily reduced. The rest of the addition agents appear not to be significantly active in the solutions.

Sect (4-3.4) The Effects of Addition Agents on the morphology of the Copper Deposits:

(A) Deposits obtained from H_2SO_4 solutions:-

The pyramidal form of deposit (fig 4-12,p225) obtained from pure copper sulphate solution at 6.25mA/cm^2 supports the bunching concept. This is because the flat portions of the pyrimidal faces may be pictured as composed of many thin, possibly monoatomic, steps assumed to be originate at the top of the pyramids and spreading in this region one after another. Approaching the base, however, smaller steps cluster and join into larger and eventually visible steps, with the distances between them increasing as they propagate[93].

Grain sizes at 6.25mA/cm^2 were very much larger than those at higher current densities (C.D.s) (table 4-5,p249). This is probably because at low current density there are very few hydrogen ions which are present in the diffusion layer at the cathode, which adsorb on the electrode. Hence at any instant, the majority of the sites suitable for crystal growth are free. Therefore, the mobility of the metal ions over the surface is not reduced. Thus there is a tendency for the crystal to grow into a reasonable size from each nuclei, and a large-grained deposits results.

As the current densities increase from 25mA cm^{-2} to 100mA cm^{-2} grain sizes also increase from about 3μm to 6.1 μm (table 4-5,p249). This is probably because the growing electrodeposit is inadequately supplied with ions at 100mA cm^{-2}, since the rate of Cu^{2+} consumption increases with current density. Therefore, further growth of electrodeposit prefers to concentrate in those parts which are easily accessible by copper ions. As a result the deposit has a larger grain size and these grains tend to form on the peak instead of the recessed parts of the electrode. The overall microscopic appearance of the deposit is that there are rows of cauliflower type of grains and with a gully in between the rows. Macroscopically edges of the electrode will be rough since they are more accessible to metal ions.

The grains change from a pyramidal form to boulder type and the cauliflower types at higher current densities (fig 4-13 to 4-15,p225). Possible reasons are the adsorption of hydrogen on the cathode which affects the growth of the deposit, and the depletion of Cu^{2+} ions at high current densities.

(B) Deposits obtained from imidazole-$CuSO_4$ and Histamine - $CuSO_4$ solutions:

Forms of deposits obtained at 6.25 mA cm^{-2} are of the boulder type (fig 4-19 to 4-22,p227). These grain boundaries are as well defined as those deposits obtained from sulphate solution. The grain sizes are reasonably larger than those obtained at high current densities. The common characteristics from deposits obtained in sulphate solution suggest that, at this low current density, the imidazole and histamine do not affect the mobility of Cu^{2+} ions significantly.

At higher current densities the shape of the grains are not distinctive and grain boundaries are no longer well defined (fig 4-17and 4-18,p226; 4-20 to 4-22,p227). Also grain sizes do not increase as the current density increases (table 4-6 and 4-7,p250 and 251). The above characteristics show that imidazole and histamine have quite a significant effect on the growth of deposits. This is probably due to the adsorption of some organic molecules.

At 100 mA cm^{-2} the same type of rough edges around the electrodes are also observed. This suggests that both imidazole and histamine are not levelling agents which will reduce roughness on the surface of an electrode. The deposits do not have a bright appearance but a normal metallic brown colour. This also shows that imidazole and histamine do not act as brighteners in copper sulphate solution.

(C) Deposits obtained from dimethyl thiourea -$CuSO_4$ Janus Green B - $CuSO_4$, and di-methyl thiourea with Janus Green B - $CuSO_4$ solutions:

At C.D. of 6.25 mA cm^{-2}, the microscopic appearance of the deposits obtained from dimethyl thiourea containing solutions are quite different from those obtained in janus green B - $CuSO_4$ solution. Irregular and random pyramidal type of grains (fig 4-23,p228) appear in the deposits obtained from janus green B - $CuSO_4$ solution. Clusters of small spherical grains were formed in solutions containing dimethyl thiourea (fig 4-27 and 4-31,p229-230). The grain sizes at this low current density are very much smaller than those grains obtained from $CuSO_4$ solution (i.e. < 1.70 ± 0.46 μm, table 4-8 to 4-10,p 252). This suggests that adsorption of di-methyl thiourea and janus green B molecules on copper cathodes inhibit the crystal growth process, and small-grained deposits result.

The dark brown precipitate type of deposits obtained at low current density from dimethyl thiourea containing solutions indicate that the deposits probably contain other compounds. Also (in dimethyl thiourea -$CuSO_4$ solution), two types of deposits appear on the cathode after electrodeposition. Parts of

the electrode were covered with bright deposit and the remainder with layers of dark brown precipitate type. Only the dark brown precipitate type of deposits obtained from di-methyl thiourea with janus green B - $CuSO_4$ solution suggest that janus green B is a levelling agent.

At higher current densities the grain sizes of the deposits obtained from dimethyl - $CuSO_4$ solutions do not reduce significantly (table 4-9,p253). The grain size from other solutions reduce to less than half of their sizes (table 4-8,4-10,p252,254). The general forms of these grains obtained from dimethyl thiourea containing solutions do not vary much from those of lower current density (4-27 to 4-34,p229 and p230). On the other hand, the grains obtained from janus green B - $CuSO_4$ solutions lost their slight pyramidal forms, into an irregular shape (fig 4-23 to 4-26,p228). This probably suggests that there might be an increase of adsorption of janus green B molecules on the cathode at higher current densities. This will affect the crystals growth process.

Macroscopically all the deposits obtained at high current densities (100mA cm^{-2}) (table 4-8 to 4-10, p252 to 254) do not have rough edges. This suggests that dimethyl thiourea or perhaps its disulphide and janus green B molecules preferentially adsorb on the microscopic peak of the electrode, until the recessed parts of the electrodes are levelled with a copper deposit.

(D) Deposits obtained from thioglycolic acid + others - $CuSO_4$ Solutions:

Two types of deposits were obtained at 6.25 mA cm^{-2} (fig 4-35,p231) on one electrode. The micrograph shows that they are normal small spherical grains and a spongy precipitate. The small grained deposit probably consists of metallic copper, and the spongy deposit of copper chloride. Macroscopically the deposit is brown/yellowish green in colour. Also the presence of chloride had been confirmed with a silver nitrate test. A smalll amount of sodium chloride had been added into the plating bath as a lustrous builder. Since the deposit was obtained using the galvanostatic pulsed method, a small amount of cuprous chloride will be formed[33](or see p165).

The grain sizes vary significantly at different current densities (table 4-11,p255). Also,microcracks appear on the deposits which were obtained at 50mA cm^{-2} (fig 4-37,p231). The deposits obtained at 25 mA cm^{-2}, 50 mA cm^{-2} and 100 mA cm^{-2} (table 4-11,p255) show that the individual grain sizes do not determine the brightness of the deposits. This is because all the deposits were bright and their grain sizes differ from an inmeasurable small to about 6 μm.

(E) Bright Deposits:

Bright copper deposits can only be obtained at reasonably high current desnities (i.e > 25mA cm^{-2}) in copper sulphate solutions containing dimethyl thiourea or thioglycolic acid as brighteners. It is observed here that the grains of bright deposits have the following features:

(i) Uniformly spherical grains which are small, and form reasonably smooth surfaces(fig 4-28, 4-30, 4-34, p229, p230)

(ii) Very smooth surface and the grains, very small (fig (4-37, p231).

(iii) Large and smooth oval shaped grains which may cluster togerher to form a dough like structure (4-38, p231).

The common physical property of the above three features is that light can be easily reflected without being blocked by adjacent grains or clusters of grains. This property probably gives the brightness of the deposits.

(F) The Levelling action of Janus Green B:-

Janus green B is a huge molecule and its structure is as follows:

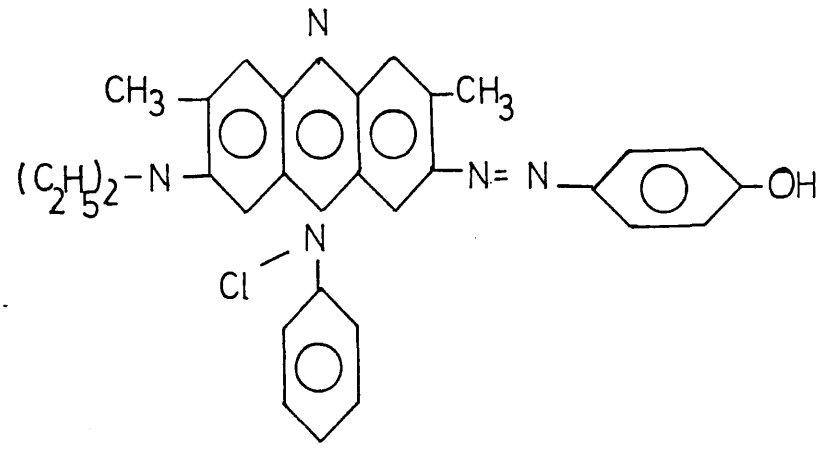

Assuming the diffusion-layer thickness between the surface of the electrode and the electrolyte has a linear variation of concentration with distance, using Fick's law of diffusion one has[102].

$$\frac{i}{nF} = J_D = -D \left(\frac{dc}{dx}\right)_{x=0} \qquad E(4\text{-}15)$$

or

$$\frac{i}{nF} = -D \frac{C^o - C_{x=0}}{\delta} \qquad E(4\text{-}16)$$

Therefore the diffusion current i is given by

$$i = -DnF \frac{C^o - C_{x=0}}{\delta} \qquad E(4\text{-}17)$$

When the heights between peaks and recesses on the electrode is small compared with the diffusion layer thickness, δ_{peak} will be less than δ_{recess} and as a result of this, more electrodeposition will take place on the peaks than on the flat or recess surface.

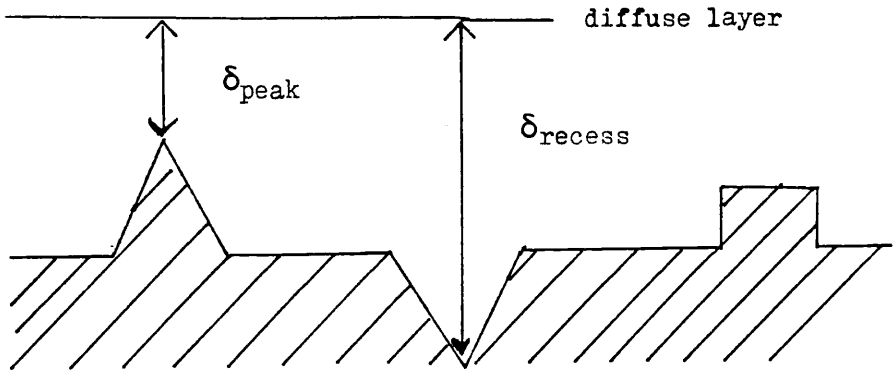

fig (4-56)

In order to slow down the rate of deposition on the peaks, levelling agents such as janus green B might be used. The mechanism of the inhibition process by janus green (B) molecule is proposed.

Considering janus green B molecule is adsorbed on a peak fig (4-57).

When the current is switched on, the coppper atoms will deposit on those vacant sites such as surface 1,2,3 and 4 (fig 4-57).

Fig (4-57)

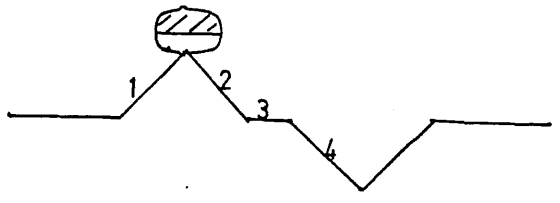

In the first step of depositon fig (4-58), the rate of deposition of copper atoms will be slightly faster in surfaces 1,2, and 3.The 4th surface has the slowest rate since its diffusion layer thickness is the largest.

Fig (4-58)

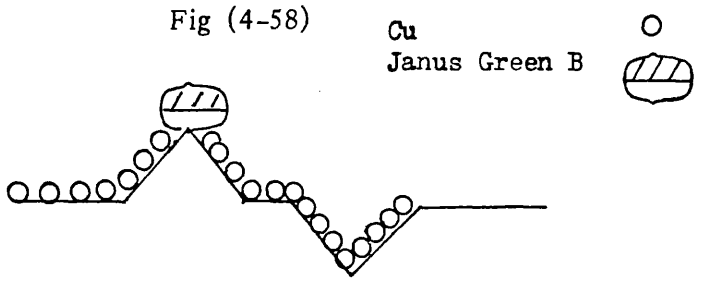

In the second step, the rate of deposition on surfaces 1 and 2 is reduced. This is because the adsorbed janus green molecule is obstructing the movement of Cu^{o} atoms. The rate of deposition of the 4th surface is accelerated since now its diffusion layer thickness is reduced and there is no obstacle for Cu^{2+} ions to deposit on its surface.

The deposition rate . of copper on surface 3 is probably not increased since this surface is getting crowded (fig 4-59)

Fig (4-59)

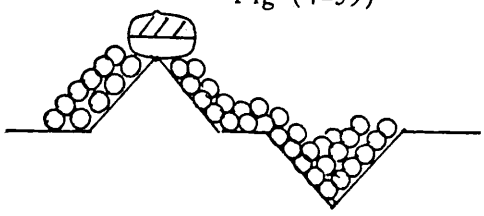

As the deposition process proceeds, the rate of depositon on surface 4 increases. Therefore, within the same time of depositions with surface 1,2,3, they will be more layers of copper atoms deposited on surface 4 than 1,2, and 3. The mobility of depositing atoms of surface 3 is restricted since it is also getting crowded due to the surface 2. As a result the number of atoms intending to deposit on surface 3 also reduced. Also forces due to the packed conditons on surface 1,2 and 3 begin to exert moment of force on the adsorbed molecule (fig 4-60).

FIg (4-60)

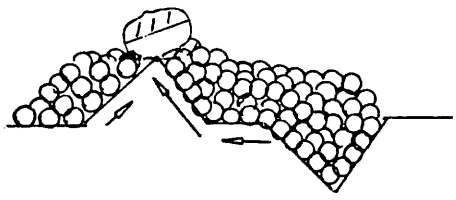

In the final stage, forces due to the densely packed condition on surface 2 and 3 will exert a very strong force on the adsorbed molecule. If the opposing force from the deposited atoms on surface 1 is not strong, it is quite likely for the adsorbed molecule willbe tumbled over towards the side nearer to surface 1 fig (4-61) and may be attracted to another close by peak. If the opposing force from surface 1 is also strong, it is quite likely that attractive force of the adsorbed molecules might be reduced and thus desorbed from the peak. The peak is now exposed to the depositing copper atoms. As a result, copper atom will deposit on the peak and the rest of surfaces with the same rate of deposition. This is because the diffusion layer thickness on the new surface is reasonably uniformed. A level surface is then obtained and this process is repeated until the surface of the electrode is smooth.

Fig (4-61)

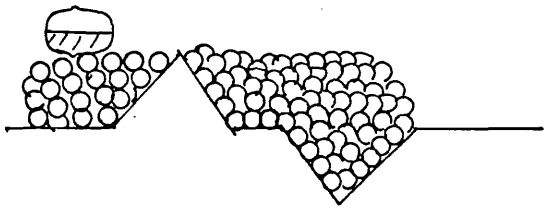

CONCLUSIONS

A galvanostatic pulse technique has been used to study the complex reactions of copper in copper (II) halide solutions. More understanding of these complex reactions have been achieved. From experimental results and with the aid of computer calculated results, it is known now that the $CuCl^+$ and $CuBr^+$ complexes are the main species which determine the Cu(I)Cl and Cu(I)Br formation reactions, ($25^oC \pm 0.5^oC$ and using total halide concentrations of less than 0.7 mol dm^{-3}).

The results of cyclic voltammetric show that brighteners, thioglycolic acid and dimethyl thiourea are readily oxidised and janus green B is easily reduced. This indicates that an addition agent probably needs to be reactive or easily adsorbed within the range of deposition overpotentials, in order to function well as a brightener or levelling agent.

Sulphur atoms were confirmed to be embedded in deposits but not as CuS

APPENDIX (1)

Computer Programme

This computer program was used in calculating the copper complexes in cupric sulphate solutions containing halides. The details of the program are as follows:

```
c            PROGRAM EQUIL
c       Equil calculates the equilibrium concentrations of
c       copper complexes.
c       K(I.J.) is the stability constant of Cu(J) L (I) where I is
c       the oxidation state of Cu, and J is the number of ligands
c       G(I,J) is the associated free energy change KCu is the
c       equilibrium constant for 2Cu+ = Cu2+ + Cu
c       Cul(I,J) is the equilibrium concentration of
c       Cu(J) L (I-1). J and I as before
c       TL is the total concentration of ligand
c       TCu is the total concentration of copper
c       L is the equilibrium concentration of ligand
c       GuessC is the tinitial value of the Cu2+ concentration
c       GuessL is the initial value of the ligand concentration
c       IP = 1  if you want the results of each iteration
c       MAXIT  The maximum number of iterations
```

```
      COMMON /B1/ Cul(5,2), K(4.2), L,KCU,TCU,TL
      REAL K,L,KCU
      DIMENSION G(4,2), B(4,2)
      CHARACTER *80 ITITLE
      EXTERNAL DIFFL
      READ (5, '(A80)' )ITITLE
      READ (5,100) T, KCU
      READ (5,100)K
      WRITE (6, '(//10X, '' Total copper concentration ?
      (E10.3).....'', $)' )
      READ (2,100) TCU
      WRITE (6, '(//10X, '' Total ligand concentration ?
      (E10.3).....'',  $)')
      READ (2,100)TL
C     Calculate free energy
      DO 1   I =1,2
      DO 1   J =1,4
      G(J, I) = 0
      If (K(J, I)  GT. O.)G(J, I) = -8.314*T*ALOG (K(J, I) )
    1 Continue
      B(1, 1) = K(1, 1)
      B(1, 2) K=(1, 2)
      DO 3  I=1, 2
      DO 3  J=2, 4
```

```
    3   B(J, I) =B(J-1, I) *K(J, I)
        WRITE (6, ' (//////20X, '' Ligand is '', A80) ') ITITLE
        WRITE (6,1000) ((K(I, J), B(I,J), G(I,J), I=1,4),J=1,2)
 1000 FORMAT (6X, 'K', 18X, 'B', 19X, 'G' /
    1            8(1X, 1PE10.3,2(10X,E10.3)/))
        WRITE (6,1001)TCU, TL, KCU
 1001 FORMAT(//1X, 'TOTAL COPPER = ', F10.7, 10X,
         'TOTAL LIGAND = ', F10.7
        1/10X, ' Equilibrium constant for Cu2+ + Cu- > 2Cu+ =',
        1PE10.3/////)
        IFAIL = 1
        MAXIT = 1000
        ERF = 1.E-7
        CALL BIN (DIFFL,TCU, O., X ,ERF, MAXIT, IFAIL)
        Cul (1, 1) = X
        R = DIFFL (X)
        CALL FUN (F, GG)
        WRITE (6,3001)
    3001 FORMAT (/20X, ' BINARY SEARCH HAS CONVERGED')
     999 WRITE (6,2000) Cul (1,1 ), Cul(1,2), ((Cul(J,I), J=2,5)
    1       I = 1, 2), L, F, GG, R
    2000 FORMAT (////2X, 10('*'), 1X, 'RESULTS', 1X, 10('*')//2X,
    1  'Cu2+ = ', 1PE10. 3,20X, 'Cu+ = ',
    1  E10.3/1X, 'Cu2+ + Ligands', 4(5X, E10.3)/1x,' Cu+ + Ligands',
    2  4(5X, E10.3)/1X 'Free ligand = ', E10.3//5X,
```

```
     5'Difference in total concentrations', 5X,2(3X, E10.3)
     6/5X, 'Value of function DIFFL = ', E10.3)
100  FORMAT (8E10.3)
c    Calculate ionic strength of soultion
     STR = 0
     DO  I= 1,2
         DO  J = 1,5
         STR = STR + Cul (J, I)*FLOAT (4 - I - J)**2
         ENDDO
     ENDDO
     STR = (STR + TCU* 4.0 + TL)/2.
     STR2 = TL + TCU* 4.0
      WRITE(6,4000)STR, STR2
4000 FORMAT(//20X, 'Ionic strength of solution :', F10.5,
     1   //2x, 'Ionic strength in terms of initial concentrations:'
     2         F10.5/)
       STOP
        END
       FUNCTION DIFFL (X)
```

```
c           Calculates difference between the concentration
c           of ligand at copper conc.  X which give F = 0 and
c           G = 0
      Common /B1/  Q(20), TCU, TL
      EXTERNAL FUNL, GUNL
      Q(1) = X
      IFAIL = 1
      MAX = 1000
      ERF = (TCU + TL) * 1. E-7
      CALL BIN1 (FUNL, TL,0., Y, ERF, MAX, IFAIL)
      If (IFAIL, EQ.  -1)Y = TL +1
      If (IFAIL, EQ.   1)Y = -1
      If (IFAIL. EQ.   2) Then
            WRITE(*,' (10X, '' Error in DIFFL with IFAIL = 2'',
            10X,
     1            ''X = '', 1PE10.3)')X
          STOP 4
      ENDIF
      IFAIL = 1
      MAX = 1000
      CALL BIN1 (GUNL, TL, 0., Z, ERF, MAX, IFAIL)
      DIFFL = Z - Y
      RETURN
      END
      FUNCTION FUNL (X)
```

```
c       Calculates value of SUMC - TC at ligand conc. X.
      COMMON /B 1/  Q(20), TCU, TL
      Q(19) = X
      CALL FUN (F, G)
      FUNL = F
      RETURN
      END
      FUNCTION GUNL (X)
c       Calculates value of SUML - TL at ligand conc. X.
      COMMON /B1/  Q(22)
      Q(19) = X
      CALL  FUN (F,G)
      GUNL = G
      RETURN
      END
      Subroutine BIN(F, YU, YL, X, ERF, MAXIT, IFA)
```

```
c       Conducts binary search between limits XU and XL
c       F(X) Generates values of the function
c       X is the final vaue returned when ABS(F(X)) < ERF
c       IFA   ----- on entry = 0 program will stop on finding
        error
c                              =1 program will reset IFA and continue
c             on exit          =0 successful operation
c                               =1 initial function values both + VE
c                               =-1 initial function values both - VE
c                               =2 Maxit iterations performed
      XU = YU
      XL = YL
      FU = F(XU)
      FL = F (XL)
      If (FU*FL .GT. 0.) Then
c               Error FU and FL same sign
        IFAIL =1
        If(FU .LT. 0) IFAIL =-1
        If(IFA.EQ. 0) Then
c                 Hard fail option
            WRITE(*,1000)IFAIL, XU,XL, FU,FL
                  STOP2
       ELSE
                IFA = IFAIL
        ENDIF
    ELSE
        IC =0
1       If(IC, EQ. MAXIT) Then
```

```
                    IFAIL =2
                    If(IFA. EQ. 0) Then
                WRITE(*,1000)IFAIL, XU,XL, FU,FL
                    STOP3
            ELSE
                IFA = IFAIL
                RETURN
            ENDIF
        ELSE
            IC = IC + 1
            X = (XU - XL)/2. + XL
            FX = F(X)
            If (FX*FL. LE. 0)Then
                        XU =X
            ELSE
                        XL =X
                        FL =FX
        ENDIF
        IF (ABS(FX) . GT. ERF) GOTO1
    ENDIF
    IFA = 0
```

```
      ENDIF
      RETURN
 1000 FORMAT (///10X, 'Error in binary search with IFAIL =', 3/
     110X, 'Status at time of error'/10X, 'XUPPER = ', 1PE10.3,
     2 5X, 'XLOWER = ', E10.3, 5X, 'F(XU) = ', E10.3,5X,' F(XL) =
     ' , E10.3)
      END
      Subroutine  BIN1 (F, YU, YL, X, ERF, MAXIT, IFA)

c           Conducts binary search between limits XU and XL
c           F(X) Generates values of the function
c           X is the final value returned when ABS(F(X))<ERF
c           IFA ------- on entry = 0 program will stop on
c           finding error
c                                =1 program will reset IFA and continue
c                 on exit        =0 successful operation
c                                 =1 initial function values both +VE
c                                 =1 initial function valuse both -VE
c                                 =2 MAXIT iterations performed
      XU=YU
      XL=YL
      FU=F(XU)
      FL=F(XL)
      IF(FU*FL .GT. 0)Then
c                   Error FU and FL same sign
        IFAIL =1
        IF(FU. LT. 0)IFAIL =-1
        IF(IFA. EQ.  0)Then
```

```
c                   Hard fail option
                       WRITE(*, 1000)IFAIL,XU,XL,FU,FL
                       STOP2
            ELSE
                       IFA=IFAIL
            ENDIF
 ELSE
            IC=0
1           IF(IC. EQ. MAXIT)Then
                    IFAIL =2
                    IF(IFA. EQ. 0)Then
                            WRITE(*,1000)IFAIL,XU,XL,FU,FL
                            STOP3
                  ELSE
                            IFA=IFAIL
                            RETURN
                ENDIF
          ELSE
                    IC=IC+1
                    X=(XU-XL)/ 2.+ XL
                   FX=F(X)
                   IF(FX*FL. LE. 0)Then
                               XU=X
```

```
                ELSE
                        XL=X
                        FL=FX
              ENDIF
              IF(ABS(FX). GT. ERF)GOTO1
          ENDIF
         IFA=0
        ENDIF
        RETURN
1000 FORMAT(///10X,'Error in BIN1 with IFAIL =',13/
     110X, 'Status at time of error'/10X, 'XUPPER=', 1PE10.3
     2 5X, 'XLOWER=  ', E10.3,5X, 'F(XU) = ', E10.3,5X,'F(XL)= 'E10.3)
    END
          Subroutine FUN(F,GG)
        Common /B1/ Cul(5,2),K(4,2),L,KCU,TCU,TL
        Real K,L,KCU
        SUML =L
        Cul(1,2)= SQRT(KCU*Cul (1,1))
        SUMCU  = Cul (1,2) + Cul (1,1)
        DO  2  I= 1,2
        DO  2  J=2,5
        Cul(J,I) = K(J-1,I)*L*Cul(J-1,I)
        SUMCU=SUMCU+Cul (J,I)
        SUML = SUML + Cul (J,I)*FLOAT(J-1)
2       Continue
```

```
F=SUMCU-TCU
GG=SUML -TL
   RETURN
   END
```

Appendix (2)

Abbreviations

a_{ox}	activity of oxidisable reactant
a_{red}	activity of reducible reactant
A	absorbance
C^o	bulk concentration
$C_{x=}$	concentration of ions at distance x from the interface
C_o	the equilibrium adions concentration
$\bar{C}_t$	the average surface concentration of adions at a time t.
$C_{M^{n+}}$	the bulk concentration of metal M ions
C_R	concentration of species R
C	capacitance
C_{dl}	double layer capacitance
C_{ads}	double layer capacitance due to adsorbed molecules
D	diffusion coefficient
E	potential difference at non standard condition
E^o	potential difference at standard condition
E_R	reversible potential of copper in electrolyte
E_1^e	equilibrium potential of reaction E(3-4,p121)
E_2^e	equilibrium potential of reaction E(3-6,p122)
F	Faraday
i	current density
i_A	anodic current density
i_c	cathodic current density
i_L	limiting current density
i_{dl}	double layer current density
i_{ct}	charge transfer current density
i_o	equilibrium exchange current density

J_D	diffusion flux
K_M	chemical reaction rate constant involving reactant M
KX	Equilibrium constant of reaction X
K_c	rate constant of charge transfer cathodic deposition
K_A	rate constant of charge transfer anodic reaction
K_p	proportionl constant
M_X	molecular weight of substance X
n	number of electrons
N_{Cu}	mol m^{-2} of copper
N_{CuX}	mol m^{-2} of copper(1) halide
$P_{i,cath}$	the order of the cathodic reaction of the reactant
Q	number of coulombs
r	radius of atoms or molecules
r'	factor of rate determining step
R	the gas constant
t'	total CuX formation reaction time
T	temperature
T_{ss}	measured time for the overpotential to reach steady state
T_{on}	pulse on time
T_{off}	relaxation time
V_t	the potential difference across a parallel plate capacitor at time t

V	the final steady state potential difference
V'	electrode potential vs. standard hydrogen electrode
W_{AA}	weight of copper in deposit
W_E	measured weight of electrode
W_{CuCl}	weight of copper (I) chloride
W_{pc}	theotrical weight of copper deposited by pulse current
α_a	anodic transfer coefficient
α_c	cathodic transfer coefficient
β_n	gross constant n
β	symmetry factor
γ_c	number of electrons transferred preceding the rate determining step for the cathodic process
δ	diffusion layer thickness
ν'	stoichiometric number of reaction
ν	sweep rate
τ	The time notation
τ''	transition time
τ''_{ct}	transition time of charge transfer reaction
$\Delta\Phi$	potential difference across interface
$\Delta\Phi_e$	equilibrium potential difference
ΔW	increase in weight of copper(I) halide
$\Delta E^{\neq}$	change in activation energy

η	overpotential
η_d	diffusion overpotential
η_c	concentration overpotential
η_{ct}	charge transfer overpotential
η_{cr}	crystallization overpotential
η_r	reaction overpotential
η_Ω	ohmic overpotential (IR drop)
η_t	overpotential at time t
η_∞	steady state overpotential
θ_e	fraction of electrode covered by adsorbed species at equilibrium
θ_t	fraction of electrode covered by adsorbed species at time t
θ	angle of resolution
ψ_s	potential of bulk solution
ϕ_M	inner potential at the metal
z_i	the valence of the species i
e_o	the electronic charge
Ψ_M	the outer potential due to the charge on the metal electrode
q_d	diffuse charge density
q_M	net charge density on the electrode

REFERENCES

1. J.O'M Bockris and A.K.N. Reddy, in "Modern Electrochemistry", Vol 2, Chap 4, Plenum Publishing Corporation, London.
2. E. Mattsson and J.O'M Bockris, Trans. Faraday Soc., 55, 1586 (1959).
3. D.S. Peter and S.A. Cruser, J. Electroanal. Chem., 9, 27 (1965).
4. D.B. Hibbert, H. Sugiarto and A.C.C. Tseung, J. Chemical Soc., Faraday Trans. I, 74, 1973 (1978).
5. O.R. Brown and H.R. Tuirsk, Electrochim. Acta, 10, 383 (1965)
6. J.O'M. Bockris and M. Enyo, Trans. Faraday Soc., 58, 1187 (1962).
7. J.O'M Bockris and H. Kita, J. Electrochem. Soc., 109, 928 (1962).
8. Q.J.M. Slaiman and W.J. Lorenz, Electrochim. Acta, 19, 791 (1974).
9. T. Hurlen, G. Ottesen and A. Staurset, ibid., P39-44, vol 23 (1978).
10. H.J. Pick, G.G. Storey and T.B. Vaughon, Electrochim Acta, 2, 165 (1960).
11. H.J. Pick and T.B. Vaughon, ibid., 2, 179 (1960).
12. S.C. Barnes, G.G. Storey and H.J. Pick, ibid., 2, 195(1960).
13. A. Damjanovic, T.H.V. Setty and J.O'M Bockris, J. Electrochem. Soc., 113, 429 (1966)
14. G. Carneval and J.B de Cusminsky, ibid., 128 (1981).
15. R. Walker and R.C. Benn, Plating, 58, 479 (1971).
16. Leonard Karasyk and Henry B. Linford, J. Electrochem. Soc., 110, 895 (1963).

17. Shinzo Okada and Saburo Magori, ibid., 102, 580 (1955).

18. W.H. Gauvin and C.A. Winkler, J. ibid., 99, 71 (1952).

19. Yu Lin Yao, Trans. Electrochem. Soc., 86, 365 (1944).

20. Wolfgang DAhms, U.S. Pat 4, 181, 582 (1980).

21. Yu Lin Yao, Trans. Electrochem, Soc., 86, 371 (1944).

22. J.F. Beaver, U.S. Pat.2, 602, 774 (1952).

23. M.A. Mosher, J. Electrochem. Soc., 107, 7C (1960).

24. L. Stephenson and J.H. Bartlett, ibid., 101, 571(1954).

25. R.S. Cooper, ibid, 103, 307 (1956).

26. R.S. Cooper and J.H. Bartlett, ibid, 105,109 (1958).

27. R.S. Cooper, ibid, 105, 506 (1958).

28. T. Hurlen, Acta Chem. Scand., 15, 1231 (1961).

29. T. Hurlen, ibid, 15, 1246 (1961).

30. A.C.C. Tseung and M.N. Mahmood, Electrochim. Acta, 341 (1977).

31. D.J. Doan, in "The Primary Battery", Vol 2, ed Cahoon and Heise, Wiley, New York (1976).

32. Nehemiah Margalit, J. Electrochem. Soc., 122, 1005 (1975).

33. C.W. Yeow and D.B. Hibbert, ibid, 130, 786 (1983).

34. M. Schlotter, Tran-Far. Soc., 31, 1177 (1935).

35. L. Mandelcorn, W.B. McConnel, W. Gauvin and C.A. Winkler, J. Electrochem. Soc., 99, 84(1952).

36. S.M. Mayanna, J. Electrochem. Soc., 121, 251 (1974).

37. S. Nagesevar, Electrodeposition and Surface Treatment, 3, 369 (1975).

38. C.H. Bonfiglio, H.C. Albaya and O.A. Cubo, Corrosion Science, 13, 717 (1973).

39. Moritz Braun and Ken Nobe, J. Electrochem. Soc., 126, 1666 (1979).

40. C. Ogden and D.Tench . Plating and Surface Finishing, 66, 30 (1979).

41. C. Ogden and D. Tench , ibid, 66, 45(1979).

42. C. Ogden and D.Tench, ibid., 68, 52 (1981).

43. D. Tench and C. Ogden, J. Electrochem. Soc., 125, 194 (1978).

44. D. Tench and C. Ogden, ibid., 125, 1218 (1978).

45. D. Fletcher, in "Industrial Electrochemistry", p48, Chapman and Hall, London (1978).

46. Baconke, J.J. Hoekstra, Bienvenido C. Sison, Jr. and D. Trivich, J. Electrochem. Soc., 106, 382(1959).

47. G.G. Storey and S.C. barnes, J. of the Institute of metals, 90, (1962).

48. F.T. Gucker and R.L. Seifert, in "Physical Chemistry", P.337-353, Flectcher and Son, Norwich (1967).

49. L.V. Azaroff in "Elements of X-ray Crystallograph", P.102-105, McGraw Hill, New York (1968).

50. S. Okada, S. Magari and K. Katsui, J. Electrochem. Soc., 103, 557(1956).

51. T. Berzins and P. Delahay, J.Am Chem., 77, 6448 (1955).

52. H. Eyring, D. Henderson and W. Jost, in "Physical Chemistry an Advanced Treatise", P399-450, Academic Press, New York (1970).

53. Ibid p352-399.

54. K.B. Oldham and R.A. Osteryoung, J. Electroanal. Chem., 11, 397 (1966).

55. M. Rubinstein, Metal Finishing, 48, 5, 54; 78,8, 51, 58 (1950).

56, J.A. Henricks, Trans. Electrochem. Soc., 82,113 (1942).

57. S.C. Barnes, J. Electrochem. Soc., 113,296 (1964).

58. H. Seiter and H. Fischer, Z. Electrochem., 63, 249 (1959).

59. D.R. Turner and G.R. Johnson, J. Electrochem. Soc., 109, 798 (1962).

60. L.L. Shreir and J.W. Smith, Trans. Faraday Soc., 50, 393(1954).

61. G.T. Rogers and M.J. Ware, J. Electrochem. Soc., 107,677 (1960).

62. R. Weil, Plating, 61,654 (1974).

63. J.J. McMullen and N. Hackerman, J. Electrochem. Soc., 106, 341 (1959).

64. B.D. Cahan, J.B. Ockerman. R.F. Amile and P. Ruetschi, ibid, 107, 725 (1960).

65. M. Babai, N. Tshernikovski and E. Gileadi, ibid, 119, 1018(1972).

66. N. Tshernikovski and E. Gileadi, Electrochim. Acta, 16, 579 (1971).

67. J.O'M. Bockris and A.K.N. Reddy, in "Modern Electrochemistry", Vol 2, P1173-1182, Plenum Press, London (1977).

68. L.V. Azaroff, in "Elements of X-ray Crystallography, P504-517, McGraw-Hill Book Co., New York (1968).

69. Ibid. P461-491.

70. I. Rubeska and B. Moldan, in "Atomic Absorption Spectrophotometry", P.161, Iliffe books Ltd, London (1969).

71. W.J. Price, in "Analytical Atomic Absorption Spectrometry", P18-21, Heyden and Son Ltd., London (1972).

72. F.T. Gucker and R.L. Seifert, in "Physical Chemistry", P580-583, the English Universities Press Ltd., London (1967).

73. A. M. James and F.E. Prichard, in"Practical Physical Chemistry", 3rd edition, P307, Longman Group Ltd,Essex (1974).

74. J.O'M Bockris and A.K.N. Reddy, in "Modern Electrochemistry", Vol 2, P 892-894, Plenum Press, London (1970).

75. Ibid. P1185-1195.

76. J.O'M. Bockris and B.E. Conway, in "Modern Aspects of Electrochemistry", No.3 p226-232, Butterworths, London (1964).

77. J.O'M Bockris and A.K.N. Reddy, in "Modern Electrochemistry", Vol 2, P623-803, Plenum Press, London (1970)

78. J.O'M Bockris and B.E. Conway, in "Modern Aspects of Electrochemistry", Vol 5, P253, Plenum Press, London (1969).

79. J.O'M Bockris and A.K.N. Reddy, in "Modern Electrochemistry", Vol 2, P997-1012, Plenum Press, London (1970).

80. Ibid, p868-873, 918-929.

81. K.W. Sykes, in "Stability Constant Supplement No.1", P285-286, 322-323.

83. H.Y. Cheh, H.B. Linford and C.C. Wan, Plating and Surface Finishing 66, (1977).

84. Powder Diffraction File, J.C.P.D.S., Easton Maryland (1972).

85. "Handbook of Chemistry and Physics, "53rd ed, Chemical Rubber Co., Ohio, F177 (1973).

86. G.Milazzo and S.Caroli, in "Tables of Standard Electrode Potentials ", P23, J.Wiley and Sons, Chichester (1978).

87. R.C. Weast and M.J. Astle - "Handbook of Chemistry and Physics, 63rd edition, D-175 (1983).

88. E.H. Rodd, in "Chemistry of Carbon compounds", Vol 1, p 924-926, Elsevier Plubishing Co., London (1952).

89. Saul Patai, in " The Chemistry of the thiol group," P 785-833, J. Wiley and Sons, London (1974).

90. Ibid, P123-125

91. Ibid, P670

92. J.L. Dye and O.J. Klingenmaier, J. Electrochem, Soc., 104, 275 (1957).

93. J.O'M Bockris and B.E. Conway, in "Modern Aspects of Electrochemistry", Vol 3, P301, Butterworth, London (1977).

94. R.A. Fellows, G. Pointe, E.W. Hoover and H. Brown U.S. Pat. No. 2733318 (1956).

95. M.M. Baizer, in " Organic Electrochemistry" P749-752 Marcel Dekker, Inc. New York.

96. Ibid, P554-556

97. Eyring, Henderson and Jost, in "Physical Chemistry an Advanced Treatised", P254-256, Academic Press, New York (1970).

98. Kirk Othmer, in "Encyclopedia of Chemical Technology" Vol 6, P 286, J. Wiley and Sons. New York 3rd Edition.

99. J.O.M. Bockris and Conway, in "Modern Electrochemistry", Vol 2, p788-732, Plenum Press, New York (1977).

100. Arthur I Vogel, in "Macro and Semi Micro Qualitative Inorganic Analysis", P337, Longman, 4th edition.

101. V. Kondratyev in "The structure of Atoms and molecules", P474, Printed in the Union of Soviet Socialist Republic.

102. J.O'M Bockris and A.K. N. Reddy, in "Modern Electrochemistry", Vol 12, P1055, Plenum Press (1977).

103. A.C.C. Tseung, H.K. ng and D.B. Hibbert. J. of the Electrochem. Soc., 127, 1034 (1980).

104. K.I.Popov, D.N. Keca, S.I. Vidojkovic, B.J. Lazarevich, and V.B. Milojkovic. J. Appl. Electrochem, 6, 365 (1976).

105. A.J. Sukava and C.A. Winkler, Canadian J. of Chemistry, 33, 961 (1955).

106. R.A. Fellows G. Pointe E.W. Hoover and H. Brown, U.S. Pat. 2,738,318 (1956).

Reprinted from JOURNAL OF THE ELECTROCHEMICAL SOCIETY
Vol. 130, No. 4, April 1983
Printed in U.S.A.

Galvanostatic Pulse Plating of Copper and Copper (I) Halides from Acid Copper (II) Halide Solutions

C. W. Yeow and D. B. Hibbert*

Department of Chemistry, Bedford College, University of London, Egham Hill, Egham, Surrey, England

ABSTRACT

CuX (X = Cl or Br) is formed during the galvanostatic pulse plating of copper from acid solutions containing Cu^{2+} and X^-. The reaction $Cu^{2+} + Cu^\circ + 2X^- \rightarrow 2CuX$ occurs in the relaxation period of the pulse. Copper (I) chloride anodes for reserve seawater batteries may be made by this method. CuBr is oriented in the {220} plane when deposited on copper foil with the {200} plane uppermost. CuCl tends to dissolve in solutions containing Cl^- to give soluble copper (I) halides. Corrosion rates at pure copper were determined from the pulse-plating experiments.

Studies (1-3) of copper plating from acid baths by a variety of pulse methods have been made to improve efficiency and plate quality, especially in cathode geometries having small holes or pores (1). Different additives may also improve plate quality by complexing with ions in solution or by adsorption at the plating surface. This investigation was instituted to observe the effect of additives on pulse plating. Copper halides were chosen as model systems because of the availability of data and the body of previous work.

The corrosion of copper in solutions of copper(II) chloride has been studied by Hurlen (4, 5) who showed that layers of copper(I) chloride are formed which subsequently dissolve giving soluble species such as $CuCl_2^-$. The rate of copper(I) chloride formation is slow after an initial monolayer because of the need for solid-state movement of chloride ions to the underlying bulk copper. Numerous workers (4, 6-8) have studied the anodic behavior of copper in halide media. Copper dissolves to $CuCl_2^-$, $CuCl_3^{2-}$, and $CuCl_4^{3-}$ via films of CuCl.

Copper(I) chloride is used as an anode for reserve seawater batteries (9), which may be fabricated by mixing copper(I) chloride with an organic binder and graphite, or by dipping copper plates into molten copper(I) chloride (9). A method of manufacture by direct reaction at a copper electrode, as described in this paper, may provide electrodes which are more conducting, have a known discharge capacity, and ultimately be more economical.

Experimental

Materials

All materials were of Analar grade and used without further purification. Electrodes were 2 × 2 cm copper foil (BDH 99.999%) or 2 × 2 cm platinum foil (Johnson Matthey 99.99%) on which a thin layer of copper was plated from acid copper sulfate solution.

Methods

Corrosion of copper in solutions containing halide ions.—A clean copper foil was suspended from a balance (CI Electronics Microforce II) in a solution containing 1 mol dm^{-3} H_2SO_4, 0.34 mol dm^{-3} $CuSO_4$, and 0.1 or 0.34 mol dm^{-3} KCl or KBr. The solution was thermostated to 25°C (±0.5°C). During the experiment, the level of the solution was adjusted relative to the electrode to correct for the buoyancy of the electrode. The increase in weight of the foil was measured (±0.01 mg) with time. Similar experiments were attempted with solutions containing fluoride and iodide ions.

Pulse plating.—Copper was galvanostatically (300 mA) pulse plated from a series of electrolytes containing 1 mol dm^{-3} H_2SO_4, 0.1 to 0.34 mol dm^{-3} $CuSO_4$, and 0.05 to 0.34 mol dm^{-3} KCl or KBr. A single compartment cell was used with a copper or platinum foil anode. The potential of the working electrode was monitored by an oscilloscope against a saturated calomel reference electrode connected with the Luggin capillary by a salt bridge. The cell was continuously purged with nitrogen during all experiments, and thermostated to 25°C (±0.5°C). A train of square wave pulses was produced by a Chemical Electronics pulse generator (CE RB1) and the current controlled by a potentiostat (Thompson Associates 125)' working in a galvanostatic mode. The range of pulse periods was 0.5-10 msec, and relaxation times of 10-1000 msec. For analysis of the deposited layer, plated platinum electrodes were used.

Analysis of plated layers.—Plated electrodes were washed with distilled water and dried in a nitrogen atmosphere to constant weight. For copper-plated

* Electrochemical Society Active Member.
Key words: pulse plating, battery anodes, corrosion.

platinum electrodes, the weight of the initial copper layer was subtracted from the total deposit weight. The total copper content was determined by atomic absorption spectroscopy of a solution obtained from dissolution of the deposit in nitric acid. Copper(I) halide was determined by cathodic coulometry in nitrogen-purged sulfuric acid at 25°C. A potentiostatic step, OCV to 0.1V (*vs.* SHE) for CuCl, and to −0.05V for CuBr, was applied to the copper(I) halide electrode and the current measured with time. The charge passed as CuX was cathodically reduced to copper and X^- (Eq. [1]) gave the amount of halide in the electrode

$$CuX + e \rightarrow Cu + X^- \qquad [1]$$

for X = Cl, E^o = 0.137V; X = Br, E^o = 0.033V. An x-ray diffraction pattern of the deposit was obtained by placing an electrode at the focal plane of a Phillips diffractometer. For comparison, the x-ray pattern of a copper foil was also recorded.

Results

Corrosion of copper in copper(II) halide solutions.—Figures 1 and 2 show the increase in weight of electrodes immersed in acid copper chloride and bromide solutions having 0.1 mol dm^{-3} and 0.34 mol dm^{-3} halide. It is seen that the corrosion rate for solutions containing bromide increases with increasing bromide concentration. In the case of chloride, the weight eventually decreases due to dissolution of CuCl giving soluble copper(I) chlorides, this effect being greater at higher concentrations. No action of solutions of F^- was noted. Solutions containing I^- and Cu^{2+} reacted extremely quickly giving CuI as a white precipitate which easily scaled from the foil.

Pulse Plating in Halide Solutions

Analysis of deposit.—For all conditions of plating, the weight of the deposit calculated from the total copper content and the amount of copper(I) halide agreed with the measured weight showing that the only species present in the deposit were Cu, and CuCl or CuBr. Table I contains x-ray data for a copper foil, and for foils coated with CuCl and CuBr. For the coated foils, a background pattern of the underlying copper was also observed.

Dependence of the formation of CuX on plating conditions.—Figure 3 shows the percentage of cop-

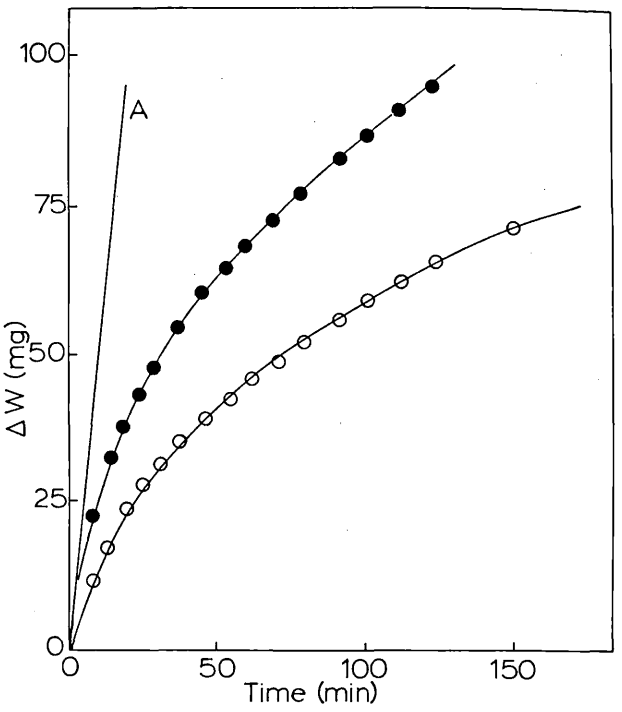

Fig. 2. Increase in weight (Δw) of an 8 cm^2 copper foil immersed in acid copper bromide solutions at 25°C. $CuSO_4$ = 0.34 mol dm^{-3}, H_2SO_4 = 1.76 mol dm^{-3}. ○: KBr = 0.1 mol dm^{-3}; ●: KBr = 0.34 mol dm^{-3}. Line A is the limiting corrosion rate calculated from Eq. [5].

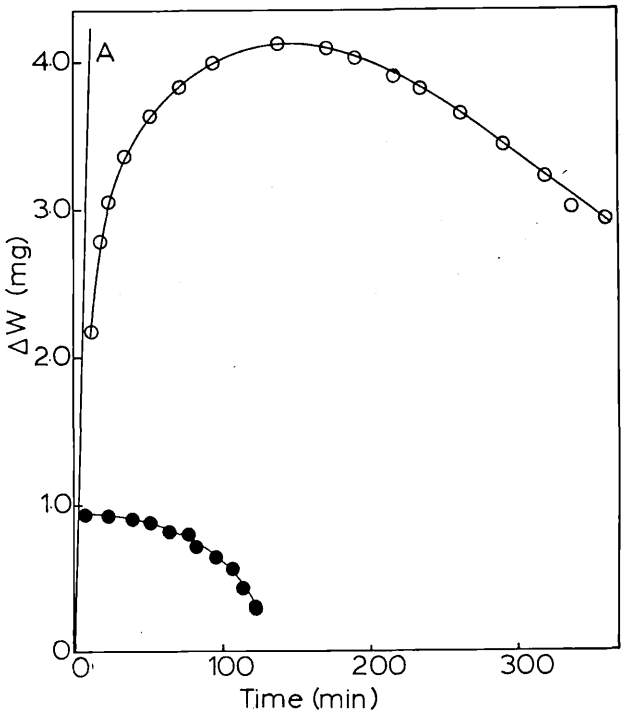

Fig. 1. Increase in weight (Δw) of a 8 cm^2 copper foil immersed in acid copper chloride solutions at 25°C. $CuSO_4$ = 0.34 mol dm^{-3}, H_2SO_4 = 1.76 mol dm^{-3}. ○ : KCl = 0.1 mol dm^{-3}; ●: KCl = 0.34 mol dm^{-3}. Line A is the limiting corrosion rate calculated from Eq. [5] and Fig. 6.

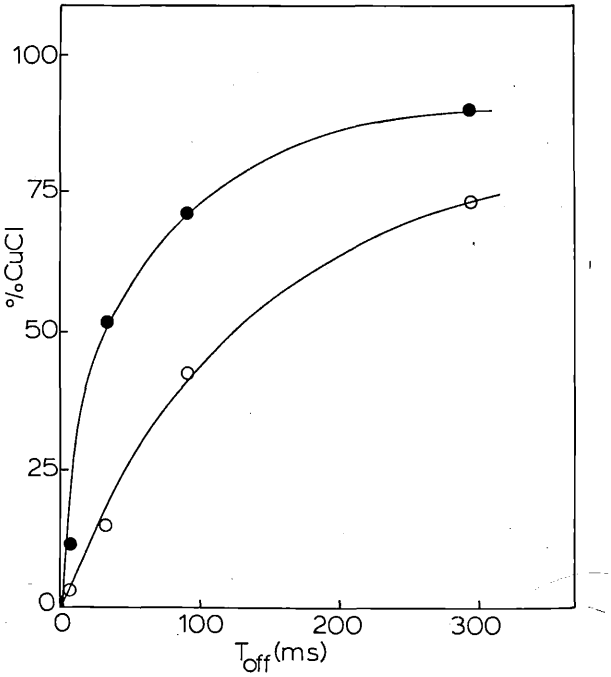

Fig. 3. Percentage of CuCl in the plated deposit as a function of relaxation time of the pulse, during pulse plating in acid copper chloride solution at 25°C. $CuSO_4$ = 0.34 mol dm^{-3}, H_2SO_4 = 1.76 mol dm^{-3}, KCl = 0.34 mol dm^{-3}. ●: Pulse length = 10 msec; ○: Pulse length = 2 msec.

Table I.

Cu						CuCl						CuBr					
d/A	I_{exp}	I_{th}	h	k	l	d/A	I_{exp}	I_{th}	h	k	l	d/A	I_{exp}	I_{th}	h	k	l
2.085	100	100	1	1	1	3.135	100	100	1	1	1	3.302	100	100	1	1	1
1.807	>800	46	2	0	0	2.722	4	8	2	0	0						
1.280	36	20	2	2	0	1.920	44	55	2	2	0	2.021	>800	60	2	2	0
1.090	21	17	3	1	1	1.633	23	30	3	1	1	1.722	50	35	3	1	1
						1.243	4	10	3	3	1	1.308	90	10	3	3	1

X-ray diffraction data for copper foil, and for copper foil coated by pulse-plated CuCl and CuBr. Theoretical intensities from Ref. (10).

per(I) chloride in the plate as a function of relaxation time at constant pulse length. For steady-state plating, no copper halides were found in the deposit. A similar plot is given for copper(I) bromide in Fig. 4 which shows the increase in percentage of CuBr with bromide concentration.

The effect of concentration of Cu^{2+} and Cl^- at constant pulse length and relaxation time was studied. The results are shown in Fig. 5.

Discussion

The reaction between copper and copper(II) halides.—In this study we have confirmed the corrosive action of halide ions in copper(II) solutions. The reaction to give copper(I) halide is

$$Cu + Cu^{2+} + 2X^- \rightarrow 2CuX \quad [2]$$

We have found that the order of reactivity of halides to Eq. [2] is $F^- < Cl^- < Br^- < I^-$. This is supported by thermodynamic data (13) which shows a similar increase in reduction potential for Eq. [2], E° = 0.401V, 0.607V, 1.045V for Cl^-, Br^-, and I^-, respectively. The reaction with chloride is complicated by dissolution of CuCl giving $CuCl_2^-$, $CuCl_3^{2-}$, and possibly $CuCl_4^{3-}$. This is seen from Fig. 1 where, on increasing the concentration of chloride, the increase in the weight of the foil is less by the reaction

$$CuX + X^- \rightarrow CuX_2^- \quad [3]$$

For X = Br, dissolution of CuBr is not so important. The equilibrium constant for Eq. [3] is 2.8×10^{-2} for X = Cl and 4.5×10^{-3} for X = Br (14). Conversion of $CuBr_2^-$ to further species is also less thermodynamically favorable (14).

For chloride and bromide solutions, therefore, the corrosion rate at a fresh copper surface is great, and it is this fact which is used in the pulse-plating experiments. During the pulse, approximately a monolayer of copper is formed which, during the relaxation time, reacts to give the copper(I) halide by Eq. [2]. Optimum production of CuX occurs when the relaxation time is sufficient to allow reaction of the monolayer of plated copper, but not so great as to allow dissolution of the halide layer.

The stoichiometry of the reaction forming CuCl and CuBr during pulse plating.—Noting that formation of CuX occurs only in the relaxation time of the pulse by corrosion of the newly plated copper, it is possible to obtain the stoichiometry of the reaction with respect to copper and halide ion and, thus, confirm that Eq. [2] is indeed of the reaction which produces CuX. Analysis of the layers formed gives the total copper content and the total weight of the deposit. The total charge passed is also known, and by coulometry of the reduction of CuX, the amount of CuX may be determined. Experiments have established that in steady-state plating under the same conditions, 100% current efficiency for

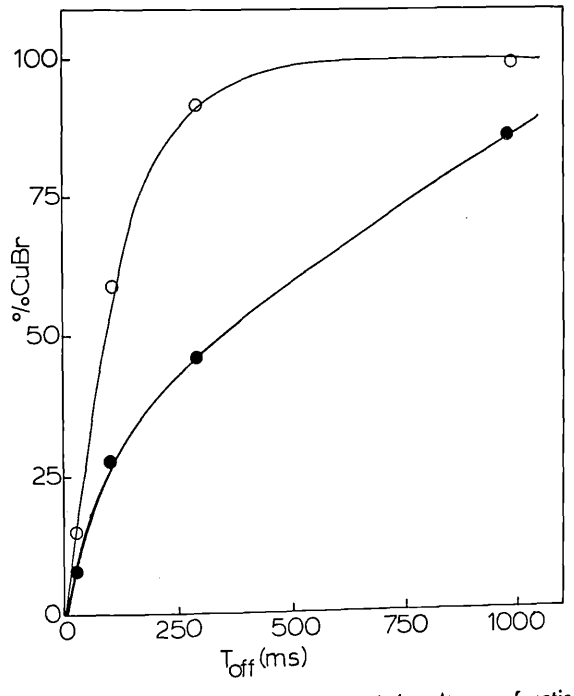

Fig. 4. Percentage of CuBr in the plated deposit as a function of relaxation time of the pulse, during pulse plating in acid copper chloride solution at 25°C. $CuSO_4$ = 0.34 mol dm^{-3}, H_2SO_4 = 1.76 mol dm^{-3}, pulse length = 30 msec. ○: KBr = 0.34 mol dm^{-3}; ●: KBr = 0.10 mol dm^{-3}.

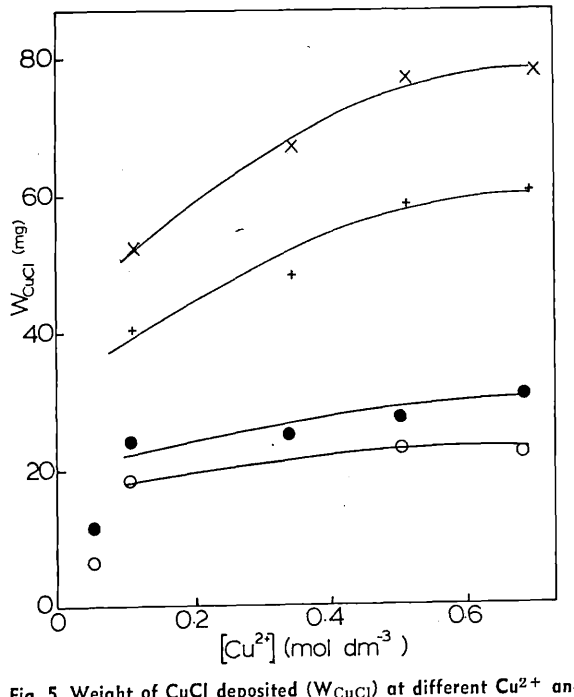

Fig. 5. Weight of CuCl deposited (W_{CuCl}) at different Cu^{2+} and Cl^- concentrations at 25°C. H_2SO_4 = 0.34 mol dm^{-3}, pulse length = 10 msec, relaxation time = 90 msec. Duration of plating = 103 min. ○: Cl^- = 0.05 mol dm^{-3}; ●: Cl^- = 0.10 mol dm^{-3}; +: Cl^- = 0.20 mol dm^{-3}; ×: Cl^- = 0.34 mol dm^{-3}.

plating copper is obtained. If the total charge passed during plating is Q coulombs, the copper deposited is $Q/2\mathbf{F}$ g atoms where $\mathbf{F}$ is the Faraday. If Q_2 coulombs are passed during reduction of CuX (molecular weight M_{CuX}), the amount of CuX formed is $Q_2/\mathbf{F}$ mol. Let a g atom of Cu° react with 1 g atom of X^- during the formation of CuX. Therefore, the amount of copper remaining after this reaction is $(Q/2\mathbf{F} - aQ_2/\mathbf{F})$ g atom. The total weight (W_T) of the deposit is, therefore

$$W_T = (Q/2\mathbf{F} - aQ_2/\mathbf{F}) \times 63.54 + M_{CuX} \times Q_2/\mathbf{F} \quad [4]$$

and thus, a may be found from the measured weight. Results during pulse plating in copper chloride gave $a = 0.51 \pm 0.03$ (from 12 experiments) and for copper bromide $a = 0.49 \pm 0.05$ (from 6 experiments). This treatment is, therefore, in agreement with a mechanism in which reaction occurs during the off time of the pulse according to Eq. [2].

Calculation of corrosion rates.—The rate of corrosion at a fresh copper surface may be determined from the formation of the copper(I) halide at different relaxation times. If conditions are chosen such that conversion to CuX is low, a constant corrosion rate may be assumed. Let n_{Cu} mol m^{-2} of copper be plated during the period of the pulse T_{on} sec, at a current density i A m^{-2}. Therefore

$$n_{Cu} = T_{on}i/2\mathbf{F} \quad [5]$$

At a corrosion rate of C mol sec^{-1} m^{-2} during the relaxation period, T_{off}, n_{CuX} mol m^{-2} are formed, *i.e.*, $n_{CuX} = CT_{off}$. Thus

$$n_{CuX}/n_{Cu} = C/(i/2\mathbf{F}) \times (T_{off}/T_{on}) \quad [6]$$

The ratio n_{CuX}/n_{Cu} calculated for a single pulse applies equally to any number of pulses. A plot of n_{CuX}/n_{Cu} against T_{off}/T_{on} should give, from its limiting slope at low relaxation times, a value for the corrosion rate C. Figure 6 shows such a plot for the corrosion of copper in 0.34 mol dm^{-3} $CuSO_4$ and 0.34 mol dm^{-3} KCl. The limiting corrosion rate is 1.10×10^{-4} mol m^{-2} sec^{-1}, which in terms of the increase in weight of a 8 cm^2 copper foil is 0.356 mg min^{-1}. This rate is drawn in Fig. 1 as line A. It is seen that the rate of corrosion by chloride stays close to the limiting value for several minutes until the effect of dissolution becomes important. A similar plot for corrosion in bromide solution gave $C = 9.30 \times 10^{-4}$ mol m^{-2} sec^{-1}, or 4.97 mg min^{-1} for an 8 cm^2 foil (line A in Fig. 2). Thus, for those metals which may be plated from solution, the pulse plating method may be used to give accurate values for corrosion rates at fresh metal surfaces.

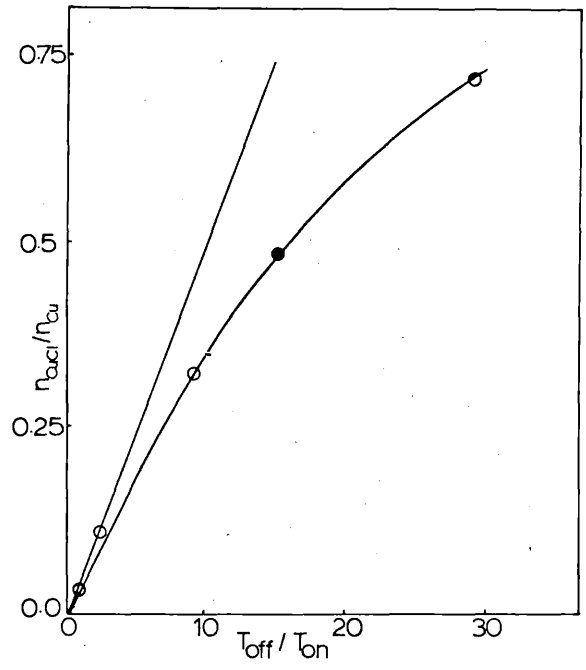

Fig. 6. Ratio of CuCl (n_{CuCl}/mol) formed in the relaxation time (T_{off}) to copper plated (n_{Cu}/mol) during the pulse (T_{on}), as a function of T_{off}/T_{on} at 25°C. $CuSO_4$ = 0.34 mol dm^{-3}, H_2SO_4 = 1.76 mol dm^{-3}, KCl = 0.34 mol dm^{-3}. ○: Pulse length = 10 msec; ●: Pulse length = 2 msec.

Reactions occurring during pulse plating.—The analysis of the processes above assumes that during the pulse copper alone is deposited by

$$Cu^{2+} + e \rightarrow Cu^+ \quad [7]$$

$$Cu^+ + e \rightarrow Cu \quad [8]$$

where Cu^{2+} and Cu^+ may be complexed by halide ion, and that the reaction in the relaxation time is given by Eq. [2]. The potential at the electrode during pulse plating (150-200 mV *vs.* SHE) allowed copper deposition to take place, but was not sufficient to result in reduction of the copper(I) halide via the reaction given by Eq. [1]. No evidence was found for the direct reduction of Cu^{2+} in the presence of halide ion

$$Cu^{2+} + X^- + e \rightarrow CuX \quad [9]$$

Orders of reaction with respect to Cu^{2+} and X^-.—The corrosion Eq. [2], which produces copper(I) halide, may be written as a pair of redox reactions of which Eq. [9] is the reduction, and

$$Cu + X^- \rightarrow CuX + e \quad [10]$$

If Eq. [10] is rate limiting, for a reaction at a monolayer of copper which does not involve diffusion, the reaction would be expected to be first order in halide and zero order in Cu^{2+}. Figure 5 shows that the production of CuCl is influenced more by chloride concentration than copper concentration, but that it is not possible to determine exact reaction orders. As Cu^{2+}, Cu^+, and Cl^- are complexed, a series of reactions involving $CuCl^+$, $CuCl_2$, $CuCl_3^-$, $CuCl_4^{2-}$, and $CuCl_2^-$, $CuCl_3^{2-}$, $CuCl_4^{3-}$ would need to be considered for a full analysis of the system.

Structure of the copper halide deposits.—The copper foil electrodes used in this work were oriented along

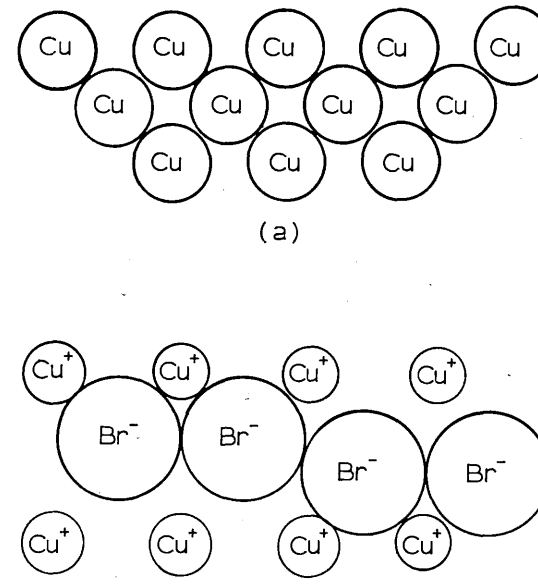

Fig. 7. (a) {200} plane of copper, (b) {220} plane of copper (I) bromide.

the {200} plane. From the x-ray results, copper bromide appears to have been deposited with the {220} plane uppermost. Copper crystallizes in a face-centered cubic arrangement with a unit cell length of 3.615Å (10). The {200} plane of copper is shown in Fig. 7a. Copper bromide exhibits a zinc blende structure in which copper is found in tetrahedral holes formed by bromide ions with $a = 5.691$Å (11). Figure 7b gives the {220} plane of CuBr in which the radius of Cu^+ and Br^- are 0.96 and 1.96Å, respectively (12). It is seen that the Cu-Cu distance in the x direction of the two planes is similar (3.6Å in copper and 3.9Å in copper(I) bromide), and thus, a CuBr lattice may be built up by the insertion of bromide ions with a limited relaxation of copper ions from the underlying lattice. Such an obvious orientation is not seen with CuCl, although geometrically the same considerations apply. Dissolution of CuCl as $CuCl_2^-$ may result in the reorganization of the CuCl layers.

The production of seawater battery anodes.—Pulse plating may be a useful method for the production of copper chloride anodes for reserve seawater batteries. Control of plating conditions can produce a nearly pure CuCl deposit of any required thickness and discharge capacity. A small amount of copper in the layer gives the anode conductivity which is an advantage for such electrodes.

Manuscript submitted Aug. 9, 1982; revised manuscript received Nov. 16, 1982.

Any discussion of this paper will appear in a Discussion Section to be published in the December 1983 JOURNAL. All discussions for the December 1983 Discussion Section should be submitted by Aug. 1, 1983.

REFERENCES

1. A. C. C. Tseung, H. K. Ng, and D. B. Hibbert, *This Journal*, **127**, 1034 (1980).
2. H. Y. Cheh, H. B. Linford, and C. C. Wan, *Plating and Surface Finishing*, **64**, 66 (1977).
3. K. I. Popov, D. N. Keca, S. I. Vidojkovic, B. J. Lazarevich, and V. B. Milojkovic, *J. Appl. Electrochem.*, **6**, 365 (1976).
4. T. Hurlen, *Acta. Chem. Scand.*, **15**, 1231 (1961).
5. T. Hurlen, *ibid.*, **15**, 1246 (1961).
6. C. H. Bonfiglio, H. C. Albaya, and O. A. Cobo, *Corros. Sci.*, **13**, 717 (1973).
7. M. Turner and P. A. Brook, *ibid.*, **13**, 973 (1973).
8. J. O'M. Bockris, B. T. Ruben, A. Despic, and B. Lovrcek, *Electrochim. Acta*, **17**, 973 (1972).
9. D. J. Doan, in "The Primary Battery," Vol. II, G. W. Heise and N. C. Cahoon, Editors, Wiley-Interscience, New York (1976).
10. Powder Diffraction File, J.C.P.D.S., Easton, Maryland (1972).
11. "Handbook of Chemistry and Physics," 53rd ed., Chemical Rubber Co., Ohio, F177 (1973).
12. G. Milazzo and S. Caroli, "Tables of Standard Electrode Potentials," Wiley-Interscience, New York (1978).
13. "Stability Constants," The Chemical Society special publication 17, London (1964).